ABSTRACT

YANG, XIN. Effects of Sucrose on the Foaming and Interfacial Properties of Egg White Protein and Whey Protein Isolate. (Under the direction of Dr. E. Allen Foegeding).

Proteins are present in aerated foods to stabilize the air/water interface by lowering the interfacial tension and forming strong interfacial films. Sugars are known to influence the functional properties of protein foams. This study investigated the mechanism responsible for sucrose effects on the foaming and interfacial properties of egg white protein (EWP) and whey protein isolate (WPI), and thereby on the functionality of their foams in food products.

In the first study, 12.8% (w/v) sucrose was added into 10% (w/v) protein solutions of EWP, WPI, or WPI-EWP combinations, with the physical properties of pre-foam solutions, foams, air/water interfaces, and angel food cakes investigated. Sucrose greatly increased the stability (longer drainage ½ life) of EWP, but slightly affected that of WPI and WPI-EWP combinations, which cannot be explained by solution apparent viscosity (μ). The dilational elasticity (E') of EWP interfacial films increased with sucrose addition, while that of WPI and WPI-EWP combinations decreased. The interfacial tension (γ) of WPI-EWP combinations followed the temporal pattern of WPI. Angel food cake prepared from 25% WPI/75% EWP foam showed comparable cake volume as that from EWP foam but a coarse structure similar to that from WPI foam. These results suggested that WPI dominated the air/water interface in mixed systems, leading to lower stability of wet foams and angel food cake batters.

Secondly, sucrose (0 to 63.6 g/100 mL) was added into 10% (w/v) protein solutions of EWP and WPI to establish its effects on protein solutions and foams. Confocal microscopic images showed that sucrose slowed the bubble size growth over time. A linear correlation was established between the change of bubble size over 20 min and the drainage ½ life, regardless of protein type. Relationships between the change of bubble size over 20 min and E'/γ suggested that interfaces with E'/γ>2 can effectively slow bubble size growing in EWP foams, confirming theoretical predictions (Walstra, 2003). The drainage ½ life was proportionally correlated to $\mu \times E'/\gamma$, independent of protein type, showing the foam stability can be enhanced by a viscous continuous phase and elastic interfaces. Sucrose addition altered the volume of angel food cakes prepared from WPI foams but showed no improvement on the coarse structures. In conclusion, sucrose can modify solution viscosity and interfacial elasticity, altering the foam microstructure and improving the stability of wet foams. However, the poor stability of WPI in the conversion from a wet to a dry foam (angel food cake) cannot be changed with sucrose addition.

Finally, sucrose effects on the E' of individual protein components in WPI or EWP were evaluated. The major protein components of EWP (ovalbumin) and WPI (β-lactoglobulin) were separated and compared with the ovalbumin and β-lactoglobulin depleted fractions. Addition of 44.3% (w/v) sucrose decreased E' of α-lactalbumin and the β-lactoglobulin depleted fraction, resembling the characteristics of WPI. However, sucrose showed no major effect on the E' of β-lactoglobulin interfacial films. Sucrose increased the E' of EWP and the ovalbumin depleted fraction but did not change that of ovalbumin. The E'

of protein mixtures suggested that the interfacial domination priority followed the order of α-lactalbumin > β-lactoglobulin > egg white proteins.

Overall, sucrose can cause a general increase in protein foam stability due to increased viscosity of the continuous phase, and a protein-specific effect on stability factors associated with interfaces. The E' of EWP increased with sucrose addition while that of WPI decreased, mainly associated with α-lactalbumin, leading to different stability of protein foams.

Effects of Sucrose on the Foaming and Interfacial Properties of Egg White Protein and Whey Protein Isolate

by
Xin Yang

A dissertation submitted to the Graduate Faculty of
North Carolina State University
In partial fulfillment of the
Requirements for the degree of
Doctor of Philosophy

Food Science

Raleigh, North Carolina

2008

APPROVED BY:

E. Allen Foegeding, Ph.D. Committee Chair	Jan Genzer, Ph.D. Minor representative
Christopher Daubert, Ph.D.	Jack P. Davis, Ph.D.

DEDICATION

This dissertation is dedicated to my parents and my husband, who always supported me no matter what.

谨以此文献给我的家人。

BIOGRAPHY

Xin Yang was born in Nanchang, a beautiful city in China, on November 2, 1981. She is the only daughter of Yichuan Yang and Ping Wang. In 1998, she went to Wuxi and stayed for 7 years to receive her Bachelor and Master degrees from Food Science and Technology Department in Jiangnan University. In 2004, she followed her advisor Dr. Fang Zhong to Dr. Charlie Shoemaker's lab at UC Davis as an exchange student and completed part work of her master project there. In 2005, she joined in Dr. Allen Foegeding's lab at NC State and started her PhD study on foaming and interfacial properties of food proteins. During the years at NC State, she met her husband Jian Wu and married on August 2007.

ACKNOWLEDGMENTS

In no particular order, I would like to thank:

- Dr. Allen Foegeding for giving me this opportunity to work on "protein foams" in his lab, and for all the support and guidance throughout these years.
- Dr. Christopher Daubert, Dr. Jack Davis, and Dr. Jan Genzer for serving as my committee and their invaluable inputs through the course of this project.
- The entire Foegeding lab: Paige for keeping the lab so organized and always willing to answer my silly questions; Tristan for being my best co-worker, providing me with unique insights in research, and helping me with confocal microscopy and image analysis; Jeab and Yiehui for all the help, encouragement, and fruitful discussions; Jason and Paula for all the help during my first year; Nin for all the suggestions and encouraging words; Mallory, Esra, Hicran, Tookta, Neal, Joseph, Kelsey, Leann, Yvette, Heather, Renee and Mary Susan for making our lab a lovely place.
- Ms. Sharon Ramsey for her assistance with my rheology experiments.
- Dr. Eva Johannes for her assistance with conforcal microscopy and image analysis.
- Mr. Roger Thompson for his help with the freeze drying equipment.
- Ms. Penny Amato for her help with the freeze drying equipment.
- The whole food science department. This department is a center of learning, offering just about any kind of environment or facilities that one could wish for. I would like to thank the food science students and the food science club for all the wonderful memories during these years. Deep appreciations are given to Junhua Zhang and Ying Chen for providing me a path to follow and their help during my first struggling year. Many

thanks are given to Youwen Pan, Weimin Gu, and all the Chinese students for the happiness we enjoyed together. Special thanks are given to Lei for our friendship and all the tough days we've been through.

- My best friends. They are Zuxu Chen & Chia-Cheng Chen, Lihua Qiu & Bin Wei, Jing Zheng & Wei Xie, Leshuai Zhang & Ying Xue, and Chunmiao Feng. A friend in need is a friend indeed. It means all of you.
- My family. Without the support from my dear parents and beloved husband, I could never make this happen.
- And more. There are so many people to whom I want to show my appreciation. I've been receiving loads of help here and will remember them for my whole life.

TABLE OF CONTENTS

LIST OF TABLES

LIST OF FIGURES

CHAPTER 1

LITERATURE REVIEW

Foams

A foam can be defined as a colloidal dispersion in which gas is dispersed in a continuous liquid or solid phase. Foams are used in various applications, in industrial processes, and for synthesis of new materials (Rieger, 1996; Cooke and Hirt, 1996; Briggs, 1996; Prud'homme and Warr, 1996; Exerova and Kryglyakov, 1998; Mills, 2007). In the food industry, foams provide a unique way to alter food structure and thereby the eating experience (Campbell and Mougeot, 1999). A typical example is cake, in which bubbles can be generated by a whipping process (air bubble) as well as released from a leavening agent (CO_2) during mixing and baking. Champagne and sparking wines are considered as foamy foods as they contain bubbles due to carbonation from a second fermentation process. An important aspect of a beer is formation of an attractive head of foam, which is primarily stabilized by adsorbed proteins. Foams are also incorporated into confectionery. Marshmallow as a tradition aerated candy is favored by consumers either as a final product or as an ingredient for food preparations. Aerated chocolate has been become popular in the market because of the special texture. More examples include soufflés, mousses, ice cream, Cappuccino, raised bread, etc. The quality of the aerated food products is attributed to the generation, physical properties and stability of foams.

Foam generation

Generating a liquid foam usually involves four factors: dispersed phase (gas), continuous phase (water), surfactant, and energy. Since the continuous phase does not have the thermodynamic desire to wet the dispersed phase, interfacial tension existed between two phases. The role of the surfactant is to bridge the two phases in a way that it's hydrophobic or non-polar segment is exposed to the gas phase and its hydrophilic or polar segment touches the aqueous phase, minimizing the interfacial tension. Energy is input during the dispersion process, which enlarges the contact area between the two phases, and hence increases the interfacial free energy of the system (Walstra, 2003). Note that the presence of surfactants can lower but not eliminate interfacial tension; a foam is still a thermodynamically unstable system. The input of energy only produces a kinetically stable system, which will eventually separate into the component phases as time progresses. Several methods can be used to create foams, such as agitation, injection, and supersaturation (Walstra, 2003). Whipping is perhaps a most common way in food preparation. During whipping, the blade rapidly agitates the pre-foam solution, generating large amount of bubbles. The bubble sizes are further reduced by the shearing forces of the blades. The Laplace pressure (Equation 1) will increase with the reduction of bubble size, preventing additional breakup of bubbles. The lower interfacial tension in the presence of surfactant contributes to less Laplace pressure, and thereby promotes breakup of bubbles into smaller ones. The Laplace pressure (P_L) is the pressure difference between the concave side ($P_{concave}$) and the convex side (P_{convex}) of a curved interface:

$$P_L = P_{concave} - P_{convex} = \gamma(\frac{1}{R_1} + \frac{1}{R_2}) \quad \text{Equation 1}$$

where γ is the interfacial tension, R_1 and R_2 are the two principle radii of curvature (Walstra, 2003). Therefore, the final bubble size in the foam depends on whipping condition and the solution composition. A higher whipping speed may agitate the solution effectively and involved large amounts of air. However, agitation during whipping also cause local pressure fluctuations and can possibly rupture the bubbles if beyond a certain whipping speed (Dickinson, 1992). Whipping for too long time may cause "overbeating" of globular proteins, due to their coagulation and loss of water-holding capacity at the interface (Dickinson, 1992). Suitable whipping speed and whipping time are required for optimum foam physical properties and stability. In addition to the whipping conditions, the concentration and type of surfactants are critical for foam generation, which has been studied by several groups (Kim et al., 1987; Binks, 2002; Aryana et al., 2002; Murray and Ettelaie, 2004). The solution viscosity is also an important factor. A low viscosity may cause less stable foam while a high viscosity can limit the amount of air being incorporated (Dickinson, 1992; Walstra, 2003).

An alternative method is sparging, in which the air bubbles are injected into the pre-foam solution through an orifice (Pugh, 1996). This process provides an accurate control of the amount of air being incorporated and the flow rate. The bubble size can be roughly estimated using the buoyancy force and interfacial tension force (Dickinson, 1992):

$$r = (3\gamma r_0 / 2\rho g)^{1/3} \quad \text{Equation 2}$$

where r and r_0 are the radii of the bubble and orifice respectively, γ is the interfacial tension and ρ is the specific gravity of the liquid, g is the gravity constant. However, the bubble

radius in practice may be larger than the predicted value due to the higher interfacial tension of the growing bubble than the equilibrium tension in the presence of surfactants (Dickinson, 1992). This method is frequently used in laboratory studies (Lage and Espósito, 1999; Magrabi et al., 1999; Wong et al., 2001; Polli et al., 2002; Pugh, 2005; Eisner et al., 2007).

Supersaturation is normally used for gas-containing beverages. The gas (usually CO_2) is dissolved in a liquid under pressure; and the gas bubbles are formed once the pressure is released. The gas should have a suitable solubility to obtain a large volume of bubbles. Bubbles can also be generated *in situ*. In the case of fermentation products (breads, beer, sparkling wine, etc.), gas is produced along with the growth of yeasts. Chemical leavening agents can also be added to food products to generate bubbles through chemical reactions. Novel aeration methods are still growing in food preparation. One example is the instant ice cream, in which liquid nitrogen is added into liquid ice cream mixtures. This freezes the solution as well as creates bubbles simultaneously through evaporation.

Overrun

One important physical property of foam is the amount of gas being incorporated into the structure, which can be represented by % overrun (Equation 3) or air phase fraction (ϕ) (Equation 4) (Campbell and Mougeot, 1999). Air phase fraction can vary from 0 (no dispersed gas) to 1 (completely gas).

$$\%\text{Overrun} = \frac{(\text{wt.}100\text{ mL solution}) - (\text{wt.}100\text{ mL foam})}{\text{wt.}100\text{ mL foam}} \times 100 \qquad \text{Equation 3}$$

$$\text{Air phase fraction } (\phi) = \frac{\%\text{overrun}}{(\%\text{overrun} + 100)} \qquad \text{Equation 4}$$

The major contributors to foam overrun include the concentration and type of surfactants, and the beating process (Walstra, 2003). The concentration of surfactants is important because sufficient surfactants are required to cover the total air-water interface in order to reach a certain overrun. Various surfactants have different interfacial activities and molecular characteristics, leading to dissimilarities in their foamability. Protein hydrolysates often have superior foaming properties due to faster unfolding of smaller peptides (Kilara and Panyam, 2003). The foam overrun is dependent on the beating conditions and beating time. Long beating time usually generated higher foam overrun (Pernall et al., 2002a); however, "overbeating" may occur for globule proteins due to their interfacial denaturation and aggregation, which causes a decrease in foam overrun.

The presence of non-surfactant co-solutes is also important for the foam overrun. Firstly, other ingredients such as salt can influence the interfacial activity of the surfactants and their foamability. Decreased foam overrun has been observed in whey protein isolate foams after adding salts (Davis et al., 2004). Secondly, the solution viscosity may be altered by addition of other ingredients, such as sugar. A high solution viscosity can retard molecule diffusion and its interfacial adsorption rate, along with impede gas dispersion. It has been indicated in several studies that incorporation of sugar decreased the overrun of protein foams due to an increase in the solution viscosity (Philips et al., 1989; Lau and Dickinson 2005; Raikos et al., 2007).

Yield stress

When the air phase fraction (ϕ) of a foam reaches a critical value, the bubbles can compress each other against the Laplace pressure, forming a "polyhedral" foam. The critical value for the arrangement of touching bubbles in an uniform monodispersion is ϕ=0.7405 based on a foam model with a unit cell of rhomboidal dodecahedron (RDH) (Edwards and Wasan, 1996). Formation of polyhedral structure can cause solid-like characteristics, usually described as "to stand up in well-defined peaks" in cookbooks. This property is exhibited as a yield stress value, which can be measured using a vane method (Pernell et al., 2000). The rheological behavior of polyhedral foams has been theoretically predicted based on 2 or 3 dimensional geometrical models, and attributed to several factors including air phase fraction, solution viscosity, interfacial tension, interfacial rheology, bubble size distribution, and bubble size shape (Narsimhan and Ruckenstein, 1986; Kraynik and Hansen, 1987; Princen and Kiss, 1989; Herzhaft, 1999). Princen and Kiss (1983) started with a theoretical 2 dimensional model consisting of mono-dispersed hexagonal cell structure as ϕ=1 and lately established a theoretical model (Equation 5) to predict yield stress for a three-dimensional system (Princen and Kiss, 1989).

$$\tau_0 = \frac{\gamma}{R_{32}} \phi^{\frac{1}{3}} Y(\phi) \qquad \text{Equation 5}$$

where τ_0 is yield stress, γ is interfacial tension, R_{32} is surface-volume mean bubble radius, ϕ is the volume fraction of the dispersed phase, and $Y(\phi)$ is an experimentally derived fitted parameter. It should be noted that several assumptions in this equation are not realistic including the monodisperse distribution of bubble size and a constant interfacial tension

through the system. The validity of this model was established using a series of emulsions over a range of ϕ from 0.8333 to 0.9756, with a relationship of $Y(\phi) = -0.080 - 0.114\log(1-\phi)$ (Princen and Kiss, 1989). Pernell et al. (2002) applied this model in protein foams generated from whey and egg white proteins and found a similar positive relationship between $Y(\phi)$ and ϕ. However, the range of $Y(\phi)$ was higher for egg white protein foams than for whey protein foams and concentrated emulsions, which was suggested to be related to some connectivity between the protein absorbed on the interface and the protein distributed in the lamellae between bubbles (Pernell et al., 2002a). Several studies revealed positive correlations between the foam yield stress and the interfacial rheological properties for whey protein-based foams (Davis et al., 2004; Davis and Foegeding, 2005; Berry, 2008), suggesting that the interfacial tension in Equation 5 can be replaced by the interfacial elasticity (Foegeding et al., 2006). However, this relationship has not been extended to foams prepared from egg white protein, which exhibited a unique behavior separated from whey protein and the mixtures of whey and egg white proteins (Berry, 2008). This may be due to the higher $Y(\phi)$ value of egg white foams than those of the others as observed by Pernell et al. (2002a). In addition, samples of egg white protein foams were not enough to establish any relationship between foam yield stress and interfacial elasticity. In all the above research, the bubble size distribution in a 3-dimensional foam was not directly measured because the R_{32} was represented by an average radius of circles or calculated using an intercept length from 2 dimensional bubble images (Pernell et al., 2002a; Berry, 2008).

Bubble size distribution

Most foams are polydisperse systems, composing of bubbles in a range of sizes. It is generally incomplete to characterize a foam in term of an average bubble size. The bubble size distribution has been correlated with the rheological properties of foam. Calvert and Nezhati (1987) found a dependence of the foam yield stress on the bubble size distribution when studying the flow properties of a foam passing through a pipe. Gardiner et al. (1998) indicated that yield stress in a foam can be determined as a function of the gas fraction and the bubble size. Princen and Kiss (1989) established the relationship (Equation 5) between foam yield stress and Sauter mean droplet radius for a series of emulsions. Pernell et al. (2002a) extended this relationship to protein foams generated from whey and egg white proteins. Berry (2008) again indicated the dependence of foam yield stress to the bubble size for protein foams of whey and egg white mixtures.

Bubble size distribution has also been correlated with the foam stability. Coalescence and disproportionation will alter bubble size distribution; meanwhile a large variation of bubble sizes can promote disproportionation as well. Sarma and Khilar (1988) suggested that the gas diffusion can be reduced with a more uniform bubble-size distribution and high initial gas volume fraction, contributing to more stable foams. Theoretical models have been developed to predict the coarsening and disproprotionation of foams by simulating bubble size change with time (Colella et al., 1999; Magrabi et al., 1999). The change of bubble size histograms over time may correspond to a transition from a Kugelschaum or sphere foam to a Polyederschaum or thin film structure caused by drainage (Pugh, 2005). As an important aspect of aerated foods, the change of bubble size distribution due to coalescence and

breakup has been studied when varying the pressure (Murray et al., 2005; Heuer et al., 2007; Sceni and Wagner, 2007). Therefore, knowledge of the bubble size distribution is essential for a better understanding of the properties and stability of foams and the aerated foods.

The bubble size distribution can be detected using several techniques. Chang et al. (1956) measured the bubble size distribution by freezing the foam and examination of a cross section. In this method, the freezing process may influence the bubble size distribution of foams. Conductivity (Lewis et al., 1984) and optical (Bisperink et al., 1992) probes have been used to measure bubble sizes. When the probes were moving across foams, an alternating signal was obtained due to the different reflected electric or light signals from liquid and gas phases, corresponding to the chord length of the bubbles through which the probes travelled. A capillary device has also been used to measure bubble size distribution (Selecki and Wasiak, 1984; Besio et al., 1985). In this method, foam was continuously sucked into a glass capillary that has a smaller diameter than the smallest bubble in the foam. The distance between liquid films in the capillary were measured and used to calculate the bubble sizes. This method causes distortion of bubbles and can only be used for stable foam. Light scattering methods (Durian et al., 1991a, 1991b; Rusu and Peuvrel-Disdierb, 1999; Sceni and Wagner, 2007) have also been used to determine bubble sizes. With the development of microscopy technique, the characteristics of the bubbles in a foam can be directly captured using a video camera. This has been widely used in sparging foams by imaging the bubbles in a column (Lage and Espósito, 1999; Magrabi et al., 1999; Wong et al., 2001; Polli et al., 2002; Pugh, 2005; Eisner et al., 2007). Du et al. (2001) used a photographic sensor to capture the images of continuous foam streams through a capillary

tube. Labbafi et al. (2007) developed an on-line image acquisition device to observe the bubble size distribution in aerated food emulsions. The microstructure of foams generated from other devices (whipping foam) can be determined by observing the foam slices under microscopy (Bals and Kulozik, 2003; Rouimi et al., 2005). Confocal microscopy has been used to determine bubble size in foams (Pernell et al., 2002a; Lau and Dickinson, 2004; Berry, 2008). This method allows for the capturing of images from several layers of bubbles to give a representative picture (Murray, 2007). Thresholding is a process of selecting the pixels that make up the objectives (bubbles), converting the original image to a binary image and allowing the objects to stand out against the background. This process provides relatively accurate comparisons for a series images by setting the same threshold value. After images have been thresholded, the quantitative information of bubbles can be obtained from the pixel numbers for each objective. Multiply features of images can be analyzed using computer software, such as counting the bubble number, measuring the bubble area, calculating the intercept length, and computing the fraction of the points that fall onto the objectives after placing a grid of points on the image (Russ, 2005). The bubble size distribution can be determined from these parameters. It should be noted that there are several potential errors in image analysis to determine bubble size distribution: 1) Foams are continuously changed as a thermodynamically unstable system, leading to variations due to imaging time; 2) Gravity may cause a vertical gradient in volume fraction, leading to variations due to sampling position; 3) Large amounts of bubbles are needed for analysis to reduce the statistical sampling bias; 4) Bubbles can be distorted during sample slice preparation; 5) Manual corrections are unavoidable in some image analysis due to the limitations of techniques,

causing problems like undercounting small circles because they are not clearly visible or clustered.

Statistical probability functions have been used to fit the frequency histogram of bubble size distributions. The frequently used functions are log normal distributions (Lage and Espósito, 1999; Wong et al., 2001; Du et al., 2003) and weibull-type distributions (Magrabi et al., 1999). In these studies, the parameters in the statistical probability function for the bubble size distribution have been correlated with the foam generation conditions, such as the size of the orifice, and the flow rate of the gas. Modeling the particle size distribution by a weibull distribution function has been suggested to facilitate the use of stereology methods for unfolding 3-dimensional size distributions with minimal irregularities (Fang et al., 1993). After obtaining the probability function, moments of bubble size can be calculated using Equation 6:

$$M_n = \int_0^\infty D^n f(D)\mathrm{d}D \qquad \text{Equation 6}$$

where M_n is the moment of bubble size, n is the integer value (typically positive), D is the bubble diameter, $f(D)$ is the probability function (Babinsky and Sojka, 2002) . It's often desirable to represent a bubble size distribution in terms of a single number. Various mean diameters can be calculated according to Equation 7:

$$D_{pq} = \left[\frac{\int_0^\infty D^p f(D)\mathrm{d}D}{\int_0^\infty D^q f(D)\mathrm{d}D} \right]^{1/(p-q)} \qquad \text{Equation 7}$$

where p and q are integer values (typically positive). Commonly used diameters include the arithmetic mean diameter (D_{10}), the surface mean diameter (D_{20}), the volume mean diameter

(D_{30}), the surface-volume mean diameter or Sauter mean diameter (D_{32}), and the de Brouckere mean diameter (D_{43}). The surface-volume mean bubble radius or Sauter radius (R_{32}) is used in the Prince and Kiss (1989) model (Equation 5). Monodisperse system should have equal values of these mean diameters. The dissimilarities of the various mean diameters to some extend indicate the characteristic of the probability function for a polydisperse system. For example, a right skewed distribution usually have an order of $D_{43}>D_{32}>D_{30}>D_{20}>D_{10}$. Other expressions can also be calculated from the statistical probability function, including the mode (maximum value), the coefficient of skewness and the coefficient of kurtosis. Calculation of these values provides a quantitative way to compare bubble distribution patterns among foams.

Even if one was observing a foam of spherical bubbles, the actual bubble radii in a 3-dimentional foam are not equal to the observed circle radii in a 2-dimentional image because a cross section is in general not made through the middle of the bubbles. The 3-dimentional characteristics of a foam can be obtained by optical tomography methods, where 2-dimentional images of successive slices are taken over a certain depth and then combined into a 3-dimentional reconstruction using computer software (Pugh, 2005; Lim and Barigou, 2004). However, the quantitative analysis of the 3-dimentional reconstruction is complicated and hard to achieve using routine software. The interior characteristics of foams can also be probed by other techniques, such as magnetic resonance imaging and multiple-light scattering methods (Pugh, 2005). Yet again, few of these techniques can provide accurately quantitative bubble size information. The stereology method has been developed to acquire 3-dimentional structure information from 2-dimentional section images using mathematical

tools (Russ, 2005). The principle of this method is to assume some small circles are due to the non-equatorial cut of large bubbles, and to subtract these circles from the small size categories. The circles are usually classified into 10 to 15 size bins. The largest circle can only come from near-equatorial cut through the largest bubbles, corresponding to the size of the largest bubbles. With the knowledge of this bubble size, the distribution of circle sizes from random intersections through the largest bubble can be calculated. Therefore, the smaller circles produced by the largest bubble can be subtracted from the corresponding smaller size bins. This process can be repeated from the largest size category to the smallest one. However, this stepwise approach may lead to very large statistical errors accumulating for the smallest size bins (Russ, 2005). To solve this problem, a set of simultaneous equations is solved for all the bins in the distribution at the same time, producing a table of coefficients. The number of bubbles in each size class (i) is calculated as the sum of the number of circles in each size class (j) times the alpha coefficients (Equation 8).

$$N_{V_i} = \sum \alpha_{ij} \cdot N_{A_j} \qquad \text{Equation 8}$$

where N_{V_i} and N_{A_j} are the bubble numbers in the corresponding size class *i* (2D) and *j* (3D) respectively. One widely used version (Cruz-orive matrix) is shown in Table 1.

Table 1 Matrix of Alpha Value Used to Convert the Distribution of Number of Circles per Unit Area to Number of Sphere per Unit Volume (Cruz-Orive)

$N_A(1)$	$N_A(2)$	$N_A(3)$	$N_A(4)$	$N_A(5)$	$N_A(6)$	$N_A(7)$	$N_A(8)$	$N_A(9)$	$N_A(10)$	$N_A(11)$	$N_A(12)$	$N_A(13)$	$N_A(14)$	$N_A(15)$
0.26491	-0.19269	0.01015	-0.01636	-0.00538	-0.00481	-0.00327	-0.0025	-0.00189	-0.00145	-0.00109	-0.0008	-0.00055	-0.00033	-0.00013
	0.27472	-0.19973	0.01067	-0.01691	-0.00549	-0.00491	-0.0033	-0.0025	-0.00186	-0.00139	-0.00101	-0.00069	-0.0004	-0.00016
		0.28571	-0.20761	0.01128	-0.01751	-0.0056	-0.00501	-0.00332	-0.00248	-0.0018	-0.0012	-0.00087	-0.00051	-0.0002
			0.29814	-0.21649	0.012	-0.01818	-0.00571	-0.00509	-0.00332	-0.00242	-0.00169	-0.00113	-0.00066	-0.00026
				0.31235	-0.2263	0.01287	-0.01893	-0.00579	-0.00516	-0.00327	-0.0023	-0.0015	-0.00087	-0.00034
					0.3288	-0.23834	0.01393	-0.01977	-0.00584	-0.00518	-0.00315	-0.00208	-0.00117	-0.00045
						0.34816	-0.25208	0.01527	-0.02071	-0.00582	-0.00512	-0.00288	-0.00167	-0.00062
							0.37139	-0.2685	0.01704	-0.02176	-0.00565	-0.00488	-0.00234	-0.00094
								0.4	-0.28863	0.01947	-0.02293	-0.00516	-0.00427	-0.00126
									0.43644	-0.31409	0.02308	-0.02416	-0.00393	-0.00298
										0.48507	-0.34778	0.02903	-0.02528	-0.00048
											0.5547	-0.3955	0.04087	-0.02799
												0.66667	-0.47183	0.08217
													0.89443	-0.68328
														1

(Russ, 2005)

Half of the matrix of alpha value is empty because no large circles can be produced by small bubbles. An important assumption to use Cruz-orive matrix is that the shapes of all objectives are spheres. This is not always true in foams, especially in the case of "polyhedral" foam. Berry (2008) analyzed the shape factors of bubbles in the confocal images of protein foams and indicated that bubbles were not perfect spheres. However, the sphere shape assumption has been commonly used in image analysis of foams for obvious simplifications (Magrabi et al., 1999; Polli et al., 2002; Pernell et al., 2002a).

Foam destabilization

As a thermodynamically unstable system, foam will finally develop to two phases allowing enough time. The foam destabilization processes are critical to the quality and shelf life of aerated foods. For example, substituting egg white with whey protein in angel food cakes produced a coarse cake structure due to poor foam stability (Arunepanlop et al., 1996; Berry, 2008). Foam destabilization mechanisms have been broadly discussed (Murray and Ettelaie, 2004; Damodaran, 2005). It is commonly agreed that three primary processes contributing to foam destabilization are creaming, disproportionation, and coalescence (Walstra, 2003).

Creaming

Creaming always happened in foam as the density of gas is much smaller than that of continuous phase. The creaming velocity of gas bubbles in a continuous phase can be described by Stokes law (Equation 9).

$$V = \frac{2r^2(\rho_0 - \rho)}{9\eta_0} g \qquad \text{Equation 9}$$

where r is the radius of bubbles, ρ_0 and ρ are densities of the continuous phase and dispersed phase (gas), g is gravitational constant, η_0 is the viscosity of the continuous phase (Walstra, 2003). However, Stokes' law can only predict the creaming rate of mono-dispersed and non-interacting bubbles with spherical shapes in a continuous phase. This is true for some "dilute" foams, such as carbonated beverages, but rarely valid for polyhedral foams which are composed of a large amount of bubbles and represent the major foam type in food industry (Campbell and Mougeot, 1999). Although creaming occurs in polyhedral foam, it is not the primary destabilization mechanism for such a system.

Disproportionation

Disproportionation, or Ostwald ripening, refers to the diffusion of gas from small bubbles to the large bubbles. Due to the polydispersity of bubbles, the Laplace pressure (Equation 1) in small bubbles is greater than in large bubbles, leading to increased gas solubility. The gas in small bubbles tends to be transferred into large bubbles or released from the foam through dissolving into liquid. The result of this process is that the small bubbles shrink and eventually disappear while large bubbles continuously expand. One way to prevent disproportionation is to create foam composed of uniformly sized bubbles. However, this is hard to achieve in practice. Another way is to select a gas with less solubility in the continuous phase. It's practical but with a lot of limitations. For a shrinking bubble with a surfactant layer, the decrease in bubble size leads to an increase in interfacial

area and the interfacial load of surfactants. This induces further reduction of interfacial tension (γ) and thereby an increase of Laplace pressure, which can prevent the additional shrinking of bubbles. The decreasing extent of γ with bubble shrinkage is dependent on the interfacial dilational elasticity (E'). According to this model, the disproportionation of bubbles can be ceased with a condition of $E'/\gamma > 1/2$ (Dickinson, 1992); while a condition of $E'/\gamma > 2$ is more realistic in practice (Walstra, 2003). Dickinson et al. (2002) observed the shrinkage of single air bubbles beneath a planar air-water interface for four types of proteins. They found that the rates of change of bubble radius for the proteins forming an elastic film were slower than the rates expected from a theoretical model without consideration of interfacial elasticity, fitting to the prediction of a theoretical model involving the contribution of interfacial elasticity. In addition, the bubbles of β-lactoglubulin, which forms a strong and coherent interfacial film, formed residual protein particles and faded slowly at the end of the shrinking process; while the bubbles of other proteins disappeared rapidly. These observations suggested that the interfacial elasticity of protein films can slow the disproportionation of bubbles.

Coalescence

Coalescence in foam is an irreversible merging of two or more bubbles to form a larger single one. When two bubbles come close together, the film between them thins and finally ruptures. One way to stabilized foam against coalescence is to retard film thinning, which corresponds to drainage. Drainage can be counteracted by increasing the continuous phase viscosity (Walstra, 2003) or increasing repulsions between bubbles (Damodaran,

2005). Another way to impede coalescence is to prevent the rupture of thin film through developing a high interfacial elasticity (Wilde, 2000). Protein layers at an interface usually provide resistance to film breakup due to intermolecular cross-links (Murray, 2002). The presence of small molecule surfactants can replace proteins at the interface, greatly impairing film stability (Wilde et al., 2004). The detrimental effect of small lipid-like particles to foam stability can also be explained by film rupture. These particles tend to bridge two neighboring bubbles and promote merging due to their hydrophobicity (Walstra, 2003).

Foam drainage

Foams with a high air phase fraction (ϕ) are described as "polyhedral" or "dry" structures. It takes time to obtain a "dry" foam since the "excess" liquid in the foam film always drains into the Plateau borders (due to a lower pressure), then flows down through thin films and additional Plateau borders (Exerowa and Kruglyakov, 1998). The main driving force for drainage is gravity and suction of the Plateau border (Dickinson, 1992). The drainage process of a single vertical film due to gravity has been modeled in Equation 10:

$$t(\delta) \approx 3\frac{\mu h}{\rho g \delta^2} \qquad \text{Equation 10}$$

where δ and h are thickness and height of the film, ρ and μ are density and dynamic viscosity of the continuous phase, g is gravitational constant, and $t(\delta)$ is the time required for the film to reach a thickness δ (Walstra, 2003). In this equation, the only driving force involved is the gravity of the continuous phase. Consideration of lamella film drainage between two bubbles is only meaningful when the two bubbles get very close. In this situation, the disjoining

pressure between the interfaces of lamella film becomes a dominant resistance and should be involved. If bubble shape is assumed as a hexagon, drainage in a foam can be represented by the thinning of the lamella film between two bubbles (Figure 1).

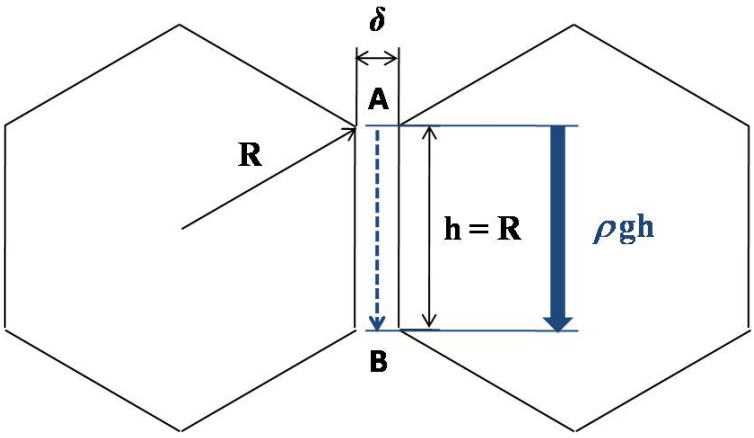

Figure 1. A schematic representation of the film drainage between two bubbles. Bubble shape is assumed as a hexagon. R is the side of the hexagon. h and δ are respectively the height and thickness of the lamella film. Dash blue arrow indicates the flowing direction. Solid blue arrow corresponds to the hydrostatic pressure from A to B (ρgh).

We can assume that one bubble is immobile while the other one is approaching it. The approaching rate can be estimated using Equation 10. After replacing h by R (Figure 1) and the driving force (ρgh) by ΔP, which is the difference between the capillary hydrostatic pressure (P_c) and the disjoining pressure (Π_d) between the interfaces of lamella film, we transformed Equation 10 to:

$$t(\delta) \approx 3\frac{\mu h^2}{(\rho gh)\delta^2} = \frac{3\mu R^2}{\Delta P \delta^2} \qquad \text{Equation 11}$$

Consequently, the approaching rate of two neighboring bubbles can be calculated as:

$$V' = -\frac{d\delta}{dt} = -\frac{1}{dt/d\delta} = -\frac{1}{\left(3\mu R^2/\Delta P\right)(-2)\delta^{-3}} = \frac{\delta^3 \Delta P}{6\mu R^2} \qquad \text{Equation 12}$$

Since the two bubbles are approaching each other, this velocity should be doubled:

$$V = 2V' = \frac{\delta^3 \Delta P}{3\mu R^2} \qquad \text{Equation 13}$$

Damodaran (2005) developed a theoretical model for the drainage rate of film between bubbles (Equation 14):

$$V = \frac{2\delta^3 \Delta P}{3\mu R^2} \qquad \text{Equation 14}$$

where δ is the lamella film thickness, μ is dynamic viscosity, R is the radius of the bubble, and ΔP is the difference between the capillary hydrostatic pressure (P_c) and the disjoining pressure (Π_d) between the interfaces of lamella film. This velocity is twice as the velocity predicted by Equation 13. This is possibly due to the thinning of lamella films on other sides of bubbles also contributes to the approaching of two bubbles (Figure 2).

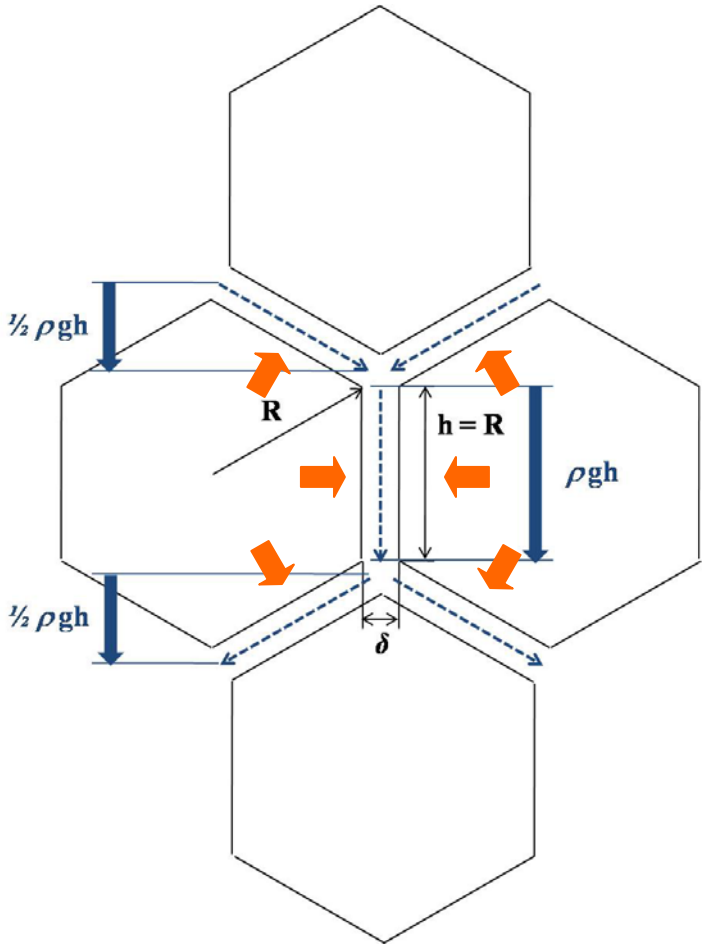

Figure 2. A schematic representation of the film drainage among bubbles. Bubble shape is assumed as a hexagon. R is the side of the hexagon. h and δ are respectively the height and thickness of the lamella film. Dash blue arrows indicate the flowing direction. Solid blue arrows correspond to the hydrostatic pressure for lamella films. Solid orange arrows indicate the moving directions of bubbles due to thinning of lamella films.

In addition, we substitute ρgh, which is the maximum hydrostatic pressure (at point A) in the lamella film between bubbles (Figure 1), with ΔP, which is the average driving pressure for the thinning of the lamella film. This may lead to different predictions of drainage velocity. Nevertheless, the film drainage rate is dependent on continuous phase viscosity (μ), lamella film thickness (δ), bubble radius (R), and the pressure difference (ΔP)

between the capillary hydrostatic pressure (P_c) and the disjoining pressure (Π_d) between the interfaces of lamella film, with a relationship of $V \propto \frac{\delta^3 \Delta P}{\mu R^2}$. This suggests that the high viscosity and low density (low hydrostatic pressure) of continuous phase can retard drainage. The effect of sugar on foam stability has been associated with the increase in solution viscosity (Phillips et al., 1989; Lau and Dickinson, 2005; Raikos et al., 2007). Likewise, longer foam drainage time in foams containing polymerized whey protein isolate are attributed to the higher solution viscosity (Davis and Foegeding, 2004). Power-law and logarithmic functions have been used to fit the relationships between foam drainage ½ life and solution apparent viscosity (Lau and Dickinson, 2005; Foegeding et al., 2006). The drainage rate can also be slowed by thinner lamella film (less h and thereby less mass of liquid) and bigger bubble size (larger R) according to Equation 10. Drainage is unavoidable in food foams because that P_c is always higher than Π_d (Damodaran, 2005). The disjoining pressure Π_d is increased with the development of an osmotic pressure between the lamella fluid and the bulk phase when two bubbles are approaching each other; and therefore reduce foam drainage rate (Damodaran, 2005). Damodaran (2005) suggested that protruding electrolyte chains of the surfactant film can cause a counter ion cloud around the surfaces and promote hydration repulsion forces. Not only osmotic pressure, but also any repulsive effects between bubble surfaces can prevent the approaching of two bubbles and thereby retard drainage. The contributors to the repulsion effect include electrostatic repulsion, solvation forces, and steric forces (Israelachvili, 1991). Alargova et al. (2004) produced extremely stable foams using hydrophobic polymer microrods, in which the bubbles were sterically

stabilized by the dense thick “hairy” layers. In the case of small molecular weight surfactants, the Gibbs-Marangoni effect also contributes to impede foam drainage due to a prevention of bubble approaching (Wilde, 2000). Note that the foam destabilization by coalescence and disproportionation changes bubble radius and the thickness of film between bubbles, thereby altering foam drainage.

Foam drainage can be determined by recording the time required for half mass of the foam to drain (drainage ½ life) (Phillips et al., 1987) or measuring the change of conductivity in the foam using a probe (Kato et al., 1983). The drainage profiles of egg white froth were also measured using a nuclear magnetic resonance imaging (NMRI) method (McCarthy et al., 1990; Stevenson et al., 2007). Measuring foam drainage by mass flow is a simple procedure, in which the foam is fixed and gravitational drainage occurs without any disturbance. The possible experimental errors are the temperature or humidity fluctuations during measurements, which showed no adverse effects to the foaming process within normal laboratory conditions (Phillips et al., 1987). However, it must be remembered that it is likely that disproportionation and coalescence occurs simultaneously during drainage measurements.

Air-water interface

Foam generation is also a process to create large area of air-water interface. Surfactants are known to stabilize the interface by lowering the interfacial tension. Surfactants can be classified into two categories. Small molecule surfactants include emulsifiers, detergents, and lipids, and usually form a compact adsorbed layer with a low

surface tension. Polymers are referred to macromolecule surfactants, such as proteins, and typically form a visco-elastic, irreversibly adsorbed layer (Wilde, 2000). The composition, structure, and properties of the adsorbed layer are of considerable importance for the formation and stability of foams (Dickinson, 1992).

Interfacial tension

It is commonly recognized that a colloidal system tends to minimize its interfacial area between two phases. The interface exerts a tension on its boundaries, which is called interfacial tension or surface tension for air-water interfaces. Interfacial tension for pure water and air is 72.3 mN/m at room temperature (25 °C) (Speight, 2005). Interfacial tension is caused by the difference of intermolecular forces between two phases. Adsorption of surfactants at the interface can reduce the dissimilarities between two phases, and thereby lower the interfacial tension. Under an ideal condition, the chemical potential of the surfactant is equal in the solution and at the interface according to Gibbs (Equation 15):

$$\Gamma = -\frac{\alpha}{RT}\frac{d\gamma}{d\alpha} = -\frac{1}{RT}\frac{d\gamma}{d\ln\alpha} \text{ or } \Gamma = -\frac{C}{RT}\frac{d\gamma}{dC} = -\frac{1}{RT}\frac{d\gamma}{d\ln C} \qquad \text{Equation 15}$$

where R is the gas constant; T is the absolute temperature; Γ is the interface excess concentration of the surfactant (with a unit of mol.m^{-2}); α and C are the respective thermodynamic activity and the bulk concentration of the surfactant in the solution (Walstra, 2003). In a very dilute solution (close to an ideal condition), α and C are approximately equal. This model can be used to describe the adsorption behavior of small molecule surfactants at low concentrations. Adsorption behavior of macromolecules, like proteins, is

difficult to predict because the molar interfacial area change with adsorption conditions (Miller et al., 2001). Nearly all protein adsorption are characterized by extremely non-ideal behavior because of the complex intermolecular interactions and intramolecular rearrangements (Dickinson, 1999; Tronin et al., 1996; Clarkson et al., 1999). At a general level, the extent of protein adsorption is influenced by its surface hydrophobicity and charge (Wilde et al., 2004).

Interfacial tension (γ) can be measured by several devices, such as the Du Nouy Ring and the Wilhelmy plate. Most of these methods are good for static γ measurement but not suitable for measuring dynamic γ changes. A pendant drop goniometer was developed as a useful tool to study the dynamic characteristics of interfaces between fluid phases. The principle of this device is that the shape of a droplet generated from one phases to another is determined by its interfacial force (depend on interfacial tension and area) and gravity (depend on density and volume). With known density of the two phases, the interfacial properties can be analyzed using the geometry information of a sessile or pendant droplet (Evans and Wennerström, 1999). Dynamic measurements can be obtained by recording the images of a droplet continuously via a video camera. The interfacial tension is calculated from the shape parameters for a pendant drop according to Equation 16:

$$\gamma = \frac{\Delta\rho g R_0^2}{\beta} \qquad \text{Equation 16}$$

where $\Delta\rho$ is the mass density difference between the drop and the surrounding medium, g is the gravity constant, R_0 is the radius of curvature at the drop apex (Figure 3) and β is the

shape factor, as defined by this equation. Note that $\Delta\rho$ and β are positive for sessile drops and negative for pendant drops (Hansen, 1993).

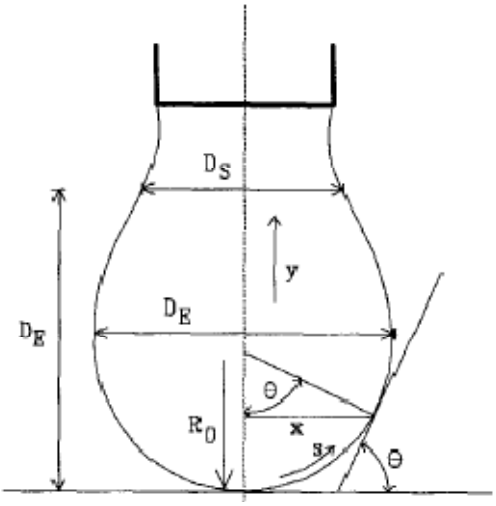

Figure 3. Geometry of a pendant drop with variables. R_0 is the radius of curvature at the drop apex; D_E is the maximum diameter; D_S is the diameter at the distance D_E from the drop apex; the co-ordinates x, y, s and θ are illustrated. (Hansen and Rødsrud, 1991)

"Normal" pendant drops are sufficiently long to measure D_S (Figure 3). The ratio $\sigma=D_S/D_E$ (D_E is the maximum diameter showed in Figure 3) is used to calculate the shape factor β (negative value), according to $\beta = -0.12836 + 0.7577\sigma - 1.7713\sigma^2 + 0.5426\sigma^3$ (Hansen and Rødsrud, 1991). This equation was obtained by using polynomial regression analysis on σ-data produced from numerous theoretical dimensionless profiles (Hansen and Rødsrud, 1991). For the pendant droplets too short to determine D_S, and for all sessile drops, the drop "height", H and the "radius" $R= D_E/2$ (Figure 4) are used to determine interfacial tension according to Equation 17:

$$\gamma = \frac{\Delta\rho g H^2}{B} \approx \frac{\Delta\rho g H^2}{4.308\left[1 - H/R\right]} \qquad \text{Equation 17}$$

where $\Delta\rho$ is the mass density difference between the drop and the surrounding medium, g is the gravity constant, H is the drop "height" (the distance between the maximum diameter D_E and the drop apex) (Figure 4), $R = D_E/2$ is the drop "radius"; B is a transformed shape parameter (Hansen, 1993).

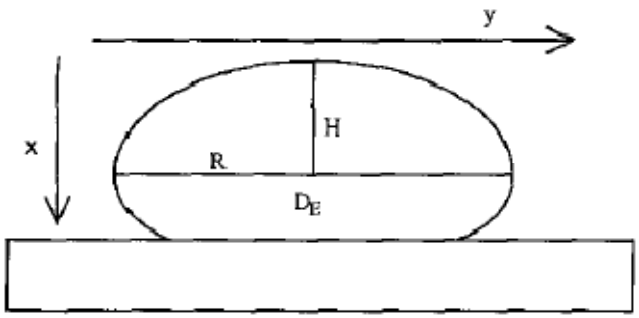

Figure 4. Geometry of a sessile drop with variables. H is the drop "height", the distance between D_E and the drop apex; D_E is the maximum diameter; $R=D_E/2$ is the drop "radius"; the co-ordinates x and y are illustrated. (Hansen, 1993)

The R_0 in Equation 16 is substituted by H in Equation 17. The parameter B may be derived from Equation 16 and Equation 17 as a function of the ratio $\xi = H/R$ (Hansen, 1993). After calculating a large number of theoretical profiles, Hansen (1993) gave an approximate relationship between γ and H/R for drops that do not deviate too much from spherical shape (Equation 17). More precise polynomial approximations of B from ξ were used to calculate γ in the DropImage program (Hansen, 1993). The whole procedure of parameter measurement and calculation is controlled and analyzed using the computer software – DropImage program (Hansen, 1993). The high resolution and excellent accuracy of this method provides a useful tool for studying the dynamic changes of γ and the dynamic properties of the interface.

Interfacial Rheology

Protein molecule can form a continuous film at the interface via intermolecular interactions and impact the structural rigidity to the interface (Dickinson, 1992). In contrast, small molecule surfactants do not cross-link at interface and tend to form a compact adsorbed layer that shows little rigidity (Wild et al., 2004). The adsoption/desorption behaviors of surfactants during the dilation process also cause viscoelastic characteristic of interface (Lucassen-Reynders, 1993). The interfacial rheology gives insight into interactions and changes of molecules at interfaces rather than equilibrium properties and plays an essential role in foam stability and physical properties (Prins, 1992; Lucassen-Reynders, 1993; Fruhner et al., 1999; Murray, 2002; Foegeding et al, 2006).

Various modes of deformation can be applied in interfacial rheology. Two primary types are shearing and dilation/compression. Shearing involves perturbing a two dimensional interfaces in a direction parallel to the interfacial plane. The shape of perturbed interface changes but the area remains constant. Dilation involves changes in interfacial area while maintaining a constant shape. An essential difference between interfacial shearing and dilational rheology is that in the shearing case the surfactant concentration at interface is a constant, whereas in the dilational case the concentration varies as the surface area is enlarged or diminished.

Similar to 3-dimensional bulk rheology, the interfacial shear modulus (E^{SS}) and the apparent interfacial shear viscosity ($\eta_a{}^{SS}$) are defined in a 2-dimensional (2-D) interface by Equation 18:

$$p_{xy} = E^{SS} e_{xy};\ p_{xy} = \eta_a^{SS} \frac{de_{xy}}{dt} \qquad \text{Equation 18}$$

where p_{xy} and e_{xy} are the interfacial shear stress and strain components respectively, t is the time (Dickinson, 1999; Walstra, 2003). Note the units are based on a 2-D system, in forms of $N.m^{-1}$ for interfacial shear modulus and $N.s.m^{-1}$ for interfacial shear viscosity. Most interfacial layers show shear shinning properties, and therefore the apparent interfacial shear viscosity (η_a^{SS}) is determined at a certain shear rate ($\frac{de_{xy}}{dt}$). The interfacial shear viscosity is primarily due to the friction between surfactant molecules. In general, the η_a^{SS} for interfacial films of small molecule surfactants are immeasurably small (about 10^{-5} $N.s.m^{-1}$) compared to that of adsorbed polymers (between 10^{-3} and 1 $N.s.m^{-1}$) (Walstra, 2003). The η_a^{SS} of some protein layers was observed to increase with time and was related to the slow rearrangements of molecular structure and/or the formation of intermolecular bonds. The interfacial shear elasticity is caused by the attractive forces between surfactant molecules, which form a more or less continuous two dimensional network (Dickinson, 1999; Walstra, 2003).

The interfacial dilational properties are directly related to changes in interfacial tension (γ) with interfacial area (A). The interfacial dilational modulus (E^{SD}) and interfacial dilational viscosity (η^{SD}) are defined by Equation 19:

$$E^{SD} = \frac{d\gamma}{d\ln A};\ \eta^{SD} = \frac{\Delta\gamma}{dInA/dt} \qquad \text{Equation 19}$$

where t is for time (Dickinson, 1999; Walstra, 2003). The units for interfacial dilational modulus and interfacial dilataional viscosity are $N.m^{-1}$ and $N.s.m^{-1}$ respectively. An apparent interfacial dilational viscosity can be measured and tends to be strongly strain rate thinning

(Walstra, 2003). For soluble surfactants, the values of E^{SD} are time dependent because exchange of surfactant between interface and bulk occurs during dilation process. In the case of protein layers, the formation of cross-link film further contribute to the interfacial dilational modulus. Generally speaking, rheological parameters of protein films reach maximum values at the isoelectric point, due to an optimization of intra- and intermolecular cohesion (Dickinson, 1992). The interfacial dilational rheology can be influenced by surfactant solubility, surfactant concentration and the time scale of dilational deformation process (Dickinson, 1992; Walstra, 2003).

It turns out that the interfacial dilational modulus (E^{SD}) for many interfaces contain both an elastic component (E') and a viscous component (E'') given by eq. 20:

$$E^{SD} = E^* = E' + iE''; \; E' = |E|\cos(\phi); \; E'' = |E|\sin(\phi) = \omega\eta^{SD} \qquad \text{Equation 20}$$

where $|E|$ is the absolute value of the complex modulus (E^* or E^{SD}) and ϕ is the phase angle (Myrvold and Hansen, 1998). The E' corresponds to the energy recovered in the interfacial perturbation while E'' is related to the energy lost due to relaxations (Lucassen-Reynders, 1993).

Numerous techniques have been developed to study interfacial shear and dilational rheology (Miller et al. 1996). Typically, shear deformation can be achieved by rotating the probe or cup, while the probe is placing at the interface and cup is holding the solution (Gaub and McConnell, 1986; Ghaskadvi et al., 1996; Brooks et al., 1999). Dilational deformations are accomplished by moving the probe at an interface (changing the area of the interface) or oscillating the volume of a droplet (Maru and Wasan, 1979; Kokelaar et al., 1991; Prins, 1992; Murray and Nelson, 1996; Myrvold and Hansen, 1998). The encountered resistance are

monitored by measuring the 2-D stress (interfacial tension) or the 2-D strain (deformation) and used to determine interfacial rheology.

Surfactant plays an important role at the interface and influences the foam characteristics. A common foaming ingredient in food industry is egg white protein, while whey protein isolate shows a comparable foaming capacity (Foegeding et al., 2002).What follows is a general overview of the compositions and foaming functionalities of the two ingredients.

Egg White Protein

Egg white is a traditional ingredient using for foam generation in food industry. Egg white or albumen contains approximately 10.5% (w/w) proteins and can be utilized in liquid or powder forms (Burley and Vadehra, 1989). Spray-dried egg white powder is an ingredient used in food applications; however, the drying process may cause changes in egg white functional properties (Kitabatake et al., 1989; Mine, 1997; Lechevalier et al. 2005; Lechevalier et al. 2007). Physical, chemical, biological and functional properties of egg white will also change during the storage of shell eggs (Reddy and Panda, 1969; Kato et al., 1970; Koehler, 1974; Li-Chan and Nakai, 1989; Schäfer et al., 1999). Changes are depending on temperature, relative humidity and time. The increase of egg albumen pH during storage is attributed to the loss of carbon dioxide through pores in the shell. Thinning of egg white is not clearly explained and postulated to be due to ovomucin, the most viscous protein component (Li-Chan and Nakai, 1989). The functional properties of egg white protein,

namely foaming and gelation, are attributing to a combination of various proteins rather than a single one.

Compositions of egg white protein

The complexity of egg white protein composition has been recognized for a while and not yet fully defined. Li-Chan and Nakai (1989) reviewed extensive studies concerning the biochemistry of egg white protein and described the physicochemical properties of the 13 major proteins (Table 2).

Table 2 Composition and some physicochemical and functional characteristics of proteins in egg white

Protein	Percent of total protein	Molecular weight	Isoelectric point	Carbohydrate moiety	Important characteristics
Ovalbumin	54	45,000	4.5	Yes	Phosphoglycoprotein, foaming and gelling; immunogenic
Ovotransferrin	12-13	77,700	6.0	Yes	Binds iron; antimicrobial
Ovomucoid	11	28,000	4.1	Yes	Trypsin inhibitor
Ovomucin	1.5-3.5	$0.23–8.3\times10^6$	4.5–5.0	Yes	Viscous; role in age-thinning; viral hemagglutination inhibitor
Lysozyme	3.4-3.5	14,300	10.7	No	Lysis of bacterial cell wall; antimicrobial
G2 globulin	4.0 (?)	49,000	5.5	Yes	?
G3 globulin	4.0 (?)	49,000	5.8	Yes	?
Ovoinhibitor	0.1-1.5	49,000	5.1	Yes	Serine proteinase inhibitor; wide spectrum of inhibitory activity
Ovoglycoprotein	0.5-1.0	24,400	3.9	Yes	?
Ovoflavoprotein	0.8	32,000	4.0	Yes	Binds riboflavin
Ovomacroprotein	0.5	$0.76–0.90\times10^6$	4.5–4.7	Yes	Strongly antigenic; high immunological cross-reactivity
Cystatin	0.05	12,700	5.1	No	Thiol proteinase inhibitor
Avidin	0.05	68,300	10.0	Yes	Binds biotin; antimicrobial

Note: ? refers to unknown or uncertain data. (Li-Chan and Nakai, 1989)

With the development of proteomic techniques, many polymorphisms of known proteins and lots of new minor proteins have been identified (Desert et al., 2001; Raikos et al., 2006; Guérin-Dubiard et al., 2006; Mann, 2007). Guérin-Dubiard et al. (2006) reported two new proteins. Tenp is a protein with strong homology with bacterial permeability-increasing protein (BPI); and VMO-1 is an outer layer vitelline membrane. Mann (2007) identified 78 chicken egg white proteins, 54 of which were reported for the first time. However, most of the protein components are polymorphisms and "similar-to" forms of the identified major proteins. For example, Guérin-Dubiard et al. (2006) separated 4 isoforms and 6 polymer forms for ovalbumin as well as 3 spots for a genetic variant of ovalbumin Y and 5 spots for ovalbumin-related Y proteins on 2D electrophoresis gels from egg white protein. These polymorphisms for ovalbumin were identified by mass spectrometry. However, they appeared in different MW ranges on the 2D electrophoresis gels as various phosphorylated forms, polymeric forms and genetic variants. The functional differences among polymorphisms of a protein are unclear. Generally speaking, the studies of egg white protein functionality in food systems have focused on whole egg white protein or mixtures of several major protein components.

Ovalbumin constitutes roughly 54% of the egg white proteins by weight. It can be isolated by crystallization in an ammonium sulfate solution or anion-exchange methods (Johnson and Zabik, 1981b; Vachier et al., 1995; Croguennec et al., 2000; Kosters et al., 2003). The ovalbumin protein of chicken egg white is made up of 385 amino acids, with the complete amino acid sequence being reported by Nisbet et al (1981). Ovalbumin has one solvent-accessible disulfide bridge and four free sulfhydryl groups buried in the interior of

the protein. It is the only egg white protein to contain free sulfhydryl groups likely to enhance sulfhydryl-disulfide interchange reactions (Fothergill and Fothergill, 1970; Lechevalier et al., 2003). During the storage of shell eggs, ovalbumin tends to transform to a more thermostable form, S-ovalbumin, probably by a thioldisulfide exchange reaction (Smith and Back, 1962; 1965; Takahashi et al., 1996; Sugimoto et al., 1999). Alkaline treatment of ovalbumin also promots a change to S-ovalbumin (Arii et al., 1999). Differential scanning calorimetric study showed that the denaturation temperatures were 84.5 °C for ovalbumin and 92.5 °C for S-ovalbumin at pH 9 (Donovan and Mapes, 1976). No difference in amino-acid compositions can be demonstrated between the two forms of ovalbumin. Hydrodynamic analysis showed that S-ovalbumin is more compact, possibly contributing to the superior thermostability (Takahash et al. 2005). The isoelectric point of S-ovalbumin is slightly more acidic than that of ovalbumin according to the isoelectric focusing of egg white protein before and after six-week storage (Schäfer et al., 1999).

The viscous characteristic of egg white is attribution to ovomucin, which is a sulfated glycoprotein with a highly viscous and gel-like nature. Egg white can be regard as a system consisting of ovomucin fibers in an aqueous protein solution, due to the low solubility of ovomucin (Rabouille et al., 1990). Therefore, ovomucin can be precipitated by adding fresh egg white slowly to three volumes of water and standing overnight at 4 °C (Kato A et al., 1985). The molecule weight of soluble ovomucin was reported in a range of $0.23 – 8.3 \times 10^6$ Da depending on various factors, including the method of isolation, pH and ionic strength of the medium and the presence of reducing agents (Table 2). The carbohydrate content and composition were described with some variablility, with a possible total carbohydrate content

of 33% (Li-Chan and Nakai, 1989). Three subunits of ovomucin, α_1-, α_2-, and β-ovomucin, are known to differ in molecular mass, solubility, carbohydrate content and composition (Itoh et al., 1987; Robinson and Monsey, 1975; Hayakawa et al. 1983; Watanabe et al., 2004). The thinning (viscosity decrease) of egg white has been attributed to differences in relative amounts of α- and β-ovomucin in thick and thin egg white, dissociation of ovomucin-lysozyme complex, changes in pH and disulfide bonds as well as degradation of carbonhydrate moieties of ovomucin (Li-Chan and Nakai, 1989).

Three globulins, G1, G2, and G3 were firstly identified from egg white by Longsworth et al. (1940). The G1 globulin was later identified as lysozyme, which is a relatively small protein in egg white with a molecular weight of 14.3 kDa (Table 2). Lysozyme with a basic isoelectric point of pH 10.7 is positively charged at a neutral pH and has the potential to form complex with other negatively charged proteins through electrostatic interactions. G_2 and G_3 globulins are two genetic variations and each comprises about 4% of the egg white proteins (Li-Chan and Nakai, 1989). The molecular weights of G_2 and G_3 globulins were roughly estimated as 49 kDa from SDS-disc gel electrophoresis (Table 2). Guérin-Dubiard et al. (2006) did not detected G2 and G3 globulin on 2D electrophoresis gels and suggested they were corresponding to the spots of two isoforms of ovalbumin gene-related proteins.

Ovotransferrin or conalbumin accounts for roughly 12% of the egg white proteins. It has a large size with a molecular weight of 77.7 kDa and a close to neutral isoelectric point of 6.0 (Table 2). The biological functions of ovotransferrin have been identified as inhibiting

bacteria growth and binding ferric ions (Alderton et al., 1946; Li-Chan and Nakai, 1989; Jeffrey et al., 1998).

Ovomucoid is a glycoprotein and constitutes around 10% of the egg white proteins. The carbohydrate moieties in ovomucoid are attached at asparaginyl residues and represent up to 25-30% of the molecular weight (Yamashita et al., 1982). Ovomucoid has a molecular weight of 28 kDa and an isoelectric point of 4.1 (Table 2). It is the dominant allergenic protein in hen's egg (Cooke and Sampson, 1997).

Other protein components are of minor concentrations in egg white proteins and are rarely considered for functional applications in food industry.

Egg white protein in wet foams and dry foams, and at interfaces

The functional properties of egg white proteins have been studied extensively and reviewed by several publications (Li-Chan and Nakai, 1989; Dickinson, 1992; Mine, 1995; Campbell et al., 2003; Li et al., 2004). Egg white is well known for its excellent foaming properties and has been traditionally used as a whipping agent in food products. In addition to a high foaming capacity, egg white is known for foam stability when subjected to heating. Formation of a very stiff foam texture is also critical for many applications of egg white foams. To elucidate the principles behind these properties, many studies were conducted on egg white foaming and interfacial behaviors.

Nakamura (1963) reported the foaming power of egg white proteins decreased in the order of: ovomucin, globulin, ovotransferrin, ovalbumin, ovomucoid, and lysozyme. However, a different importance order was given by Johnson and Zabik (1981b) as: globulin,

ovalbumin, ovotransferrin, lysozyme, ovomucoid and ovomucin. Controversial results on the foamability of ovomucin are possibly due to the composition variation of this fraction from different purification processes. Ovomucin showed no foaming capacity because of an extremely high viscosity (Johnson and Zabik, 1981b). It may stabilize foam because its long protein strands linked with polysaccharides, which can prevent water drainage in foam (Kato et al., 1978). Kato et al. (1985) studied the functional and structural properties for three types of (soluble, sonicated, and reduced) ovomucins, and suggested that the foaming properties of ovomucins were dependent upon viscosity. Likewise, thick egg white showed superior foam stability than thin egg white due to a higher viscosity (Hammershøj et al., 2008). Therefore, different compositions of ovomucin fractions may exhibit dissimilar foaming capacity, leading to controversial conclusions. Not much difference was observed among the foaming capacities of ovalbumin, ovotransferrin, and lysozyme, which were all far less than that of globulin and egg white control (Johnson and Zabik, 1981b). Nakamura (1963) suggested that protein foamability is related to their denaturation at an interface. The proteins which are easily interfacial denatured can form a well-developed network, promoting foam generation. The disulfide bonds contribute to the structural rigidity of lysozyme and ovomucoid, and thereby restrict their unfolding and denaturation at an interface, resulting in low foaming powers. Although lysozyme showed poor foamability alone, it may interact with other components, especially ovomucin, enhancing foam stability and leading to larger cake volumes (Johnson and Zabik, 1981a, 1981b; Dickinson, 1992). However, the formation of lysozyme-ovomucin complex reduces foaming capacity of the solutions (Johnson and Zabik, 1981a, 1981b). The better foamability of older eggs than fresh ones is also due to the

dissociation of lysozyme-ovomucin complex during storage (Ternes, 2001; Hammershøj and Qvist, 2001). Addition of lysozyme has been observed to improve the foamability and foam stability for other acidic food proteins, particularly strong for globular proteins β-lactoglobulin and bovine serum albumin (Phillips et al., 1989; Dickinson, 1992). The substantial reduction in foam stability with addition of electrolyte demonstrated that the lysozyme enhancing effects of protein foam stability was because of the electrostatic interactions (Dickinson, 1992). A study on competitive adsorption of EWP at air-water interface showed lysozyme will not adsorb at the interface at high ionic strength solvent, however, it adsorbed along with other egg white proteins at low ionic strength, possible through electrostatic interactions (Damodaran et al., 1998). Mine et al. (1991) found that the emulsifying activity of ovalbumin was higher in the acidic pH region than in the neutral pH, corresponding to the greater surface hydrophobicity and flexibility of molecules. MacDonnell et al. (1954) determined constant cysteine values before (pre-foam solutions) and after foaming (drip solutions) during several rewhipping process, suggesting no net change in free sulfhydryl groups in ovalbumin through the repeated whipping. Kitabatake and Doi (1987) detected a molecular confirmation change in ovalbumin after adsorbing at an air-water interface. They suggested that the conformation change exposed interior sulfhydryl residues that interacted with each other forming disulfide bridges at the interface, enhancing the foam stability. Lechevalier et al. (2003) investigated the structural modifications of protein molecules at air-water interface and confirmed the formation of insoluble polymers of ovalbumin through intermolecular disulfide bonds.

Johnson and Zabik (1981a, 1981b) found that the globulin alone exhibited good foaming properties and produced a large cake with excellent texture, while its combinations with ovomucin resulted in reduced cake volume. Good foamability of globulin and ovomucin mixture was reported by MacDonnell et al. (1954). The globulin and ovomucin mixture can make an excellent angel food cake batter; however the batter rises normally but then collapses on baking. Addition of ovalbumin into this mixture can result in a normal cake volume, indicating ovalbumin is critical for the structure formation during heating (MacDonnell et al., 1954). Ovalbumin alone can generate no less cake volume than egg white if given a long whipping time; but the cake structure is coarser (MacDonnell et al., 1954; Johnson and Zabik, 1981b). Ternes (2001) indicated that ovalbumin is responsible for the rough texture of egg white protein foams while globulins provide the stability of fine bubbles.

In general, globulins and ovalbumin are major contributors to EWP foamability, foam stability and foamy structure formation during baking. Ovomucin adds viscosity of pre-foam solutions and can reduce the foamability but prevent foam drainage. Lysozyme may form complexes with other proteins, especially ovomucin, through electrostatic interactions, and thereby contribute to the film strength and foam stability.

The foaming properties of egg white protein are influenced by various factors, such as protein concentration, pH, ionic strength, co-solutes, whipping time and egg source (Dickinson, 1992; Hammershøj et al., 1999; Pernell et al., 2002a; Hammershøj et al.; 2006), and therefore can be optimized at a certain condition. Numerous modifications of protein molecules have also been applied to improve the foaming behavior of egg white protein,

including pre-heat treatment, forming protein-carbohydrate conjugates and enzymatic hydrolysis (Handa and Kuroda, 1998; Hagolle et al., 1998; Aoki et al., 1999; Relkin et al., 1999; Hagolle et al., 2000; Campbell et al., 2003; Baron et al., 2003; Croguennec et al., 2007; Hammershøj et al., 2008). The enhancing effect of copper on stability of egg white foams has been noted for a while. It's recommended to beat egg white in a copper vessel in order to obtain a better foam. The hypothetical principle for this effect is the formation copper-conalbumin-complex, which denatures at the air-water interface easier than the iron-conalbumin-complex (Ternes, 2001). The mild pre-heat treatment of ovalbumin caused a decrease of the secondary structures at neutral pH, and thereby enhanced foaming functionality by increasing molecular flexibility and surface hydrophobicity (Relkin et al., 1999; Hagolle et al., 1998). However, treatment at high temperature range (>60 °C) promoted formation of ovalbumin aggregates, leading to decreased interfacial activity (Hagolle et al., 1998). Covalently linking a carbohydrate moiety to a protein has been observed to improve the functionality of egg white proteins, possibly due to the enhanced amphiphilic characteristics (Mine, 1995; Campbell et al., 2003). Hammershøj et al. (2008) hydrolyzed ovomucin using four types of proteinases, and found an optimum foam capacity at DH of 15–40% but no significant changes of foam stability. The enhanced foaming power of ovomucin after enzyme hydrolysis was correlated with a fast initial adsorption rate at interface, due to the small molecular size or modified surface hydrophobicity of the hydrolysates. Modifications of functional properties of egg white protein are associated with the molecular structure changes induced by each treatment. Exploring the mechanisms

involved in the structure-function relationship would enable us to develop novel protein ingredients from other sources, such as whey protein products.

Whey and Whey Protein Isolate

Whey refers to the remaining liquid after enzymatic (sweet whey) or isoelectric (acid whey) precipitation of casein from milk. It is a dilute solution of lactose, proteins, inorganic salts, vitamins and several constituents at trace levels (Fox 2003). The protein content in whey is approximately 0.6% and can be further increased by removing other fractions (Foegeding et al. 2002). Separation technologies include ultrafiltration, microfiltration and ion exchange (Varnam and Sutberland, 2001; Fox, 2003). Two major whey protein-enriched products are whey protein concentrates (25-80% protein) and whey protein isolates (>90% protein). The high nutritional value and functional properties, including gelling, emulsifying and foaming properties allow for a wide utilization of whey protein ingredients in food products (Swaisgood, 1982; Kinsella and Whitehead, 1989; Wong et al., 1996; Swaisgood, 1996; Foegeding et al., 2002; Fox, 2003; Kilara and Vaghela, 2004).

Composition of whey protein isolate

The main proteins in bovine whey are β-lactoglobulins (~50%), α-lactoalbumins (~25%), proteose-peptone (partly derived from hydrolysis of β-casein), serum albumin, and immunoglobulins (Swaisgood, 1982). β-lactoglobulin is the major whey protein and was isolated and crystallized from milk by Palmer (1934). It was initially called "β-lactalbumin" but later renamed "β-lactoglobulin". On one hand, it behaves like an albumin in that it is

soluble in half-saturated $(NH_4)_2SO_4$ or saturated $MgSO_4$. On the other hand, it shows some characteristics of globulins in that it is insoluble in pure water at the isoelectric point (pH 5.2) but can be dissolved in dilute salt solutions (Fox, 2003). The solubility of β-lactoglobulin in sodium sulphate, ammonium sulphate, and trichloroacetic acid solution at low pH has been used to isolate this protein (Swaisgood, 1982).

More than 20 genetic variants of β-lactoglobulins were identified in ruminant species; while more distinct genes appear in other mammals (Sawyer, 2003). β-lactoglobulins A and B are the most predominant and occur at nearly equal frequencies, while the other variants are very rare. β-lactoglobulins A and B differ by two amino acids, where the Asp_{64} and Val_{118} in variant A were replaced by Gly_{64} and Ala_{118} in variant B, and exhibit minor changes in structural characteristics (Qin et al., 1999). The monomer of β-lactoglobulin consists of 162 amino acids, including two disulphides (Cys_{66}-Cys_{160} and Cys_{106}-Cys_{119}) and one free thiol group (Cys_{121}) that becomes reactive at pH values above ~7.5 (Uhrinova et al., 2000; Tanford et al., 1959). It has a MW of approximately 18.3 kDa (18367 Da for cow variant A and 18281 Da for cow variant B calculated from the amino acid sequences using PIR software (http://pir.georgetown.edu/pirwww/search/comp_mw.shtml)) (Sawyer, 2003).

The monomer of β-lactoglobulin has a very compact globular structure and exists almost as a sphere about 3.6 nm in diameter (Figure 5).

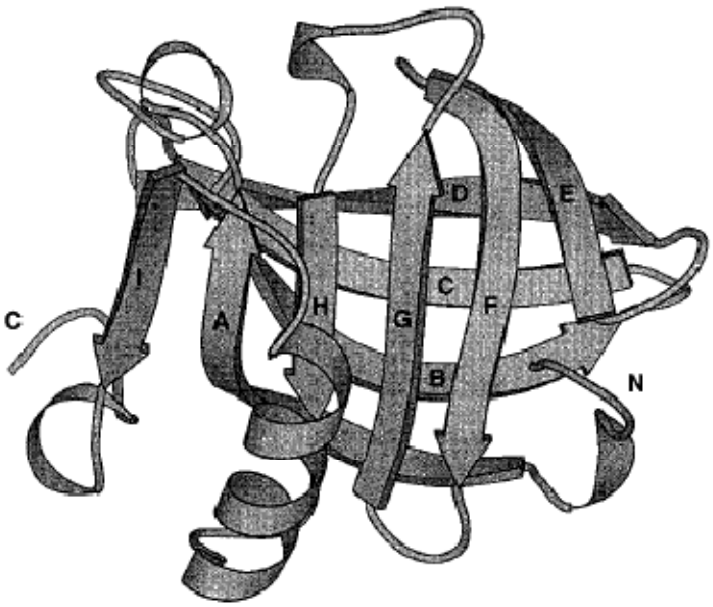

Figure 5. A schematic representation of the arrangement of secondary structure elements (residue 6 – 160) in β-lactoglobulin monomer. A-I are nine strands of anit-parallel β-sheets. The α-helix is between strands H and I. (Uhrinova et al., 2000)

This monomer consists of nine strands of anti-parallel β-sheet, eight of which (stands A-H in Figure 5) create an inside barrel. The stand I exists on the outside, so is able to form part of the dimer interface. β-lactoglobulin forms dimers of two monomeric subunits between pH 5.5 and 7.5 through non-covalent interactions. When < pH 3.5 and > pH 7.5, the dimer dissociates to monomers as the charge density increased. Between pH 3.5 and 5.2, β-lactoglobulin A can form octamers of MW of ~ 144 kDa while the β-lactoglobulin B variant octamerizes to a much smaller extent (Walstra and Jenness, 1984). During denaturation, bovine β-lactoglobulin undergoes an initial dissociation of dimer to monomer followed by a change in conformation, and subsequent aggregation. Early work indicates that dimer dissociation occurs between 30 and 55°C (Sawyer, 1969). At higher temperature, the molecules unfold with increased thiol reactivity (Larson and Jenness, 1952). Dimer

dissociation followed by monomer unfolding permit high sulphydryl reactivity that can lead to disulphide interchange and aggregation (Sawyer, 2003). After unfolding, the previous buried hydrophobic regions are also exposed and promote the hydrophobic interactions and aggregation. Heat denaturation of β-lactoglobulin, as monitored by differential scanning calorimetry, depends upon pH, ionic strength and protein concentration (de Wit and Klarenbeek, 1981). The presence of sugars showed a stabilizing effect on heat denaturation of β-lactoglobulin (Park and Lund, 1984; Boye and Alli, 2000; Anema et al., 2006).

α-lactalbumin is the second most prevalent protein in whey, with a MW of 14186 Da calculated from the amino acid sequences of bovine α-lactalbumin using PIR software (http://pir.georgetown.edu/pirwww/search/comp_mw.shtml) and an isoelectric point of ~pH 4.8 (Brew, 2003). It is a regulatory protein of the lactose synthase enzyme system, which catalyzes and regulates the biological synthesis of lactose (Brew, 2003). α-lactalbumin and lysozyme share many structural similarities. Not only 54 out of a total of 123 residues in α-lactalbumin primary structure are identical to lysozyme, but also the four disulphide bonds have similar locations in the main chain (Swaisgood, 1982; Walstra and Jenness, 1984; Brew, 2003). α-lactalbumin contains 4 intramolecular disulphide bonds and no free sulphydryl groups. Heat denaturation temperature of α-lactalbumin is 63.7 °C at neutral pH (McGuffey et al., 2005). Heat denaturation and disulfate aggregation at temperatures of 75, 80, 85 °C of α-lactalbumin were described as first order reactions, being unaffected by protein concentration (Anema, 2001). The presence of sugars stabilizes α-lactalbumin against thermal denaturation (Boye and Alli, 2000; Anema et al., 2006).

Normal bovine whey contains a small amount of bovine serum albumin (0.3-1.0% of total N). It has a molecular weight of 69323 Da calculated from the amino acid sequence in GenBank (accession number NP_851335) using PIR software (http://pir.georgetown.edu/pirwww/search/comp_mw.shtml) and an isoelectric point of pH 4.7~4.9 (Suttiprasit et al., 1992). Bovine serium albumin is composed of 582 amino acids, with 17 disulphide bonds and 1 free sulfhydryl group (Fox, 2003). This globular protein has an elliptical shape (Fox and McSweeney, 1998).

Other protein components in whey include proteose-peptone, immunoglobulins and serum albumin. They have relatively low concentrations and are seldom considered for the overall functionality of whey protein ingredients. However, the existence and variation of these components should be awarded when comparing the functional properties of whey protein ingredients from different sources.

Foaming and interfacial properties of whey protein isolate

Whey protein ingredients are utilized in many food products, providing the functional properties like gelation, emulsifying, and foaming (Foegeding et al., 2002). The comparable foaming power of whey protein isolate to egg white protein has been recognized; however, the yield stress and stability of whey protein isolate foams were quite lower (Pernell et al., 2002a; Davis and Foegeding, 2007). Additionally, longer whipping time and higher protein concentration are required for whey protein isolate to establish the foam stiffness (measurable yield stress) (Pernell et al., 2002a). The foaming capacity of whey protein isolate is mainly attributed to β-lactoglobulin (Kim et al., 1987). Luck et al. (2001) varied the ratio

of β-lactoglobulin/α-lactalbumin in protein foams and found overrun linearly increased with the percentage of β-lactoglobulin. The foam generated from α-lactalbumin only exhibited half overrun as that from β-lactoglobulin at the same concentration of 15% (w/w). The foam yield stress of β-lactoglobulin/α-lactalbumin mixtures showed a similar result as overrun, with a linear correlation between foam yield stress (τ_0) and the cube root of the air phase volume ($\phi^{1/3}$) (Equation 5). Linear relationships between τ_0 and $\phi^{1/3}$ were also observed on whey protein isolate (WPI) and egg white protein (EWP) by varying the protein concentration and whipping time (Pernell et al., 2002a). However, a higher slope was observed for EWP than WPI, corresponding to a greater combined variables of $\gamma/R_{32}Y(\phi)$ (Equation 5). Pernell et al. (2002a) observed the microstructures of WPI and EWP foams using confocal imaging and indicated a smaller bubble size (R_{32}) of EWP. They indicated that the experimentally derived fitted parameter $Y(\phi)$ was positively correlated with ϕ, which for WPI foams conformed to the general trend observed on emulsions while which for EWP foams showed a more rapid increase at lower ϕ range (Princen and Kiss, 1989). The dependence of foam yield stress to bubble size was further demonstrated by Berry (2008). She established positive linear relationships between foam yield stress and total interfacial area of bubbles for WPI and EWP-WPI mixtures. However, EWP showed a different characteristic from those of WPI and EWP-WPI mixtures. The unique behavior of EWP regarding foam yield stress has been suggested to be due to some connections between proteins at interface and protein in the lamellae (Pernell et al., 2002a).

Luck et al. (2001) found that the addition of $CaCl_2$ was able to enhance the foam overrun and yield stress of β-lactoglobulin and α-lactalbumin, and suggested it was due to

changes of rheological properties of the interfacial protein film or protein aggregation or network formation in the lamella. Davis et al. (2004) estabilished a positive correlation between foam yield stress (τ_0) and interfacial dilational elastic modulus (E') for whey protein isolate and β-lactoglobulin foams over a range of pH levels and salt concentrations, suggesting that the various effects from electrostatic forces on protein foams can be explained by the interfacial rheology. They also indicated that the presence of α-lactalbumin in WPI may weaken interfacial elasticity, and thereby cause lower foam yield stress as reported by Luck et al. (2001). The postive relationship between τ_0 and E' was also confirmed for polymerized WPI and hydrolysates from β-lactoglobulin (Davis and Foegeding, 2004, Davis et al. 2005). Foegeding et al. (2006) suggested that the interfacial tension (γ) in Equation 5 can be replaced by interfacial rheology (E') when applying this model in protein foams. Berry (2008) developed the correlations between τ_0 and E' in the same way as those between τ_0 and γ for WPI and EWP mixtures, and established two types of linear relationships respectively. However, the relationships did not hold across the protein types since the EWP exhibited much higher foam yield stress at the same E' range (Davis and Foegeding, 2007; Berry, 2008).

Whey protein isolate foams have lower stability (drainage time) than egg white protein foams and are unable to form a batter that can produce an angel food cake (Richert, 1979; Arunepanlop et al., 1996; Pernell et al., 2002b; Davis and Foegeding, 2007; Berry, 2008). Heat polymerization of whey protein isolate can retard foam drainage by increasing the continuous phase viscosity and increase cake volume (Pernell et al., 2002b; Davis and Foegeding, 2004). Davis and Foegeding (2007) suggested the longer foam drainage ½ life of

EWP is due to a higher foam yield stress in comparison to WPI, which is corresponding to smaller bubbles. This is in agreement with the smaller bubble size of EWP than WPI observed by Pernell et al. (2002a) and Berry (2008). Substituting egg white protein with whey protein isolate in angel food cakes results in lower volume and coarser cake structure (DeVilbiss et al., 1974; Mohamed et al., 1995; Arunepanlop et al., 1996; Pernell et al., 2002b; Berry, 2008). Pernell et al. (2002b) measured the cake height changes during baking and found that cakes containing whey proteins had a poor ability to prevent collapse once starch gelatinization started. The angel food cake batter of EWP is more elastic than WPI at high temperature, preventing the collapse of the cake matrix. Up to 25% of the EWP can be substituted by WPI without adversely affecting cake volume; however, a 75%EWP/25%WPI cake has a coarser structure with a predomination of larger air cells, differing from the fine structured matrix of 100% EWP cake (Arunepanlop et al., 1996; Berry, 2008). Addition of xanthan gum improved the volume and air dispersion in 75%EWP/25%WPI cakes, but not to the extent of 100% EWP cakes (Arunepanlop et al., 1996; Pernell et al., 2002b). The poor functional performance of WPI in angel food cakes revealed its inability to prevent the overexpansion and/or destabilization changes of bubbles during baking. Berry (2008) observed the changes of cake batters during heating and found that some destabilization changes occurred in cake batters containing WPI even before heating. They suggested that the addition of cake flour and powdered sugar along with the action of folding dry ingredients into the protein foams may increase the instability of WPI foam but do not generate adverse effect on EWP foam.

The foaming properties of whey proteins can be modified by heat polymerization, high pressure treatment, glycated with sugars and enzyme hydrolysis (Zhu and Damodaran, 1994; Chevalier et al., 2001; Foegeding et al., 2002; Kilara and Panyam, 2003; Davis and Foegeding, 2004; Davis and Foegeding, 2005; Bouaouina et al., 2006; Tosi et al., 2007; Lim et al., 2008). Mild heat treatments can promote the formation of WPI polymers via sulfhydryl-disulfide interexchange reactions, and thereby enhance foam stability by increasing continuous phase viscosity (Zhu and Damodaran, 1994). Davis and Foegeding (2004) found the mixtures of native WP and polymerized WPI showed higher foam yield stress than native WPI, corresponding to a greater interfacial elasticity. They suggested that polymerized WPI coadsorbed with native WPI and contributed to the interfacial rheology.

Dynamic high pressure treatment can dissociate large protein aggregation without alternation of protein confirmation, leading to exposure buried hydrophobic groups with no loss of solubility (Bouaouina et al., 2006; Lim et al., 2008). The high pressure treated proteins can interact with each other through exposed hydrophobic groups, enhancing the viscoelasticity of the adsorbed film and the foam stability (Bouaouina et al., 2006). Chevalier et al. (2001) obtained β-lactoglobulin glycated with six types of sugars through Maillard reactions and revealed the best foam stability of β-lactoglobulin glycated with glucose or galactose as determined by a conductivity method. The drainage ½ life values of β-lactoglobulins glycated with six sugars were all longer than native β-lactoglobulin. The conjugation of a sugar moiety may support the liquid retention in the foam.

Higher foam overruns and yield stress values were observed on whey proteins after enzyme hydrolysis (Luck et al., 2001; Davis and Foegeding 2005). This corresponds to a

more rapid interfacial adsorption rate and higher interfacial elasticity for β-lactoglobulin after hydrolysis (Davis and Foegeding, 2005). Enzyme hydrolysis decreases molecular size and changes the surface hydrophobicity, promoting the interfacial adsorption and the viscoelastic film formation.

Protein/Sugar interactions in solution, foam and at interface

Two common and important ingredients often found in aerated food products are protein and sugar. Proteins play an important role as macromolecular surfactants. During the foaming process, the proteins rapidly adsorb at the newly formed air-water interfaces and lower the interfacial tension. Immediately after and during the initial adsorption, the adsorbed proteins partially unfold and form a viscoelastic layer, further promoting foam stability (Dickinson, 1999; Wilde, 2000). The interfacial functionality of proteins is determined by their structure and interactions in the adsorbed layer (Damodaran, 2005). In many foam applications, it is suggested to add sugar slowly along with the continued beating after the protein solution has been beaten into a stable foam (Dickinson, 1992). Sugar is mainly to increase the continuous phase viscosity, and therefore to prevent drainage of liquid. If it's added too early, the high viscosity of the continuous phase may reduce the foam overrun. The presence of sugar can also directly affect the thermodynamic and functional properties of protein molecules, especially the adsorption and aggregation behaviors (McClements, 2002; Semenova et al., 2002; Guzey et al., 2003; Lau and Dickinson, 2005; Raikos et al., 2007; Davis and Foegeding, 2007; Herceg et al. 2007).

The presence of sugar can influence protein behaviors in bulk solutions. The stabilizing effect of sugar on heat denaturation of proteins has been revealed in many studies (Back et al., 1979; Lee and Timasheff, 1981; Anema, 2006). Sucrose and glycerol can strengthen the pair-wise hydrophobic interaction between hydrophobic groups for proteins (Back et al., 1979). The preferential hydration of proteins with solvent was enhanced with incorporations of lactose, glucose or several neutral osmolytes (Lee and Timasheff, 1981; Arakawa and Timasheff, 1982; Arakawa and Timasheff, 1985; Wilde et al., 1997). Therefore, addition of sugars stabilizes protein structure and promotes more compact molecular conformation, facilitating the diffusion of proteins as their size is smaller. However, the bulk phase viscosity is increased with sugar addition, causing a contradicted retarding effect on protein molecular diffusion.

Many studies have focused on the influence of sugars on the air-water interfacial characteristics of globular proteins, i.e. adsorption kinetics, interfacial activity, and interfacial rheology. The increase of interfacial adsorption rate of bovine serium albumin (BSA) with addition of sucrose (<1M) was suggested due to a fast diffusion rate of the compact protein molecules in the presence of sucrose (Rodríguez Patino and Niño, 1995; Niño et al., 2002). It has also been speculated that the addition of sucrose may reduce protein aggregation, allowing more protein to be involved in film formation at interfaces (Wilde et al., 1997). However, the interfacial adsorption rate of BSA shows the opposite trend of decreasing when the sucrose concentration is above 1M, due to the high solution viscosity impeding molecule diffusion (Niño et al., 1997). Complicated effects of sucrose on the interfacial adsorption behavior of soy proteins were also observed by Ruíz-Henestrosa et al. (2008). Ovalbumin

was found to adsorb less rapidly at the air-water interface due to the increase of protein surface hydrophilicity in the presence of sucrose (Antipova et al., 1999). In the case of sodium caseinate, the presence of sugar causes a dissociation of casein aggregates and increases protein hydrophobicity (Antipova et al., 1999). Guzey et al. (2003) studied the interfacial adsorption rate of BSA and attributed the sugar effects to three aspects: 1) an increase in solution viscosity; 2) a decrease in hydrophobicity of protein surfaces due to direct preferential interactions with sugars; 3) an increased hydrophilicity of protein surfaces due to preferential hydration. Note that sugar can alter the interfacial tension of water by itself. The sugar type and concentration, protein concentration, the presence of other solutes and pH also influence the adsorption kinetics of protein at interface.

Niño et al. (1997) found the air-water interfacial viscoelasticity of BSA decreased with increasing sucrose concentration, suggesting reduced protein-protein interactions in the adsorbed layer. Davis and Foegeding (2007) indicated that the presence of sucrose has an enhancing effect on the interfacial dilational elasticity for EWP and a reducing effect for WPI; however, sucrose can promote the interfacial elasticity for β-lactoglobuin and ovalbumin. The reason for the dissimilarity of the sucrose effect on the interfacial rheology of WPI and β-lactoglobuin is not clear. Addition of sucrose into the aqueous phase also generates complex effects on the interfacial elasticity of soy proteins (Ruíz-Henestrosa et al., 2008). The presence of sucrose can alter the molecular surface amphiphilic characteristics due to changes of the molecular conformation and aggregation in solution and/or influence the protein unfolding and interactions at the interface, modifying the interfacial rheology.

Furthermore, the effect of sucrose on interfacial dilational viscoelasticity can also be attributed to the adsorption/desorption behaviors of proteins.

Addition of sugars usually caused a decrease in foam overrun and an increase in foam stability, mainly attributed to the enhanced solution viscosity (Haggett, 1976; Phillips et al., 1989; Yankov and Panchev, 1996; McClements, 2002; Herceg et al., 2007). A straight-line plot was established between foam drainage ½ life and solution apparent viscosity on a log-log scale for egg white protein with addition of different amounts of sugar (Lau and Dickinson, 2005). Sugar was found to delay egg white foam formation, again attributing to an increase in viscosity (Lau and Dickinson, 2004; Lau and Dickinson, 2005; Raikos et al., 2007). Dynamic image analysis of egg white foam microstructure indicated that the destabilization changes mainly involved creaming of large bubbles and disproportionation of neighbor bubbles, which were accelerated after reducing sugar content (Lau and Dickinson, 2005). Raikos et al. (2007) indicated that the bubble size of egg white foams reduced with sugar addition, corresponding to a decrease of foam overrun; while the incorporation of salt can further reduce the bubble size and enhance overrun. Ruíz-Henestrosa et al. (2008) established positive correlations between foam drainage ½ life and interfacial dilational elasticity for soy proteins, suggesting that the modification of interfacial viscoelasticity induced by sugar may influence the foam stability. Davis and Foegeding (2007) found that sucrose (25% w/w) increased the foam yield stress and drainage resistance for egg white protein whereas it minimally affected these properties for whey protein isolate, possibly due to its opposite effects (positive on egg white protein and negative on whey protein isolate) on the interfacial rheology. So far only a few relationships have been established between foam

stability and interfacial dilational elasticity for protein foams in the presence of sucrose. This is one of the primary goals of the study presented in chapter 2.

As a major ingredient in angel food cakes, sugar plays an important role as a bulking agent. Due to the increasing demands for low-calories foods, the replacements of sugar with other polyols, oligosaccharides or polysaccharides were investigated in cakes (Attia, 1993; Pateras et al., 1994; Baeva et al., 2000; Ronda et al., 2005). Although similar qualities can be reproduced using other types of sweeteners or bulking agents, it's believed that the overall contributions of sucrose to the products are irreplaceable. Pateras (1994) observed the microstructure of cake batter and found that replacing sucrose by polydextrose increases the mean bubble size and introduces a large variance into the initial bubble size distribution, causing a faster bubble expansion during heating. Pernell et al. (2002b) indicated that sucrose increases the protein denaturation temperature and may influence the cake matrix formation. Egg white protein showed a higher denaturation temperature than whey protein isolate in the presence of sugar, possibly contributing to the stability of bubbles in cake batters during baking. Berry (2008) found that the network formation of egg white protein foam occurs at a lower temperature than that of whey protein isolate foam in the presence of sugar. The foam network formation temperature (45 °C) of egg white protein is much lower than its denaturation temperature (85 °C) in a protein-sugar solution, postulated to be due to the partial denaturation of proteins at the interface (Berry, 2008). She also suggested that the incorporation of powdered sugar and flour introducing destabilizing effect on angel food cake batters containing whey protein isolate, while causing no detrimental effects to cake batter of egg white protein (Berry, 2008).

Impetus for further study

The comparable foaming power of whey protein isolate provides a prospective possibility to replace egg white protein in aerated food products. However, the lack of foam stability of whey protein isolate was observed either at room temperature or during heating, resulting in a coarser cake structure and lower cake volume in angel food cakes. The sugar effects on the interfacial rheology and foam stability (drainage and microstructure) suggest that one functional difference between whey and egg white proteins is how they interact with sucrose. Accordingly, the major goal of this study is to investigate the mechanisms responsible for the sucrose effect on foaming and interfacial behaviors of whey and egg white proteins, and therefore to facilitate the application of whey protein ingredients in food products.

A review of previous literatures indicates that sucrose generates complicated effects on protein behaviors in foams and at air-water interface. However, few investigations were conducted to explore the sucrose effect on the foaming and interfacial characteristics as well as the foam functionality in cakes simultaneously. A second goal of this study is to develop correlations among various properties, including foam rheology, foam stability, interfacial rheology, foam microstructure and solution viscosity, via varying the sucrose concentration in protein solutions. The establishment of relationships among foam, interface, and bulk phase, leads to further developments of existing models.

Last but not least, this study investigates the contributions of individual proteins to the interfacial properties of the mixtures, complimenting the previous observations on the interfacing properties of whey protein isolate. It reveals the key element corresponding to the

poor interfacial viscoelasticity of whey protein isolate in the presence of sucrose, suggesting development of novel whey-protein-based foaming ingredients in the future.

REFERENCES

Alargova RG, Warhadpande DS, Paunov VN, Velev OD. 2004. Foam superstabilization by polymer microrods. Langmuir. 20: 10371-10374.

Alderton G, Ward WH, Fevold HL. 1946. Identification of the bacteria-inhibiting iron-binding protein of egg white as conalbumin. Arch Biochem Biophys 11: 9.

Anema SG. 2001. Kinetics of the irreversible thermal denaturation and disulfide aggregation of alpha-lactalbumin in milk samples of various concentrations. J Food Sci 66: 2-9.

Anema SG, Lee SK, Klostermeyer H. 2006. Effect of protein, nonprotein-soluble components, and lactose concentrations on the irreversible thermal denaturation of β-lactoglobulin and α-lactalbumin in skim milk. J Agric Food Chem 54: 7339-7348.

Antipova AS, Semenova MG, Belyakova LE. 1999. Effect of sucrose on the thermodynamic properties of ovalbumin and sodium caseinate in bulk solution and at air-water interface. Colloids Surf B: Biointerfaces 12: 261-270.

Aoki T, Hiidone Y, Kitahata K, Sugimoto Y, Ibrahim HR, Kato Y. 1999. Improvement of heat stability and emulsifying activity of ovalbumin by conjugation with glucuronic acid through the
Maillard reaction Food Res Int 32: 129–133.

Arakawa T, Timasheff SN. 1982. Stabilization of protein structure by sugars. Biochemistry 21: 6536–6544.

Arakawa T, Timasheff SN. 1985. The stabilization of proteins by osmolytes. Biophysical Journal 47: 411–414.

Arii Y, Yakahashi N, Tatsumi E, Hirose M. 1999. Structural properties of recombinant ovalbumin and its transformation into a thermostabilized form by alkaline treatment. Biosci Biotechnol Biochem 63: 1392-1399.

Arunepanlop B, Morr CV, Karleskind D, Laye I. 1996. Partial Replacement of Egg White Proteins with Whey Proteins in Angel Food Cakes. J Food Sci 61: 1085-1093.

Aryana KJ, Haque ZZ, Gerard PD. 2002. Influence of whey protein concentrate on the functionality of egg white and bovine serum albumin. Int J Food Sci and Tech 37: 643-652.

Attia EA. 1993. An alternative formula for the sweetening of reduced-calorie cakes. Food Chem 48: 169-172.

Babinsky E, Sojka PE. 2002. Modeling drop size distribution. Prog Energy Combust Sci 28: 303-329.

Back JF, Oakefull D, Smith MB. 1979. Increased thermal stability of proteins in the presence of sugars and polyols. Biochem 18: 5191-5196.

Baeva MR, Panchev IN, Terzieva VV. Comparative study of texture of normal and energy reduced sponge cakes. Nahrung/Food 44: 242–246.

Bals A, Kulozik U. 2003. Effect of pre-heating on the foaming properties of whey protein isolate using a membrane foaming apparatus. Int Dairy J 13: 903-908.

Baron F, Nau F, Guerin-Dubiard C, Gonnet F, Dubois JJ, Gautier M. 2003. Effect of dry heating on the microbiological quality, functional properties, and natural bacteriostatic ability of egg white after reconstitution. J Food Prot 66(5): 825–832.

Berry TK. 2008. Foaming Properties, Interfacial Properties, and Foam Microstructure of Egg White Protein and Whey Protein Isolate, Alone and in Combination. Thesis and dissertation. North Carolina State University.

Besio GJ, Oyler G, Prud'homme RK. 1985. Automated system for the characterization of liquid foam. Rev Sci Instrum 56: 746.

Binks BP. 2002. Particles as surfactants – similarities and differences. Curr Opin Colloid Interface Sci 7: 21-41.

Bisperink CGJ, Ronteltap AD, Prins A. 1992. Bubble size distribution in foams. Adv Colloid Interface Sci 38: 13-32.

Bouaouina H, Desrumauxa A, Loisela C, Legrand J. 2006. Functional properties of whey proteins as affected by dynamic high-pressure treatment. Int Dairy J 16: 275 – 284

Boye JI, Alli I. 2000. Thermal denaturation of mixtures of alpha-lactalbumin and beta-lactoglobulin: a differential scanning calorimetric study. Food Rec Int 33: 673-682.

Brew K. 2003. α-lactalbumin. In “Advanced Dairy Chimestry – 1 Proteins” Edited by Fox PF and McSweeney PLH. p387-412.

Briggs T. 1996. Foams for firefighting. Chapter 12 in “Foams: theory, measurements and applications” Edited by Prud'homme RK and Khan SA. New York Marcel Dekker, Inc., p465.

Brooks CF, Fuller GG, Frank CW, Robertson CR. 1999. An interfacial stress rheometer to study rheological transitions in monolayers at the air-water interface. Langmuir 15: 2450-2459.

Burley RW, Vadehra DV. 1989. The avian egg: chemistry and biology. New York : Wiley. p65-128.

Calvert JR, Nezhai K. 1987. Bubble size effects in foams. Int J heat fluids 8: 102-106.

Campbell GM, Mougeot E. 1999. Creation and characterization of aerated food products. Trends Food Sci and Technol 10: 283-296.

Campbell L, Raikos V, Euston SR. 2003. Modification of functional properties of egg white proteins. Nahrung/Food 47: 369-376.

Chang RC, Schoen HM, Grove CS. 1956. Bubble Size and Bubble Size Determination. Ind Eng Chem 48: 2035.

Chevalier F, Chobert JM, Popineau Y, Georgette M, Haertle N, Haertle T. 2001. Improvement of functional properties of b-lactoglobulin glycated through the Maillard reaction is related to the nature of the sugar. Int Dairy J 11: 145–152.

Clarkson JR, Cui ZF, Darton RC. 1999. Protein denaturation in foam. II – Surface activity and conformational change. J Colloid Interface Sci 215: 333-338.

Colella D, Vinci D, Bagatin R, Masi M, Abu Bakr E. 1999. A study on coalescence and breakage mechanisms in three different bubble columns. Chem Eng Sci 54: 2331.

Cooke SK, Sampson HA. 1997. Allergenic properties of ovomucoid in man. J Immunology 159(4): 2026-2032.

Cooke TF, Hirt DE. 1996. Foam wet processing in the textile industry. Chapter 9 in “Foams: theory, measurements and applications” Edited by Prud'homme RK and Khan SA. New York Marcel Dekker, Inc., p339.

Croguennec T, Nau F, Pezennec S, Brule G. 2000. Simple Rapid Procedure for Preparation of Large Quantities of Ovalbumin. J Food Chem 48: 4883-4889.

Croguennec T, Renault A, Beaufils S, Dubois JJ, Pezennec S. 2007. Interfacial properties of heat-treated ovalbumin. J Colloid Interface Sci 315: 627-636.

Damodaran S, Anand K, Razumovsky L. 1998. Competitive Adsorption of Egg White Proteins at the Air-Water Interface: Direct Evidence for Electrostatic Complex Formation between Lysozyme and Other Egg Proteins at the Interface. J Agric Food Chem 46: 872-876.

Damodaran S. 2005. Protein Stabilization of Emulsions and Foams. J Food Sci 70: R54-R64.

Davis JP, Foegeding EA, Hansen FK. 2004. Electrostatic effects on the yield stress of whey protein isolate foams. Colloids Surf B: Biointerfaces 34: 13-23.

Davis JP, Foegeding EA. 2004. Foaming and Interfacial Properties of Polymerized Whey Protein Isolate. J Food Sci 69: C404-C410.

Davis JP, Doucet D, Foegeding EA. 2005. Foaming and interfacial properties of hydrolyzed β-lactoglobulin. J Colloid Interface Sci 288: 412-422.

Davis JP, Foegeding EA. 2007. Comparisons of the foaming and interfacial properties of whey protein isolate and egg white proteins. Colloids Surf B: Biointerfaces 54: 200-210.

de Wit JN, Klarenbeek G. 1981. A differential scanning calorimetric study of the thermal behavior of bovine β-lactoglobulin at temperatures up to 100 °C. J of Dairy Res 48: 293-302.

Desert C, Guérin-Dubiard C, Nau F, Jan G, Val F, Mallard J. 2001. Comparison of Different Electrophoretic Separations of Hen Egg White Proteins. J Agric Food Chem 49: 4553-4561.

Dickinson E. 1992. An Introduction to Food Colloids. Oxford: Oxford University Press. p135, 216.

Dickinson E. 1999. Review: Adsorbed protein layers at fluid interfaces: interactions, structure and surface rheology. Colloids Surf B: Biointerfaces 15: 161-176.

Dickinson E, Ettelaie R, Murry BS, and Du Z. 2002. Kinetics of disproportionation of air bubble beneath a planar air-water interface stabilized by food proteins. J Colloid Interface Sci 252: 202-213.

DeVilbiss ED, Holsinger VH, Posati LP, Pallansch MJ. 1974. Properties of whey protein concentrate foams. Food Technol 28: 40-48.

Donovan JW, Mapes CJ. 1976. A differential scanning calorimetric study of conversion of ovalbumin to S-ovalbumin in eggs. J Sci Food Agric 27: 197.

Du L, Prokop A, Tanner RD. 2003. Variation of bubble size distribution in a protein foam fractionation column measured using a capillary probe with photoelectric sensors. J Colloid and Interface Sci 259: 180-185.

Durian DJ, Weitz DA, Pine DJ. 1991a. Multiple light-scattering probes of foam structure and dynamics. Science 252: 686-688.

Durian DJ, Weitz DA, Pine DJ. 1991b. Scaling behavior in shaving cream. Physical review A 44: 7902-7905.

Edwards DA, Wasan DT. 1996. Foam rheology: the theogy and role of interfacial rheologycial properties. Chapter 3 in "Foams: theory, measurements and applications" Edited by Prud'homme RK and Khan SA. New York Marcel Dekker, Inc., p189.

Eisner MD, Jeelani SAK, Bernhard L, Windhab EJ. 2007. Stability of foams containing proteins, fat particles and nonionic surfactants. Chem Eng Sci 62: 1974-1987.

Evans DF, Wennerström H. 1999. The Colloidal Domain. Where Physics, Chemistry, Biology, and Technology Meet. 2nd Edition. New York: Wiley-VCH. p63.

Exerova DR, Kryglyakov PM. 1998. Foam and foam films: theory, experiment, application. New York: Elsevier p381.

Fang Z, Patterson PR, Turner Jr. ME. 1993. Modeling particle size distributions by the Weibull distribution function. Mater charact 31:177-182.

Foegeding EA, Davis JP, Doucet D, McGuffey MK. 2002. Advances in modifying and understanding whey protein functionality. Trends Food Sci Technol 13: 151-159.

Foegeding EA, Luck PJ, Davis JP. 2006. Factors determining the physical properties of protein foams. Food Hydrocolloids 20: 284–292.

Fothergill LA, Fothergill JE. 1970. Thiol and Disulphide Contents of Hen Ovalbumin. Biochem J 116: 555-561.

Fox PF. 2003. Milk proteins: General and historical aspects. In "Advanced Dairy Chemistry – 1 Proteins" Edited by Fox PF and McSweeney PLH. p1.

Fox PF, McSweeney PLH. 1998. Dairy Chemistry and Biochemistry. New York: Blackie Academic & Professional, p189.

Fruhner H, Wantke KD, Lunkenheimer K. 1999. Relationship between surface dilational properties and foam Stability. Colloids Surf A: Physicochemical and Engineering Aspects 162: 193–202.

Gardiner BS, Dlugogorski BZ, Jameson GJ. 1998. Yield stress measurements of aqueous foams in the dry limit. J Rheol 42(6): 1437-1450.

Gaub HE, McConnell HM. 1986. Shear viscosity of monolayers at the air-water interface. J Phys Chem 90: 6830-6832.

Ghaskadvi RS, Ketterson JB, MacDonald RC, Dutta P. 1996. Apparatus to measure the shear modulus of Langmuir monolayers as functions of strain amplitude and frequency. Rev Sci Instrum 68(4): 1792-1795.

Guérin-Dubiard C, Pasco M, Molle D, Desert C, Croguennec T, Nau F. 2006. Proteomic analysis of hen egg white. J Agric and Food Chem 54: 3901-3910.

Guzey D, McClements DJ, Weiss J. 2003. Adsorption kinetics of BSA at air-sugar solution interfaces as affected by sugar type and concentration. Food Res Int 36: 649-660.

Haggett TOR. 1976. The whipping, foaming and gelling properties of whey protein concentrates. New Zealand J Dairy Sci Techno 11: 251-256.

Hagolle N, Launay B, Relkin P. 1998. Impact of structural changes and aggregation on adsorption kinetics of ovalbumin at the water/air-interface. Colloids Surf B: Biointerfaces 10(4): 191–198.

Hagolle N, Relkin P, Popineau Y, Bertrand D. 2000. Study of the stability of egg white protein-based foams: effect of heating protein solution. J Sci Food Agric 80(8): 1245-52.

Hammershoj M, Prins A, Qvist KB. 1999. Influence of pH on surface properties of aqueous egg albumen solutions in relation to foaming behaviour. J Sci Food Agric 79: 859–868.

Hammershoj M, Qvist K B. 2001. Importance of hen age and egg storage time for egg albumen foaming. Lebensmittel Wissenschaft und Technologie 34(2): 118–120.

Hammershoj M, Nording JA, Rasmussen HC, Carstens JH, Pedersen H. 2006. Dry-pasteurisation of egg albumen powder in a fluidised bed. I. Effect on microbiology, physical and chemical parameters. Int J Food Sci Technol 41: 249–261.

Hammershoj M, Nebel C, Carstens JH. 2008. Enzymatic hydrolysis of ovomucin and effect on foaming properties. Food Res Int 41: 522-531.

Handa A, Kuroda N. 1999. Functional Improvements in Dried Egg White through the Maillard Reaction. J Agric Food Chem 47: 1845-1850.

Hansen FK. 1993. Surface tension by image analysis: fast and automatic measurements of pendant and sessile drops and bubbles. J Colloid Interface Sci 160: 209-217.

Hansen FK, Rødsrud G. 1991. Surface tension by pendant drop I. A faster standard instrument using computer image analysis. J Colloid Interface Sci 141(1): 1-9.

Hayakawa S, Kondo H, Nakamura R, Sato Y. 1983. Effect of β-ovomucin on the solubility of α-ovomucin and further inspection of the structure of ovomucin complex in thick egg white. Agric Bio Chem 47: 815–820.

Herceg Z, Rezek A, Lelas V, Kresic G, Franetovic M. 2007. Effect of carbohydrates on the emulsifying, foaming and freezing properties of whey protein suspensions. J Food Eng 79: 279-286.

Herzhaft B. 1999. Rheology of Aqueous Foams: a literature review of some experimental works. Oil Gas Sci Technol 54(5): 587-596.

Heuer A, Cox AR, Singleton S, Barigou M, Ginkel M. 2007. Visualisation of foam microstructure when subject to pressure change. Colloids Surf A: Physicochemical and Engineering Aspects 311: 112-123.

Israelachvili. 1991. Intermolecular and surface forces. 2nd Edition. San Diego: Academic Press. p139-330.

Itoh T, Miyazaki J, Sugawara H, Adachi S. 1987. Studies on the characterization of ovomucin and chalaza of the hen's egg. J Food Sci 52: 1518–1521.

Jeffrey PD, Bewley MC, MacGillivray RTA, Mason AB, Woodworth RC, Baker EN. 1998. Ligand-induced conformational change in transferrins: crystal structure of the open form of the N-terminal half molecule of human transferring. Biochem 37: 13978-13986.

Johnson TM, Zabik ME. 1981a. Response surface methodology for analysis of protein interactions in angel food cakes. J Food Sci 46: 1226-1230.

Johnson TM. Zabik ME. 1981b. Egg albumen proteins interactions in an angel food cake system. J Food Sci 46: 1231-1236.

Kato A, Nakamura R, Sato Y. 1970. Studies on changes in stored shell eggs. V. The difference in the chemical and physicochemical properties of ovomucin β between the thick and thin white. Agric Biol Chem 34: 854.

Kato A, Hirata S, Kobayashi K. 1978. Structure of the sulfated oligosaccharide chain of ovomucin. Agric Bio Chem 42: 1025–1029.

Kato A, Oda S, Yamanaka Y, Matsudomi N, Kobayashi K. 1985. Functional and structural properties of ovomucin. Agric Bio Chem 49: 3501.

Kilara A, Panyam D. Peptides from milk proteins and their properties. Crit Rev Food Sci Nutr 2003; 43(6):607-633.

Kilara A, Vaghela MN. 2004. Whey proteins. In "Proteins in food processing" Edited by Yada RY. Washington DC: CRC Press. p 72-99.

Kim YA, Chism GW, Mangino ME. 1987. Determination of the beta-Lactoglobulin, alpha-Lactqdbumin and Bovine Serum Albumin of Whey Protein Concentrates and Their Relationship To Protein Functionality.J Food Sci 53(1): 124-127.

Kinsella JE, Whitehead DM. 1989. Proteins in whey: chemical, physical, and functional properties. Adv Food Nutr Res 33: 344-438.

Kitabatake N, Doi E. 1987. Conformational change of hen egg ovalbumin during foam formation detected by 5, 5'-dithiobis (2-nitrobenzoic acid). J Agric Food Chem 35: 353-357.

Kitabatake N, Indo K, Doi E. 1989. Changes in interfacial properties of hen egg ovalbumin caused by freeze-drying and spray-drying. J Agric Food Chem 37: 905-910.

Koehler HH. 1974. Physicochemical appraisal of changes in egg white during storage. J Agric Food Chem 22: 288-293.

Kokelaar JJ, Prins A, Gee MD. 1991. A new method for measuring the surface dilational modulus of a liquid. J Colloidal Interfacial Sci 146(2): 507-511.

Kosters HA, Broersen K, de Groot J, Simons JWFA, Wierenga P, de Jongh HHJ. 2003. Chemical processing as a tool to generate ovalbumin variants with changed stability. Biotechnol Bioeng 84: 61-70.

Kraynik AM, Hansen MG. 1986. Foam and emulsion rheology: a quasistatic model for large deformations of spacially-periodic cells. J Rheol 30: 409-415.

Labbafi M, Thakur RK, Vial C, Djelveh G. 2007. Development of an on-line optical method for assessment of the bubble size and morphology in aerated food products. Food Chem 102: 454-465.

Lage PLC, Espósito RO. 1999. Experimental determination of bubble size distributions in bubble columns: prediction of mean bubble diameter and gas hold up. Powder technology 101: 142-150.

Larson BL, Jenness R. 1952. Characterization of the sulfhydryl groups and the kinetics of the heat denaturation of crystalline β-lactoglobulin. J Amer Chem Soc 74: 3090-3.

Lau CK, Dickinson E. 2005. Instability and structural change in an aerated system containing egg albumen and invert sugar. Food Hydrocolloids 19, 111-121.

Lau CK, Dickinson E. 2004. Structural and rheological properties of aerated high sugar systems containing egg albumen. J Food Sci 69(5): E232-E239.

Lechevalier V, Croguennec T, Pezennec S, Guérin-Dubiard C, Pasco M, Nau F. 2003. Ovalbumin, ovotransferrin, lysozyme: three model proteins for structural modifications at the air-water interface. J Agric Food Chem 51: 6354-6361.

Lechevalier V, Perinel E, Jeantet R, Lesaffre C, Croguennec T, Guérin-Dubiard C, Nau F. 2005. Statistical analysis of effects of industrial processing steps on functional properties of pasteurised liquid egg white. J Sci Food Agric 85: 757-769.

Lechevalier V, Jeantet R, Arhaliass A, Legrand J, Nau F. 2007. Egg white drying: influence of industrial processing steps on protein structure and functionalities. J Food Eng 83: 404-413.

Lee JC, Timasheff SN. 1981. The stabilization of proteins by sucrose. J Bio Chem 256: 7193-7210.

Lewis DA, Nicol RS, Thompson JW. 1984. Measurement of bubble sizes and velocities in gas-liquid dispersions. Chem Eng Res Des 62: 334-336.

Li CP, Ibrahim HR, Sugimoto Y, Hatta H, Aoki T. 2004. Improvement of functional properties of egg white protein through phosphorylation by dry-heating in the presence of pyrophosphate. J Agric Food Chem 52: 5752-5758.

Li-Chan E, Nakai S. 1989. Biochemical Basis for the Properties of Egg White. CRC Crit Rev Poultry Biology 2: 21-58.

Lim KS, Barigou M. 2004. X-ray micro-computed tomography of cellular food products. Food Res Int 37: 1001-1012.

Lim SY, Swanson BG, Clark S. 2008. High hydrostatic pressure modification of whey protein concentrate for improved functional properties. J Dairy Sci 91(4): 1299-1307

Longsworth LG, Cannan RK, MacInnes DA. 1940. An electrophoretic study of the proteins of egg white. J Amer Chem Soc 62: 2580.

Lucassen-Reynders EH. 1993. Interfacial Viscoelasticity in Emulsions and Foams. Food Structure 12: 1-12.

Luck PJ, Bray N, Foegeding EA. 2001. Factors Determining Yield Stress and Overrun of Whey Protein Foams. J Food Sci 65: 1677-1681.

MacDonnell LR, Feeney RE, Hanson HL, Campbell A, Sugihara TF. 1954. The functional properties of the egg white proteins. Food Technol 8: 49-53.

Magrabi SA, Dlugogorski BZ, Jameson GJ. 1999. Bubble size distribution and coarsening of aqueous foams. Chem eng sci 54: 4007-4022.

Mann K. 2007. The chicken egg white proteome. Proteomics J 7: 3558-3568.

Maru HC, Wasan DT. 1979. Dilational viscoelastic properties of fluid interfaces – II Experimental study. Chem Eng Sci 34: 1295-1307.

McCarthy KL, Heil JR. 1990. Internal liquid flow during foam drainage: Comparison of theory and experiment. AIChE Symposium Series 86(277): 71–75.

McClements DJ. 2002. Modulation of globular protein functionality by weakly interacting cosolvents. Crit Rev Food Sci Nutr 42: 417-471.

McGuffey MK, Epting KL, Kelly RM, Foegeding EA. 2005. Denaturation and aggregation of three α-lactalbumin preparations at neutral pH. J Agric Food Chemi 53: 3182-3190.

Miller R, Wustneck R, Kragel J, Kretzschmar G. 1996. Dilational and shear rheology of adsorption layers at liquid interfaces. Colloids Surf A: Physcicochemical and Engineering Aspects 111: 75-118.

Miller R, Aksenenko EV, Fainerman VB, Pison U. 2001. Kinetic of adsorption of globular proteins at liquid/fluid interface. Colloids Surf A: Physicochemical and Engineering Aspects 183-185: 381-390.

Mills N. 2007. Polymer foams handbook. Engineering and biomechanics applications and design guide. Oxford: Butterworth Heinemann.

Mine Y, Noutomi T, Haga N. 1991. Emulsifying and structural properties of ovalbumin. J Agric Food Chem 39: 443-446.

Mine Y. 1995. Recent advances in the understanding of egg white protein functionality. Trends Food Sci and Technol 6: 225-232.

Mine Y. 1997. Effect of dry heat and mild alkaline treatment on functional properties of egg white proteins. J Agric Food Chem 45: 2924-2928.

Mohamed S, Mawar-Md-Lajis S, Abdul-Hamid N. 1995. Effects of protein from different sources on the characteristics of sponge cakes, rice cakes (Apam), doughnuts and frying batters. J Sci Food Agric 68, 271-277.

Murray BS, Nelson PV. 1996. A novel Langmuir trough for equilibrium and dynamic measurements on air-water and oil-water monolayers. Langmuir 12: 5973-5976.

Murray BS. 2002. Interfacial rheology of food emulsifiers and proteins. Curr Opin Colloid Interface Sci 7: 426-431.

Murray BS, Ettelaie. 2004. Foam stability: proteins and nanoparticles. Curr Opin Colloid Interface Sci 9: 314–320.

Murray BS, Dickinson E, Lau CA, Nelson PV, Schmidt E. 2005. Coalescence of protein stabilized bubbles undergoing expansion at a simultaneously expanding planar air-water interface. Langmuir 21: 4622-4630.

Murray BS. 2007. Stabilization of bubbles and foams. Curr Opin Colloid Interface Sci 12: 232-241.

Myrvold R, Hansen FK. 1998. Surface elasticity and viscosity from oscillating bubbles measured by automatic axisymmetric drop shape analysis. J Colloid Interface Sci 207: 97-105.

Nakamura R. 1963. Studies on the foaming property of the chicken egg white. VI. Spread monolayer of the protein fraction of the chicken egg white. Agric Bio Chem 27: 427.

Narsimhan G, Ruckenstein E. 1986. Effect of bubble size distribution on the enrichment and collapse in foams. Langmuir 2: 494-508.

Niño MRR, Wilde PJ, Clark DC, Husband FA, Rodríguez Patino JM. 1997. Rheokinetic analysis of protein films at the air-aqueous phase interface. 2. Bovine serum albumin adsorption from sucrose aqueous solutions. J Agric Food Chem 45: 3016-3021.

Niño MRR, Rodríguez Patino JM. 2002. Effect of the aqueous phase composition on the adsorption of bovine serum albumin to the air-water interface. Ind Eng Chem Res. 41: 1489-1495.

Nisbet AD, Saundry RH, Moir AJG, Fothergill LA, Fothergill JE. 1981. The complete amino-acid sequence of hen ovalbumin. Europe J Biochem 115: 335.

Palmer AH. 1934. The preparation of a crystalline globulin from the albumin fraction of cow's milk. J Biol Chem 104: 359-372.

Park KH, Lund DB. 1984. Calorimetric study of the thermal denaturation of β-lactoglobulin. J Dairy Sci 67: 1699-1706.

Pateras IMC, Howells KF, Rosenthal AJ. 1994. Hot-stage microscopy of cake batter bubbles during simulated baking: sucrose replacement by polydextrose. J Food Sci 59: 168-170, 178.

Pernell CW, Foegeding EA, Daubert CR. 2000. Measurement of the yield stress of protein foams by vane rheometry. J Food Sci 65: 110.

Pernell CW, Foegeding EA, Luck PJ, Davis JP. 2002a. Properties of whey and egg white protein foams. Colloids Surf A: Physicochemical and Engineering Aspects 204: 9-21.

Pernell CW, Luck PJ, Foegeding EA, Daubert CR. 2002b. Heat-induced Changes in Angel Food Cakes Containing Egg-white Protein or Whey Protein Isolate. J Food Sci 67: 2945-2951.

Phillips LG, Hague Z, Kinsella JE. 1987. A method for the measurement of foam formation and stability. J Food Sci 52: 1074-1077.

Phillips LG, Yang ST, Schulman W, Kinsella JE. 1989. Effects of lysozyme, clupeine, and sucrose on the foaming properties of whey protein isolate and beta-lactoglobulin. J Food Sci 54: 743-747.

Polli M, Stanislao MD, Bagatin R, Bakr EA, Masi M. 2002. Bubble size distribution in the sparger region of bubble columns. Chem Eng Sci 57: 197–205.

Princen HM, Kiss AD. 1989. Rheology of foams and highly concentrated emulsions IV: An experimental study of the shear viscosity and yield stress of concentrated emulsions. J Colloid Interface Sci 128(1): 176-187.

Prins A. 1992. Surface rheology and practical behavior of foams and thin liquid films. Chem Ing Technol 64: 73-75.

Prud'homme RK, Warr GG. 1996. Foams in mineral flotation and separation processes. Chapter 13 in "Foams: theory, measurements and applications" Edited by Prud'homme RK and Khan SA. New York Marcel Dekker, Inc., p511.

Pugh RJ. 1996. Foaming, foam films, antifoaming and defoaming. Adv Colloid Interface Sci 64: 67-142.

Pugh RJ. 2005. Experimental techniques for studying the structure of foams and froths. Adv Colloid Interface Sci 114-115: 239-251.

Qin BY, Bewley MC, Creamer LK, Baker EN, Jameson GB. 1999. Functional implications of structural differences between variants A and B of bovine β-lactoglobulin. Protein Sci 8: 75–83.

Rabouille C, Ano MA, Muller G, Cartaud J, Thomas D. 1990. The supermolecular organization of ovomucin. Biochem J 266: 697-706.

Raikos V, Hansen R, Campbell L, Euston SR. 2006. Separation and identification of hen egg protein isoforms using SDS–PAGE and 2D gel electrophoresis with MALDI-TOF mass spectrometry. Food Chem 99: 702–710

Raikos V, Campbell L, Euston SR. 2007. Effects of sucrose and sodium chloride on foaming properties of egg white proteins. Food Res Int 40: 347-355.

Reddy MS, Panda B. 1969. Chemical changes occurring in shell eggs during storage – a review. J Food Sci Technol 6: 257.

Relkin P, Hagolle N, Dalgleish DG, Laurey B. 1999. Foam formation and stabilization by pre-denatured ovalbumin. Colloids Surf B: Biointerfaces 12: 409–416.

Richert SH. 1979. Physical-chemical properties of whey protein foams. J Agric Food Chem 27: 665-668.

Rieger M. 1996. Foams in personal care products. Chapter 10 in "Foams: theory, measurements and applications" Edited by Prud'homme RK and Khan SA. New York Marcel Dekker, Inc., p413.

Robinson DS, Monsey JB. 1975. The composition and proposed subunit structure of egg-white b-ovomucin. Biochem J 147: 55–62.

Rodríguez Patino JM, Niño MRR. 1995. Protein adsorption and protein-lipid interactions at the air aqueous solution interface. Colloids Surf A: Physicochemical and Engineering Aspects 103: 91-103.

Ronda F, Gómez M, Blanco CA, Caballero PA. 2005. Effects of polyols and nondigestible oligosaccharides on the quality of sugar-free sponge cakes. Food Chem 90: 549-555.

Rouimi S, Schorsch C, Valentini C, Vaslin S. 2005. Foam stability and interfacial properties of milk protein-surfactant system. Food Hydrocolloids 19: 467-478.

Ruíz-Henestrosa VP, Sánchez CC, Rodríguez Patino JM. 2008. Effect of sucrose on functional properties of soy globulins: adsorption and foam characterisitics. J Agric Food Chem 56(7): 2512-2521.

Russ JC. 2005. Image Analysis of Food Microstructure. CRC Press LLC. p5.

Rusu D, Peuvrel-Disdierb E. 1999. In situ characterization by small angle light scattering of the shear induced coalescence mechanisms in immiscible polymer blends. J Rheol 43(6): 1391-1409.

Sarma DSHSR, Khilar KC. 1988. Effects of Initial gas volume fraction on stability of aqueous air foams. Ind Eng Chem Res 27: 892-894.

Sawyer WH. 1969. Complex between β-lactoglobulin and κ-casein. J Dairy Sci 52: 1347-55.

Sawyer L. 2003. β-lactoglobulin. In "Advanced Dairy Chimestry – 1 Proteins" Edited by Fox PF and McSweeney PLH. New York: Kluwer Academic/Plenum Publishers. p319-63.

Sceni P, Wager JR. 2007. Study on sodium caseinate foam stability by multiple light scattering. Food Sci Technol Int 13(6): 461-468.

Schäfer A, Drewes W, Schwägele F. 1999. Effect of storage temperature and time on egg white protein. Nahrung 43(2): 86–89.

Selecki A, Wasiak R. 1984. The continuous direct method of bubble size determination in static foams. J Colloid Interface Sci 102(2): 557-559.

Smith MB, Back JF. 1962. Modification of ovalbumin in stored eggs detected by heat denaturation. Nature 193: 878-879.

Smith MB, Back JF. 1965. Studies on ovalbumin II. The formation and properties of S-ovalbumin, a more stable form of ovalbumin. Aust J Biol Sci 18: 365-377.

Speight JG. 2005. Lange's Handbook of Chemistry. 16th edition. New York : McGraw-Hill, Professional. p1.226.

Stevenson P, Mantle MD, Hicks JM. 2007. NMRI studies of the free drainage of egg white and
meringue mixture froths. Food Hydrocolloids. 21: 221-229.

Sugimoto Y, Sanuki S, Ohsako S, Higashimoto Y, Kondo M, Kurawaki J, Ibrahim HR, Aoki T, Kusakabe T, Koga K. 1999. Ovalbumin in developing chicken eggs migrates from egg white to embryonic organs while changing its conformation and thermal stability. J Bio Chem 274(16): 11030-11037.

Suttiprasit P, Krisdhasima V, Mcguire J. 1992. The surface activity of α-lactalbumin, β-lactoglobulin, and bovine serum albumin. I. Surface tension measurements with single-component and mixed solutions. J Collid Interface Sci 154(2): 316-326.

Swaisgood HE. 1982. Chemistry of Milk Protein. Developments in Dairy Chemistry – 1. Edited by Fox PF. Applied Science Publishers LTD. p1-59.

Swaisgood HE. 1996. Characteristics of Milk. Food Chemistry. Edited by Fennema O.R. New York Marcel Dekker, Inc., p841-879.

Takahashi N, Tatsumi E, Orita T, Hirose M. 1996. Role of the intrachain disulfide bond of ovalbumin during conversion into S-ovalbumin. Biosci Biotechnol Biochem 60: 1464-8.

Takahashi N, Onda M, Hayashi K, Yamasaki M, Mita T, Hirose M. 2005. Thermostability of Refolded Ovalbumin and S-Ovalbumin. Biosci Biotechnol Biochem 69: 922-931.

Tanford C, Brunville LG, Nozaki Y. 1959. The reversible transformation of β-lactoglobulin at pH 7.5. J Amer Chem Soc 81: 4032-4036.

Ternes W. 2001. Egg proteins. In Chemical and functional properties of food proteins. Edited by Sikorski ZE. Lancaster, PA: Technomic Publishing Co. Inc., p335-71.

Tosi E, Canna L, Lucero H, Re E. 2007. Foaming properties of sweet whey solutions as modified by thermal treatment. Food Chem 100: 794–799.

Tronin A, Dubrovsky T, Dubrovskaya S, Radicchi G, Nicolini C. 1996. Role of protein unfolding in monolayer formation on air-water interface. Langmuir 12: 3272-3275.

Uhrinova S, Smith MH, Jameson GB, Uhrin D, Sawyer L, Barlow PN. 2000. Structural changes accompanying pH-induced dissociation of the β-lactoglobulin dimer. Biochem 39: 1113-23.

Vachier MC, Piot M, Awade AC. 1995. Isolation of hen egg white lysozyme, ovotransferrin and ovalbumin, using a quaternary ammonium bound to a highly crosslinked agarose matrix. J Chromatograph B 664: 201-210.

Varnam AH, Sutberland JP. 2001. Milk and Milk Products: Technology, Chemistry and Microbiology. Gaithersburg, Md: Aspen.

Walstra P. 2003. Physical Chemistry of Foods. New York: Marcel Dekker. p355,

Walstra P, Jenness R. 1984. Dairy Chemistry and Physics. A Wiley-Interscience Publication.

Watanabe K, Shimoyamada M, Onizuka T, Akiyama H, Niwa M, Ido T, Tsuge Y. 2004. Amino acid sequence of α-subunit in hen egg white ovomucin deduced from cloned cDNA. DNA Sequence 15(4): 251–261.

Wilde PJ, Niño MRR, Clark DC, Rodríguez Patino JM. 1997. Molecular diffusion and drainage of thin liquid films stabilized by bovine serum albumin—Tween 20 mixtures in aqueous solutions of ethanol and sucrose. Langmuir 13: 7151–7157.

Wilde PJ. 2000. Interfaces: their role in foam and emulsion behavior. Curr Opin Colloid Interfaces Sci 5: 176-181.

Wilde P, Mackie A, Husband F, Gunning P, Morris V. 2004. Proteins and emulsifiers at liquid interfaces. Adv Colloid Interfaces Sci 108-109: 63-71.

Wong CH, Hossain MM, Davies CE. 2001. Performance of continuous foam separation column as a function of process variable. Bioprocess Biosyst Eng 24: 73-81.

Wong YC, Herald TJ, Hachmeister KA. 1996. Comparison between irradiated and thermally pasteurized liquid egg white on functional, physical, and microbiological properties. Poultry Sci 75: 803-808.

Yamashita K, Kamerling JP, Kobata A. 1982. Structural study of the carbohydrate moiety of hen ovomucoid. J Biol Chem 257(21): 12809-12814.

Yankov S, Panchev I. 1996. Foaming properties of sugar-egg mixtures with milk protein concentrates. Food Res Int. 5-6: 521-525.

Zhu H, Damodaran S. 1994. Proteose peptones and physical factors affect foaming properties of whey protein isolate. J Food Sci 59: 554-560.

CHAPTER 2

Manuscript in submission for publication

Foaming and Interfacial Properties of Egg White Protein and Whey Protein Isolate, Alone and in Combination

Authors: Xin Yang, Tristan K. Berry, and E. Allen Foegeding

Abstract

Foaming properties of whey protein isolate (WPI), egg white protein (EWP), and combinations of the two (WPI/EWP), were compared in model and food systems. Physical properties of foams (overrun, drainage 1/2 life, and yield stress), angel food cakes (volume), and air/water interfaces (interfacial tension and interfacial rheology) were investigated. Progressive substitution of WPI for EWP decreased foam stability (drainage 1/2 life). Incorporation of 12.8% (w/v) sucrose greatly increased EWP foam stability but had little effect on the stability of WPI and WPI/EWP foams. Changes in interfacial tension showed that even the lowest level of WPI substitution (25% WPI) was enough to cause the temporal pattern of interfacial tension to mimic the pattern of WPI instead of EWP, suggesting that whey proteins dominated the interface. Yield stress (τ_0) and interfacial dilational elastic moduli (E') of WPI and WPI/EWP combinations decreased with sucrose addition, with a positive relationship established between τ_0 and E'. The presence of sucrose increased angel food cake volume when EWP proportion was higher than 50%. Although EWP and 25% WPI/75% EWP treatments showed similar cake volumes, cross-sections of 25% WPI/75% EWP cakes showed larger air cells, reminiscent of WPI cakes. These results indicated that foam functionality using blends of WPI and EWP was not additive and suggested that whey proteins dominated the air/water interface in mixed systems. This decreased the stability of wet foams and thereby decreased the stability of angel food cake batters during heating.

Key words: whey protein, egg white, foam, interfacial tension, angel food cake

Introduction

Foams are defined as a gas dispersed in a solid or liquid phase. Although structurally complex, food foams are encountered daily, from cakes and breads to champagne, beer, meringues and ice cream. Angel food cakes are of particular interest among food foam products because the protein foam is generated independently then combined with other ingredients, allowing for separate investigation of the properties of the foam and food product.

Although egg white protein (EWP) is the traditional standard for culinary foams, whey protein isolate (WPI) shows comparable foaming functionality on some levels. Peter and Bell (1930) noted that whey protein may be a suitable, economical replacement for egg white in foaming applications, except for those applications involving heating or baking. Richert (1979) confirmed whey protein's foaming capabilities as comparable to egg white in overrun, whipping time, and foam stability, but also observed the lack of stability during heating. DeVilbiss et al. (1974) demonstrated differences in thermal stability by showing that angel food cakes made with whey proteins expanded quickly to a maximum volume and then collapsed during baking, while the cakes containing EWP held their shape. Further experiments on angel food cakes made with WPI and EWP showed similar expansion during the initial phase of baking but a deviation in the later stage where cakes containing WPI collapsed (Pernell et al., 2002b). Arunepanlop et al. (1996) showed that up to 25% of EWP could be substituted with whey proteins and produce an angel food cake without significant change in cake texture (springiness, hardness, and cohesiveness). However, increasing substitution of whey protein showed progressively lower cake volumes and coarser bubble

structures. The mechanisms responsible for the effect of whey proteins in the cakes were not established but speculated to be due to differences in thermal stability among egg white and whey proteins.

The role of individual proteins in the foaming functionality of egg white and whey protein has been a topic of study. Johnson and Zabik (1981) investigated angel food cakes made with individual egg white proteins and noted both positive and negative protein-protein interactions on foaming and angel food cake applications. Overall, the foaming functionality of egg white appears to be the result of complex interactions between the individual proteins rather than attributable to a single protein component. Moreover, the interactions are still not completely understood (Damodaran, 2005). Similarly, previous research has investigated the effects of individual whey proteins on foaming properties. In foams made from mixtures of the two major whey protein, β-lactoglobulin and α-lactalbumin, increasing the amount of β-lactoglobulin causes a linear increase in overrun and a non-linear increase in yield stress (Luck et al., 2002). In another investigation, combinations of whey protein concentrate and egg white protein were shown to have a synergistic effect on foam stability (Aryana et al., 2002). The mechanism causing an increase in stability was not established.

The goal of this investigation was to better understand what contributes to the foaming properties in mixtures of EWP and WPI. This was done by first determining how combinations of EWP and WPI alter the physical properties (foam overrun, stability and yield stress) of foams and air-water interfaces (interfacial tension and dilatational elasticity). These combinations were additionally examined in an angel food cake to determine if properties of wet foams had any bearing on functionality in a heat-set foam. Reported herein

are the results covering foam, interfacial and cake properties; changes in foam and cake batter microstructure will be covered in a separate article.

Materials and Methods

Materials

Two commercial samples of whey protein isolate (WPI 1 and WPI 2) were obtained. Provon 190 (91% protein, dry basis) was supplied by Glanbia Foods, Inc. (Twin Falls, ID) and BiPro (93% protein, dry basis) was supplied by Davisco Foods International, Inc. (Le Sueur, MN). Both WPIs were stored at room temperature (22 ± 2 °C). Spray dried egg white protein (P-18J, 81% protein, dry basis) was obtained from Henningsen Foods, Inc. (Omaha, NE) and stored at 4 °C. The sodium hydroxide (ACS pellets) and sucrose (ACS) were purchased from Fisher Scientific Inc. (Fair Lawn, NJ). Hydrochloric acid was obtained from Mallinckrodt Inc. (Hazelwood, MO). Cake flour and 10x powdered sugar were purchased from a local grocery store. Deionized water was obtained using a Dracor Water Systems (Durham, NC) purification system. The resistivity was a minimum of 18.2 MΩ cm.

Methods

Protein solutions

Protein powders were mixed with deionized water and stirred overnight (14 to 16 hours) at room temperature (22 ± 2 °C) to allow for full hydration. When required, sucrose was added to the protein solutions on a 12.8% w/v basis prior to pH adjustment. Before final adjustment to 10% w/v protein, the pH was adjusted to 7.0 using 1N NaOH or 1N HCl.

Protein solutions of five WPI/EWP ratios (100/0, 75/25, 50/50, 25/75 and 0/100) were prepared by mixing WPI and EWP solutions.

Foam Generation

A Kitchen Aid Ultra Power Mixer (Kitchen Aid, St. Joseph's, MI) with a 4.3 L stationary bowl and rotating beaters was used to generate the foams from protein solutions. Two hundred mL of protein solutions were whipped for 20 min at a speed setting of 8 (planetary rpm of 225 and beater rpm of 737), both in the presence and absence of 12.8% (w/v) sucrose.

Overrun

Overrun was measured according to the method of Phillips et al. (1987). Foam was gently scooped into a standard weigh boat (100 mL), leveled using a rubber spatula, and weighed. This process was repeated a minimum of 10 times per foam and was completed within 20 min after whipping. The 10 overrun data points were found to be stable over the measurement time (Figure 1).

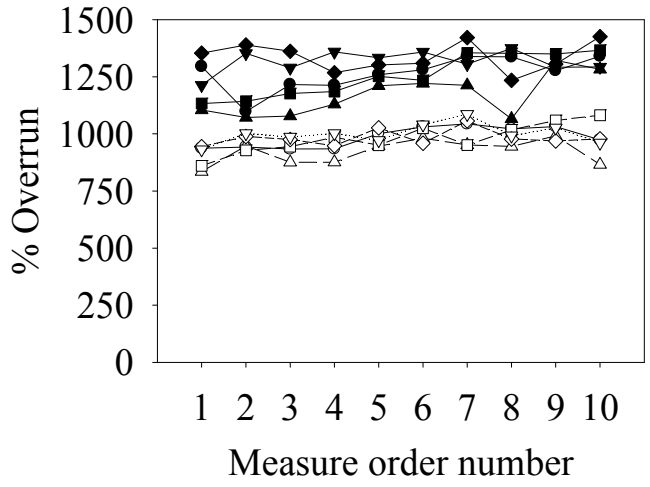

Figure 1. Sequential overrun measurements of foams prepared from 10% (w/v) protein solutions at pH 7, both in the presence (open symbols) and absence (closed symbols) of 12.8% (w/v) sucrose. Overrun measurement were competed within 20 min. All foams were prepared from WPI 1. ● WPI ▲75WPI/25EWP ■ 50WPI/50EWP ◆ 25WPI/75EWP ▼ EWP

The mean of 10 weights was used for overrun and air phase fraction calculations according to Equation 1 and Equation 2 (Campbell and Mougeot, 1999):

$$\%\text{Overrun} = \frac{(\text{wt.100 mL solution}) - (\text{wt.100 mL foam})}{\text{wt.100 mL foam}} \times 100 \qquad \text{Equation 1}$$

$$\text{Air phase fraction } (\phi) = \frac{\%\text{overrun}}{(\%\text{overrun} + 100)} \qquad \text{Equation 2}$$

Each treatment was replicated a minimum of three times.

Yield stress

Yield stress was measured using a vane attachment to a Brookfield 25xLVTDV-ICP viscometer (Brookfield Engineering Laboratories, Inc., Middleboro, MA) (Pernell et al., 2000). Immediately after foam generation, the vane (10 mm in diameter and 40 mm in length) was gently inserted into the foam until the top edge was even with the foam surface.

The vane was then rotated at a speed of 0.3 rpm. Maximum torque response (M_0) was used to calculate yield stress according Equation 3 (Dzuy and Boger, 1985; Steffe, 1992):

$$\tau_0 = \frac{M_0}{\left(\frac{h}{d} + \frac{1}{6}\right)\left(\frac{\pi d^3}{2}\right)} \qquad \text{Equation 3}$$

where τ_0 is the yield stress, and h and d are the height and diameter of the vane. Three consecutive measurements throughout the bowl were completed within 5 min after foam generation and averaged. A minimum of three replications were conducted for each treatment.

Foam stability (drainage ½ life)

Foam stability was measured by recording the length of time required for half of the pre-foam mass to drain (Phillips et al., 1990). Special bowls with a 6-mm diameter hole were used for stability measurements. After foam generation, the bowl was placed in a ring stand over a scale with a weigh boat and the hole uncovered. The time necessary for half the mass to drain was recorded as the drainage ½ life. A longer drainage ½ life corresponds to greater foam stability. Each treatment was replicated for a minimum of three times to obtain average drainage ½ life.

Viscosity measurements

Viscosity of pre-foam protein solutions was measured on a controlled stress rheometer (StressTech; Reologica Instruments AB, Lund, Sweden) using cup and bob geometry (measuring system CCE25) according to the method of Davis and Foegeding (2004). After a pre-shear at 50 s^{-1} for 30 s, viscosity was tested over a range of shear rates

(0.5 s^{-1} to 225 s^{-1}). The rheological behavior of protein solutions was described by a power law model as shown in Equation 4:

$$\sigma = K\dot{\gamma}^{n} \qquad \text{Equation 4}$$

where σ and $\dot{\gamma}$ are shear stress and shear rate, and K and n are consistency constant and flow behavior index, respectively. Shear stress and shear rate data was fit to a power law model and the consistency constant and flow behavior index were calculated. All measurements were carried out at room temperature (22 ± 2 °C) and replicated a minimum of three times.

Interfacial tension

Interfacial tension of pre-foam solution bubbles was measured using a pendant drop method (Myrvold and Hansen, 1998). An automated contact angle goniometer (Rame-Hart Inc, Mountain Lakes, NJ) was used for data collection and calculations in combination with the DROPimage computer program. A 16 μL pendant drop of pre-foam solution was generated by a computer-controlled syringe from a stainless-steel capillary into an environmental chamber with standing water at its bottom to minimize evaporation. A digital camera captured the image of the pendant drop every 2 s for a total of 600 s and interfacial tension was calculated based on shape parameters. All samples were equilibrated to room temperature (22 ± 2 °C) before measurement. Values reported are the averages of a minimum of three replications. The system was calibrated using HPLC water with an interfacial tension of 72.3 mN/m at room temperature (22 ± 2 °C). The estimated experimental error is ± 1.0 mN/m. Values reported are represents of a minimum of three replications.

Interfacial dilational modulus

To measure dilational visco-elasticity of the interfaces, sinusoidal oscillations of the drops' areas (Myrvold and Hansen, 1998) were increased by volume amplitude of 0.5 μL at a frequency of 0.1 Hz. The resulting changes in interfacial tension and interfacial area were collected and used to calculate the dilational modulus utilizing the DROPimage software. Drops were suspended for 300 s before measurement. Values reported are the averages of a minimum of three replications.

Density determination

DROPimage software requires inputs of component phase densities to calculate interfacial tension from drop shape analysis. A Mettler-Toledo DE40 density meter (Mettler-Toledo, Columbus, OH) equipped with a viscosity correction card was used to measure the density of each solution at room temperature (22 ± 2 °C). The accuracy of the instrument is 1 $\times 10^{-4}$ g/cm^3. Each solution was evaluated in triplicate and averaged.

Angel Food Cake Preparation

Angel food cakes were prepared based on the method of Pernell et al. (2002b). Two cake formulas were used to determine the effect of sucrose. The control cake was made by foaming 200 mL of a 10% w/v protein, 12.8% powdered sucrose solution and combining it with flour (66 g) and powdered sucrose (151.6 g). The "no-sucrose" treatment did not contain sucrose in the foaming solution, nor was it added to the foam. Solutions were prepared as described above. Foams were generated by the same method as stated above except whipping time was 15 min. The dry blend (flour and sugar) was sifted 3 times and gently folded into the foam using a balloon whisk in 3 installments and no more than 20

strokes total. The batter was poured into 3 cake pans (size 6.5 cm × 13 cm × 5.5 cm) with 75.0 g batter in each pan. The cakes were baked in a conventional oven at 204 °C for 14 min. After baking, the cakes were cooled upside down on a wire rack for 30 min at room temperature. After cooling, cake volume was measured using a rapeseed displacement method (Pernell et al., 2002b). Six cakes were made from each batch of batter per treatment and all treatment were replicated twice.

Statistical Analysis

Data for foams (overrun, drainage 1/2 life, and yield stress), cakes (volume), pre-foam solutions (viscosity), and interfaces (interfacial tension) were analyzed using the General Linear Model procedure of the SAS statistical software package (Version 9.1; SAS Institute, Inc., Cary, NC, USA). Analysis of variance (ANOVA) was conducted with means separation to determine differences between treatments. Significant differences were established at $P < 0.05$.

Results and Discussion

Statistical Analysis

Whey protein isolates from two manufacturers (WPI 1 and WPI 2) were used to cover some of the differences that may be found among manufacturing processes. This was intended to establish the general effects of WPI rather than link to differences between sources of WPI. Table 1 shows the statistical results when WPI sources were analyzed jointly.

Table 1. Tests of factor effects, using analysis of variance (ANOVA) (Data of WPI 1 and WPI 2 were analyzed jointly.)

Source of variance	*Properties*	*F*	*p-value*
WPI source	Overrun	9.47	0.0036
	Yield stress	1180	<0.0001
	Drainage 1/2 life	82.5	<0.0001
	Dynamic viscosity	16.6	0.0002
	Interfacial tension	68.6	<0.0001
	Cake volume	74.2	<0.0001
WPI/EWP ratio	Overrun	3.84	0.0094
	Yield stress	232	<0.0001
	Drainage 1/2 life	185	<0.0001
	Dynamic viscosity	14.9	<0.0001
	Interfacial tension	120	<0.0001
	Cake volume	121	<0.0001
Sucrose	Overrun	52.8	<0.0001
	Yield stress	68.8	<0.0001
	Drainage 1/2 life	126	<0.0001
	Dynamic viscosity	759	<0.0001
	Interfacial tension	0.99	0.323
	Cake volume	92.9	<0.0001

Significant differences ($P < 0.05$) existed for all properties when analyzed between WPI 1 and WPI 2, among five WPI/EWP ratios (100/0, 75/25, 50/50, 25/75 and 0/100), and between no sucrose and 12.8% (w/v) sucrose content (with the exception of the insignificant sucrose effect on interfacial tension). Since significant differences were detected for all properties between two sources of WPI (Table 1), data for WPI 1 and WPI 2 were analyzed separately (Table 2).

Table 2. Tests of factor effects, using analysis of variance (ANOVA) (Data of WPI 1 and WPI 2 were analyzed separately.)

Source of variance	*Properties*	*WPI*	*F*	*p-value*
WPI/EWP ratio	Overrun	WPI 1	3.19	0.0354
		WPI 2	1.97	0.133
	Yield stress	WPI 1	171	<0.0001
		WPI 2	268	<0.0001
	Drainage 1/2 life	WPI 1	78.5	<0.0001
		WPI 2	232	<0.0001
	Dynamic viscosity	WPI 1	19.5	<0.0001
		WPI 2	1.39	0.274
	Interfacial tension	WPI 1	69.1	<0.0001
		WPI 2	52.9	<0.0001
	Cake volume	WPI 1	31.6	<0.0001
		WPI 2	120	<0.0001
Sucrose	Overrun	WPI 1	102	<0.0001
		WPI 2	0.71	0.407
	Yield stress	WPI 1	117	<0.0001
		WPI 2	4.12	0.0605
	Drainage 1/2 life	WPI 1	7.20	0.0136
		WPI 2	464	<0.0001
	Dynamic viscosity	WPI 1	373	<0.0001
		WPI 2	386	<0.0001
	Interfacial tension	WPI 1	0.01	0.909
		WPI 2	3.51	0.0716
	Cake volume	WPI 1	49.0	<0.0001
		WPI 2	44.6	<0.0001

Changes in the WPI/EWP ratio cause significant effects ($P < 0.05$) in all properties for WPI 1 but failed to be significant for WPI 2 regarding overrun and dynamic viscosity. Likewise, sucrose had a significant ($P < 0.05$) effect on all properties of WPI 1 except for interface tension, while sucrose did not alter overrun, yield stress and interfacial tension for WPI 2 (Table 2). The mechanisms for these differences will be discussed in the following sections.

Foam Stability (drainage ½ life)

Polyhedral foams are composed of air bubbles separated by thin films, with Plateau borders at the intersection of three thin films. Gravity causes liquid to move through the network of Plateau borders and thin films, resulting in foam drainage (Wang and Narsimhan, 2006). The rate of film drainage between bubbles can be predicted by the theoretical model shown in Equation 5:

$$V = \frac{2h^3 \Delta P}{3\mu R^2} \qquad \text{Equation 5}$$

where h is the lamella film thickness, μ is dynamic viscosity, R is the radius of the bubble, and ΔP is the difference between the capillary hydrostatic pressure (P_c) and the disjoining pressure (Π_d) between the interfaces of lamella film (Damodaran, 2005).

A high continuous phase dynamic viscosity can slow the rate of drainage (Pugh, 1996). Foam drainage ½ life was plotted against dynamic viscosity of pre-foam solutions (Figure 2) to explore relationships between the two parameters as described by Equation 5.

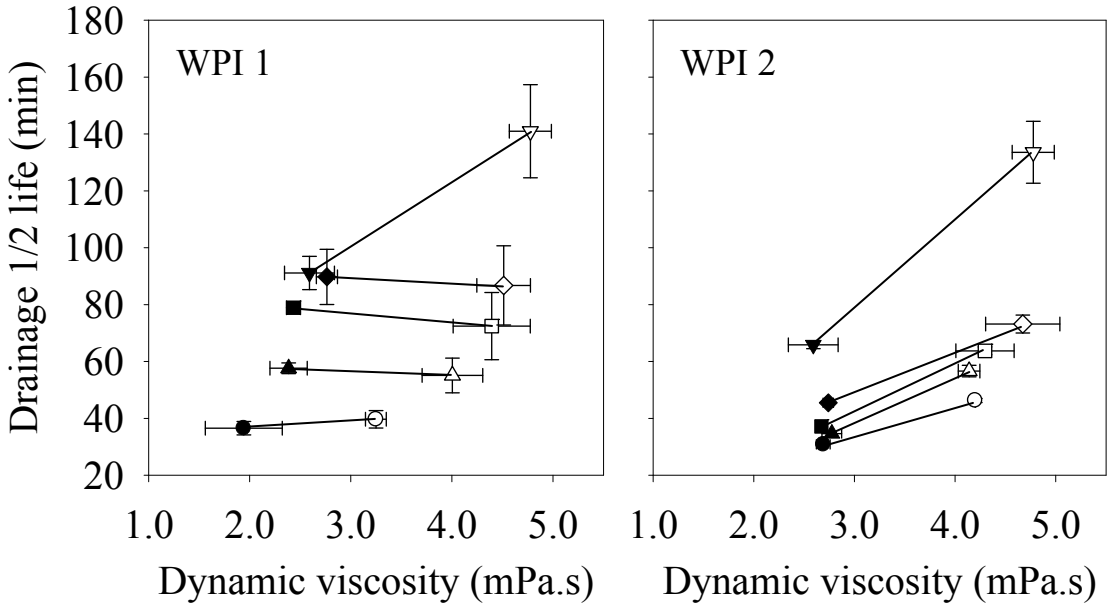

Figure 2. Foam drainage ½ life against pre-foam solution dynamic viscosity of 10% (w/v) protein solutions at pH 7, both in the presence (open symbols) and absence (closed symbols) of 12.8% (w/v) sucrose. ● WPI ▲75WPI/25EWP ■ 50WPI/50EWP ◆ 25WPI/75EWP ▼ EWP. Error bars are standard deviations of mean values. Viscosity data are calculated from power law model at a shear rate of 8.5 s^{-1}. The lines are drawn to guide the eye.

Apparent dynamic viscosity data of all solutions were calculated at 8.5 s^{-1} based on a power law model fit of the shear rate sweep (Equation 4). A shear rate of 8.5 s^{-1} was chosen because the typical shear rates experienced by materials under gravity induced drainage range from 0.1 s^{-1} to 10 s^{-1} (Barnes et al., 1989). The addition of sucrose showed a systematic viscosity increase in all treatments (Figure 2). Drainage 1/2 life was lowest for WPI and increased with progressive substitution of EWP. Most treatments followed the general trend of sucrose addition increasing viscosity but showing little effect on drainage 1/2 life, with the exception of 100% EWP. The addition of sucrose nearly doubled the drainage 1/2 life for 100% EWP foams, although the viscosity did not increase more for EWP than other treatments. This observation suggests the sucrose retarding effect on EWP foam drainage

was not simply due to increasing solution viscosity, since the WPI and WPI/EWP combination solutions also increased in viscosity. In addition to continuous phase dynamic viscosity, the radius of bubbles, thickness of lamella film, and ΔP also contribute to drainage rate according to Equation 5. Changes in bubble size and number are always occurring, corresponding to the processes of disproportionation and coalescence. The thickness of lamella film and ΔP are also altered. Sucrose possibly changed these parameters in different ways for whey and egg white proteins, resulting in a great decrease in EWP foam drainage and only slight effects on WPI and WPI/EWP foam drainage. With incorporation of WPI into EWP solutions, even with 25% replacement, the sucrose retarding effect on foam drainage was lowered compared to EWP alone. One hypothesis to explain this observation is that WPI may dominate bubble interfaces and determine foam properties when two proteins are mixed.

Interfacial Tension

Foam physical properties and stability also depend on characteristics of the air/water interfaces of bubbles. To investigate interfacial properties, interfacial tension and interfacial dilational rheology of pre-foam solutions were measured. Adsorption rates at the air/water interface of WPI, EWP and WPI/EWP solutions were evaluated by the rate of interfacial tension decline for newly formed drops (Myrvold and Hansen, 1998). Dynamic changes seen in interfacial tension of protein solutions are illustrated in Figure 3.

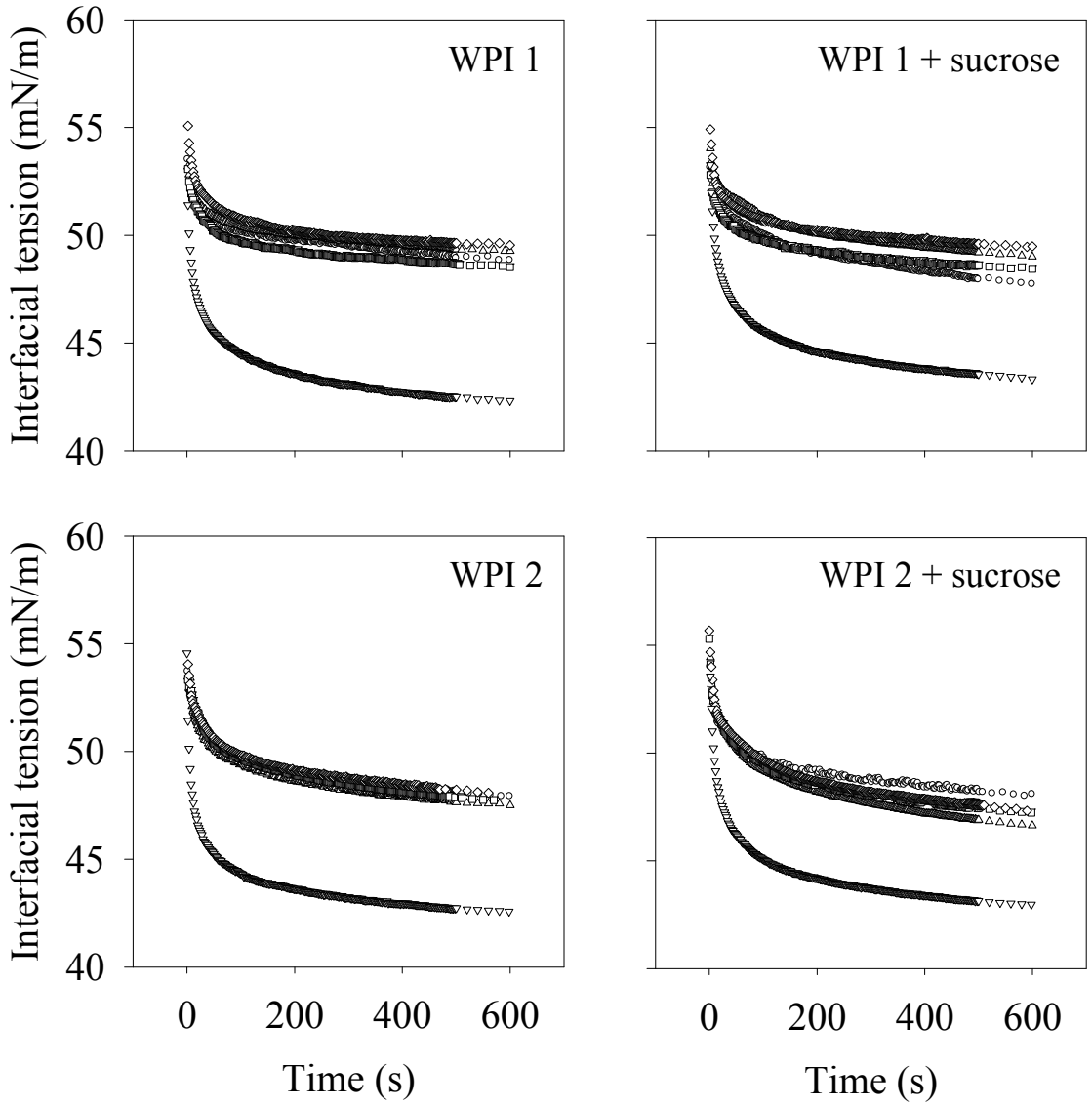

Figure 3. Typical dynamic interfacial tension measurements of 10% (w/v) protein solutions at pH 7, both in the presence and absence of 12.8% (w/v) sucrose. ○ WPI Δ 75WPI/25EWP □ 50WPI/50EWP ◊ 25WPI/75EWP ∇ EWP

EWP solutions exhibited the most rapid decreasing rates of interfacial tension, whereas all WPI/EWP solutions followed the pattern of WPI, both in the presence and absence of 12.8% (w/v) sucrose. Sucrose did not alter the adsorption patterns of protein

solutions except for a slightly increased EWP interfacial tension at the initial stage of adsorption.

The more rapid decreasing rates and lower values of interfacial tension of EWP than WPI were also previously reported by Davis and Foegeding (2007). Although EWP exhibited a more rapid adsorption rate, similar interfacial tension decline patterns of WPI/EWP and WPI solutions indicated that the surface active molecules in WPI rather than those in EWP appeared to occupy the interface when the two proteins were mixed. A similar relationship was observed in mixtures of β-casein and β-lactoglobulin at the air-water interface, where β-casein tended to dominate interfacial properties of the mixed system (Ridout et al., 2004). Competitive adsorption at an interface depends on factors beyond interfacial activity. If the protein reaching the interface first does not have a chance to unfold, it can be displaced by competing proteins (Dickinson, 1999). As a result, WPI/EWP interfaces demonstrated similar interfacial properties to WPI, in agreement with observations that foam properties of WPI/EWP foams tended to follow the pattern of WPI.

The major component in EWP, ovalbumin was found to adsorb less rapidly at the air/water interface in the presence of sucrose (Davis and Foegeding, 2007). In aqueous solutions, ovalbumin forms hydrogen bonds with sucrose, increasing the hydrophilic nature of the protein and decreasing its activity at the air-water interface (Antipova et al., 1999). The decreased hydrophobicity of ovalbumin with sucrose may explain the slightly higher interfacial tension of EWP at the initial adsorption stage after sucrose addition. Since the protein concentration (10%, w/v) was very high, the interfacial tension decreased rapidly after the initial stage due to the large amount of molecules available for adsorption.

The interfacial tension reached a more slowly declining value after 600 s of aging. The interfacial tension at 600 s was recorded and the averages for three replications of data are shown in Figure 4.

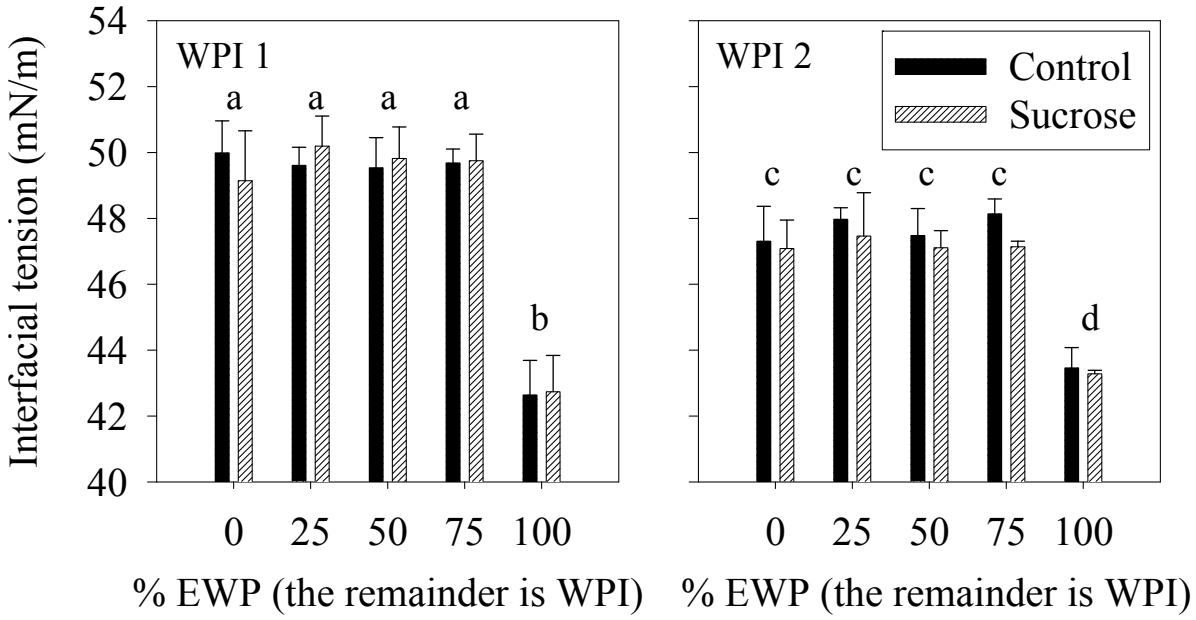

Figure 4. Interfacial tension at 600 s of 10% (w/v) protein solutions at pH 7, both in the presence and absence of 12.8% (w/v) sucrose. Error bars represent one standard deviation. Symbols appear on the figure. Means marked with the same letter are not significantly different from each other.

No significant difference was observed in interfacial tension of WPI and WPI/EWP within a type of WPI (WPI 1 or WPI 2), whereas interfacial tension of EWP was significantly lower than those of WPI and WPI/EWP. Sucrose had no significant effect (P = 0.909 for WPI 1 and P = 0.0716 for WPI 2, Table 2) on interfacial tension of all protein solutions.

Foam Yield Stress and Interfacial Rheology

Foams transform from viscous fluids to semi-solid like structures and exhibit yield stress values when the air phase fractions increase above the random close pack air phase fraction of 0.64 (Mason, 1999). As the air phase fractions of all samples were greater than 0.9, yield stress values were measured by a vane method. Foam yield stress has been previously modeled based on the model proposed by Princen and Kiss (1989) (Pernell et al., 2002a; Davis and Foegeding, 2004; Davis et al., 2004):

$$\tau_0 = \frac{\gamma}{R_{32}} \phi^{1/3} Y(\phi) \qquad \text{Equation 6}$$

where τ_0 is yield stress, γ is interfacial tension, R_{32} is surface-volume mean drop radius, ϕ is the volume fraction of the dispersed phase, and $Y(\phi)$ is an experimentally derived fitted parameter.

Foegeding et al. (2006) suggested that the Princen and Kiss (1989) model could be modified for protein foams by replacing interfacial tension with interfacial dilational elasticity, as positive correlation between interfacial dilational elastic moduli and foam yield stress was observed in previous studies on WPI (Davis and Foegeding, 2004; Davis et al., 2004, 2005). A plot of interfacial dilational elastic moduli (E') verses foam yield stress (τ_0) (Figure 5) displayed a similar positive relationship between E' and τ_0 as was observed in previous studies; however, this was only true for WPI and WPI/EWP combinations.

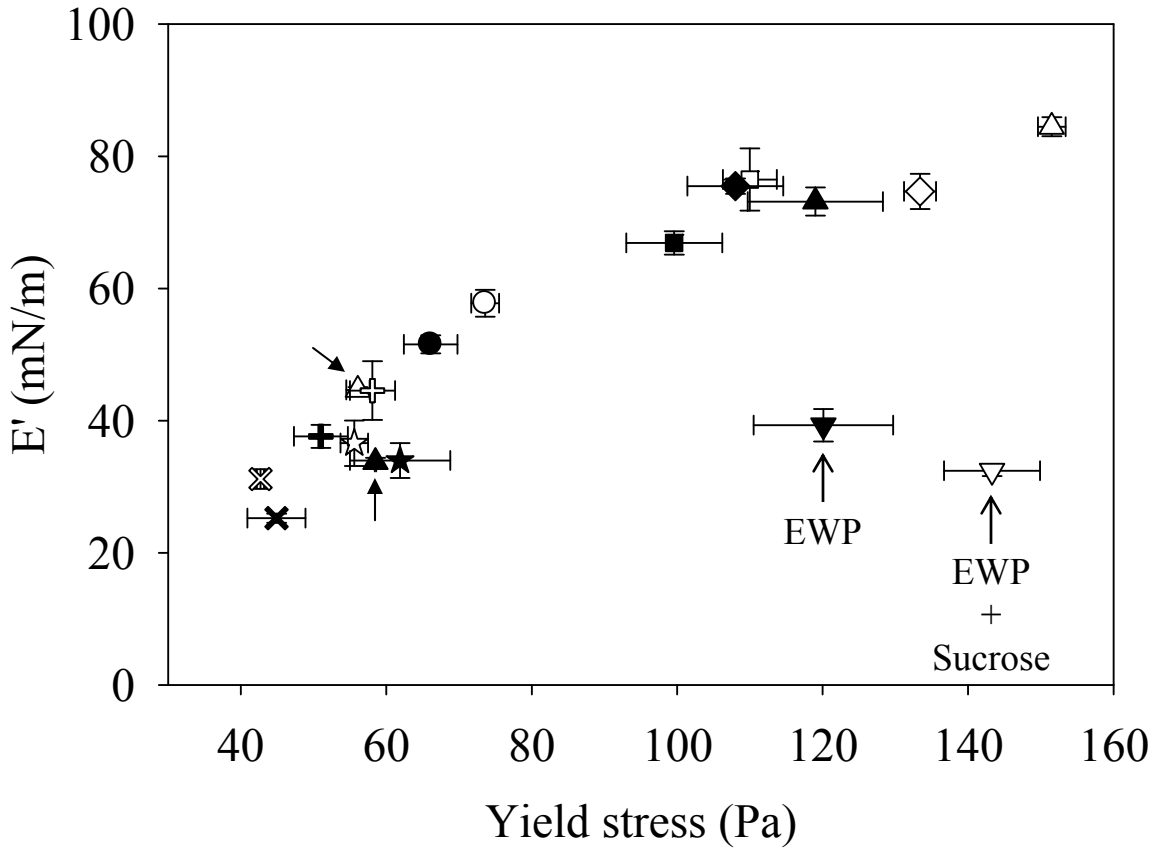

Figure 5. Changes in interfacial dilational elasticity with yield stress. 10% (w/v) protein solutions at pH 7, both in the presence (closed symbols) and absence (open symbols) of 12.8% (w/v) sucrose. ● WPI 1, ▲ 75WPI 1/25EWP, ■ 50WPI 1/50EWP, ◆ 25WPI 1/75EWP, X WPI 2, ▲ 75WPI 2/25EWP (with arrow indicated), + 50WPI 2/50EWP, ★ 25WPI 2/75EWP, ▼ EWP. Symbols for EWP and EWP + sucrose appear on the figure. Error bars are standard deviations from mean values.

The deviation of EWP from this relationship further supports the dissimilarity of EWP from WPI and WPI/EWP combinations in interfacial and foam properties. The E' and τ_0 of WPI 1 and WPI 1/EWP combinations were higher than those of WPI 2, but the general relationship between E' and τ_0 was observed for both WPI 1 and WPI 2. Interestingly, the

mixed WPI/EWP solutions had higher E' and τ_0 values than WPI alone. Sucrose decreased E' and τ_0 of WPI and WPI/EWP combinations.

E' reflects the resistance of the adsorbed molecules to dilational deformations and depends on molecule adsorption/desorption, inter-molecular structural rearrangement, and intra-molecular interactions at interfaces. The same interfacial tension of WPI and WPI/EWP combinations revealed that a component of WPI dominated the interface. This was true for both WPI 1 and WPI 2. The presence of EWP molecules in WPI/EWP combinations may affect interfacial tension gradients and inter-molecular interactions at air/water interfaces, resulting in higher E' of WPI/EWP combinations than WPI. In addition, the presence of EWP also decreased the concentration of WPI in solutions and influenced the adsorption/desorption rates of molecules during dilational deformation. The foam yield stress of WPI/EWP combinations changed with the interfacial rheology variations accordingly. This supports the hypothesis that whey proteins dominate interfaces in mixed systems.

The incorporation of 12.8% (w/v) sucrose had no significant effect on interfacial tension; but it decreased E' of WPI and WPI/EWP solutions and increased E' of EWP. The presence of 25% (w/w) sucrose was also found to decrease E' of WPI and to increase E' of EWP (Davis and Foegeding, 2007). Wilde et al. (1997) suggested that the addition of sucrose reduced protein aggregations and allowed more proteins to be involved in film formation at interfaces, resulting in a higher interfacial elasticity. However, Niño et al. (1997) observed that interfacial viscoelasticity of bovine serum albumin (BSA) decreased with increasing sucrose concentration, suggesting possible reduced protein-protein interactions in the

adsorbed layer. In our work, sucrose had opposite effects on interfacial rheology of WPI and EWP and introduced the same effect on WPI/EWP combinations as on WPI.

Angel Food Cakes

Angel food cake, a simple system composed of protein foam, sucrose, and flour, provides a model to study protein foam stability during heating. Because of the high sucrose content (~36% w/w in cake batters before baking) in angel food cakes, no-sucrose angel food cakes were prepared and compared to normal angel food cakes. Cake volumes are compared in Figure 6.

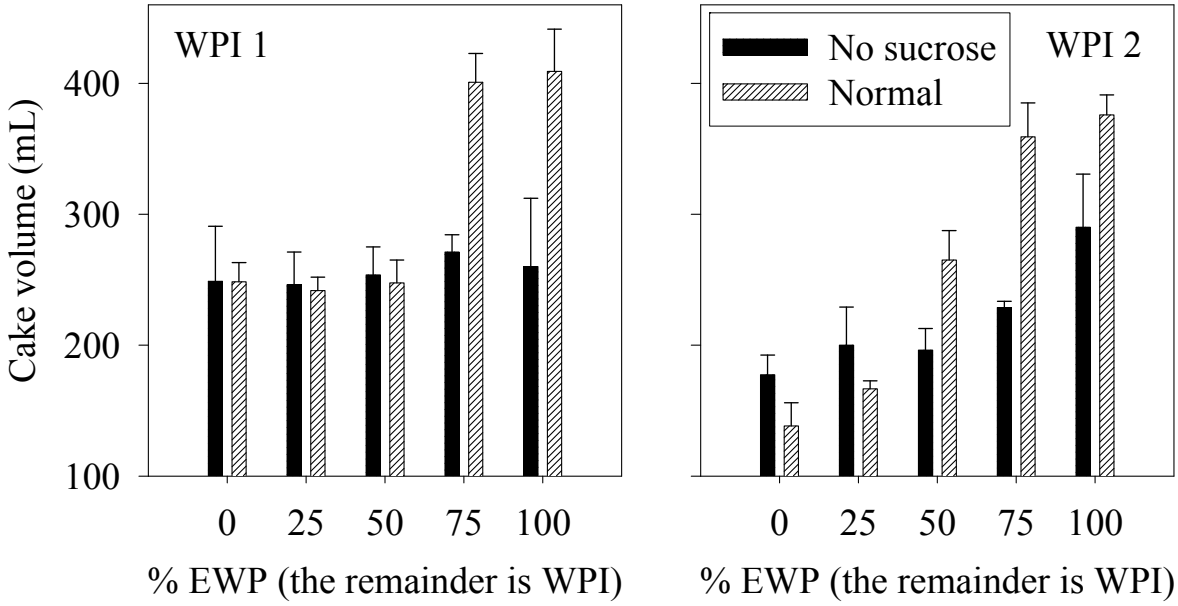

Figure 6. Volume of angel food cake prepared from 10% (w/v) protein solutions at pH 7. Error bars are standard deviations from mean values. Symbols appear on the figure.

The main trend seen in angel food cake volumes was the increased volume of normal cakes made with 100% EWP and 25% WPI/ 75% EWP. This is similar to what was observed by Arunepanlop et al. (1996). Within each type of WPI (WPI 1 or WPI 2), these two

treatments were not significantly different from each other, but were statistically different from cakes produced with 50% or more WPI.

The addition of sucrose improved angel food cake volume when cakes contained a majority of EWP (>50%). A cake matrix is built on a protein foam structure resulting from the thermal denaturation of proteins and starch gelatinization during baking (Pernell et al., 2002b). Addition of sucrose can increase the starch gelatinization temperature and decrease the percent gelatinization (Munzing and Brack, 1991). This effect slows down the cake matrix solidification and allows further expansion of cake batters at high temperature. Pernell et al. (2002b) measured the cake height changes of angel food cake containing WPI or EWP during baking and found that cakes containing whey proteins had a lower ability to prevent collapse once starch gelatinization started during baking. As sucrose increases the starch gelatinization temperature, cake batters containing EWP can achieve further expansion at high temperature range before starch gelatinization and maintain this volume till the end of baking; however, cake batters with WPI cannot and collapsed at the high temperature range. Our results suggested that the angel food cake batters rich in EWP (>50%) have the ability to prevent collapse at the high temperature range and resulted in increased cake volume due to the combined effects of sucrose and egg white proteins.

As seen in Figure 6, 25% WPI/75% EWP and 100% EWP normal angel food cakes exhibited similar volumes for both WPI 1 and WPI 2. However, images of freshly cut cake sections revealed differences in internal structural features of the two cakes (Figure 7).

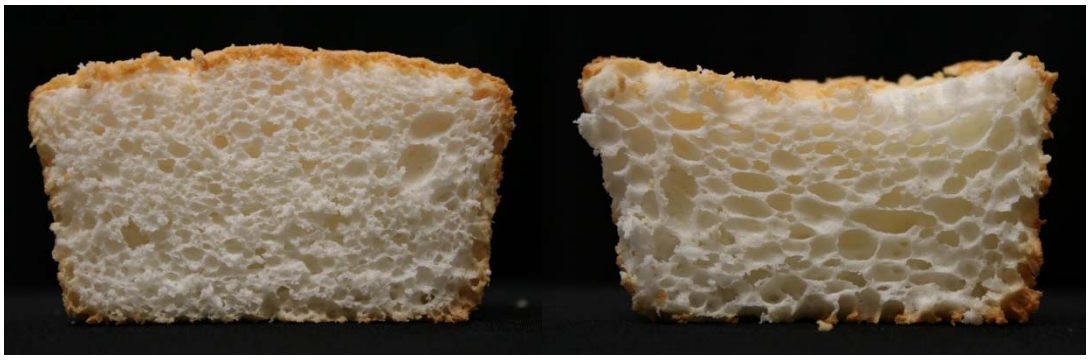

Figure 7. Cross section images of angel food cakes prepared with 100% EWP (left) and 25% WPI/75% EWP (right).

The concave shape of the 25% WPI/75% EWP cake cross-section (Figure 7) reflected some collapse. Previous studies indicated that angel food cakes made with whey proteins expanded to a maximum height then collapsed during baking (DeVilbiss et al., 1974; Pernell et al., 2002b). The 100% EWP cake displayed a fine structured matrix with many small, uniformly sized air cells and only a few larger air cells. The 25% WPI/75% EWP cake showed a coarser structure with a predominance of larger air cells. Foam destabilization processes such as coalescence and disproportionation caused an increase in air bubble size and a decrease in cake quality. In contrast, the fine structure of the EWP cake revealed the ability of EWP to maintain smaller bubble size during baking. The coarse structure and predominance of large air cells in 25% WPI/75% EWP cakes indicated loss of this ability after replacing 25% EWP with WPI. Based on interfacial results, this appears to be due to whey proteins displacing egg white proteins at the air-water interface and forming an interfacial film that was less stable during heating as compared to an egg white protein film.

Arunepanlop et al. (1996) observed the inadequate performance of WPI in EWP replacement angel food cakes in an earlier study and considered the intrinsic compositional and conformational differences in WPI and EWP that affect their heat-induced denaturation

and coagulation properties as the reasons. We have shown that WPI dominated the interfaces of protein mixtures and that the interfacial characteristics of bubbles in WPI/EWP cake batters followed that of WPI. The presence of EWP in the liquid phase surrounding the bubbles probably assisted cake matrix formation of WPI/EWP angel food cakes, producing cakes of similar volumes (e.g. at 25%WPI/75%EWP) but different textures.

Conclusions

Combinations of WPI and EWP did not show an additive effect in foaming properties, interfacial measurements, or cake volume. The addition of 12.8% (w/v) sucrose showed a large increase in foam stability for foams made with EWP but exhibited little impact on stability for foams made with WPI or WPI/EWP combinations. This increased stability cannot be explained by an increase in viscosity. Interfacial tension measurements showed that WPI/EWP combinations followed the pattern of WPI, indicating that WPI was dominating the interface when both proteins were present. Angel food cakes produced with and without sugar resulted in high volume cakes only in the presence of sugar and at levels of 75% EWP or 100% EWP, leading to the hypothesis that sugar and >50% of EWP needs to be present to stabilize cake volume. However, although cakes containing 25% WPI had volumes similar to 100% EWP, the texture was different with whey proteins causing a coarser bubble structure and concave shape. Changes in foam properties and angel food cake quality in egg white and whey protein mixtures can be attributed to whey proteins dominating the air/water interface, and different effects of sugar on egg white and whey protein interfacial elasticity.

REFERENCES

Antipova AS, Semenova MG, Belyakova LE. 1999. Effect of sucrose on the thermodynamic properties of ovalbumin and sodium caseinate in bulk solution and at air-water interface. Colloids Surf B: Biointerfaces 12: 261-270.

Arunepanlop B, Morr CV, Karleskind D, Laye I. 1996. Partial replacement of egg white proteins with whey proteins in angel food cakes. J Food Sci 61: 1085-1093.

Aryana KJ, Haque ZZ, Gerard PD. 2002. Influence of whey protein concentrate on the functionality of egg white and bovine serum albumin. Int J Food Sci Tech 37: 643-652.

Barnes HA, Hutton, JF, Walters K. 1989. An introduction to rheology. Amsterdam: Elsevier. p199.

Campbell GM, Mougeot E. 1999. Creation and characterization of aerated food products. Trends Food Sci Tech 10: 283-296.

Damodaran S. 2005. Protein stabilization of emulsions and foams. J Food Sci 70: R54-R66.

Davis JP, Foegeding EA. 2004. Foaming and interfacial properties of polymerized whey protein isolate. J Food Sci 69: C404-C410.

Davis JP, Foegeding EA. 2007. Comparisons of the foaming and interfacial properties of whey protein isolate and egg white proteins. Colloids Surf B: Biointerfaces 54: 200-210.

Davis JP, Doucet D, Foegeding EA. 2005. Foaming and interfacial properties of hydrolyzed β-lactoglobulin. J Colloid Interface Sci 288: 412-422.

Davis JP, Foegeding EA, Hansen FK. 2004. Electrostatic effects on the yield stress of whey protein isolate foams. Colloids Surf B: Biointerfaces 34: 13-23.

DeVilbiss ED, Holsinger VH, Posati LP, Pallansch MJ. 1974. Properties of whey protein concentrate foams. Food Tech 28: 40-48.

Dickinson E. 1999. Review: Adsorbed protein layers at fluid interfaces: interactions, structure and surface rheology. Colloids Surf B: Biointerfaces 15: 161-176.

Dzuy NQ, Boger DV. 1985. Direct Yield Stress Measurement with the Vane Method. J Rheology 29: 335-347.

Foegeding EA, Luck PJ, Davis JP. 2006. Factors determining the physical properties of protein foams. Food Hydrocolloids 20: 284-292.

Johnson TM, Zabik ME. 1981. Egg albumen proteins interactions in an angel food cake system. J Food Sci 46: 1231-1236.

Luck PJ, Bray N, Foegeding EA. 2002. Factors determining yield stress and overrun of whey protein foams. J Food Sci 67: 1677-1681.

Mason TG. 1999. New fundamental concepts in emulsion rheology. Curr Opin Colloid Interface Sci 4: 231-238.

Munzing K, Brack G. 1991. DSC-studies of flour confectionery. Thermochimica Acta 187: 167-173.

Myrvold R, Hansen FK. 1998. Surface elasticity and viscosity from oscillating bubbles measured by automatic axisymmetric drop shape analysis. J Colloid Interface Sci 207: 97-105.

Peter PN, Bell RW. 1930. Normal and modified foaming properties of whey-protein and egg-albumin solutions. Ind Eng Chem 22: 1124-1128.

Pernell CW, Foegeding EA, Daubert CR. 2000. Measurement of the yield stress of protein foams by vane rheometry. J Food Sci 65: 110-114.

Pernell CW, Foegeding EA, Luck PJ, Davis JP. 2002a. Properties of whey and egg white protein foams. Colloids Surf A: Physicochemical and Engineering Aspects 204: 9-21.

Pernell CW, Luck PJ, Foegeding EA, Daubert CR. 2002b. Heat-induced changes in angel food cakes containing egg-white protein or whey protein isolate. J Food Sci 67: 2945-2951.

Phillips LG, Haque Z, Kinsella JE. 1987. A method for the measurement of foam formation and stability. J Food Sci 52: 1074-1077.

Phillips LG, Geman JB, Oneill TE, Foegeding EA, Harwalkar VR, Kilara A, Lewis BA, Mangino ME, Morr CV, Regenstein JM, Smith DM, Kinsella JE. 1990. Standardized procedure for measuring foaming properties of three proteins, a collaborative study. J Food Sci 55: 1441.

Princen HM, Kiss AD. 1989. Rheology of foams and highly concentrated emulsions. 4. An experimental study of the shear viscosity and yield stress of concentrated emulsions. J Colloid Interface Sci 128:176-187.

Pugh RJ. 1996. Foaming, foam films, antifoaming and defoaming. Adv Colloid Interface Sci 64: 67-142.

Richert SH. 1979. Physical-Chemical properties of whey protein foams. J Agric Food Chem 27: 665-668.

Ridout MJ, Mackie AR, Wilde PJ. 2004. Rheology of mixed β-casein/ β-lactoglobulin films at the air-water interface. J Agric Food Chem 52: 3930-3937.

Niño MRR, Wilde PJ, Clark DC, Husband FA, Rodríguez Patino JM. 1997. Rheokinetic analysis of protein films at the air-aqueous phase interface. 1. Bovine serum albumin adsorption on ethanol aqueous solutions. J Agric Food Chem 45: 3010-3015.

Steffe JF. 1992. Rheological Methods in Food Process Engineering. 2nd ed. East Lansing, MI: Freeman Press. p418.

Wang Z, Narsimhan G. 2006. Model for Plateau border drainage of power-law fluid with mobile interface and its application to foam drainage. J Colloid Interface Sci 300: 327-337.

Wilde PJ, Niño MRR, Clark DC, Rodríguez Patino JM. 1997. Molecular diffusion and drainage of thin liquid films stabilized by bovine serum albumin—Tween 20 mixtures in aqueous solutions of ethanol and sucrose. Langmuir 13: 7151–7157.

CHAPTER 3

Manuscript to be submitted for publication

Effects of Sucrose on the Foaming and Interfacial Properties of Egg White Protein and Whey Protein Isolate

Authors: Xin Yang and E. Allen Foegeding

Abstract

The effects of sucrose on the foaming and interfacial properties of egg white protein (EWP) and whey protein isolate (WPI) have been investigated for solutions containing 10% (w/v) protein. Increasing sucrose concentration (0 to 63.6 g/100 mL) gradually decreased foam overrun and increased foam drainage ½ life. Confocal laser microscopic images showed that the initial bubble size in protein foams decreased, and grew at a slower rate over time with increasing sucrose concentration. Interfacial rheology measurements indicated that sucrose enhanced the interfacial elastic modulus (E') of EWP but reduced E′ of WPI, possibly due to different interfacial tensions (γ).A linear correlation was established between the change of bubble size over 20 min and the foam drainage ½ life regardless of protein type. Relationships between the change of bubble size over 20 min and E'/γ suggested that interfaces with $E'/\gamma>2$ can effectively slow bubble size growing in EWP foams, confirming theoretical predictions (Walstra, 2003); however, WPI foams exhibited a different behavior. The foam drainage ½ life was proportionally correlated to the bulk phase viscosity and the interfacial elasticity regardless of protein type, suggesting the foam destabilization changes can be slowed by a viscous continuous phase and elastic interfaces. Addition of sucrose altered volume of angel food cakes prepared from WPI foams but showed no improvement on the coarse structure. In conclusion, sucrose can modify bulk phase viscosity and interfacial rheology and therefore alter the foam microstructure and improve the stability of wet foams. However, the poor stability of whey proteins in the conversion from a wet to a dry foam (angel food cake) cannot be changed with addition of sucrose.

Key words: foam, interfacial rheology, yield stress, microstructure, angel food cake

Introduction

Foams provide a variety of quality attributes to food products. The appearance, texture and shelf-life of aerated products are determined by the amount of air incorporated and the sizes and physical stability of the bubbles (Campbell and Mougeot, 1999). Globular proteins, such as egg white proteins, are extensively used in aerated systems to stabilize the foam and enhance desirable features. A comparable foaming capacity of whey protein has been observed for a long time (Peter and Bell, 1930; Richert, 1979; Foegeding et al., 2002). However, substitution of whey proteins for egg white in angel food cake batters results in low cake volume and coarse cake structure (Arunepanlop et al., 1996; Pernell et al., 2002b). Angel food cake batter is a wet foam containing protein, sugar and flour, and transfers to a heat-set dry foam during baking. The final cake structure depends on thermal expansion of air bubbles and formation of protein and starch networks (Pernell et al., 2002b). The lack of heat stability of whey protein foams were observed and postulated to be responsible for its poor functionality in angel food cakes (DeVilbiss et al., 1974; Arunepanlop et al., 1996; Pernell et al., 2002b). Berry (2008) investigated the microstructural change of angel food cake batters during heating process using confocal laser scanning microscopy (CLSM). She found that cake batters prepared from egg white protein foams formed a network that stabilized bubble structure; however, the bubbles in cake batters containing whey protein isolate continuously grew. In addition, the appearance of large bubbles in cake batters containing whey protein isolate was observed at room temperature, suggesting destabilization changes occurred even before heating. A critical step during cake batter preparation is to blend dry ingredients (sugar and flour) to a wet protein foam. The unstable characteristic of

whey protein cake batters can be due to mixing process or addition of sugar and flour, which involves small molecules (sugar) and polymers (starch and protein) in the systems. The concentration of sugar in a normal angel food cake is extremely high (88.6 g/100 mL pre-foam protein solutions). In Chapter 1, we found that addition of sugar assisted the formation of cake matrix for angel food cake batters containing a high percentage of egg white proteins, suggesting an important role of sugar on protein foam functionality in angel food cakes.

The effect of sucrose on the physical properties of protein foams has been investigated in several studies (Davis and Foegeding, 2007; Raiko et al., 2007; Yankov and Panchev, 1996; Phillips et al., 1989). Generally speaking, the addition of sucrose can decrease foam overrun and increase foam stability against drainage due to an increase in bulk phase viscosity. A straight-line plot was established between foam drainage ½ life and solution apparent viscosity on a log-log scale for egg white protein with addition of different amounts of sugar (Lau and Dickinson, 2005), while a positive logarithmic relationship was suggested for whey protein isolate foams (Foegeding et al., 2006). Microscopic images of egg white protein foams indicated that increasing sugar content led to much smaller bubble sizes and higher bubble density, corresponding to a decrease of foam overrun (Raikos et al., 2007). Dynamic image analysis of egg white foam microstructure indicated that the destabilization changes mainly involved creaming of large bubbles and disproportionation of neighbor bubbles, which were accelerated after reducing sugar content (Lau and Dickinson, 2005). In addition to the bulk phase viscosity, sucrose can alter the interfacial properties of proteins. Ruíz-Henestrosa et al. (2008) found that sucrose slowed the adsorption of soy globulins, contributing to the decrease of foam overrun. They also established positive

correlations between foam drainage ½ life and interfacial dilational elasticity for soy proteins, suggesting that the modification of interfacial viscoelasticity caused by sugar may influence foam stability. Davis and Foegeding (2007) found that sucrose (25% w/w) increased the foam yield stress and drainage resistance for egg white protein whereas it minimally affected these properties for whey protein isolate, possibly due to its opposite effects (positive on egg white protein and negative on whey protein isolate) on the interfacial elasticity of proteins. This suggested that sucrose can generate protein-specific effects on the interfacial and foaming properties.

Although many studies investigated sucrose effects on protein foaming properties, most of them were conducted using a single level of sucrose content. A quantitative study may provide a further view of the sucrose effect on protein foams and assist exploring the differences of foaming functionalities between whey and egg white proteins. The goal of this study is to establish quantitative relationships between foaming properties and the characteristics of protein solutions and interfaces via varying sucrose concentration. Two major foaming ingredients – egg white protein and whey protein isolate were evaluated. The foam characteristics (overrun, yield stress, drainage ½ life and microstructure), the bulk solution viscosity, and interfacial rheology were measured and correlated with each other using theoretical models.

Materials and Methods

Materials

Spray dried egg white protein (82% protein, dry basis) was obtained from Primera Foods (Cameron, WI) and stored at 4 °C. A commercial sample of whey protein isolate (BiPro, 93% protein, dry basis) was supplied by Davisco Foods International, Inc. (Le Sueur, MN) and stored at room temperature (22 ± 2 °C). Cake flour and 10x powdered sugar were purchased from a local grocery store. Sucrose (ACS) were obtained from Fisher Scientific Inc. (Fair Lawn, NJ). Sodium fluorescein was obtained from Sigma-Aldrich (St. Louis, MO). All other chemicals were of reagent grade quality. Deionized water was obtained using a Dracor Water Systems (Durham, NC) purification system. The resistivity was a minimum of 18.2MΩ cm.

Protein solutions

Protein powders were mixed with deionized water and stirred overnight (14 to 16 hours) at room temperature (22 ± 2 °C) to allow for full hydration. Before final adjustment to 10% (w/v) protein, the pH was adjusted to 7.0. When required, sucrose was added to the protein solutions on a *g/100 mL* basis.

Foam Generation

Protein foams were generated using a Kitchen Aid Ultra Power Mixer (Kitchen Aid, St. Joseph's, MI) with a 4.3 L stationary bowl and rotating beaters. Two hundred mL of protein solutions were whipped for 15 min for EWP or 20 min for WPI at a speed setting of 8 (planetary rpm of 225 and beater rpm of 737). The 15 min whip time for EWP solutions was used to prevent overbeating (Pernell et al., 2002a).

Yield stress

Yield stress was measured using a vane attachment to a Brookfield 25xLVTDV-ICP viscometer (Brookfield Engineering Laboratories, Inc., Middleboro, MA) (Pernell et al., 2000). Immediately after foam generation, the vane (10 mm in diameter and 40 mm in length) was gently inserted into the foam until the top edge was even with the foam surface. The vane was then rotated at a speed of 0.3 rpm. Maximum torque response (M_0) was used to calculate yield stress according Equation 1 (Dzuy and Boger, 1985; Steffe, 1996):

$$\tau_0 = \frac{M_0}{\left(\frac{h}{d} + \frac{1}{6}\right)\left(\frac{\pi d^3}{2}\right)} \qquad \text{Equation 1}$$

where τ_0 is the yield stress, and h and d are the height and diameter of the vane. Three consecutive measurements throughout the bowl were completed within 5 min after foam generation and averaged. A minimum of three replications were conducted for each treatment.

Overrun

Overrun was measured according to the method of Phillips et al. (1987). After yield stress measurement, the foam was gently scooped into a standard weigh boat (100 mL), leveled using a rubber spatula, and weighed. This process was repeated 3 times per foam and was completed within 10 min after whipping. The mean of 3 weights was used for overrun and air phase fraction calculations according to Equation 2 and Equation 3 (Campbell and Mougeot, 1999):

$$\%\text{Overrun} = \frac{(\text{wt. 100 mL solution}) - (\text{wt. 100 mL foam})}{\text{wt. 100 mL foam}} \times 100 \qquad \text{Equation 2}$$

$$\text{Air phase fraction } (\phi) = \frac{\%\text{overrun}}{(\%\text{overrun} + 100)} \qquad \text{Equation 3}$$

Each treatment was replicated a minimum of three times.

Foam stability (drainage ½ life)

Foam stability was measured by recording the length of time required for half of the pre-foam mass to drain (Phillips et al., 1989). Special bowls with a 6-mm diameter hole in the bottom were used for stability measurements. Immediately after the final overrun measurement, the bowl was placed in a ring stand over a scale with a weigh boat and the hole uncovered. The time necessary for half the mass to drain was recorded as the drainage ½ life. The mass of foam removed during the overrun measurements (less than 20%) was subtracted when calculating half of the pre-foam mass. The starting time for these measurements was taken as immediately after foam formation. Each treatment was replicated for a minimum of three times to obtain average drainage ½ life.

Viscosity measurements

Viscosity of pre-foam protein solutions was measured on a controlled stress rheometer (StressTech; Reologica Instruments AB, Lund, Sweden) using cup and bob geometry (measuring system CCE25) according to the method of Davis and Foegeding (2004). After a pre-shear at 50 s^{-1} for 30 s, viscosity was measured over a range of shear rates (0.5 s^{-1} to 225 s^{-1}). The rheological behavior of protein solutions was described by a power law model as shown in Equation 4:

$$\sigma = K\dot{\gamma}^{n} \qquad \text{Equation 4}$$

where σ and $\dot{\gamma}$ are shear stress and shear rate, and K and n are consistency constant and flow behavior index, respectively. Shear stress and shear rate data were fit to a power law model and the consistency constant and flow behavior index were calculated. All measurements were at room temperature (22 ± 2 °C) and replicated a minimum of three times.

Interfacial tension

Interfacial tension of pre-foam solution was measured using a pendant drop method (Myrvold and Hansen, 1998). An automated contact angle goniometer (Rame-Hart Inc, Mountain Lakes, NJ) was used for data collection and calculations in combination with the DROPimage computer program. A 16 μL pendant drop of pre-foam solution was generated by a computer-controlled syringe from a stainless-steel capillary into an environmental chamber with standing water to minimize evaporation. A digital camera captured the image of the pendant drop every 2 s for a total of 600 s and interfacial tension was calculated based on shape parameters. All samples were equilibrated to room temperature (22 ± 2 °C) before measurement. Values reported are the averages of a minimum of three replications. The system was calibrated using HPLC water with an interfacial tension of 72.3 mN/m at room temperature (22 ± 2 °C). The estimated experimental error is ± 1.0 mN/m. Values reported are represents of a minimum of three replications.

Interfacial dilational modulus

To measure dilational visco-elasticity of the interfaces, sinusoidal oscillations of the drops' areas (Myrvold and Hansen, 1998) were increased by volume amplitude of 0.5 μL at a frequency of 0.04 or 0.1 Hz. The resulting changes in interfacial tension and interfacial area

were collected and used to calculate the dilational elastic modulus (*E′*) utilizing the DROPimage software. Drops were suspended for 1 to 10 min before measurement. The *E′* values measured at 0.04 and 0.1 Hz were compared in Figure 1.

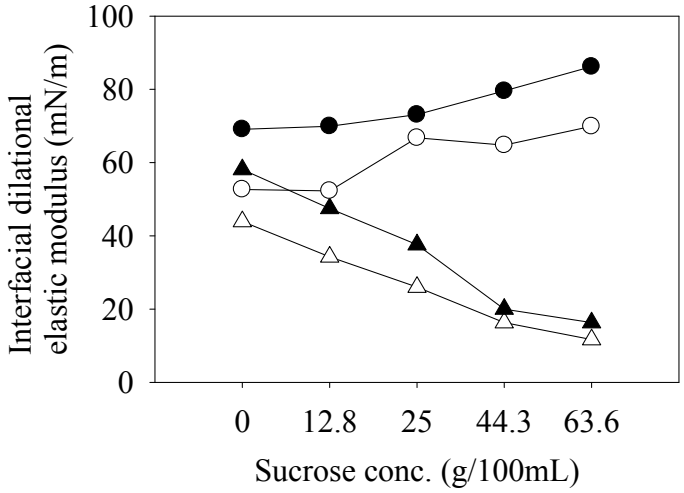

Figure 1. Interfacial dilational elastic modulus (*E′*) of 10% (w/v) protein solutions of egg white protein (EWP) and whey protein isolate (WPI) at pH 7.0 in the presence of different amounts of sucrose. Drops were suspended for 5 min before measurement. ● EWP 0.1 Hz ○ EWP 0.04 Hz ▲ WPI 0.1 Hz △ WPI 0.04 Hz.

Increasing frequency from 0.04 Hz to 0.1 Hz systematically shifted the interfacial dilational modulus values to a higher level. All the following measurements were conducted at a frequency of 0.1 Hz. Values reported are the averages of a minimum of three replications. The *E′* measured at 5 min were used for the calculations.

Density determination

DROPimage software requires inputs of component phase densities to calculate interfacial tension from drop shape analysis. A Mettler-Toledo DE40 density meter (Mettler-Toledo, Columbus, OH) equipped with a viscosity correction card was used to measure the

density of each solution at room temperature (22 ± 2 °C). The accuracy of the instrument is 1 $\times 10^{-4}$ g/cm^3. Each solution was evaluated in triplicate and averaged.

Confocal laser microscopic images

Confocal laser microscopic images of protein foams were taken on an inverted Leica DM IRBE (Heidelberg, Germany) confocal laser scanning microscope (CLSM) according to the method of Berry (2008). Sodium fluorescein was added at 0.1 mM to the protein solutions and dissolved readily before foaming. A foam sample was loaded into a single-welled microscope slide with a #1.5 cover slip attached to the bottom using silicon grease and immediately viewed. Samples were excited by an argon laser at 488nm. Light at a range from 500-550 nm was collected. A transmitted light differential interference contrast (DIC) image was recorded simultaneously. The objective used for 10x magnification was an HC PL FLUOTAR 10.0x, with a 0.30 numerical aperture. Images were viewed using Leica confocal software (version 2.61).

Time lapse data was collected for all foam samples. A single plane was focused into the foam sample immediately after foam preparation and slide loading. Images were collected every 10 s for 20 min, scanning the same position of the foam sample. A time lapse video was combined from the 120 time lapse images per treatment using the Leica software.

For image analysis, three slides were prepared per treatment, with samples taken from three random positions in a foam. The three slides were rotationally scanned under the CLSM at 5 min intervals for 20 min. The imaging time difference between slides was no more than 1 min. The image analyzing results were averaged from the three slides for each treatment.

Image analysis

Image analysis was done using MetaMorph Imaging System software, version 6.1 (Molecular Devices, Downington, PA, USA). The procedure followed the method of Berry (2008). All images were converted to binary using the same threshold, allowing objects (air bubbles) to stand out against the background aqueous phase. Overlapping or touching bubbles were manually separated using a "cut" feature. Because of the variation in pixel brightness values, pixels may be missing from the center of some small bubbles. In this case, a "join" feature was used to manually outline these bubbles and to fill in their broken centers. Object (bubble) area was measured using an integrated morphometry analysis feature. The edge bubbles with less than 50% of their estimated area visible were manually de-selected before bubble area measurement, preventing skewing the bubble sizes to smaller areas due to only a small portion of the bubble being analyzed. Observations showed that objectives with areas of less than 10 pixels were not actual bubbles. To eliminate noise, these values were excluded from image data before further analysis. For each treatment, three sets of bubble area data were obtained from images.

Mean and median bubble areas were evaluated on the bubble area data set of each image. The average and standard deviation of "mean bubble area" and "median bubble area" were calculated from the data of three images per treatment.

Unfolding bubble size distribution

Bubble size distribution was analyzed using apparent bubble diameter, which was calculated from bubble area and assuming spherical shape. Three data sets of bubble diameter for each treatment were pooled into one data set as the two dimensional (2D)

original data before analysis. Mean and standard deviation were calculated from the natural logarithm of 2D original data and fitted into Lognormal probability density function (Equation 5). The normality of the natural logarithm of 2D original data was tested using Shapiro-Wilk test in SigmaPlot version 11.0 (Systat Software, Inc.). Frequency analysis was conducted for each 2D original data set using the SAS system 8.02 (SAS Institute, Inc.). Cumulative relative frequency data were fit using a 4-parameter Weibull cumulative distribution function (Equation 6) using the non-linear regression tool in SigmaPlot version 11.0 and 2-parameter Weibull cumulative distribution function (Equation 7) using Microsoft Office Excel 2007. Fitting data into different distribution functions can facilitate the use of the Cruz-Orive method for unfolding three dimensional (3D) size distributions with minimal irregularities (Fang et al., 1993). The log normal distribution of the bubble size in a bubble or a foam column was observed by Lage and Espósito (1999) and Calvert and Nezhati (1987) using microscopy techniques combined with image analyzing software. Magrabi et al. (1999) found that a Welbull type distribution best approximated the narrow bubble size distribution produced by a compressed-air foam generator, in which the bubble size was determined by the two-dimensional photographic method. In this study, the bubble size distribution was fitted using the Lognormal and Weibull probability density functions, with two types of Weibull functions tested. The 4-parameter Weibull function provides more accurate fit to the real bubble size distribution than 2-parameter Weibull function; however, the former predicted a minimum bubble size and had a cumulative value less than 1, contradicting to the real situation. The statistic functions are as following (Merran et al., 2000):

$$f(x;\mu,\sigma)=\frac{1}{\pi\sigma\sqrt{2\pi}}e^{\frac{(\ln(x)-\mu)^2}{2\sigma^2}}$$ Lognormal probability density function

Equation 5.1

$$f(x;\mu,\sigma)=\frac{1}{2}+\frac{1}{2}erf\left[\frac{\ln(x)-\mu}{\sigma\sqrt{2}}\right]$$ Lognormal cumulative distribution function

Equation 5.2

for $x > 0$, where μ and σ are the mean and standard deviation of the variable's natural logarithm.

$$f(x;a,x_0,b,c)=\frac{ac}{b}\left(\frac{x-x_0}{b}\right)^{(c-1)}e^{-\left(\frac{x-x_0}{b}\right)^c}$$ 4-parameter Weibull probability density function

Equation 6.1

$$f(x;a,x_0,b,c)=a\left[1-e^{-\left(\frac{x-x_0}{b}\right)^c}\right]$$ 4-parameter Weibull cumulative distribution function

Equation 6.2

for $x > x_0$, where $k > 0$ is the shape parameter and $\lambda > 0$ is the scale parameter of the distribution; and for $x \leq x_0$, $f(x; k, \lambda) = 0$.

$$f(x;\kappa,\lambda)=\frac{\kappa}{\lambda}\left(\frac{x}{\lambda}\right)^{(\kappa-1)}e^{-\left(\frac{x}{\lambda}\right)^\kappa}$$ 2-parameter Weibull probability density function

Equation 7.1

$$f(x;\kappa,\lambda)=1-e^{-\left(\frac{x}{\lambda}\right)^\kappa}$$ 2-parameter Weibull cumulative distribution function

Equation 7.2

for $x > 0$, where $k > 0$ is the shape parameter and $\lambda > 0$ is the scale parameter of the distribution; and for $x \leq 0$, $f(x; k, \lambda) = 0$.

The 2D bubble diameter distribution data was expanded to 3D distribution using Cruz-Orive coefficient table (Russ, 2005). Relative frequency histograms of 2D original data were plotted using SigmaPlot software, with 15 bins divided based on the range of each data set. Relative frequency histograms of 2D Lognormal, 2D 4-parameter Weibull and 2D 2-parameter Weibull data were calculated based on the cumulative distribution function. The relative frequency histograms of 2D bubble diameter distribution were converted into relative frequency histograms of 3D bubble diameter distribution. Mean diameter (mean D), median diameter (median D), mode diameter (mode D) and the Sauter mean diameter (R_{32}) were calculated from all data sets.

Angel Food Cake Preparation

Angel food cakes were prepared based on the method of Pernell et al. (2002b). The angel food cakes preparation process was as follows: 1. Foam was generated from protein solution; 2. Dry materials (flour and/or powdered sugar) were gently mixed into the foam; 3. The batter was distributed into the cake containers and bake at 204 °C for 14 min. Two types of angel food cakes were prepared. One had all powdered sugar added before foaming (ABF cakes) and the other had sugar added after foaming (AAF cakes) (Table 1). This is different from the method of Pernell et al. (2002b), in which the powder sugar was partially added into the protein solution before foam generation and partially added into the foams. After baking, the cakes were cooled upside down on a wire rack for 30 min at room temperature. After

cooling, cake volume was measured using a rapeseed displacement method (Pernell et al., 2002b). Three cakes were made from each batch of batter per treatment and all treatments were replicated twice.

Table 1 Composition of "adding sugar before foaming" (ABF) and "adding sugar after foaming" (AAF) cakes

Cake		**Before foaming**		**After foaming**	
Sugar conc. (g/100 mL)	*Type*	*Pre-foam solutions (mL)*	*10× powdered sugar (g)*	*Flour (g)*	*10× powdered sugar (g)*
0.00		200	0	66.0	0
4.27	ABF	200	8.54	66.0	0
4.27	AAF	200	0	66.0	8.54
8.53	ABF	200	17.1	66.0	0
8.53	AAF	200	0	66.0	17.1
12.8	ABF	200	25.6	66.0	0
12.8	AAF	200	0	66.0	25.6
25.0	ABF	200	50	66.0	0
25.0	AAF	200	0	66.0	50
44.3	ABF	200	88.6	66.0	0
44.3	AAF	200	0	66.0	88.6
88.6	ABF	200	177	66.0	0
88.6	AAF	200	0	66.0	177

Results and discussion

Foam overrun and drainage ½ life

Foam overrun was determined and plotted against solution apparent viscosity at sucrose concentrations varying from 4.27 to 63.6 g/100 mL (Figure 2A).

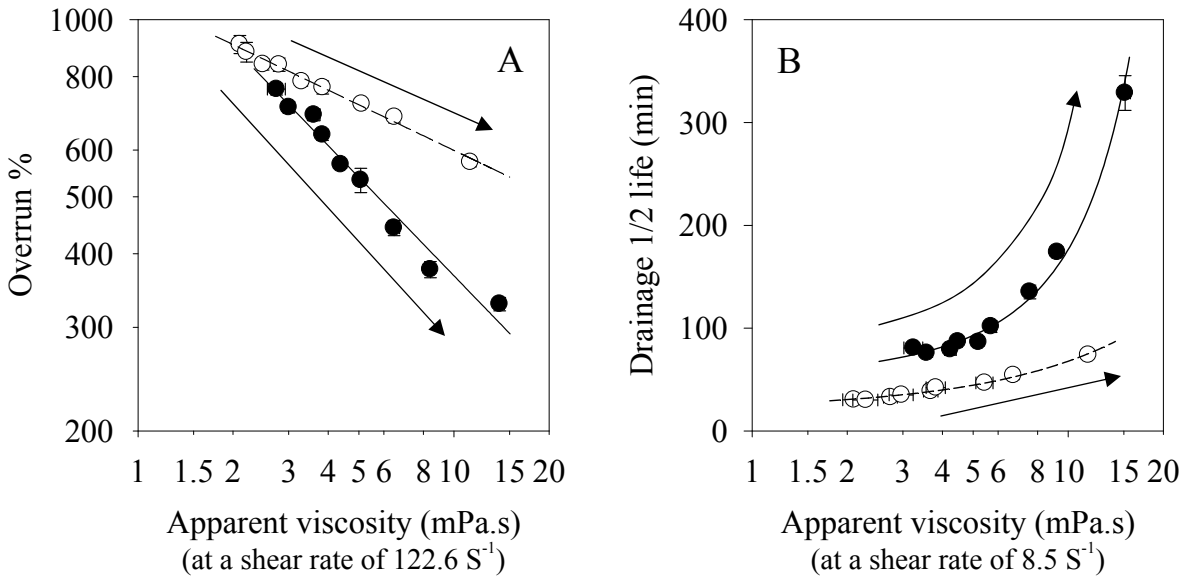

Figure 2. Changes in overrun (A) and drainage ½ life (B) with the solution apparent viscosity (at shear rates of 122.6 1/s for comparison with overrun and 8.5 1/s for comparison with drainage ½ life) for 10% (w/v) protein solutions of egg white protein (EWP, close symbols and solid lines) and whey protein isolate (WPI, open symbols and dashed lines) at pH 7.0 in the presence of different sucrose concentrations. Protein concentration is 10% (w/v) in solutions. Sucrose concentration (0.00, 4.27, 8. 56, 12.8, 19.0, 25.0, 35.0, 44.3, 63.6 g/100 mL) increased along with arrow direction.

Apparent viscosity was calculated based on the power law model (Equation 4) using a shear rate of 122.6 1/s. This shear rate is estimated from a simplified whipping model (Appendix I) and is among the typical shear rate range (10 to 10^3 1/s) for a mixing process in food industry (Steffe, 1996). WPI had a higher foam overrun than EWP at the same solution apparent viscosity (Figure 2A), suggesting a better foamability. Addition of sugar decreased protein foam overrun due to an increase in the solution viscosity, which impeded the incorporation of air bubbles (Dickinson, 1992). Two negative linear relationships were established between foam overrun and solution viscosity on a ln-ln scale for EWP and WPI respectively (Table 2).

Table 2. Relationships among physical properties of foams and interfaces for 10% (w/v) protein solutions of egg white protein (EWP) and whey protein isolate (WPI)

y	***x***	***Protein***	***Equations***	R^2
Overrun (%)	Apparent viscosity (mPa.s) (at 122.6 s^{-1})	EWP	$\ln y = 7.18 - 0.556 \ln x$	0.973
		WPI	$\ln y = 6.99 - 0.257 \ln x$	0.990
Drainage ½ life (min)	Apparent viscosity (mPa.s) (at 8.5 s^{-1})	EWP	$\ln y = 3.89 + 0.128x$	0.983
		WPI	$y = 4.66x + 21.2$	0.988
Mean bubble area (10^3 μm^2)	Apparent viscosity (mPa.s) (at 122.6 s^{-1})	All	$\ln y = 3.30 - 1.25 \ln x$	0.954
Median bubble area (10^3 μm^2)	Apparent viscosity (mPa.s) (at 122.6 s^{-1})	All	$\ln y = 2.67 - 1.29 \ln x$	0.942
Changes of mean bubble area over 20 min (10^3 μm^2)	Drainage ½ life (min)	All	$\ln y = 11.7 - 2.53 \ln x$	0.936
Changes of mean bubble area over 20 min (10^3 μm^2)	E'/γ	EWP	$y = -8.22x + 14.8$	0.753
		WPI	$y = 25.4x - 7.18$	0.846
Changes of mean bubble area over 20 min (10^3 μm^2)	E'/γ	EWP*	$y = -4.08x + 7.53$	0.967
		WPI*	$y = 32.8x - 10.8$	0.902
Drainage ½ life (min)	$\mu\left(E'/\gamma\right)$	All	$y = 11.1x + 12.8$	0.975

* The linear relationships were established based on protein solutions containing sucrose.

With increasing sucrose concentration, the foam overrun of EWP decreased in a faster rate than WPI, with an almost doubled negative slope (-0.556) than that of WPI (-0.257). If given a very low viscosity ($\mu \rightarrow 1$ mPa.s), EWP and WPI should have very similar foam overrun (the intercepts are 7.18 for EWP and 6.99 for WPI). This observation suggested that an increase in solution viscosity (altered by sucrose) can decrease the foam overrun of EWP to a greater extent than WPI. The solution viscosity can influence molecular diffusion, and therefore reduce the adsorption rate of proteins. The difference between the

two proteins may be due to the adsorption behavior of the proteins. Another important characteristic is the bubble size in a foam. Smaller bubble size corresponds to lower overrun (Raikos et al., 2007). The dissimilarity between the two protein foams can also be due to the bubble size.

Protein foam stability is influenced by the viscosity of the fluid continuous phase (Halling, 1981). A high viscosity should impede the movement of liquid through the network of thin films and plateau border, thereby slowing the drainage rate (Wang and Narsimhan, 2006). Foam drainage ½ life was plotted against solution apparent viscosity at a shear rate of 8.5 1/s (Figure 2B). This shear rate is among the typical shear rate range experienced by materials under gravity induced drainage (Barnes et al., 1989). Solution viscosity of both proteins increased gradually with sucrose concentration; however, the foam drainage ½ life of EWP increased exponentially while that of WPI increased linearly with increasing solution apparent viscosity (Figure 2B and Table 2). EWP foam had a longer drainage ½ life than WPI foam at the same solution apparent viscosity, in agreement with the observations in Chapter 2. Damodaran (2005) modeled the rate (V, with a unit of *m/s*) of film drainage between bubbles as the following equation:

$$V = \frac{2h^3 \Delta P}{3\mu R^2} \qquad \text{Equation 8}$$

where μ is the continuous phase viscosity, R is the bubble radius, h is the lamella film thickness, and ΔP is the difference between the capillary hydrostatic pressure P_c and the disjoining pressure Π_d between the interfaces of lamella film. According to Equation 8, the drainage rate is inversely proportional to the solution apparent viscosity if assuming other

parameters to be constants. The viscosity of EWP and WPI is not much different in the presence of the same amount of sucrose. Addition of sucrose increase solution density, and therefore enhance the hydrostatic pressure P_c, leading to an increase in ΔP and drainage rate. However, the increased drainage ½ life with addition of sucrose suggested that this decreasing effect was not as significant as the increase of solution viscosity. Sucrose may also alter bubble size and lamella film thickness. Smaller bubble size of a protein foam was observed after adding sucrose (Figure 5; Raikos et al., 2007). Although all these parameters can contribute to foam stability, one critical contributor to protein foam stability is interfacial elasticity, which was modified differently for EWP and WPI with sucrose addition (Davis and Foegeding, 2007). In Chapter 2, we hypothesized that the greater foam stability of EWP than WPI in the presence of sucrose might be due to the interfacial elasticity. The correlations between foam stability and interfacial elasticity for the two proteins were therefore investigated.

Interfacial rheology

The air/water interfacial adsorption behaviors of EWP and WPI at different sucrose concentrations (0 to 44.3 g/100 mL) were evaluated through the dynamic interfacial tension measurement of freshly formed pendant drops (Figure 3).

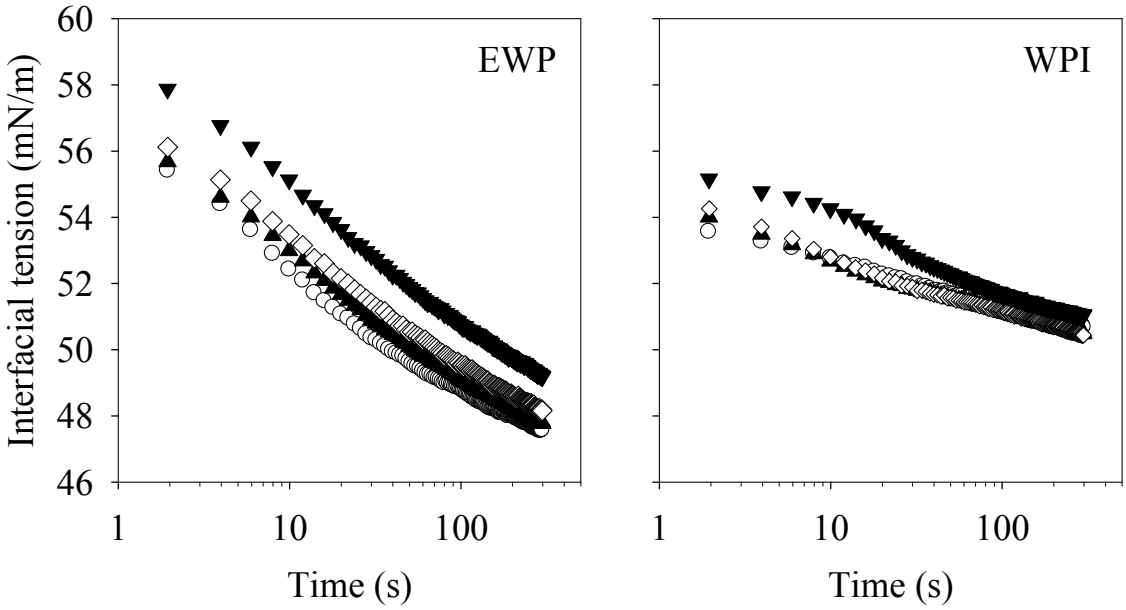

Figure 3. Typical dynamic changes of interfacial tension (γ) over time for 10% (w/v) protein solutions of egg white protein (EWP) and whey protein isolate (WPI) at pH 7.0 in the presence of different sucrose concentrations. ○ no sucrose ▲ 12.8 g/100 mL sucrose ◇ 25.0 g/100 mL sucrose ▼ 44.3 g/100 mL sucrose.

The initial interfacial tension (γ) values at 2 sec for EWP (55.5 to 58.0 mN/m) are higher than those of WPI (53.5 to 55.1 mN/m) while all initial γ values are lower than that of pure water (72.3 mN/m at 23 °C). The γ gradually decreased over time from the initial values, with faster decreasing rates of EWP than WPI (Figure 3). Protein adsorption occurs typically in three stages: 1) diffusion to the interface, 2) initial adsorption at the interface and 3) rearrangements of adsorbed molecules at the interface (Graham and Phillips, 1979). The low initial γ values of WPI suggested rapid initial adsorptions of molecules at interfaces right after droplet formation. Accordingly, WPI showed a better foamability than EWP due to a rapid interfacial adsorption rate and consequently a fast bubble formation process. After initial adsorption, protein molecules keep on adsorbing and undergo further unfolding and

rearrangements at the interface, resulting in additional γ decreasing. The faster decreasing γ of EWP may be attributed to a greater interfacial concentration or a faster structural changing rate of proteins at interface; although neither of these changes was measured. The γ of EWP reached a lower level at 5 min than the γ of WPI, in agreement with our previous observations (Davis and Foegeding, 2007). Addition of sucrose slightly increased the γ of EWP and had no effect on the γ decline patterns. The increased γ of EWP suggested that sucrose decreased protein interfacial activity. Ovalbumin was found to adsorb less rapidly at the air-water interface due to the increase of protein surface hydrophilicity in the presence of sucrose (Antipova et al., 1999). The γ values and decline patterns of WPI were not altered with addition of less than 44.3 g/100 mL sucrose. The presence of high sucrose concentration (44.3 g/100 mL) slowed down the initial γ decline rate of WPI, possibly due to a slower diffusion rate of molecules at high solution viscosity.

The interfacial dilational elastic modulus (E') of EWP and WPI (10% (w/v) protein) solutions in the presence of sucrose (0 to 44.3 g/100 mL sucrose) were measured after suspending a pendent drop for a certain time (1 to 10 min), as shown in Figure 4A. E' was also plotted against interfacial pressure ($\pi=\gamma_0-\gamma$ where γ_0=72.3 mN/m at 25 °C) in Figure 4B.

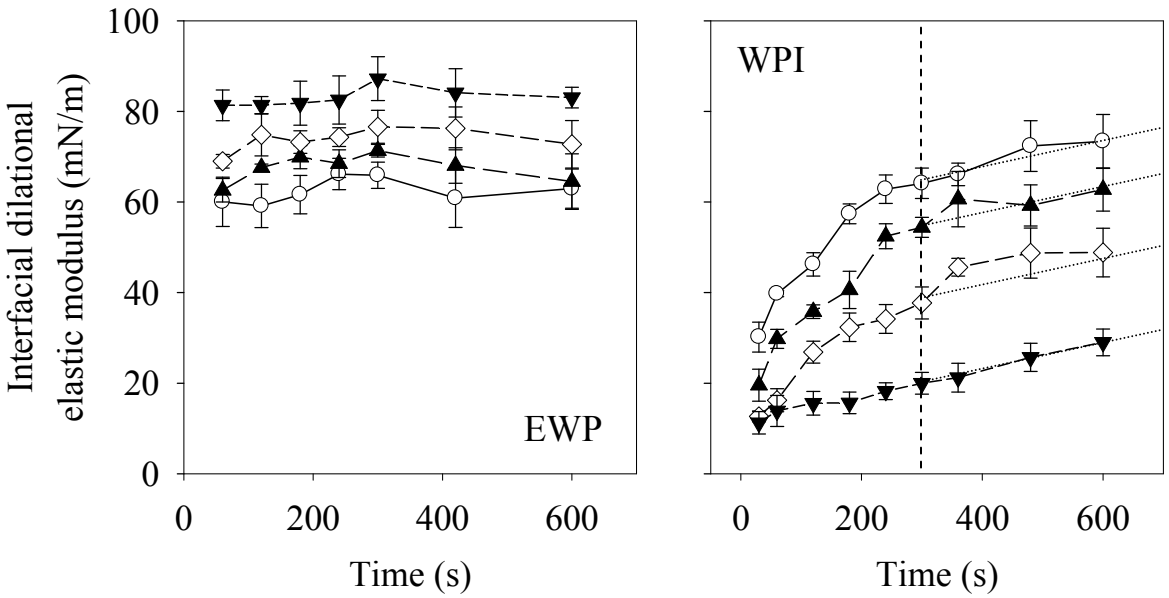

Figure 4A. Changes of interfacial dialtional elastic moduli (E') over time for 10% (w/v) protein solutions of egg white protein (EWP) and whey protein isolate (WPI) at pH 7.0 in the presence of different sucrose concentrations. ○ No sucrose ▲ 12.8 g/100 mL sucrose ◇ 25.0 g/100 mL sucrose ▼ 44.3 g/100 mL sucrose. Dash line indicates the position of 5 min. Dot lines are drawn manually to show the common increasing trend after 5 min.

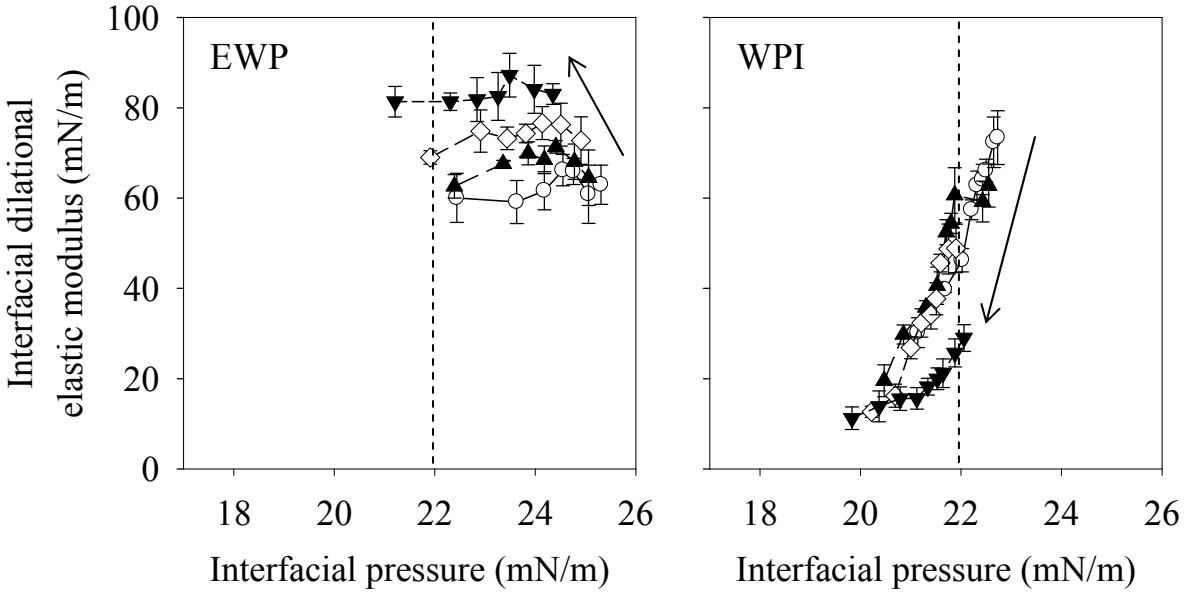

Figure 4B. Interfacial dialtional elastic moduli (E') verses interfacial pressure ($\pi=\gamma_0-\gamma$ where γ_0 is 72.3 mN/m at 25 °C) for 10% (w/v) protein solutions of EWP and WPI at pH 7.0 in the presence of different sucrose concentrations. ○ no sucrose ▲ 12.8 g/100 mL sucrose ◇ 25.0 g/100 mL sucrose ▼ 44.3 g/100 mL sucrose. Dash lines correspond to a interfacial pressure

of 22 mN/m. Arrows are drawn to indicate the change trend of E' with increasing sucrose concentration.

E' of EWP remained constant over time, while the constant value increased with increasing sucrose concentration (Figure 4A). In contrast, E' of WPI gradually increased with aging time, showing a rapid increase followed by a more constant rate after about 5 min (indicated by dot lines in Figure 4A). Addition of sucrose slowed down the initial increase in E' and progressively decreased E' of WPI, but showed no significant effect on the constant rate after 5 min (indicated by dash lines in Figure 4A). One hypothesis for E' increasing over time is that the interfacial molecules undergo a further rearrangement and/or interaction after adsorption, developing an elastic protein film. The addition of sucrose can limit protein unfolding and the development of protein-protein interactions as sucrose is known to create a less favorable thermodynamic environment for protein unfolding; however, it's difficult to disentangle the complicated interrelated effects of electrostatic interactions, hydrogen bonding and hydrophobic forces on the molecule level (Belyakova et al., 2003; Dickinson and Merino, 2002). Sugar only slowed down the initial E' increasing and did not affect the constant E' increasing rate after 5 min for WPI. This constant increasing rate is very low compared to the initial stage (Figure 4A), suggesting a relatively slow change of the interfacial film. Addition of sucrose gradually decreased E' of WPI interfacial film at this state (after 5 min). Possible explanation is that the network formation of compact molecules is weakened after addition of sucrose.

Noting the dissimilar interfacial tension among samples, we plotted the E' verses interfacial pressure π (Figure 4B). A clear difference between proteins is seen with EWP

remaining at interfacial pressures above 22 mN/m and WPI being below (indicated by dash lines in Figure 4B). This result suggests that the lower E' of WPI than EWP can be due to a lower corresponding π. Addition of sucrose decreased π, which for EWP was still higher than 22 mN/m while for WPI was shifted to an even lower value. Therefore, the dissimilar modifying effects of sucrose on E' for both proteins are partially due to the different ranges of π. Comparing the trends of E' (arrows in Figure 4B) for the proteins, we can say that E' of EWP (or WPI) gradually increased (or decreased) with increasing sucrose concentration even at the same π range. This observation indicates that the enhancing (or reducing) effect of sucrose on E' of EWP (or WPI) is not solely due to shifting interfacial pressure range and can be attributing to concentration, inter- and intra-molecular interactions, and adsoption/desorption rates of proteins at interface.

Dynamic microstructural changes

A high interfacial dilational elasticity was found to decrease the destabilization of protein foams by coalescence and/or disproportionation (Walstra, 2003). A direct result of foam disproprotionation and/or coalescence is the change of bubble sizes. The microstructural changes of protein foams were observed using confocal laser scanning microscopy (CLSM). The EWP and WPI foams with addition of different sucrose amounts were observed at 5 min intervals for 20 min (Figure 5A and 5B).

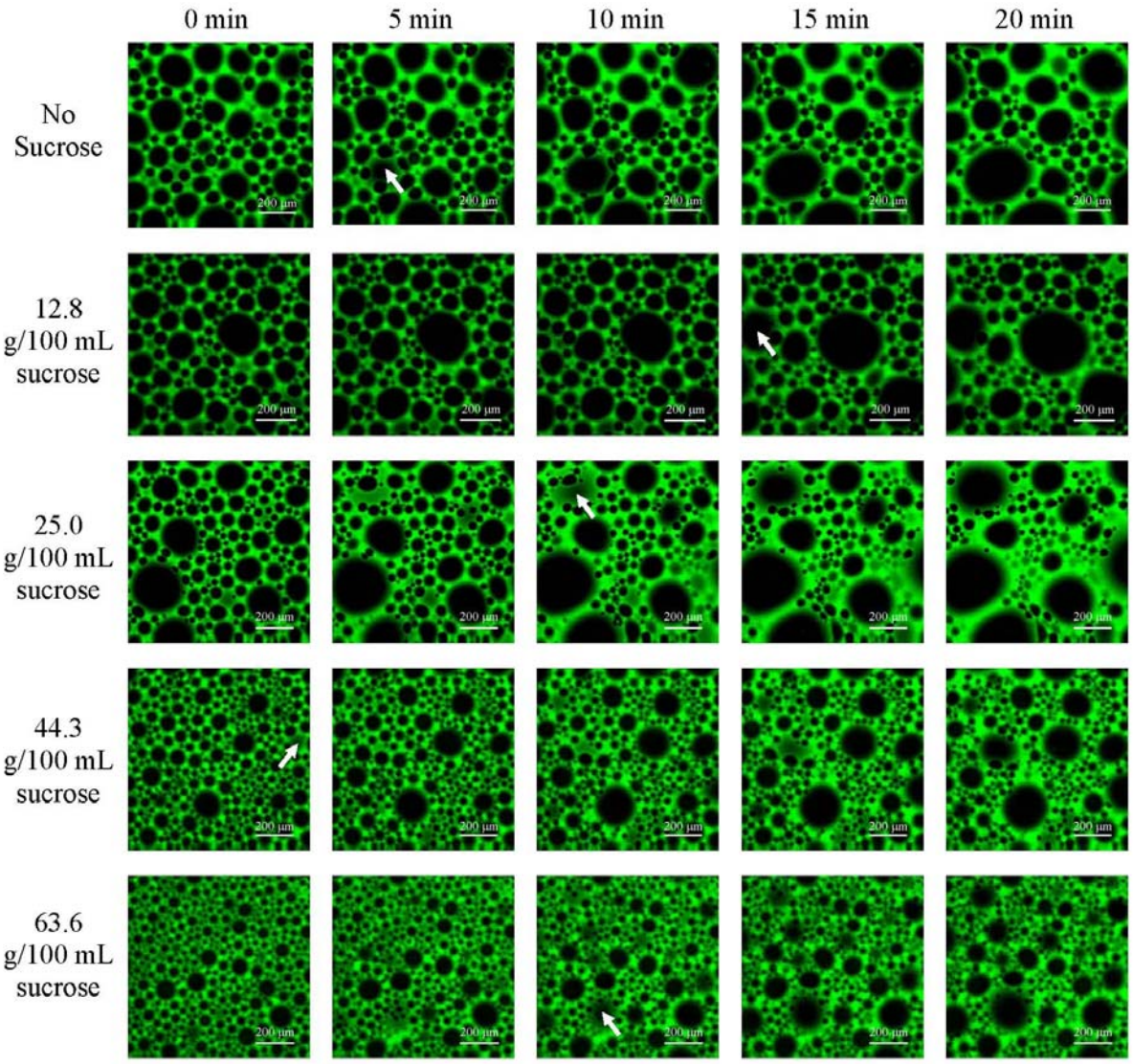

Figure 5A. Confocal image of egg white protein (EWP) foams in the presence of different amounts of sucrose from 0 to 20 min. Protein concentration is 10% (w/v) in solutions. White arrows indicate the appearance of 'new' bubbles during the period of observation.

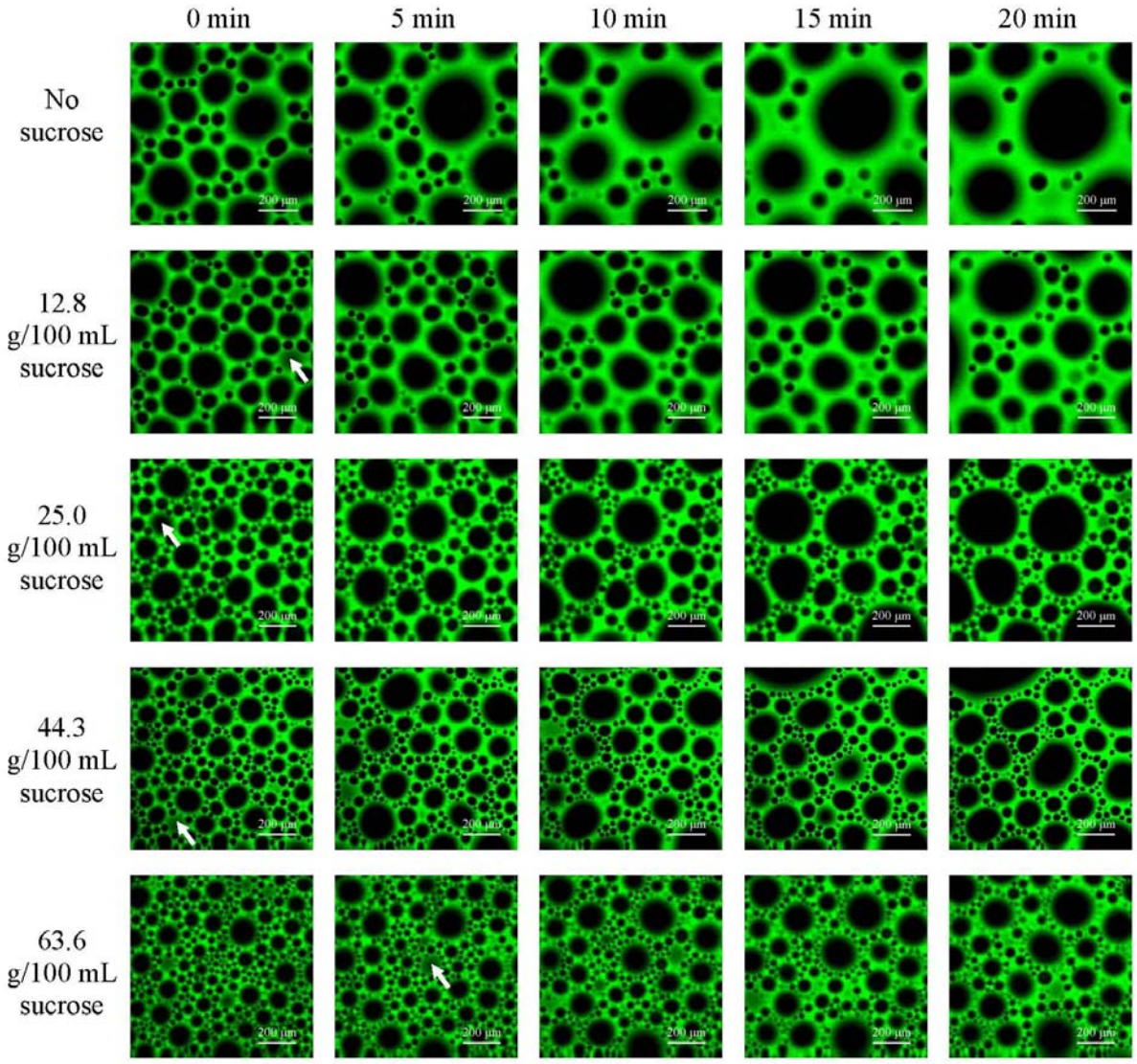

Figure 5B. Confocal image of whey protein isolate (WPI) foams in the presence of different amounts of sucrose from 0 to 20 min. Protein concentration is 10% (w/v) in solutions. White arrows indicate the appearance of 'new' bubbles during the period of observation.

With increasing sucrose concentration, foam structures evolved from low bubble density dispersions with mainly large bubbles into highly concentrated bubble dispersions containing mainly small bubbles for both EWP and WPI. From left column (0 min) to the right column (20 min), the foam structures changed into more bimodal distributions. A video

sequence was used to monitor the changes of bubble distribution within the same focal plane and indicated dynamic movements in the system. The bubbles were moving in and out the observation plane under the influence of local flow and buoyancy due to the gravity induced creaming. In some cases, 'new' bubbles came into the focal plane and grew into big bubbles during the period of the observation, with several examples marked in Figure 5A and 5B. Some small bubbles present at the beginning have disappeared during the experiment due to disproportionation of bubbles of different sizes and/or coalescence of neighboring bubbles. Although disappearance of a few small bubbles was attributing to vertically moving out of the observation plane, the total number of small bubbles in each image decreased over time, indicating that the overall bubble size is growing due to disproportionation and/or coalescence.

Bubble size can be quantitatively evaluated using the bubble area in a 2D image. Area of each bubble in an image was determined using MetaMorph Imaging System. Mean bubble area and median bubble area were calculated for each image. Since the foam characteristics may not be represented using a single image, three images were taken from each foam at every time point and used for mean (or median) bubble area computations. The average value and the standard deviation of the mean (or median) bubble area were calculated from the three images for each foam. Two linear relationships were established between the mean or median bubble area and the solution apparent viscosity (at a shear rate of 122.6 1/s) on a ln-ln scale, regardless of protein types (Figure 6 and Table 2). A shear rate of 122.6 1/s was selected for the calculation of solution apparent viscosity (Appendix I).

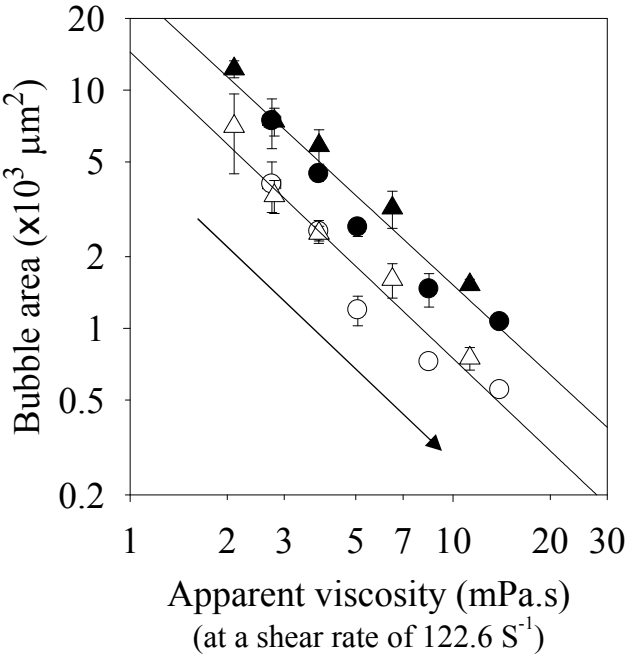

Figure 6. Relationship between median or mean bubble area and solution viscosity (at a shear rate of 122.6 1/s) for egg white protein (EWP) and whey protein isolate (WPI) in the presence of different sucrose concentrations. Protein concentration is 10% (w/v) in solutions. Sucrose concentration (0.00, 12.8, 25.0, 44.3, 63.6 g/100 mL) increased along with arrow direction. ● EWP mean bubble area ▲ WPI mean bubble area ○ EWP median bubble area △ WPI median bubble area.

The two linear relationships were parallel to each other on a ln-ln scale (Slopes were -1.25 for mean bubble area and -1.29 for median bubble area in Table 2). The median bubble areas are lower than mean bubble areas for all foams, suggesting right skewed bubble size distribution. Sucrose increased continuous phase viscosity, limiting the amount of air being incorporated into the system and leading to lower foam overrun and smaller bubble sizes. Bubble areas (mean or median) of EWP were smaller than those of WPI at the same sucrose content, contributing to lower foam overrun. Although the linear relationships between bubble area (mean or median) and solution viscosity were independent of protein types, the linear relationships between foam overrun and solution viscosity were protein-specific, with

a higher negative slope for EWP than for WPI (Table 2). This can be due to different bubble size distributions in two protein foams.

Change of mean bubble area over time is shown in Figure 7A. The bubble numbers in each image were counted, averaged and plotted against elapsed time in Figure 7B.

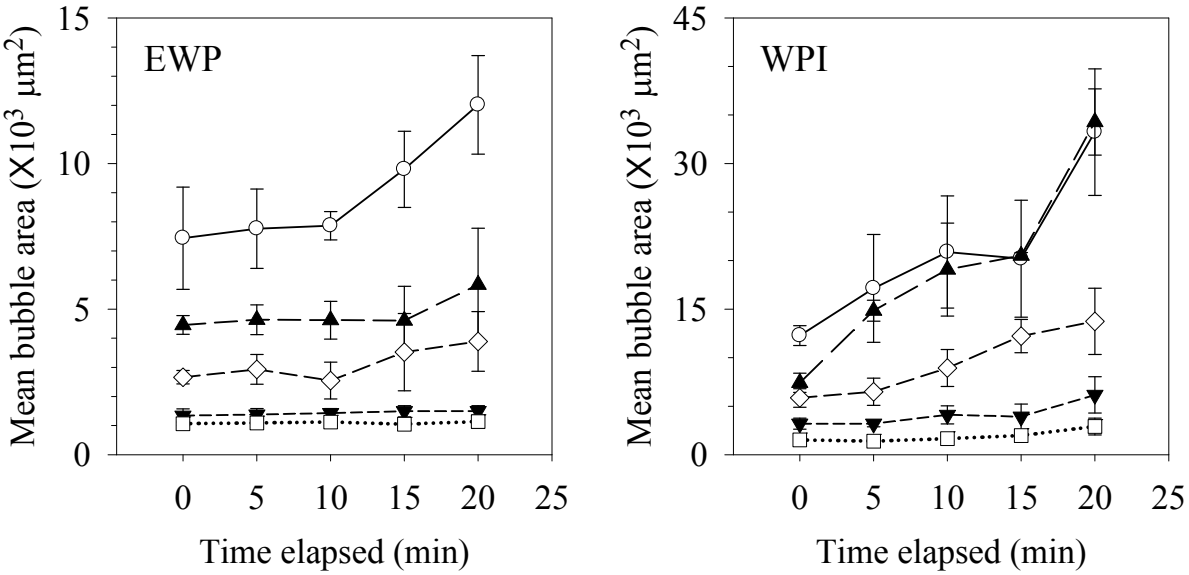

Figure 7A. Changes of mean bubble area from 0 to 20 min for egg white protein (EWP) and whey protein isolate (WPI) in the presence of different sucrose concentrations. Protein concentration is 10% (w/v) in solutions. ○ no sucrose ▲ 12.8 g/100 mL sucrose ◇ 25.0 g/100 mL sucrose ▼ 44.3 g/100 mL sucrose □ 63.6 g/100 mL sucrose.

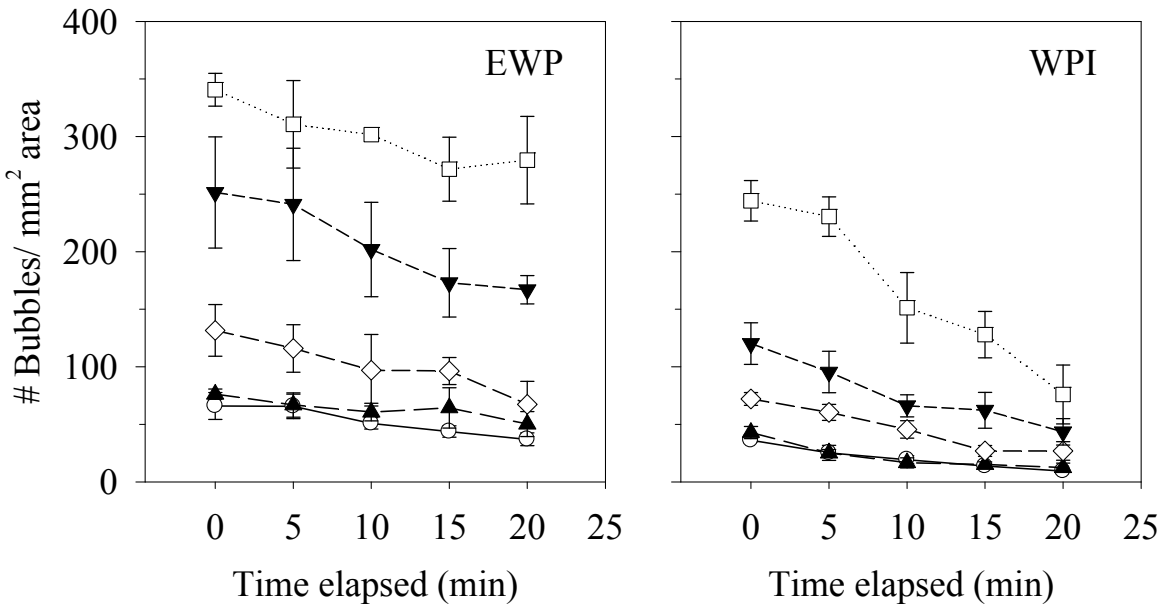

Figure 7B. Changes of bubble count per area from 0 to 20 min for egg white protein (EWP) and whey protein isolate (WPI) in the presence of different sucrose concentrations. Protein concentration is 10% (w/v) in solutions. ○ no sucrose ▲ 12.8 g/100 mL sucrose ◇ 25.0 g/100 mL sucrose ▼ 44.3 g/100 mL sucrose □ 63.6 g/100 mL sucrose.

Although bubbles were moving in and out of the observing plane during observation, overall bubble size (mean bubble area) increased over time due to disproportionation and/or coalescence (Figure 7A). The decrease of bubble count per area in each image confirmed that bubbles were getting larger over time (Figure 7B). Addition of sucrose decreased the mean bubble area at the beginning stage (0 min) and slowed down the growth of mean bubble area for both EWP and WPI foam (Figure 7A). Note the larger scale for bubble area of WPI (Figure 7A). It's hard to compare the changes of bubble area at high sucrose concentration (>44.3 g/100 mL) due to the relatively low values (Figure 7A). Comparing the bubble number in each image, we found that sucrose increased the bubble number at initial time but did not slow the decreasing rate. On the contrary, the bubble number decreasing rate of WPI foam at a high sucrose concentration (63.6 g/100 mL) was faster than others. This can be

attributed to an extremely large amount of bubbles at the initial stage. However, the initial bubble number of EWP at 63.6 g/100 mL or even 44.3 g/100 mL sucrose concentrations are greater than this WPI foam but decreased more slowly. This result suggests that the EWP bubbles are more stable and disappear in a slower rate than WPI bubbles.

Since the growing of bubble area is not a steady process with jumps at certain time points (Figure 7A), the change of mean bubble area over 20 min (the difference of mean bubble area at 20 min and at 0 min) was used to represent the overall growth of bubble area. This is the maximum change of bubble size over the observation period. A negative linear relationship was established between this change and foam drainage ½ life on a log-log scale, independent of protein types (Figure 8).

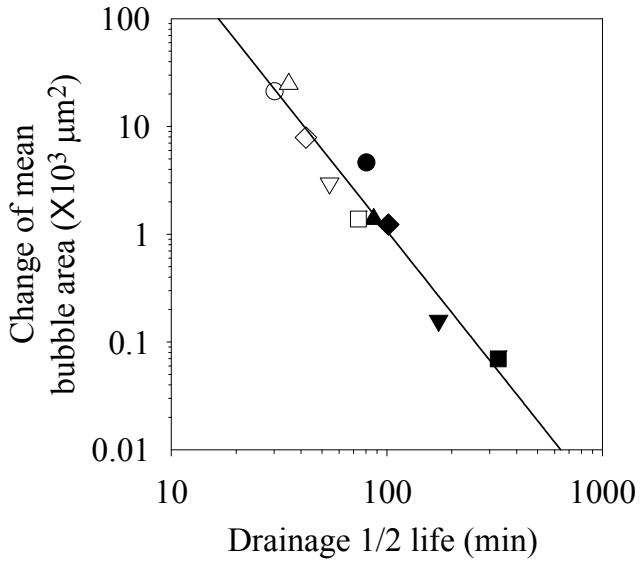

Figure 8. Relationship between the change of mean bubble area and foam drainage ½ life for egg white protein (EWP, Close symbols) and whey protein isolate (WPI, Open symbols) in the presence of different sucrose concentrations. Protein concentration is 10% (w/v) in solutions. ● no sucrose ▲ 12.8 g/100 mL sucrose ◆ 25.0 g/100 mL sucrose ▼ 44.3 g/100 mL sucrose ■ 63.6 g/100 mL sucrose.

The growth of bubble size was less in EWP foams than in WPI foams when compared at the same sucrose concentration; coinciding with a longer foam drainage ½ life. The change of bubble size corresponds to the destabilization changes of bubbles. However, destabilization changes can lead to opposite changes of bubble area. Firstly, bubbles come in and out the observation plane due to horizontal and vertical movements, causing positive or negative changes of bubble area. Secondly, big bubbles are growing while small bubbles are shrinking during disproportionation, leading to opposite changes of bubble area. Thirdly, small bubbles are merging into a big one due to coalescence, resulting in an increase of bubble area. Note that the movement of bubbles, disproportionation and colescence can influence each other as well. Although the overall changes in a foam are very complex, the bubble size is generally growing during observation (Figure 7A), resulting in a positive change of mean bubble area over 20 min. This value to some extent represents the destabilization changes of bubbles in a foam, and corresponds to performance of a foam in real foods, such as air bubble size in angel food cakes. The negative linear relationship between this value and foam drainage ½ life suggests that the change of mean bubble area over 20 min (the maximum change over observation period) can be used as an index for foam stability.

At the interfacial level, interfacial elasticity is proposed to increase bubble stability; with a cessation of disproportionation predicted at $E' > 2\gamma$ (Walstra, 2003). Dickinson et al. (2002) found that elastic interfacial film can slow the shrinkage of a single bubble beneath a planar air-water interface. We calculated E'/γ for the protein interface at 5 min (the relatively

stable E' for WPI in Figure 4A) and correlated the growth of bubble size (change of mean bubble area) min with E'/γ in Figure 9.

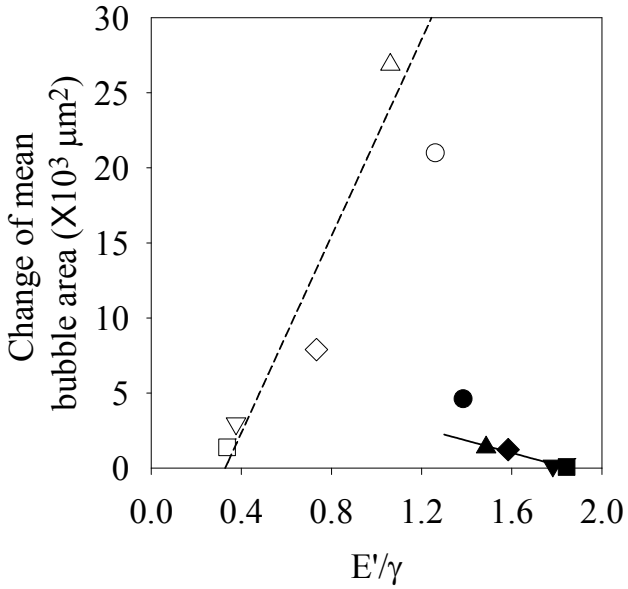

Figure 9. Relationship between the change of mean bubble area and interfacial elasticity for egg white protein (EWP, Close symbols) and whey protein isolate (WPI, Open symbols) in the presence of different sucrose concentrations. Protein concentration is 10% (w/v) in solutions. ● no sucrose ▲ 12.8 g/100 mL sucrose ◆ 25.0 g/100 mL sucrose ▼ 44.3 g/100 mL sucrose ■ 63.6 g/100 mL sucrose. The solid and dash lines correspond to the linear relationship between two variables for EWP and WPI, excluding the two points for pure protein solutions.

Two linear relationships with opposite trends were established for EWP and WPI respectively (Figure 9 and Table 2). Exclusion of the two points for pure protein solutions generated a better linear fit (higher R^2 in Table 2), suggesting the presence of sucrose changed the solution characteristics. The negative linear relationship between changes of mean bubble area and E'/γ for EWP suggested that $E'>2\gamma$ can effectively impede bubble size growth over time (Table 2). However, WPI didn't follow this pattern. While the changes of mean bubble area with drainage ½ life were similar (Figure 8), the decrease of E' with

increased sucrose caused an opposite trend in E'/γ for WPI. One potential reason is that sucrose increased the solution viscosity and therefore improved the foam stability as well as slowed down the bubble size growth; at the same time having a destabilizing effect on the interface. Consequently, a combination of solution viscosity and interfacial elasticity is necessary when analyzing sucrose effects on foam stability. Plotting foam drainage ½ life against $\mu\left(E'/\gamma\right)$ resulted in a linear relationship (R^2=0.975) between the two parts, regardless of protein types (Figure 10 and Table 2).

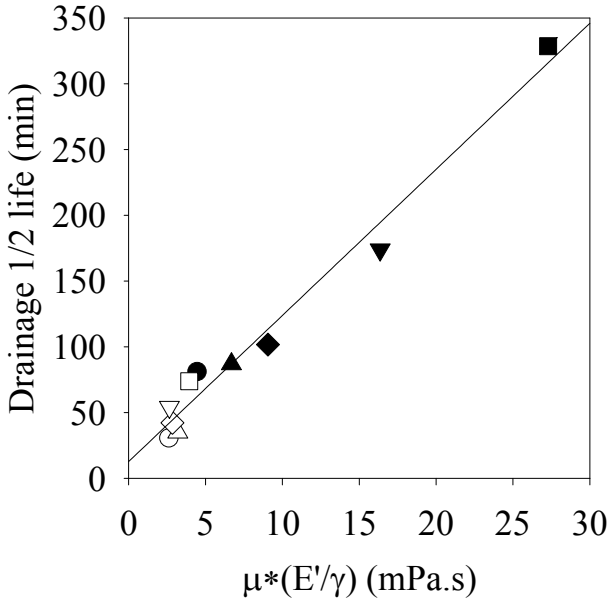

Figure 10. Relationship between foam drainage ½ life and viscosity (μ) and interfacial properties (E'/γ) for egg white protein (EWP, Close symbols) and whey protein isolate (WPI, Open symbols) in the presence of different sucrose concentrations. Protein concentration is 10% (w/v) in solutions. ● no sucrose ▲ 12.8 g/100 mL sucrose ◆ 25.0 g/100 mL sucrose ▼ 44.3 g/100 mL sucrose ■ 63.6 g/100 mL sucrose. Solid line corresponds to the linear relationship between two variables.

Changes of solution viscosity (μ) cannot explain all the sucrose effects on foam stability, resulting in two individual relationships between drainage ½ life and μ for EWP and

WPI respectively (Figure 2). The lower degree of bubble size growth and longer foam drainage ½ life of EWP than WPI can be mainly attributed to the higher interfacial elasticity. Therefore, both changes occurring in the bulk phase (viscosity) and at the interface (interfacial dilational elasticity) contribute to foam destabilization. Although sucrose increased bulk phase viscosity of EWP and WPI solutions, the opposite effects of sucrose on the interfacial dilational elasticity of the two types of proteins produced significant differences in overall stability.

Foam yield stress and microstructure

Mason (1999) indicated that foams transformed from viscous fluid to semi-solid like structures and exhibited yield stress values when the air phase fractions increased above the random close pack air phase fraction of 0.64 (or 177% overrun). Princen and Kiss (1989) predicted a model (Equation 9) for foam yield stress (τ_0) based on interfacial tension (γ), bubble surface-volume mean radius (R_{32}), air phase fraction (ϕ) and an experimentally derived fitted parameter $Y(\phi)$.

$$\tau_0 = \frac{\gamma}{R_{32}} \phi^{1/3} Y(\phi) \qquad \text{Equation 9}$$

Foegeding et al. (2006) suggested that for protein in foams, the interfacial tension (γ) in this model can be replaced by interfacial elasticity (E'), resulting in Equation 10.

$$\tau_0 = \frac{E'}{R_{32}} \phi^{1/3} Y(\phi) \qquad \text{Equation 10}$$

Berry and Foegeding (2008) deduced Equation 11 through14 from Equation 9 and 10 and found positive linear relationships between foam yield stress and approximate bubble surface area (Equation 11 and 12) or bubble count per unit area (Equation 13 and 14).

$$\tau_0 = (\gamma * Approx\ Interfacial\ Area\ per\ unit\ volume)\ \ Y(\phi) \qquad \text{Equation 11}$$

$$\tau_0 = (E' * Approx\ Interfacial\ Area\ per\ unit\ volume)\ \ Y(\phi) \qquad \text{Equation 12}$$

$$\tau_0 = \gamma * \sqrt{\frac{Bubble\ Count}{Area}}\ Y(\phi) \qquad \text{Equation 13}$$

$$\tau_0 = E' * \sqrt{\frac{Bubble\ Count}{Area}}\ Y(\phi) \qquad \text{Equation 14}$$

The approximate interfacial area per unit volume can be calculated from the surface-volume mean radius R_{32} and the volume fraction of gas phase ϕ using $a = \frac{3\phi}{R_{32}}$, where the R_{32} was approximated as $R_{32} \approx R_{20}$ = (mean bubble area / π)$^{1/2}$ or $R_{32} \approx R_{median}$ = (median bubble area / π)$^{1/2}$ in this work. However, plots of the foam yield stress against the approximate bubble interfacial area per unit volume (Figure 11A for $R_{32} \approx R_{20}$ and 11B for $R_{32} \approx R_{median}$) and the bubble count number per unit area (Figure 12) did not show logical relationships between these variables.

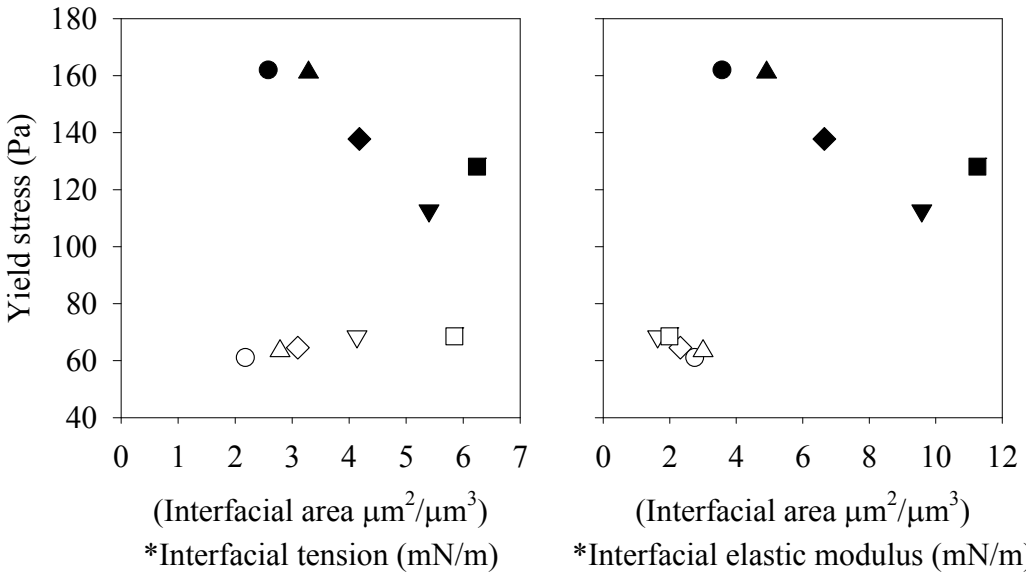

Figure 11A. Yield stress vs. interfacial area per volume * interfacial tension (γ) or interfacial elasticity (E') for egg white protein (EWP, Close symbols) and whey protein isolate (WPI, Open symbols) in the presence of different sucrose concentrations. Protein concentration is 10% (w/v) in solutions. ● no sucrose ▲ 12.8 g/100 mL sucrose ◆ 25.0 g/100 mL sucrose ▼ 44.3 g/100 mL sucrose ■ 63.6 g/100 mL sucrose. Approximate interfacial area per foam volume was calculated based on mean bubble area.

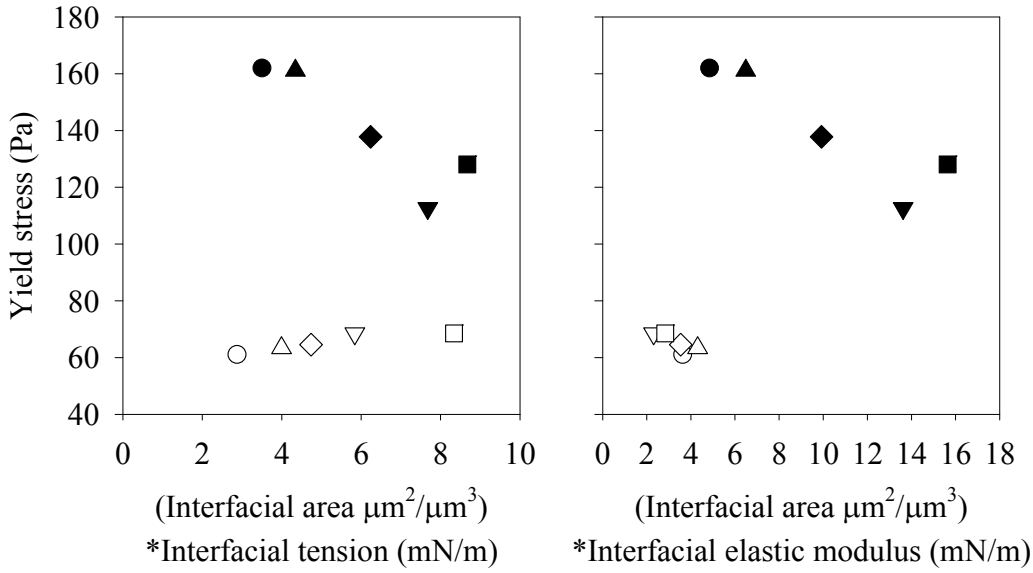

Figure 11B. Yield stress vs. interfacial area per volume * interfacial tension (γ) or interfacial elasticity (E') for egg white protein (EWP, Close symbols) and whey protein isolate (WPI, Open symbols) in the presence of different sucrose concentrations. Protein concentration is 10% (w/v) in solutions. ● no sucrose ▲ 12.8 g/100 mL sucrose ◆ 25.0 g/100 mL sucrose ▼

44.3 g/100 mL sucrose ■ 63.6 g/100 mL sucrose. Approximate interfacial area per foam volume was calculated based on median bubble area.

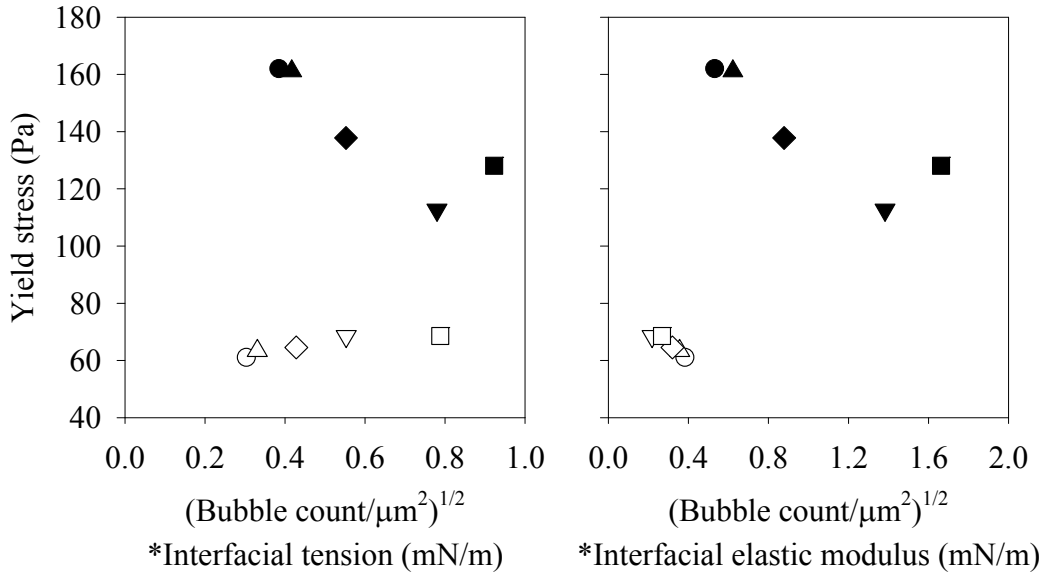

Figure 12. Yield stress vs. (bubble count per area)$^{1/2}$ * surface tension (γ) or interfacial elasticity (E') for egg white protein (EWP, Close symbols) and whey protein isolate (WPI, Open symbols) in the presence of different sucrose concentrations. Protein concentration is 10% (w/v) in solutions. ● no sucrose ▲ 12.8 g/100 mL sucrose ◆ 25.0 g/100 mL sucrose ▼ 44.3 g/100 mL sucrose ■ 63.6 g/100 mL sucrose.

This is because of the wide variation of foam air phase fractions and therefore a change of the experimentally derived fitted parameter $Y(\phi)$ among foams. The factor $Y(\phi)$ can be calculated based on τ_0 and $\phi^{1/3}$ values associated with each foam; R_{32}, calculated from $R_{32} \approx R_{20}$ = (mean bubble area / π)$^{1/2}$ or $R_{32} \approx R_{median}$ = (median bubble area / π)$^{1/2}$; and interfacial tension (γ) or interfacial dilational elasticity (E') at 5 min; according to Equation 15 and 16, which were derived from Equation 9 and 10. As the three dimensional (3D) bubble size was unknown, it's impossible to calculate R_{32} without unfolding bubble size distribution data. The unfolding process of bubble size distribution will be discussed later. In this part, we use the

area mean radius (R_{20}) calculated from mean bubble area or median radius (R_{median}) calculated from median bubble area in each image as the approximate R_{32}.

$$Y(\phi) = \frac{R_{32}}{\gamma \phi^{1/3}} \tau_0 \quad \text{or} \quad Y(\phi) = \frac{D_{32}}{2\gamma \phi^{1/3}} \tau_0 \qquad \text{Equation 15}$$

$$Y(\phi) = \frac{R_{32}}{E' \phi^{1/3}} \tau_0 \quad \text{or} \quad Y(\phi) = \frac{D_{32}}{2E' \phi^{1/3}} \tau_0 \qquad \text{Equation 16}$$

Princen and Kiss (1989) established a relationship of $Y(\phi) = -0.080 - 0.114 \log(\phi)$ within a range of ϕ between 0.8333 and 0.9756 based on a series of emulsions. Accordingly, we correlated $Y(\phi)$ and ϕ in a form of:

$$Y(\phi) = -a - b \ln(\phi) \qquad \text{Equation 17}$$

where a and b are constents (Figure 13).

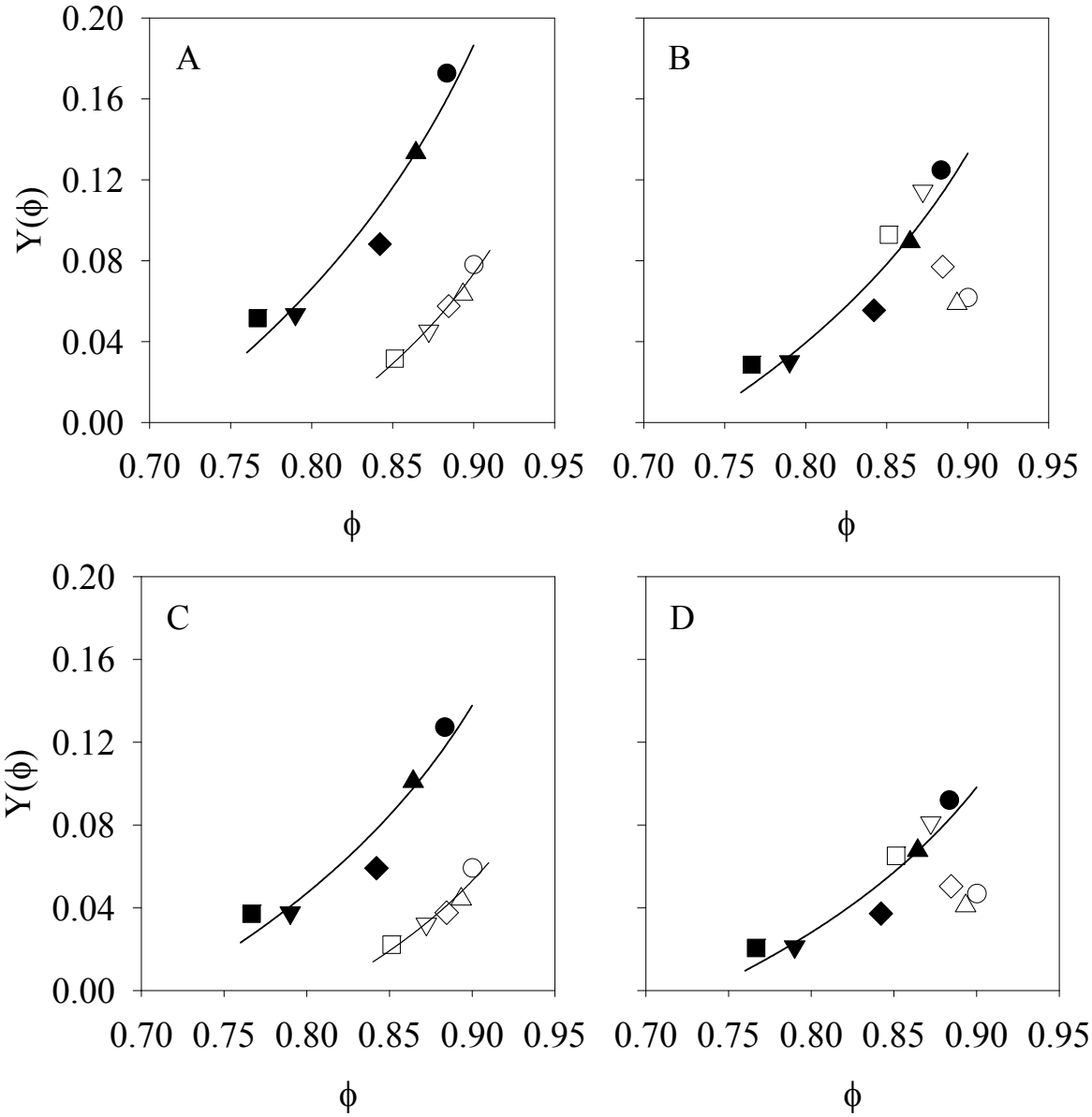

Figure 13. *Y(ϕ)* vs. *ϕ* from radius calculated from mean (R_{20}) or median (R_{median}) area for egg white protein (EWP, Close symbols) and whey protein isolate (WPI, Open symbols) in the presence of different sucrose concentrations. Protein concentration is 10% (w/v) in solutions. ● no sucrose ▲ 12.8 g/100 mL sucrose ◆ 25.0 g/100 mL sucrose ▼ 44.3 g/100 mL sucrose ■ 63.6 g/100 mL sucrose. A: *Y(ϕ)* of protein foams was calculated based on R_{20} and γ at 5 min. EWP: $Y(\phi)$=-0.174ln(1-ϕ)-0.213 (R^2=0.940) WPI: $Y(\phi)$=-0.110ln(1-ϕ)-0.179 (R^2=0.979) B: *Y(ϕ)* of protein foams was calculated based on R_{20} and E' at 5 min. EWP: $Y(\phi)$=-0.135ln(1-ϕ)-0.178 (R^2=0.926) C: *Y(ϕ)* of protein foams was calculated based on R_{median} and γ at 5 min. EWP: $Y(\phi)$=-0.131ln(1-ϕ)-0.164 (R^2=0.914) WPI: $Y(\phi)$=-0.0833ln(1-ϕ)-0.139 (R^2=0.925) D:

$Y(\phi)$ of protein foams was calculated based on R_{median} and E' at 5 min. EWP: $Y(\phi)$=-0.101ln(1-ϕ)-0.135 (R^2=0.907).

In Figure 13A, $Y(\phi)$ of protein foams was calculated based on R_{32} = (mean bubble area / π)$^{1/2}$ and interfacial tension (γ) at 5 min. The factor $Y(\phi)$ can be accurately predicted from ϕ using this model (Equation 17), with two individual curves corresponding to EWP and WPI respectively. The $Y(\phi)$ values of EWP foams are higher than those of WPI foams, whereas the $Y(\phi)$ values of protein foams are higher than those of emulsions when compared within the same ϕ range (Princen and Kiss, 1989). This is in agreement with our previous studies for egg white protein (EWP) and whey protein isolate (WPI) foams made by varying whipping time and protein concentration (Pernell et al., 2002a). However, the $Y(\phi)$ values for protein foams containing different sucrose concentrations were higher than those for pure protein foams reported by Pernell et al. (2002a). This can be attributed to different ranges of foam yield stress and bubble size in two studies. The protein concentration in our work was 10% (w/v), which was the highest value in Pernell et al. (2002a); therefore the foam yield stress values are higher, resulting in a higher range of $Y(\phi)$ values according to Equation 15 and 16. In addition, the bubble radius values calculated from mean bubble area were larger than those calculated using the mean intercept length in Pernell et al. (2002a), when comparing the pure protein foams. Our results support the validity of Princen and Kiss (1989) model for foams containing sucrose, with a higher range of $Y(\phi)$ for foams than for emulsions. The difference between foams and emulsions can be attributed to the different ranges of interfacial tension, bubble or droplet sizes, and yield stress values and different model assumptions. The range of $Y(\phi)$ for EWP was higher than that for WPI, due to higher

yield stress (τ_0) and lower interfacial tension (γ) of EWP foams than those values of WPI foams. Addition of sucrose decreased bubble size (R_{32}) and therefore decreased $Y(\phi)$ values. The larger increase in $Y(\phi)$ at lower phase volume for EWP than WPI was also observed by Pernell et al. (2002a), and was suggested to be due to some connections between proteins at interface and protein in the lamellae.

In Figure 13B, the relationship between $Y(\phi)$ and ϕ (Equation 15) was still valid for EWP but failed for WPI after substituting γ (Equation 14) with E' (Equation 15) for $Y(\phi)$ calculation. However, the $Y(\phi)$ values of EWP and WPI were in the same range after taking into account interfacial rheological properties. In addition, the two points of WPI at high sucrose concentration (44.3 and 63.6 g/100 mL) were close to the curve established for EWP points, suggesting a master curve. This result suggested that interfacial rheological properties should be incorporated into Princen and Kiss (1989) model when applying it to protein foams (Foegeding et al., 2006). The higher foam yield stress (τ_0) of EWP than that of WPI can be attributed to the higher E' rather than γ, resulting in similar ranges of $Y(\phi)$ for EWP and WPI in Figure 13B. The $Y(\phi)$ of WPI foams failed to fit Equation 17 when varying sucrose concentrations due to the deviation of three points at low sucrose concentrations (0.00, 12.8 and 25 g/100 mL). The foam yield stress (τ_0) of WPI slightly increased (Figure 11B) whereas the interfacial elasticity (E') decreased (Figure 4A) with increasing sucrose concentration, contradicting with the positive relationships established between τ_0 and E' for protein foams in our previous studies (Foegeding et al., 2006; Berry, 2008). The reasons for this phenomenon are not clear right now but hypothesized to be associated with the molecular interactions of proteins at the interface and between those at the interface and in solution. The

Princen and Kiss (1989) equation was established using a model composed of stable unit cells (droplets or bubbles) so that the yield stress can be calculated from the deformation (strain) of the unit cells and the surface tension (stress) of the interfaces (Princen, 1982). The destablization changes of bubble were not considered and may also cause deviations from the predictions.

Models built on $Y(\phi)$ calculated from median bubble area (Figure 13C and 13D) gave similar results as those from mean bubble area (Figure 13A and 13B), only with different parameters in the equations. As the median bubble areas of all foams are systematically smaller than the mean bubble areas, the $Y(\phi)$ shifted to a lower value range when using the median bubble area for calculations. In general, we demonstrated the validity of Princen and Kiss (1989) model in foams and suggested the incorporation of interfacial rheological properties into this model is necessary when apply it to protein foams.

Unfolding bubble size distributions

The basic approach to recovering the size distribution of 3D feathers from the image of 2D intersections is called “unfolding”. A common method is to calculate the number of spheres (3D) in each size class from the number of circles (2D) in size classes using a table of coefficients. This method was first described by Saltykov (1967) and has been reviewed in a summery by Cruz-Orive (1976) that includes tables of coefficients suitable for general use. From geometric probability, the frequency distribution for the number of circles in each size class is due to the three dimensional objects of each size. Therefore, the number of bubbles in each size class (i) is calculated as the sum of the number of circles in each size class (j) times the alpha coefficients (Equation 18).

$$N_{V_i} = \sum \alpha_{ij} \cdot N_{A_j} \qquad \text{Equation 18}$$

where N_{V_i} and N_{A_j} are the bubble numbers in the corresponding size class *i* (2D) and *j* (3D) respectively. A typical alpha matrix for sphere unfolding (Cruz-Orive) was used in this study. The bin width is typically chosen to permit each bin to accumulate enough counts for good statistical precision and enough bins to show the shape of the distribution (Russ and Dehoff, 2000). The bubble size was represented as bubble diameter and 15 bins were linearly spaces in size up to the largest value measured for each foam. After the unfolding process, the relative frequency of bubbles in each size class was calculated using Equation 19:

$$n_{Vj} = \frac{N_{Vj}}{\sum_{k=1}^{15} N_{Vk}} \qquad \text{Equation 19}$$

where n_{Vj} is the relative frequency of bubbles in size class j (3D).

One big problem of this unfolding method is the possibility to generate negative values in small ranges. This occurs due to undercounting the number of small particles, some of which are too small to be seen. Fang et al. (1993) used a Weibull distribution function to fit the particle size distribution before unfolding and found this could smooth the histograms and gave out better results with less negative values. Several distribution functions have been used to fit bubble size distribution in foams, including Lognormal and Weibull functions (Lage and Espósito, 1999; Calvert and Nezhati, 1987; Magrabi et al., 1999). The Lognormal, 4-parameter Weibull and 2-parameter Weibull functions were selected to fit the bubble size distribution data. Unfolding bubble size distribution processes were conducted based on the

15-bin histograms generated from the original bubble diameters and the three fitted functions respectively. The normality test (Shapiro-Wilk) results for the natural logarithm fit of bubble diameters for foams were given in Table 3.

Table 3. Normality Test (Shapiro-Wilk) of the natural logarithm values of bubble diameter

	EWP			***WPI***		
Sucrose (g/100 mL)	W-Statistic	P		W-Statistic	P	
0.00	0.976	0.002	Failed	0.969	0.028	Failed
12.8	0.988	0.056	Passed	0.986	0.323	Passed
25.0	0.993	0.103	Passed	0.994	0.560	Passed
44.3	0.996	0.303	Passed	0.997	0.851	Passed
63.6	0.997	0.052	Passed	0.996	0.045	Failed

Most of the foams passed the test (P>0.05) except for the EWP, WPI and WPI + 63.6 g/100 mL) sucrose foams. The R^2 for the fitting of 4-parameter and 2-parameter Weibull functions are shown in Table 4.

Table 4. The R^2 for the fitting of Weibull distribution of bubble size accumulative curve

	EWP		***WPI***	
Sucrose (g/100 mL)	4-parameter R^2	2-parameter R^2	4-parameter R^2	2-parameter R^2
0.00	0.996	0.990	0.993	0.978
12.8	0.998	0.984	0.993	0.967
25.0	0.998	0.933	0.998	0.967
44.3	0.998	0.938	0.998	0.954
63.6	0.998	0.944	0.999	0.952

Although the bubble size distribution was better approximated by 4-parameter weibull function (higher R^2) than 2-parameter weibull function, the cumulative probability of the former was slightly less than 1, depending on 'a' value in Equation 6. Therefore, 2-parameter Weibull function provides better prediction for the real situation than 4-parameter Weibull function. The cumulative probability curves of three functions (Figure 14B, C and D) were very similar to the curves of original bubble diameters for both EWP and WPI

(Figure 14A). The moving of this curve to a lower value range indicated the decrease of bubble size in foams with increasing sucrose concentration for both protein foams.

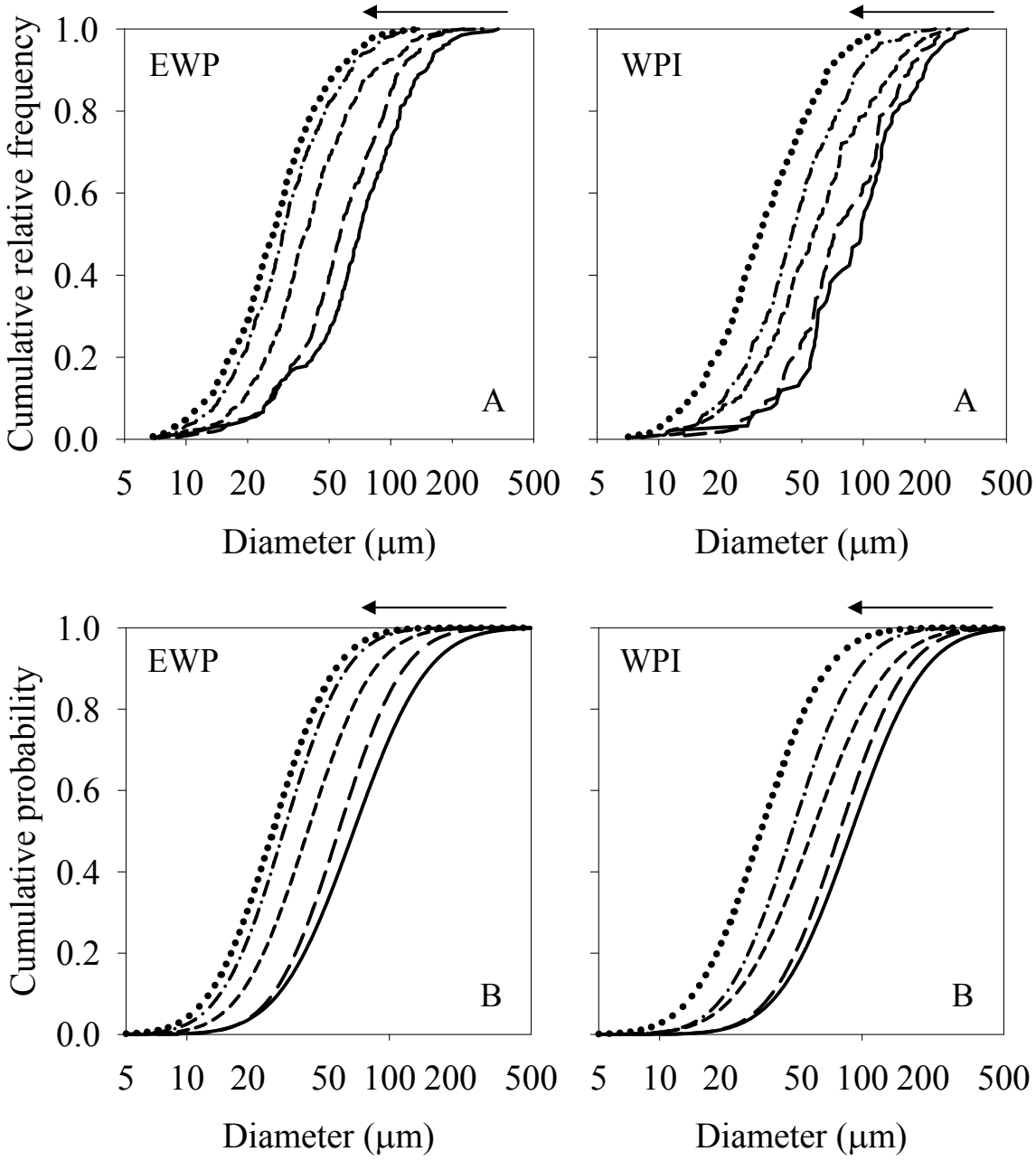

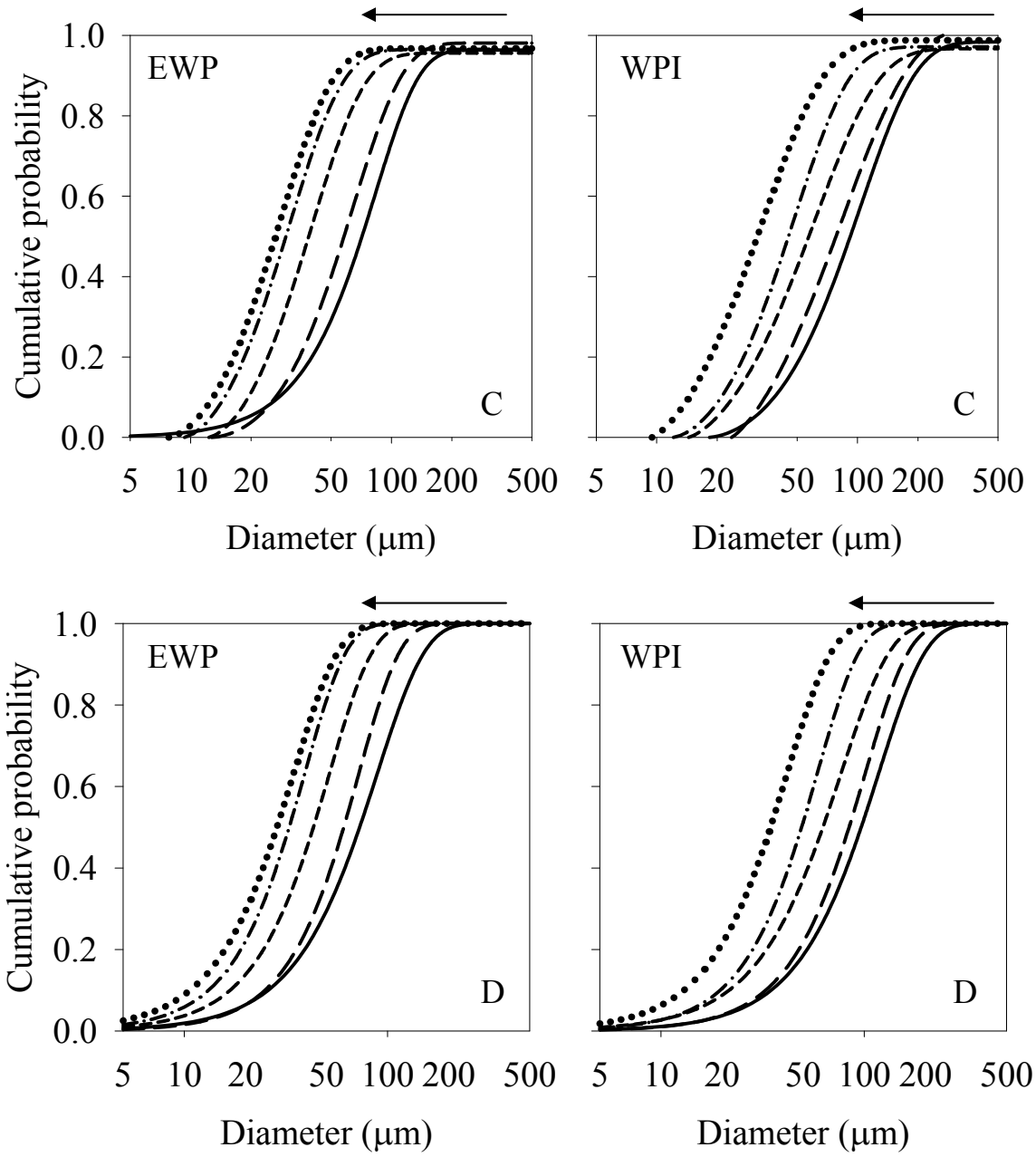

Figure 14. Cumulative relative frequency of bubble diameters for egg white protein (EWP) and whey protein isolate (WPI) in the presence of different sucrose concentrations. Protein concentration is 10% (w/v) in solutions. Sucrose concentration (0.00, 12.8, 25.0, 44.3, 63.6 g/100 mL) increased along with arrow direction from solid line to dot line. A: original data from image; B, C and D: Lognormal, 4-parameter Weibull and 2-parameter Weibull fits.

The mean diameter, median diameter, mode diameter and the Sauter mean diameter (D_{32}) were calculated from the 2D original diameter and the three statistical functions (Lognormal, 2-parameter Weibull and 4-parameter Weibull distribution functions) using the appropriate statistical equations (Merran et al. 2000). Data are listed in Table 5A and 5B.

Table 5A. Mean diameter (mean *D*), median diameter (median *D*), mode diameter or the most probability diameter (mode *D*) and the Sauter mean diameter (D_{32}) before and after unfolding (Data are for egg white protein foams in the presence of different sucrose concentrations at 0 min.)

		2D				**3D (from histogram)**			
Sucrose (g/100 mL)	*D type*	*Original*	*Log-normal*	*4-Weib*	*2-Weib*	*Original*	*Log-normal*	*4-Weib*	*2-Weib*
0.00	Mean *D*	81.18	83.14	74.07	79.58	104.4	106.4	100.0	108.5
	Median *D*	70.18	66.57	69.49	46.65	80.13	86.57	95.18	101.9
	Mode *D*	-	42.69	58.75	58.50	-	-	-	-
	D_{32}	152.1	202.2	-	126.0	218.1	190.4	127.6	146.2
12.8	Mean *D*	65.65	66.52	63.17	64.58	84.88	86.27	82.90	87.07
	Median *D*	56.69	56.16	57.36	41.60	74.78	73.62	76.46	83.64
	Mode *D*	-	40.03	42.78	54.31	-	-	-	-
	D_{32}	107.3	130.9	-	93.13	134.2	133.5	113.5	108.5
25.0	Mean *D*	47.49	47.18	41.88	46.39	49.47	57.81	50.96	61.70
	Median *D*	38.53	39.50	37.61	29.02	37.54	48.88	45.16	59.07
	Mode *D*	-	27.69	26.76	37.55	-	-	-	-
	D_{32}	105.6	96.02	-	68.88	155.7	107.0	70.77	77.90
44.3	Mean *D*	35.27	35.26	32.58	35.16	42.90	45.19	40.01	47.51
	Median *D*	29.68	30.10	29.14	22.48	33.92	38.70	36.25	45.40
	Mode *D*	-	21.93	20.40	29.29	-	-	-	-
	D_{32}	63.10	66.44	-	51.07	76.24	72.13	57.50	58.99
63.6	Mean *D*	31.07	31.04	28.75	31.07	35.65	38.53	34.93	41.41
	Median *D*	26.68	26.52	25.88	19.07	28.36	33.25	29.56	39.46
	Mode *D*	-	19.37	18.59	24.48	-	-	-	-
	D_{32}	57.51	58.22	-	47.02	71.80	64.90	49.27	53.76

Table 5B. Mean diameter (mean *D*), median diameter (median *D*), mode diameter or the most probability diameter (mode *D*) and the Sauter mean diameter (D_{32}) before and after unfolding (Data are for whey protein isolate foams in the presence of different sucrose concentrations at 0 min.)

		2D				**3D (from histogram)**			
Sucrose (g/100 mL)	*D type*	*Original*	*Log-normal*	*4-Weib*	*2-Weib*	*Original*	*Log-normal*	*4-Weib*	*2-Weib*
0.00	Mean *D*	107.1	109.8	102.8	104.9	133.8	141.0	139.5	148.4
	Median *D*	97.54	88.78	90.88	62.02	113.2	121.3	126.8	140.1
	Mode *D*	-	58.01	60.50	78.16	-	-	-	-
	D_{32}	182.3	257.2	-	164.7	222.1	213.2	198.2	195.8
12.8	Mean *D*	92.09	93.12	95.92	90.10	126.8	119.5	124.2	126.9
	Median *D*	72.28	77.67	79.63	55.98	111.5	106.0	112.7	121.5
	Mode *D*	-	54.03	38.92	72.26	-	-	-	-
	D_{32}	152.0	192.4	-	134.6	184.6	169.6	177.4	160.1
25.0	Mean *D*	70.95	71.79	65.45	68.83	90.08	92.47	82.40	95.28
	Median *D*	57.13	56.96	55.68	39.68	67.20	76.00	71.60	89.14
	Mode *D*	-	35.86	30.88	49.23	-	-	-	-
	D_{32}	138.7	181.1	-	110.8	171.5	159.0	136.9	130.6
44.3	Mean *D*	53.58	53.71	50.00	52.48	68.44	68.54	61.92	70.68
	Median *D*	45.02	45.12	44.43	33.25	50.93	57.73	56.31	67.59
	Mode *D*	-	31.84	30.27	43.21	-	-	-	-
	D_{32}	100.6	107.8	-	76.95	136.1	115.5	91.33	88.24
63.6	Mean *D*	37.65	37.79	36.70	37.46	47.59	49.12	46.39	51.74
	Median *D*	31.46	31.65	31.44	22.94	38.12	41.87	40.56	49.06
	Mode *D*	-	22.21	18.09	29.44	-	-	-	-
	D_{32}	66.85	76.78	-	56.79	83.09	76.95	73.67	67.01

The 15-bin relative frequency histograms were established for the original 2D diameter data and three statistical functions. Unfolding bubble size distribution were conducted on for the four histograms using the Cruz-Orive coefficient matrix, resulting in four 15-bin relative frequency histograms for 3D diameter. The approximate mean, median and D_{32} of diameters were calculated from the 15-bin relative frequency histograms for 3D diameter (Table 5A and 5B). The mode value cannot be predicted from a histogram. The diameter values followed the same sequence of D_{32} > Mean diameter > Median diameter > Mode diameter for all foams, suggesting right-skewed bubble size distributions. The 3D

bubble sizes were larger than 2D size because some small circles in 2D images were the small cross sections from large bubbles. Again, all types of bubble diameters decreased with increasing sucrose concentration.

The calculating process of $Y(\phi)$ is the same as shown in the previous part. The relationships between $Y(\phi)$ and ϕ for protein foams were fitted into Equation 17, giving the parameters (a and b) in Table 6A and 6B.

Table 6A. Parameters in function regression of $Y(\phi)=-a*ln(1-\phi)-b$ for egg white protein (EWP) and whey protein isolate (WPI), where $Y(\phi)$ was calculated from γ at 5 min.

			2D			3D		
Distribution	*D type*	*Protein*	*a*	*b*	R^2	*a*	*b*	R^2
Original	Mean	EWP	0.148	0.182	0.931	0.196	0.251	0.879
		WPI	0.100	0.166	0.978	0.132	0.219	0.948
	Median	EWP	0.128	0.159	0.911	0.158	0.202	0.844
		WPI	0.0888	0.149	0.933	0.120	0.206	0.870
	Mode	EWP	-	-	-	-	-	-
		WPI	-	-	-	-	-	-
	D_{32}	EWP	0.268	0.327	0.952	0.392	0.496	0.912
		WPI	0.161	0.258	0.992	0.186	0.291	0.978
Lognormal	Mean	EWP	0.152	0.189	0.925	0.197	0.247	0.915
		WPI	0.104	0.173	0.976	0.132	0.220	0.975
	Median	EWP	0.121	0.148	0.927	0.160	0.197	0.915
		WPI	0.0825	0.136	0.963	0.117	0.196	0.952
	Mode	EWP	0.0764	0.0893	0.914	-	-	-
		WPI	0.0521	0.0845	0.908	-	-	-
	D_{32}	EWP	0.376	0.499	0.886	0.345	0.440	0.922
		WPI	0.256	0.440	0.950	0.185	0.298	0.982
4-parameter Weibull	Mean	EWP	0.137	0.169	0.913	0.190	0.243	0.898
		WPI	0.101	0.168	0.929	0.140	0.239	0.919
	Median	EWP	0.129	0.162	0.909	0.185	0.241	0.895
		WPI	0.0866	0.145	0.945	0.129	0.223	0.909
	Mode	EWP	0.111	0.145	0.880	-	-	-
		WPI	0.0513	0.0860	0.813	-	-	-
	D_{32}	EWP	-	-	-	0.239	0.297	0.899
		WPI	-	-	-	0.189	0.313	0.948
2-parameter Weibull	Mean	EWP	0.144	0.176	0.927	0.196	0.242	0.923
		WPI	0.0970	0.160	0.973	0.140	0.234	0.963
	Median	EWP	0.0854	0.103	0.930	0.185	0.227	0.926
		WPI	0.0565	0.0923	0.949	0.133	0.222	0.959
	Mode	EWP	0.108	0.129	0.926	-	-	-
		WPI	0.0707	0.115	0.926	-	-	-
	D_{32}	EWP	0.224	0.280	0.909	0.262	0.328	0.904
		WPI	0.154	0.258	0.975	0.186	0.312	0.966

Table 6B. Parameters in function regression of $Y(\phi)=-a*ln(1-\phi)-b$ for egg white protein (EWP) and whey protein isolate (WPI), where $Y(\phi)$ was calculated from E' at 5 min.

		2D			3D		
Distribution	*D type*	*a*	*b*	R^2	*a*	*b*	R^2
Original	Mean	0.115	0.151	0.923	0.151	0.204	0.880
	Median	0.0992	0.132	0.906	0.121	0.164	0.861
	Mode	-	-	-			
	D_{32}	0.208	0.273	0.937	0.301	0.404	0.904
Lognormal	Mean	0.118	0.156	0.917	0.152	0.203	0.909
	Median	0.0942	0.124	0.923	0.124	0.164	0.913
	Mode	0.0602	0.0768	0.923			
	D_{32}	0.286	0.397	0.871	0.266	0.358	0.906
4-parameter Weibull	Mean	0.106	0.140	0.912	0.146	0.197	0.897
	Median	0.0996	0.133	0.905	0.141	0.193	0.891
	Mode	0.0844	0.116	0.873			
	D_{32}	-	-	-	0.185	0.245	0.904
2-parameter Weigull	Mean	0.112	0.147	0.920	0.152	0.201	0.915
	Median	0.0666	0.0867	0.930	0.144	0.189	0.919
	Mode	0.0841	0.109	0.931			
	D_{32}	0.174	0.232	0.899	0.203	0.271	0.895

No data for WPI is shown in Table 6B because no logical relationship can be established between $Y(\phi)$ and ϕ for WPI foams when calculating $Y(\phi)$ based on the interfacial elasticity model (Equation 16). The R^2 values are above 0.8 for all fit (Table 6A and 6B). $Y(\phi)$ calculated from 3D D_{32} (original, lognormal, 2-parameter weibull and 4-parameter weibull functions) and interfacial tension (or interfacial dilational elasticity) was plotted against ϕ in Figure 15A through 15H.

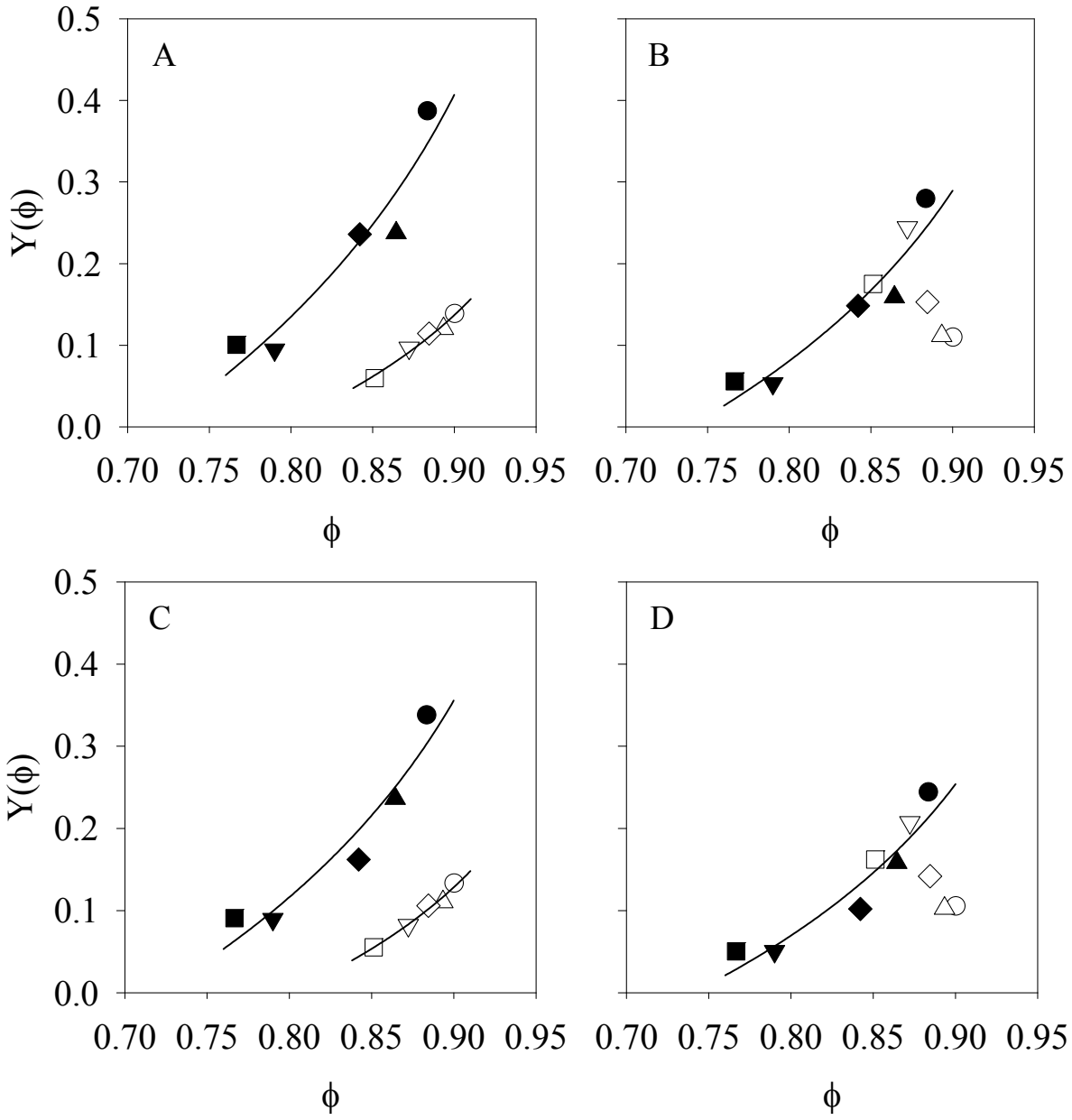
A
B
C
D
Y(ϕ)
ϕ
0.0
0.1
0.2
0.3
0.4
0.5
0.70
0.75
0.80
0.85
0.90
0.95

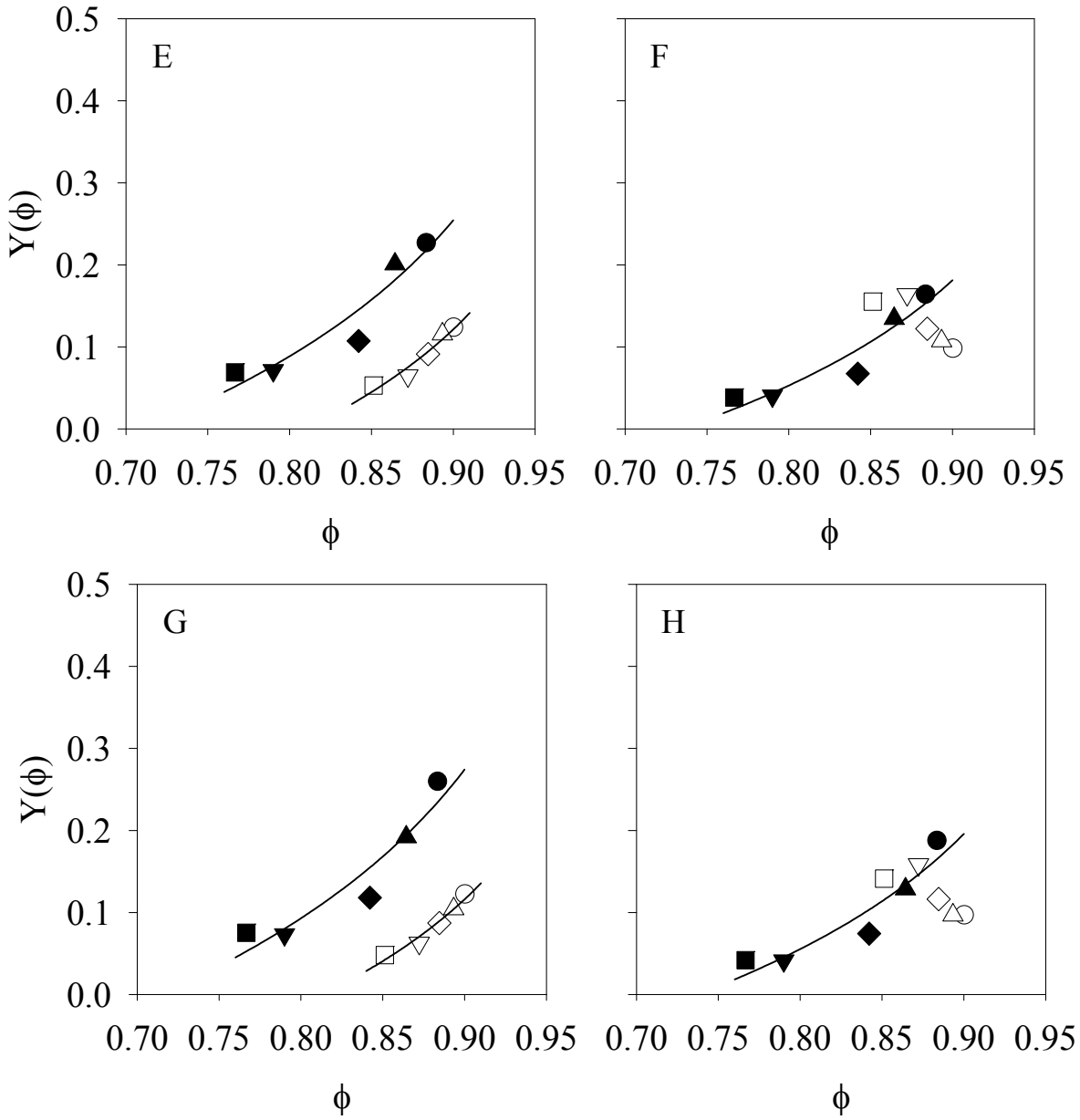

Figure 15. *Y(ϕ)* vs. *ϕ* from R_{32} calculated from the 3D bubble diameter histograms (after unfolding size distribution) for egg white protein (EWP, Close symbols) and whey protein isolate (WPI, Open symbols) in the presence of different sucrose concentrations. Protein concentration is 10% (w/v) in solutions. ● no sucrose ▲ 12.8 g/100 mL sucrose ◆ 25.0 g/100 mL sucrose ▼ 44.3 g/100 mL sucrose ■ 63.6 g/100 mL sucrose. A: *Y(ϕ)* was calculated from 3D original R_{32} and *γ*. B: *Y(ϕ)* was calculated from 3D original R_{32} and *E′*. C: *Y(ϕ)* was calculated from 3D lognormal R_{32} and *γ*. D: *Y(ϕ)* was calculated from 3D lognormal R_{32} and *E′*. E: *Y(ϕ)* was calculated from 3D 2-parameter weibull R_{32} and *γ*. F: *Y(ϕ)* was calculated from 3D 2-parameter weibull R_{32} and *E′*. G: *Y(ϕ)* was calculated from 3D 4-

parameter weibull R_{32} and γ. H: $Y(\phi)$ was calculated from 3D 4-parameter weibull R_{32} and E'. Parameters for equations were given in Table 6.

These figures have the same characteristics as discussed in Figure 13A through 13D except for a higher range of $Y(\phi)$. The range of $Y(\phi)$ depends on the type of diameter used for calculation. This result suggested that the unfolding process won't affect the validity of Princen and Kiss (1989) model in foams.

Bubble size distributions

The mean bubble diameter does not guarantee the accurate information of the bubble size distribution since different size distributions can give the same mean diameter. The bubble size distribution can be described using a histogram of bubble diameter. The original bubble diameter produced a histogram skewed toward the right, with a few large bubbles and many small ones. Plotting instead a histogram of the natural logarithm values produces a Gaussian result because the natural logarithm values of bubble diameters obey normal distribution. From the mathematic point, the natural logarithm values of bubble diameter, bubble area and bubble volume have the same distribution shape, only differing in the scale. Accordingly, the bubble size distribution histograms were plotted using the 11-bin relative frequency histograms of the natural logarithm values of bubble diameter. Figure 16A through 16E showed the relative frequency histograms of protein foams containing different amount of sucrose (0 to 63.6 g/100 mL).

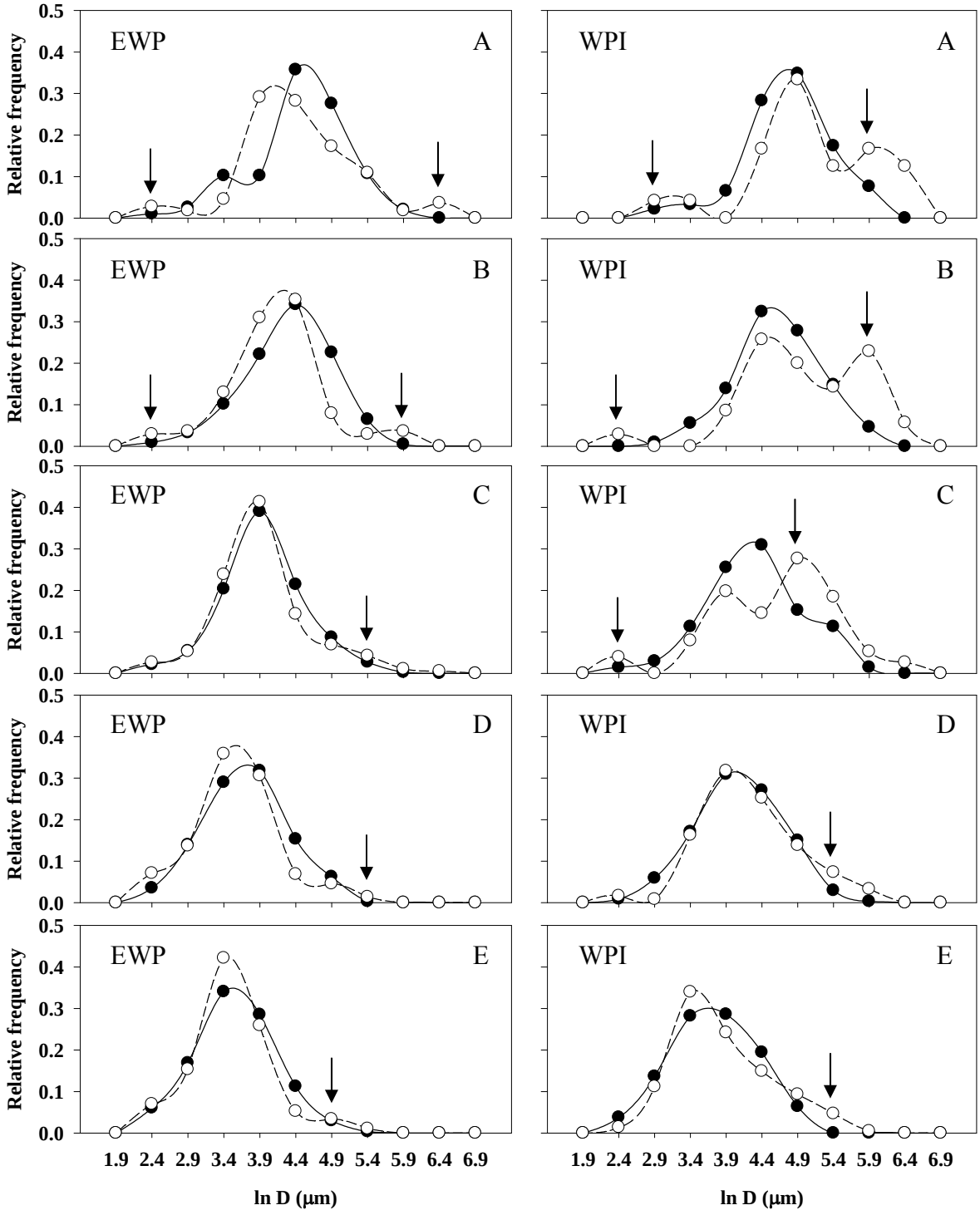

Figure 16. Changes of the histograms of logarithm values of bubble diameter from 0 to 20 min for egg white protein (EWP) and whey protein isolate (WPI) in the presence of different

sucrose concentration. Protein concentration is 10% (w/v) in solutions. A: no sucrose, B: 12.8 g/100 mL sucrose, C: 25.0 g/100 mL sucrose, D: 44.3 g/100 mL sucrose, E: 63.6 g/100 mL sucrose. Arrows indicate the position of new peaks in bubble size distribution after 20 min. in images. ● 0 min ○ 20 min

At the beginning (0 min), the histogram of each foam shows a main single symmetric peak, which shifted to the lower range with increasing sucrose concentration. After 20 min, the height of the main peak decreased while two small peaks appeared in large and small size ranges respectively, as indicated by arrows in Figure 16. This dynamic change became less obvious with increasing sucrose concentration. The change of bubble size distribution from a single peak to a bimodal pattern is corresponding to disproportionation process, in which gas transferred from small bubbles to large ones. The appearance of large bubbles also implies the possibility of coalescence. Addition of sucrose slowed down these changes mainly due to two reasons. Firstly, sucrose increased the solution viscosity and therefore limited the gas diffusion rate, which is a key step during disproportionation (Dickinson et al., 2002). The bubble movements were also impeded at a high viscosity, decreasing their approaching rate during coalescence. Secondly, sucrose changed the solvent property and thereby altered gas solubility. Air has a lower solubility at higher sucrose concentration and transfers more slowly through solvent. When sucrose concentration reached a high level (25 g/100 mL for EWP and 44.3 g/100 mL for WPI), the single peak distribution pattern didn't change significantly after 20 min. The change of foam microstructure can be easily seen in the images (Figure 5A and 5B). However, the appearance of large bubbles wasn't revealed in their relative percentage in histogram due to the high percentage of the middle size bubbles. The middle size bubble peak became even higher after 20 min (EWP: Figure 16D, 16E; WPI:

Figure 16E). The increase of large bubble percentage was indicated by arrows in Figure 16D and 16E for WPI foams. This increase was also marked by arrows but not obviously in Figure 16C, 16D and 16E for EWP foams. The change of EWP histogram was less than that of WPI when compared at the same sucrose concentrations, suggesting the better stability of EWP foam than WPI foam.

The probability curves of statistical functions were also plotted (Figure 17).

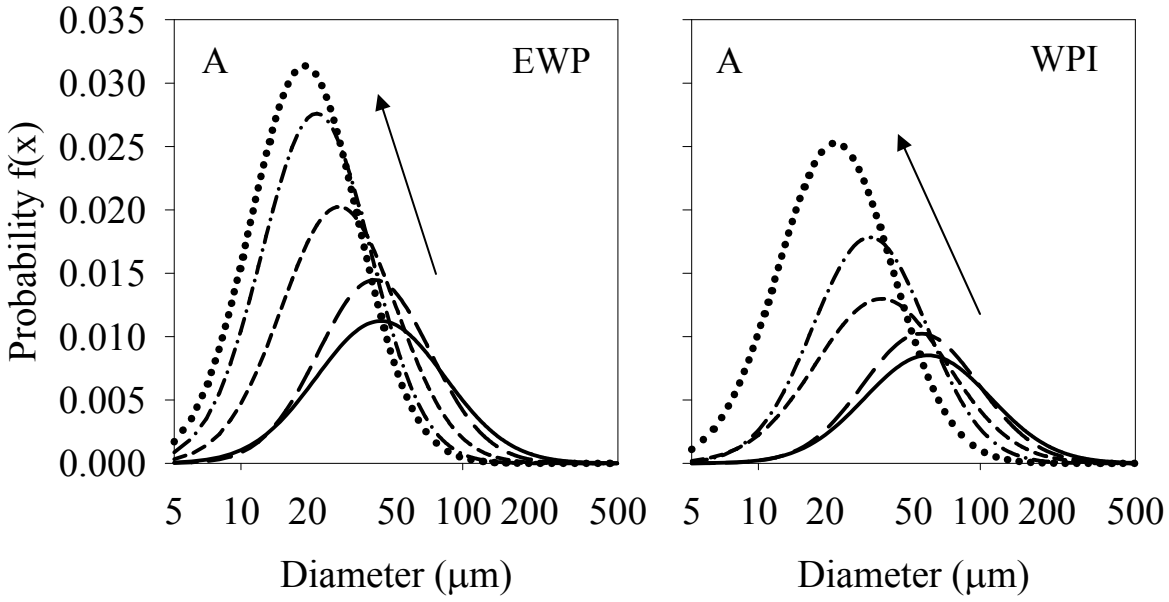

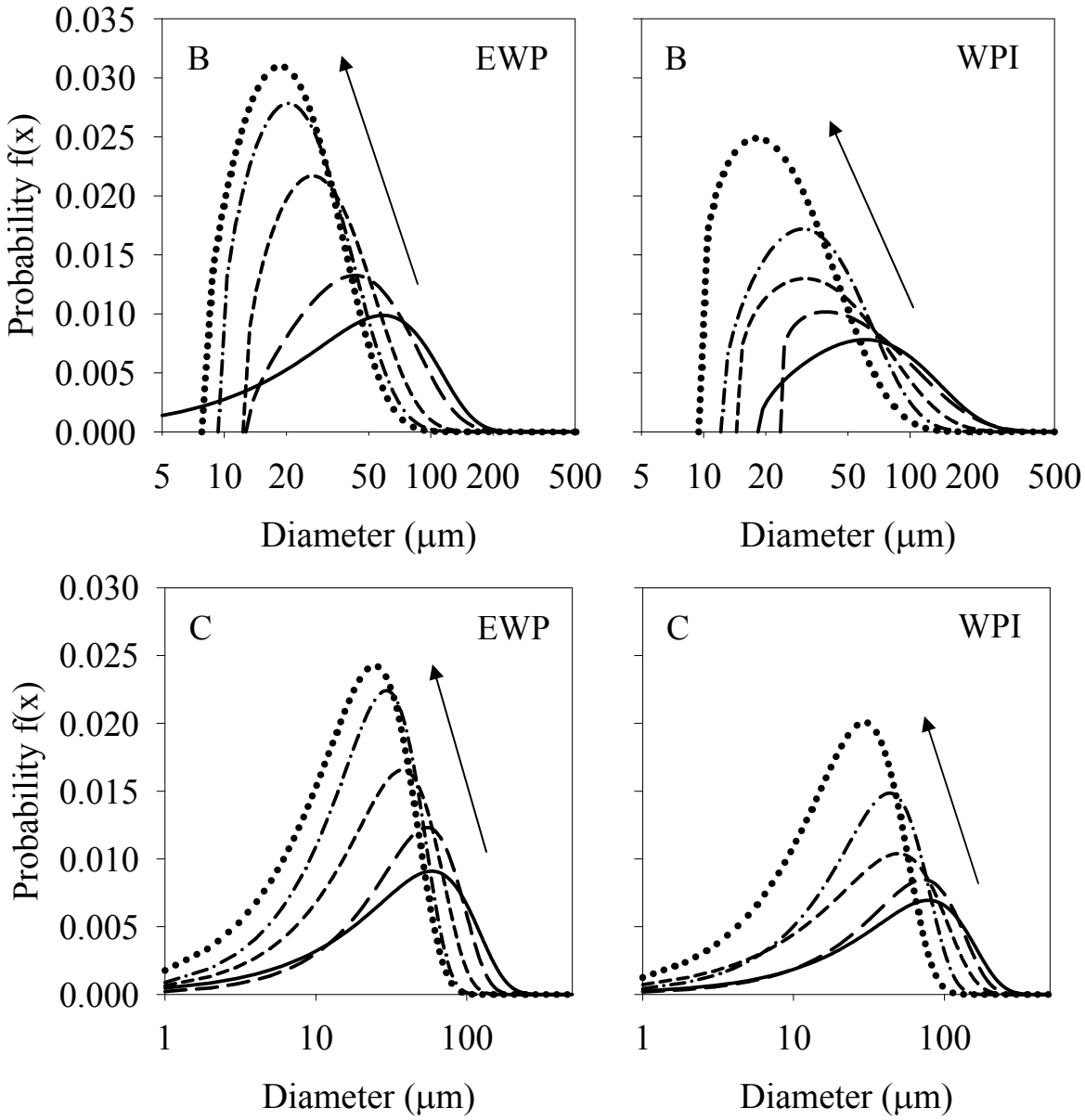

Figure 17. Probability curves of A: Lognormal, B: 4-parameter Weibull and C: 2-parameter Weibull functions for bubble diameter of egg white protein (EWP) and whey protein isolate (WPI) in the presence of different sucrose concentrations. Protein concentration is 10% (w/v) in solutions. Sucrose concentration (0.00, 12.8, 25.0, 44.3, 63.6 g/100 mL) increased along with arrow direction from solid line to dot line.

The shift of main peak to lower range with increasing sucrose concentration was coincident with the observations in the relative frequency histogram. The height of the main

peak increased gradually with sucrose addition, suggesting increasing percentages of small bubbles. There is a minimum values predicted by the 4-parameter Weibull function for each foam, which does not reflect what is observed in the real system.

Angel food cakes

Angel food cake can be used as a simple model to test protein foam stability of the wet foam and in converting to a dry foam. Studies on the EWP and WPI combinations indicated that sucrose (88.6 g/100 mL) improved the volume of angel food cakes containing EWP but not of WPI cakes (Berry, 2008). According to the previous discussion, addition of sucrose gradually changed the foaming and interfacial properties of EWP and WPI. Angel food cakes containing EWP or WPI and different amounts of sugar (0 to 88.6 g/100 mL) were made. Since sucrose changed the foam overrun, the order of sugar addition may affect the final cake volume. Two types of angel food cakes were studied; one with powdered sugar added before foaming (ABF cakes), and the other with sugar added after foaming (AAF cakes) (Table 1). The cake volumes are compared in Figure 18.

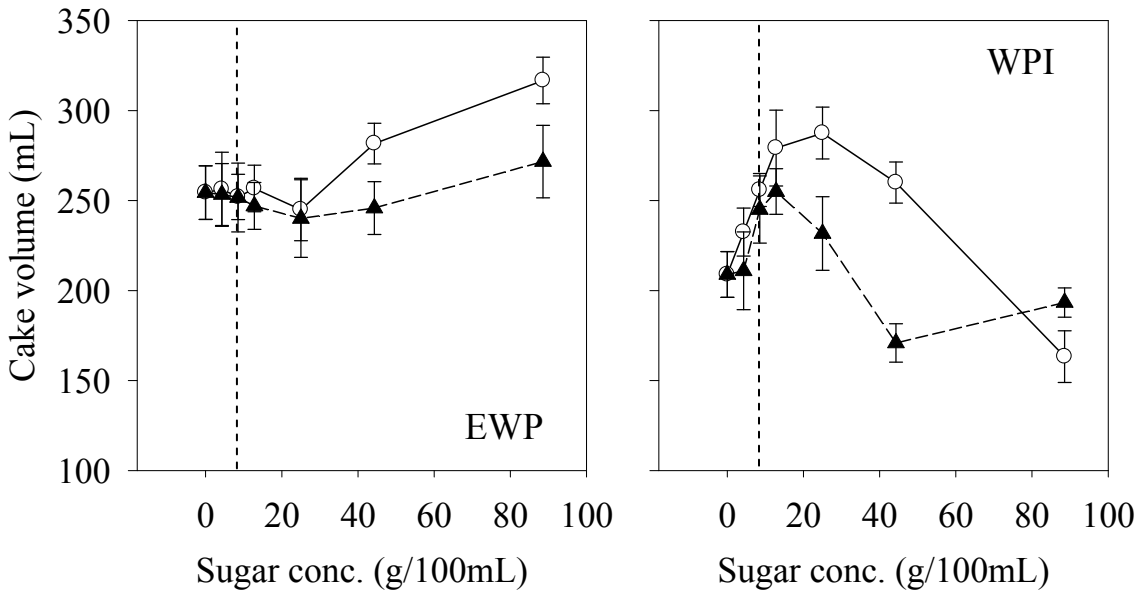

Figure 18. Cake volume of egg white protein (EWP) and whey protein isolate (WPI) in the presence of different sucrose concentrations. Protein concentration is 10% (w/v) in solutions. ○ Adding sugar after foaming (AAF) ▲ Adding sugar before foaming (ABF). The dash line indicates the sugar content in a foam for normal angel food cake preparation.

No major difference in cake volume was observed between ABF and AAF cakes when sugar content was low; while ABF cakes exhibited higher volumes than AAF cakes when sugar content was high (>44.3 g/100 mL for EWP and >25.0 g/100 mL for WPI). The exception was WPI cakes with a sugar content of 88.6 g/100 mL, in which ABF cake volume was a little higher than that of AAF cake. In the common procedure for angel food cake preparation, 12.8 g/100 mL sugar is added into protein solution before foam generation. This content is indicated by a dash line (Figure 18). When sugar content is above this value, the order of sugar addition will affect final cake volume. Addition of sugar before foam generation increased the solution viscosity and resulted in a lower overrun (Figure 2A). The decline in foam overrun became considerable and influenced the cake volume when sugar content reached a high level. Although there is a difference between ABF and AAF cakes,

the overall trends of cake volume with increasing sugar content were the same. The EWP cake volume increased with increasing sugar concentration, however, WPI cake volume resulted in a bell-shape trend with a peak value between 12.8 ~ 25.0 g/100 mL sugar concentrations. Sugar in angel food cake batters functioned as a taste ingredient as well as a bulking agent. Cake volume increased with sugar concentration due to the bulking effect. Luck et al. (2002) found a positive trend between apparent viscosity of the foaming solutions and cake volume for whey proteins, and suggested it was due to the increase of foam stability. The increased continuous phase viscosity with sucrose concentration might also contribute to cake volume. The decrease of WPI cake volume at high sugar level could be attributed to collapse of cake matrix during heating, suggesting the bulking and stabilizing effect of sugar on WPI cakes was inadequate.

The cake volume is corresponding to the air content in the final product. In addition to air content, the air bubble size distribution is another important structural characteristic of the angel food cake. Cakes of similar volume can exhibit different structure, such as 100% EWP and 75%EWP /25% WPI cakes (Figure 7 in Chapter 1). Images were taken on angel food cake cross sections (Figure 19).

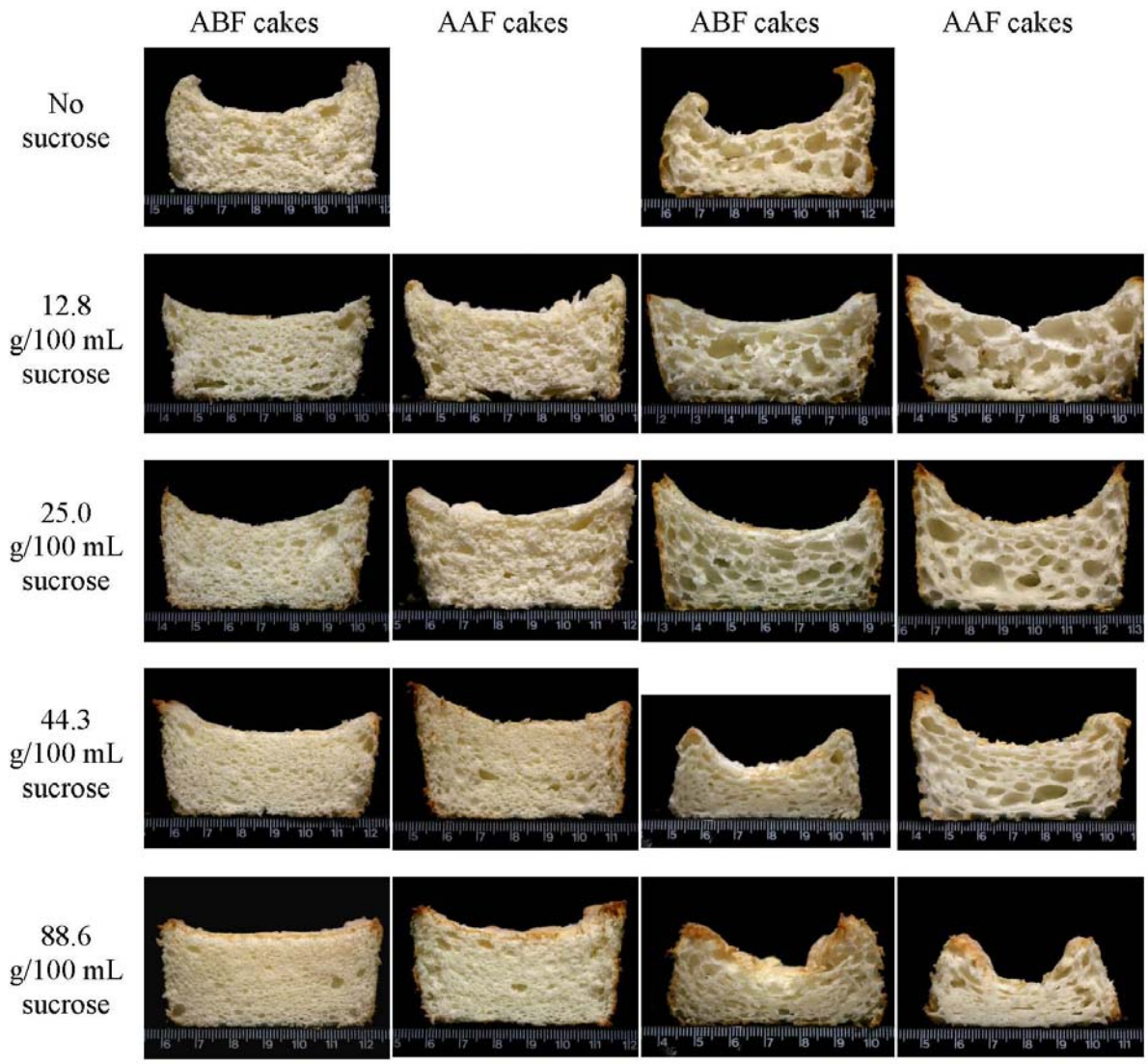

Figure 19. Photos of cross sections of angel food cakes prepared from 10% (w/v) protein solutions at pH 7.0 in the presence of different amounts of sucrose. (The unit of the scale in the images is cm.)

Although increasing sucrose concentration in foaming solutions decreased the initial bubble size (Figure 6), the ABF and AAF cakes showed similar structures at the same sugar level. The structure of angel food cakes containing EWP (column 1 and 2 in Figure 19) became finer with increasing sugar concentration; meanwhile the cake height became higher,

corresponding with a more stable foam. The concave shape of EWP cake cross section transformed to a flat shape as collapse of small bubbles was prevented with addition of sugar. The small bubbles maintained in EWP cake held the cake matrix, resulting in a higher cake volume. The structure of angel food cakes prepared from WPI foams (column 3 and 4 in Figure 19) changed from a coarse to a condense structure with increasing sugar concentration. Addition of <44.3 g/100 mL sugar improved WPI cake height and cake volume. In this case, sugar functioned as a bulking agent, assisting cake matrix formation during baking. However, it showed no improvement in the coarse cake structure. Additional increase of sugar content (>44.3 g/100 mL) in WPI cakes resulted in a condense cake structure, indicating collapse of large bubbles in the cake matrix. The concave shape of the WPI cake cross section was not altered with addition of sugar. The coarse structure and concave shape of cake are always observed in angel food cakes containing WPI (Arunepanlop et al. 1996; Berry, 2008). Addition of sugar can alter the cake volume but won't change the coarse structure of WPI cakes.

There is no major difference between ABF and AAF cakes containing EWP (column 1 and 2 in Figure 19) except for the lower cake height of ABF cakes which is corresponding to the lower cake volume. The cake structure of EWP cakes became finer with increasing sugar content, independent of the sugar adding order. However, the ABF and AAF cakes prepared from WPI foams with addition of 44.3 g/100 mL sugar showed very different structures (column 3 and column 4 in Figure 19). The condensed structure and low height of cakes when sugar was added in the foaming solution were in accordance with the low cake volume. In general, the WPI cake structure is directly related to the cake volume. All three

WPI cakes with condense structures (44.3 g/100 mL sugar ABF cake, 66.3 g/100 mL sugar AAF and ABF cakes in Figure 19) have volumes less than 200 mL (Figure 18). Addition of sugar can increase starch gelatinization and protein denaturation temperature (Munzing and Brack, 1991; Pernell et al., 2002b). During heating, air bubbles in the cake matrix expand with increasing temperature and then collapse due to film rupture. Starch gelatinizatation and protein denaturation also occurs during heating, contributing to the formation of a cake matrix. Accordingly, the final cake volume and cake structure depend on the harmonization of these processes. Large bubbles in WPI cakes indicated disproportionation and/or coalescence. Addition of sugar improved wet foam stability but could not prevent the appearance of large bubbles in WPI cakes. This is in agreement with the observation that sucrose did not slow down the decreasing rate of bubble number (Figure 7B) and the appearing of large bubbles (Figure 16) in WPI wet foams. The EWP cakes displayed a fine texture due to the heat stability of EWP foams and smaller starting bubbles (Berry, 2008). Addition of sugar improved EWP foam stability and prevented the disproportionation and/or coalescence during heating, resulting in a fine structure at a high sugar concentration. The AAF cake containing WPI and 25 g/100 mL sugar has a volume at the same level as or even higher than that of the EWP cakes. However, the cake structure was much coarser than that of EWP cakes. Although addition of sugar can improve the wet foam stability and the angel food cake volume (<25 g/100 mL) of WPI, it cannot improve the coarse cake structure.

Conclusions

Addition of sucrose gradually decreased overrun of foams made from egg white protein or whey protein isolate. Confocal laser microscopic images showed that sucrose creates an egg white foam with smaller, more stable bubbles than whey protein isolate. Foam drainage ½ life was proportional related to the solution viscosity (μ) and interfacial elasticity (E') regardless of protein type, suggesting that sucrose caused a general increase in protein foam stability due to increased viscosity of the continuous phase, and a protein-specific effect on stability factors associated with interfaces. Sucrose increases stability of whey protein isolate foam by increasing viscosity and lowering bubble size; but the loss of interfacial elasticity decreased stability. The angel food cake prepared from whey protein isolate foam showed coarse structure, unlike the fine structure of egg white protein cake, indicating poor stability of bubbles in angel food cake. The appearance of large bubbles indicated the rapid destabilization of whey protein foams during heating, which is not in harmony with structure formation associated with starch or gluten effects.

REFERENCES

Antipova AS, Semenova MG, Belyakova LE. 1999. Effect of sucrose on the thermodynamic properties of ovalbumin and sodium caseinate in bulk solution and at air-water interface. Colloids Surf B: Biointerfaces 12: 261-270.

Arunepanlop B, Morr CV, Karleskind D, Laye I. 1996. Partial replacement of egg white proteins with whey proteins in angel food cakes. J Food Sci 61: 1085-1093.

Barnes HA, Hutton JF, Walters K. 1989. An introduction to rheology. Amsterdam: Elsevier. p199.

Belyakova LE, Antipova AS, Semenova MG, Dickinson E, Merino L, Tsapkina EN. 2003. Effect of sucrose on molecular and interaction parameters of sodium caseinate in aqueous solution: relationship to protein gelation. Colloids Surf B: Biointerfaces 31: 31–46.

Berry TK. 2008. Foaming Properties, Interfacial Properties, and Foam Microstructure of Egg White Protein and Whey Protein Isolate, Alone and in Combination. Thesis and dissertation. North Carolina State University.

Calvert JR, Nezhai K. 1987. Bubble size effects in foams. Int J heat fluids 8: 102-106.

Campbell GM, Mougeot E. 1999. Creation and characterization of aerated food products. Trends Food Sci Tech 10: 283-296.

Cruz-Orive LM. 1976. Particle size-shape distributions: the general spheroid problem. J. Microscopy. 107:235 and 112:153.

Damodaran S. 2005. Protein stabilization of emulsions and foams. J Food Sci 70: R54-R66.

Davis JP, Foegeding EA. 2004. Foaming and interfacial properties of polymerized whey protein isolate. J Food Sci 69: C404-C410.

Davis JP, Foegeding EA. 2007. Comparisons of the foaming and interfacial properties of whey protein isolate and egg white proteins. Colloids Surf B: Biointerfaces 54: 200-210.

DeVilbiss ED, Holsinger VH, Posati LP, Pallansch MJ. 1974. Properties of whey protein concentrate foams. Food Tech 28: 40-48.

Dickinson E. 1992. An Introduction to Food Colloids. Oxford: Oxford University Press. p135, 216.

Dickinson E, Ettelaie R, Murry BS, and Du Z. 2002. Kinetics of disproportionation of air bubble beneath a planar air-water interface stabilized by food proteins. J Colloid Interface Sci 252: 202-213.

Dickinson E, Merino LM. 2002. Effect of sugars on the rheological properties of acid caseinate-stabilized emulsion gels. Food Hydrocolloids. 16(4): 321-331.

Dzuy NQ, Boger DV. 1985. Direct Yield Stress Measurement with the Vane Method. J Rheology 29: 335-347.

Fang Z, Patterson PR, Turner Jr. ME. 1993. Modeling particle size distributions by the Weibull distribution function. Mater Charact 31:177-182.

Foegeding EA, Davis JP, Doucet D, McGuffey MK. 2002. Advances in modifying and understanding whey protein functionality. Trends Food Sci Technol 13: 151-159.

Foegeding EA, Luck PJ, Davis JP. 2006. Factors determining the physical properties of protein foams. Food Hydrocolloids 20: 284-292.

Graham DE, Phillips MC. Proteins at liquid interfaces: I. kinetics of adsorption and surface denaturation. J Colloid Interface Sci 1979; 70(3):403-414.

Halling PJ. 1981. Protein stabilized foams and emulsions. Crit Rev Food Sci Nutr 13: 155–203.

Lage PLC, Espósito RO. 1999. Experimental determination of bubble size distributions in bubble columns: prediction of mean bubble diameter and gas hold up. Powder Technol 101**:** 142–150.

Lau CK, Dickinson E. 2005. Instability and structural change in an aerated system containing egg albumen and invert sugar. Food Hydrocolloids 19, 111-121.

Luck PJ, Bray N, Foegeding EA. 2001. Factors Determining Yield Stress and Overrun of Whey Protein Foams. J Food Sci 65: 1677-1681.

Magrabi SA, Dlugogorski BZ, Jameson GJ. 1999. Bubble size distribution and coarsening of aqueous foams. Chem Eng Sci 54: 4007–4022.

Mason TG. 1999. New fundamental concepts in emulsion rheology. Curr Opin Colloid Interface Sci 4: 231-238.

Merran E, Hastings N, Peacock B. 2000. Statistical distributions. 3rd Edition. John Wiley and Sons, Inc. p129.

Munzing K, Brack G. 1991. DSC-studies of flour confectionery. Thermochimica Acta 187: 167-173.

Myrvold R, Hansen FK. 1998. Surface elasticity and viscosity from oscillating bubbles measured by automatic axisymmetric drop shape analysis. J Colloid Interface Sci 207: 97-105.

Pernell CW, Foegeding EA, Daubert CR. 2000. Measurement of the yield stress of protein foams by vane rheometry. J Food Sci 65: 110-114.

Pernell CW, Foegeding EA, Luck PJ, Davis JP. 2002a. Properties of whey and egg white protein foams. Colloids Surf A: Physicochemical and Engineering Aspects 204: 9-21.

Pernell CW, Luck PJ, Foegeding EA, Daubert CR. 2002b. Heat-induced changes in angel food cakes containing egg-white protein or whey protein isolate. J Food Sci 67: 2945-2951.

Peter PN, Bell RW. 1930. Normal and modified foaming properties of whey-protein and egg-albumin solutions. Ind Eng Chem 22: 1124-1128.

Phillips LG, Haque Z, Kinsella JE. 1987. A method for the measurement of foam formation and stability. J Food Sci 52: 1074-1077.

Phillips LG, Yang ST, Schulman W, Kinsella JE. 1989. Effects of lysozyme, clupeine, and sucrose on the foaming properties of whey protein isolate and beta-lactoglobulin. J Food Sci 54: 743-747.

Princen HM. 1982. Rheology of foams and highly concentrated emulsions: I. Elastic properties and yield stress of a cylindrical model system. J Colloid Interface Sci 91(1): 160-175.

Princen HM, Kiss AD. 1989. Rheology of foams and highly concentrated emulsions. 4. An experimental study of the shear viscosity and yield stress of concentrated emulsions. J Colloid Interface Sci 128:176-187.

Raikos V, Campbell L, Euston SR. 2007. Effects of sucrose and sodium chloride on foaming properties of egg white proteins. Food Res Int 40: 347-355.

Richert SH. 1979. Physical-Chemical properties of whey protein foams. J Agric Food Chem 27: 665-668.

Ruíz-Henestrosa VP, Sánchez CC, Rodríguez Patino JM. 2008. Effect of sucrose of functional properties of soy globulins: Adsorption and foam characteristics. J Agric Food Chem.

Russ JC, Dehoff RT. 2000. Practical stereology. 2nd Edition. Kluwer Academic / Plenum Publishers, New York. p297.

Russ JC. 2005. Image Analysis of Food Microstructure. CRC Press LLC. 5p.
Saltykov SA. 1967. The determination of size distribution of particles in an opaque material from the measurement of the size distribution of their sections. Stereology. Springer Verlag, New York. p163.

Saltykov SA. 1967. The determination of size distribution of particles in an opaque material from the measurement of the size distribution of their sections. Stereology. New York: Springer Verlag. p163.

Steffe JF. 1996. Rheological Methods in Food Process Engineering. 2nd ed. East Lansing, MI: Freeman Press. p15, 418.

Walstra P. 2003. Physical Chemistry of Foods. New York: Marcel Dekker.

Wang Z, Narsimhan G. 2006. Model for Plateau border drainage of power-law fluid with mobile interface and its application to foam drainage. J Colloid Interface Sci 300: 327-337.

Yankov S, Panchev I. 1996. Foaming properties of sugar-egg mixtures with milk protein concentrates. Food Res Int. 5-6: 521-525.

CHAPTER 4

Manuscript to be submitted for publication

Interfacial Rheology Study of Individual Protein Components of Whey Protein Isolate and Egg White Protein in the presence of Sucrose

Authors: Xin Yang and E. Allen Foegeding

Abstract

The interfacial dilational elasticity of components in whey and egg white proteins and their mixtures were evaluated using a pendent drop method in the absence and presence of 44.3% (w/v) sucrose (half of the sucrose concentration found in an angel food cake). β-lactoglobulin was purified from whey protein isolate using a precipitation method, with the β-lactoglobulin depleted fraction collected. Ovalbumin was separated from egg white protein using ion-exchange chromatography, with the ovalbumin depleted fractions collected. Commercial samples of α-lactalbumin and β-lactoglobulin were also evaluated. Protein composition of each fraction was determined using SDS-PAGE. Addition of sucrose decreased the interfacial elasticity (E') of α-lactalbumin and the β-lactoglobulin depleted fraction, resembling the characteristics of whey protein isolate. However, sucrose showed no major effect on the E' of β-lactoglobulin. Commercial β-lactoglobulin had a lower E' than the purified β-lactoglobulin in the presence of sucrose, due to the presence of a few other fractions. Sucrose increased E' of egg white protein and the ovalbumin depleted fraction. The E' of ovalbumin was much higher than that of egg white protein, with no major change after sucrose addition. The E' of protein mixtures indicated that the interfacial domination priority followed the order of α-lactalbumin > β-lactoglobulin > egg white proteins. The properties of wet foams (overrun, yield stress, drainage ½ life and microstructure) and angel food cakes (volume and structure) were evaluated for commercial β-lactoglobulin after adding different amounts of sugar. Commercial β-lactoglobulin had longer foam drainage ½ life than that of whey protein isolate, attributing to a higher E'. However, addition of sugar did not slow down large bubbles appearing in foams, leading to a coarse structure of angel food cakes.

Key words: Interfacial rheology, foam, α-lactalbumin, β-lactoglobulin, ovalbumin

Introduction

A foam structure is an important element of many food products (Campbell and Mougeot, 1999). The majority of food foams are stabilized by an adsorbed layer of proteins at the air/water interface (Dickinson et al., 1988). The interfacial activity of proteins are attributing to several molecular properties, including size, charge, the molecule rigidity, structural feathers, stability, amphipathicity and lipophylity (Magdassi and Kamyshny, 1996). After interfacial adsorption, proteins tend to interact with each other and form a film with measurable rheological properties. The possible intermolecular interactions include hydrogen bonding, hydrophobic contacts, electrostatics, disulfate bond formation and van der Waals forces, depending on the amino acid composition and the molecular structure (Prins et al., 1998). Many proteins exhibited different interfacial rheological characteristics when having similar interfacial tension (Bos et al., 2001). The interfacial viscoelastic fingerprints have been used to as a sensitive probe to detect the competitive adsorption and cooperative interactions in mixed protein systems (Ridout et al., 2004; Dickinson et al., 1990). The interactions among proteins and other surface-active ingredients such as low molecular weight emulsifiers and lipids, have been also extensively studied using the interfacial rheological techniques (Bos et al., 2001; Dickinson, 2001; Baeza et al., 2004).

Interfacial network formation of proteins has been related to bubble stability using theoretical models (Kloek et al., 2001). Dickinson et al. (2002) observed the shrinkage of single air bubbles beneath a planar air-water interface for four types of proteins. They found that the rates of change of bubble radius for the proteins forming an elastic film were slower than the rates expected from a theoretical model without consideration of interfacial

elasticity, fitting to the prediction of a theoretical model involving the contribution of interfacial elasticity. In addition, bubbles coated with β-lactoglubulin, which forms a strong and coherent interfacial film, formed residual protein particles and faded slowly at the end of the shrinking process; while the bubbles covered with other proteins disappeared rapidly. These observations suggested that the interfacial elasticity of protein films can effectively slow the disproportionation of bubbles. Martin et al. (2002) studied the relationship between foam stability and interfacial viscoelsticity for proteins with a range of structures from flexible to rigid. They found that glycinin (pH 3) had a higher interfacial elasticity and was more stable to coarsening (bubble size growing) than β-casein whereas the abilities against foam drainage of the two proteins were almost equal. In their study, coalescence was not observed and the coarsening of protein foams was only due to disproportionation. Although interfacial elasticity is not directly correlated with film drainage, a prevention of disproportionation and/or coalescence can slow down foam drainage. In Chapter 3, we established a proportional relationship between interfacial dilational elasticity (E') and foam drainage ½ life via varying the sugar concentration in 10% (w/v) protein solutions. The key difference between whey protein isolate and egg white protein is E', which leads to dissimilar foam stability of two proteins in the presence of sucrose. Interfacial elasticity has been positively correlated with foam yield stress (τ_0) for whey protein isolates when varying the solution composition (Foegeding et al., 2006). A positive correlation was also established for whey protein isolate and whey protein isolate and egg white protein mixtures in Chapter 2. The relationship between τ_0 and E' for protein solutions containing different amounts of sucrose was described using the Princen and Kiss (1989) model after substituting interfacial

tension with E' (Chapter 3). These observations suggest that interfacial rheology can be used as an effective index to predict the effect of other components on the foaming behavior of a single protein system.

Sugar is a common ingredient in food products. The presence of sugar can influence protein functionality (McClements, 2002). For example, foam stability can be enhanced with addition of sugar, mainly due to the increase of solution viscosity (Phillips et al., 1989; Lau and Dickinson, 2005). The sugar effect on the interfacial elasticity (E') is protein-specific. Davis and Foegeding (2007) found that sucrose increased E' for egg white protein but decreased E' for whey protein isolate. These effects were confirmed in Chapter 3. However, addition of 25% (w/w) sucrose generated a decrease of E' for β-lactoglobulin while minimally affected E' of ovalbumin, dissimilar to the response of whey protein isolate and egg white protein (Davis and Foegeding, 2007). E' of bovin serum albumin was dependent on the sucrose concentration and did not decrease until sucrose concentration reached 1 M (Niño et al., 1997). The sugar effect on interfacial characteristics of proteins can be attributed to several aspects. Firstly, addition of sugar increases the bulk phase viscosity and impedes the diffusion rate of molecules. Secondly, the presence of sugar may alter the protein structure, modifying the molecular properties such as the size and hydrophobicity. Thirdly, sucrose can interact with protein molecules and change their interfacial activity directly (Antipova et al., 1999).

Egg white and whey protein are two wildly used food ingredients. The physicochemical properties of individual protein components determine the characteristics of foam-containing food products. In this study, the proteins in whey protein isolate and egg

white protein were divided into several parts – α-lactalbumin, β-lactoglobulin, ovalbumin, β-lactoglobulin depleted fraction and ovalbumin depleted fractions. The interfacial rheological properties of these components in the absence and presence of sucrose were evaluated alone and in combination. Previous studies indicated that addition of sucrose caused dissimilar modification on the interfacial elasticity of whey and egg white protein, leading to great difference in foam stability. The goal of this study is to find out the key components corresponding to the dissimilar interfacial behaviors of whey and egg white in the presence of sucrose.

Materials and Methods

Materials

Commercial samples of whey protein isolate (BiPro, 93% protein, dry basis), α-lactalbumin (BioPURE, 93% protein, dry basis) and β-lactoglobulin (BiPURE, 93% protein, dry basis) were supplied by Davisco Foods International, Inc. (Le Sueur, MN). Whey protein isolate (WPI) was stored at room temperature (22 ± 2 °C). The α-lactalbumin and β-lactoglobulin samples were stored at -20 °C. Spray dried egg white protein (82% protein, dry basis) was obtained from Primera Foods (Cameron, WI) and stored at 4 °C. Pure β-lactoglobulin and ovalbumin were separated from whey protein isolates and egg white proteins as described in the following and stored at -20°C. Cake flour and 10x powdered sugar were purchased from a local grocery store. Sucrose (ACS) was obtained from Fisher Scientific Inc. (Fair Lawn, NJ). All other chemicals were of reagent grade quality. Deionized

water was obtained using a Dracor Water Systems (Durham, NC) purification system. The resistivity was a minimum of 18.2ΩM cm.

Methods

β-lactoglobulin purification and depleted β-lactoglobulin fraction collection

β-lactoglobulin was purified from whey protein isolate powder (BioPro, 94%, Davisco Foods International, Inc.) base on the method of Mailliart and Ribadeau-dumas (1988). Briefly, whey protein isolate was dissolved in deionized water on a ratio of 150 g / 1000 mL with addition of 70 g NaCl. The pH was adjusted to 3.0. After stirring at room temperature for 30 min, the solution was centrifuged at 10000 g, 4°C for 20 min. The supernatant (β-lactoglobulin fraction) was filtered through a 0.45μm filter and adjusted to pH 6.7. After dialysis in deionized water at 4 °C, the solution was freeze dried and stored at -20 °C. The precipitation (β-lactoglobulin depleted fraction) was dissolved in deionized water and adjusted to pH 6.7. After dialysis in deionized water at 4 °C, the solution was freeze dried. The commercial samples of whey protein isolate, α-lactalbumin and β-lactoglobulin were also dialyzed in deionized water at 4 °C and then freeze dried. The protein content of each fraction was determined using BCA™ Protein Assay Kit according to the instruction manual (Pierce, Rockford, IL).

Ovalbumin purification and depleted ovalbumin fractions collection

A batch of ovalbumin was purified from commercial egg white protein powder using a modified method of Kosters et al. (2003). The process is illustrated in Figure 1.

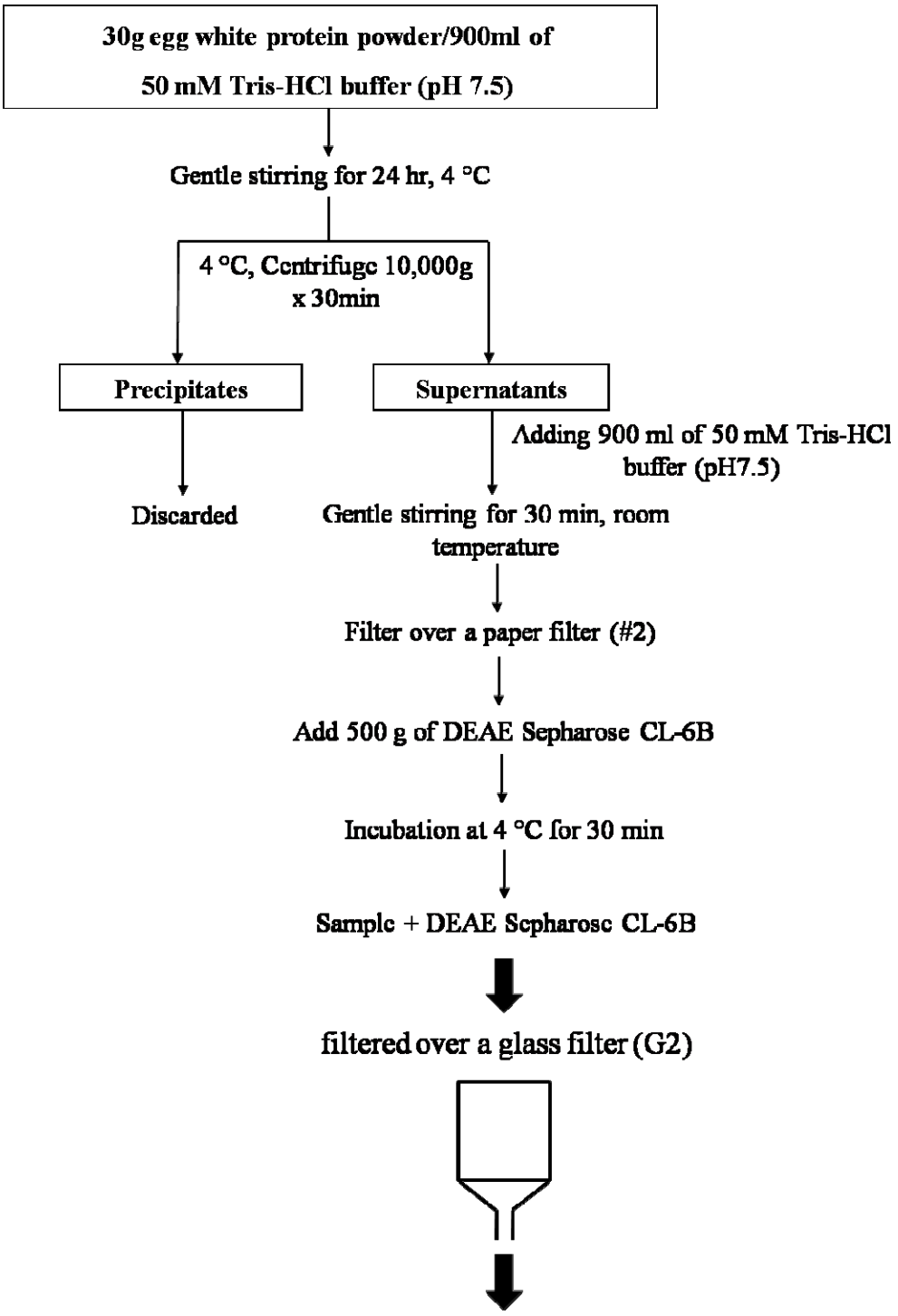
30g egg white protein powder/900ml of
50 mM Tris-HCl buffer (pH 7.5)
Gentle stirring for 24 hr, 4 °C
4 °C, Centrifuge 10,000g
x 30min
Precipitates
Supernatants
Adding 900 ml of 50 mM Tris-HCl
buffer (pH7.5)
Discarded
Gentle stirring for 30 min, room
temperature
Filter over a paper filter (#2)
Add 500 g of DEAE Sepharose CL-6B
Incubation at 4 °C for 30 min
Sample + DEAE Sepharose CL-6B
filtered over a glass filter (G2)

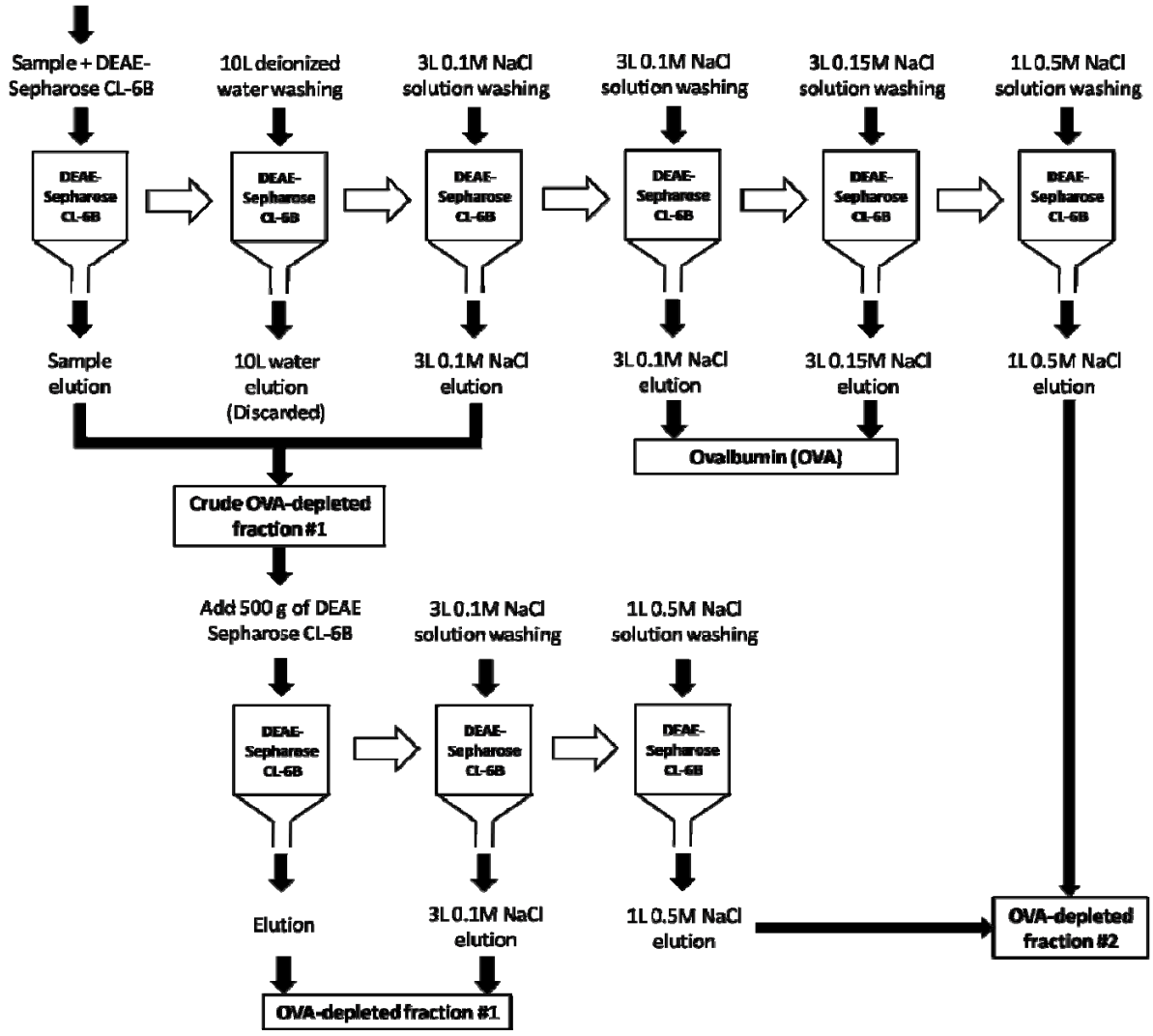

Figure 1. Purification process of egg white protein fractions. OVA is for ovalbumin.

The #2 paper filter was from Schleicher & Schuell (Keene, NH) and DEAE Sepharose Cl-6B was from Pharmacia (Uppsala, Sweden). All fractions were desalted and concentrated using a Millipore (Bedford, MA) ultrafiltration unit with an Aminco spiral ultrafiltration cartridge (Millipore) with a 10 kDa molecular mass cut-off. The concentrated solutions were freeze-dried and stored at -20°C until further use. The commercial sample of egg white protein was also desalted using the ultrafiltration system and then freeze dried. The

protein content of each fraction was determined using BCA™ Protein Assay Kit according to the instruction manual (Pierce, Rockford, IL). Generally, the ratio of the three fractions (OVA : OVA-depleted 1 : OVA-depleted 2) was 47:42:11 based on their protein content.

Polyacrylamide Gel Electrophoresis in SDS (SDS-PAGE)

The protein composition of each fraction was observed using NuPAGE® Bis-Tris Electrophoresis System. All gels and reagents were from Invitrogen Corporation (Carlsbad, CA). Proteins were separated on pre-cast NuPAGE® 4-12% Bis-Tris Gel according to the protocol in the NuPAGE® electrophoresis system instruction manual. Proteins were dissolved in NuPAGE® LDS sample buffer. Then, 20 μL of each sample containing about 10 μg protein was loaded in each cell. For reducing SDS-PAGE, the NuPage® Sample reducing agent (containing 2,3-butanediol,1,4-dimercapto-,(theta, theta)-(+/-)-) was added to the solution before loading samples. Electrophoresis in gels was performed in the XCell SureLock MiniCell system using NuPAGE® MES SDS running buffer at a constant 200V. Gels were stained with the NOVEX® Colloidal Blue Stain Kit. Dry gels were prepared using Gel-Dry™ drying solution.

Protein solutions

Protein solution was prepared by dissolving protein powders in deionized water at room temperature (22 ± 2 °C). The pH was adjusted to 7.0 before final volume adjustment to 10% w/v protein. Sucrose concentration was on % (w/v) basis in the final solution if not specifically indicated. For the study of the foaming properties for the commercial β-lactoglobulin, sucrose was added to the 10% (w/v) protein solutions on a % (w/v) basis. This

is to achieve the same concentration of sucrose and protein as in the whey protein isolate and egg white protein solutions in Chapter 3.

Interfacial tension

Air/water interfacial tension of pre-foam solution was determined using an automated contact angle goniometer (Rame-Hart Inc, Mountain Lakes, NJ) in combination with the DROPimage computer program according to the method Myrvold and Hansen (1998). A computer-controlled syringe generated a16 μL pendant drop of pre-foam solution from a stainless-steel capillary into an environmental chamber with standing water to minimize evaporation. The image of the pendant drop was captured by a digital camera immediately after the droplet formation. The shape parameter of the drop was used to calculate the air/water interfacial tension. The dynamic change of interfacial tension was measured every 2 s for 5 min for each solution. All measurements were at room temperature (22 ± 2 °C). HPLC water with an interfacial tension of 72.3 mN/m at room temperature was used as a standard solution to calibrate the system before measurements. This method has an estimated experimental error of ± 1.0 mN/m. Data reported are averages of a minimum of three replications.

Interfacial dilational modulus

To measure dilational visco-elasticity of the interfaces, sinusoidal oscillations of the drops' areas were increased by volume amplitude of 0.5 μL at a frequency of 0.1 Hz (Myrvold and Hansen, 1998). The resulting changes in interfacial tension and interfacial area were collected and used to calculate the dilational modulus using the DROPimage software.

Drops were suspended for 300 s before measurement. Values reported are averaged from a minimum of three replications.

Density determination

The phase densities of solutions are required by the DROPimage software for the interfacial tension calculation from drop shape analysis. A Mettler-Toledo DE40 density meter (Mettler-Toledo, Columbus, OH) in combination with a viscosity correction card was used to determine the density of each solution at room temperature (22 ± 2 °C). The accuracy of the instrument is 1×10^{-4} g/cm^3. Each solution was evaluated in three times and averaged.

Foaming properties

The foaming properties of commercial β-lactoglobulin were evaluated using 10% (w/v) protein solutions. Foams were generated on a Kitchen Aid Ultra Power Mixer (Kitchen Aid, St. Joseph's, MI) with a 4.3 L stationary bowl following the same method as in Chapter 2 and Chapter 3. Two hundred mL of 10% (w/v) protein solutions was whipped for 20 min at a speed setting of 8 (planetary rpm of 225 and beater rpm of 737). Foam yield stress was measured using a vane method as described by Pernell et al. (2000). Immediately after foam generation, the vane (10 mm in diameter and 40 mm in length) was gently inserted into the foam and rotated at a speed of 0.3 rpm. The maximum torque response was recorded and used to calculate foam yield stress. Foam overrun was measured according to the method of Phillips et al. (1987). After yield stress measurement, the foam was scooped into a standard weight boat (100 mL) and weighted. The weight of pre-foam solution of the same volume (100 mL) was determined as well. Foam overrun was calculated from the two weights. Foam drainage ½ life was measured by recording the time required for half the mass of a foam to

drain (Phillips et al., 1987). A bowl with a 6-mm diameter hole in the bottom was used for foam generation. Immediately after the final overrun measurement, the bowl was placed in a ring stand over a scale with the hole uncovered. The foam was drained into a weight boat and time necessary for half the mass to drain was recorded. The overrun measurements removed some mass of the foam (less than 20% of the mass of the pre-foam solution), which was subtracted when calculating half of the foam mass. Details of the three methods are found in Chapter 3. All measurement were at room temperature (22 ± 2 °C) and replicated a minimum of three times for each treatment.

Viscosity measurements

Viscosity of pre-foam solutions was measured according to the method of Davis and Foegeding (2004). A controlled stress rheometer (StressTech; Reologica Instruments AB, Lund, Sweden) equipped with cup and bob geometry (measuring system CCE25) was utilized. Samples were pre-sheared at 50 s^{-1} for 30 s and followed by viscosity measurement over a range of shear rates (0.5 s^{-1} to 225 s^{-1}). The rheological behavior of protein solutions was described by a power law model (Barnes et al., 1989). Shear stress and shear rate data for each sample were fit to the power law model, with the consistency constant and flow behavior index predicted. The apparent solution viscosity was calculated at a shear rate of 8.5 1/s based on the power law model. All measurements were at room temperature (22 ± 2 °C) and replicated a minimum of three times for each treatment.

Confocal microscopy

The microscopic structure of the protein foams were examined using an inverted Leica DM IRBE (Heidelberg, Germany) confocal laser scanning microscope (CLSM)

according to the method of Berry (2008). The protein phase was stained with 0.1mM sodium fluorescein. The foam sample was loaded into a single-welled microscope slide with a #1.5 cover slip attached to the bottom using silicon grease and scanned immediately after foam generation. The dye was excited by an argon laser at 488nm. Light at a range from 500-550 nm was collected. Three slides were prepared per treatment, with samples taken from three random positions in a foam. The three slides were rotationally scanned under the CLSM at 5 min interval for 20 min. The imaging time difference between slides was no more than 1 min. The image analyzing results were averaged from the three slides for each treatment.

Image analysis

Image analysis was done using MetaMorph Imaging System software, version 6.1 (Molecular Devices, Downington, PA, USA) following the method of Berry (2008). All images were converted to binary using the same threshold, allowing objects (air bubbles) to stand out against the background aqueous phase. Overlapping or touching bubbles were manually separated using a "cut" feature. Because of the variation in pixel brightness values, pixels may be missing from the center of some small bubbles. In this case, a "join" feature was used to manually outline these bubbles and to fill in their broken centers. The edge bubbles with less than 50% of their estimated area visible were manually de-selected, preventing skewing the bubble sizes to smaller range due to only a small portion of the bubble being analyzed. The area of the selected object (bubble) was measured using an integrated morphometry analysis feature. Observations showed that objectives with areas of less than 10 pixels were not actual bubbles. To eliminate noise, these values were excluded from image data before further analysis. Mean and median values were evaluated from the

bubble area data set for each image. The average and standard deviation of mean bubble area and median bubble area were calculated from the data of three images per treatment.

Angel Food Cake Preparation

Angel food cakes were prepared based on the method of Pernell et al. (2002). Foams were generated from 200 mL protein solutions. The dry blend (flour and powdered sugar) was sifted 3 times and gently folded into the foam using a balloon whisk in 3 installments and no more than 30 strokes total. The batter was poured into 3 cake pans with 75.0 g batter per each and baked in a conventional oven at 204 °C for 14 min. The cakes were cooled upside down on a wire rack at room temperature for at least 30 min before volume measurement. The cake volume was measured using a rapeseed displacement method (Pernell et al., 2002). Three cakes were made from each cake batter and all treatments were replicated twice.

Results and discussion

Purification of individual protein components

The major bovine milk whey proteins are β-lactoglobulin (~50%), α-lactalbumin (~25%), bovine serum albumin, and immunoglobulins (Swaisgood, 1982). All of these fractions were indentified in the non-reducing SDS-PAGE of the commercial whey protein isolate (WPI) sample (Figure 2, Column 2).

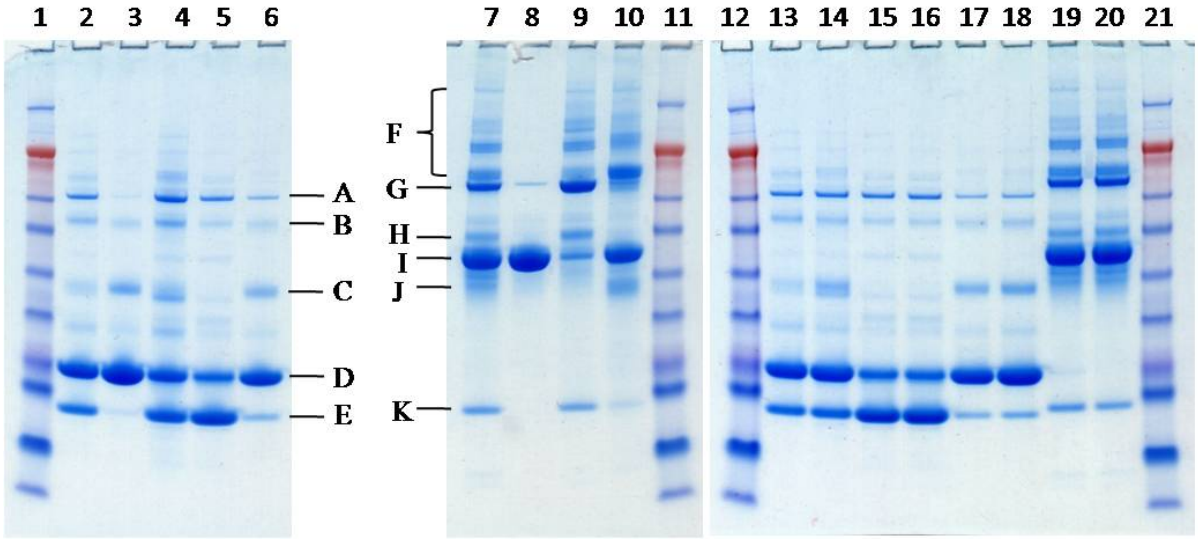

Figure 2. SDS-PAGE of protein fractions. Columns 1, 11, 12, and 21: standard; Column 2 and 13: whey protein isolates (WPI); Column 3: purified β-lactoglobulin (purified-BLG); Column 4: β-lactoglobulin depleted fraction (BLG-depleted); Column 5 and 15: commercial α-lactoalbumin (ALAC); Column 6 and 17: commercial β-lactoglobulin (commercial BLG); Column 7 and 19: egg white proteins (EWP); Column 8: purified ovalbumin (OVA); Column 9: ovalbumin depleted fraction 1 (OVA-depleted 1); Column 10: ovalbumin depleted fraction 2 (OVA-depleted 2); Column 14: Dialyzed WPI; Column 16: Dialyzed ALAC; Column 18: Dialyzed BLG; Column 20: Ultrafiltrated EWP. The molecule weights corresponding to the bands in standard are: 188 kDa (Myosin), 98 kDa (Phosphorylase), 62 kDa (BSA), 49 kDa (Glutamic Dehydrogenase), 38kDa (Alcohol Dehydrogenase), 28kDa (Carbonic Anhydrase), 17kDa (Myoglobin Red), 14kDa (Lysozyme), 6kDa (Aproinin), 3kDa (Insulin, B Chain). The standards are reduced. A: Bovine serum albumin (BSA) (~66 kDa); B: aggregates of β-lactoglobulin monomer (uncertain); C: dimer of β-lactoglobulin (~36 kDa); D: monomer of β-lactoglobulin (~18 kDa); E: α-lactablumin (~14 kDa); F: Ovomucin (α-subunit and β-subunit), ovomacroglobulin and others (uncertain); G: Ovotransferrin (~78 kDa); H: Ovoinhibitor (~49 kDa) and/or G2 and G3 ovoglobulins (~49 kDa) (uncertain); I: Ovalbumin (~45 kDa); J: ovoflavoprotein (~32 kDa) (uncertain); K: Lysozyme (~14 kDa).

The monomer of BLG has a molecular weight of ~18 kDa and usually forms dimers (~36 kDa) between pH 5.5 and 7.5 through depleted-covalent interactions (Fox, 2003). Purified BLG (Figure 2, Column 3) showed one major band at ~18 kDa and a weak band at ~36 kDa. After separating BLG, the remaining proteins in WPI were collected and

designated β-lactoglobulin depleted fraction (BLG-depleted). This fraction (Figure 2, column 4) still contains β-lactoglobulin along with α-lactalbumin (ALAC), and bovine serum albumin (BSA). Note the percentage of β-lactoglobulin in the BLG-depleted fraction is less than in whey protein isolate. The SDS-PAGE of the commercial α-lactalbumin (ALAC) (Figure 2, column 5) is very similar to that of the BLG-depleted fraction except for a higher percentage of α-lactalbumin. The commercial β-lactoglobulin (commercial BLG) (Figure 2, Column 6) contained a very small amount of α-lactalbumin and BSA.

More than half of egg white protein is ovalbumin (~54%); others include ovotransferrin (12~13%), ovomucoid (11%), G2 and G3 globulin (~8%), lysozyme (3.4~3.5%), ovomucin (1.5~3.5%), ovoinhibitor (0.1~1.5%), ovoglycoprotein (0.5~1.0%), ovoflavoprotein (~0.8%), and some minor components (Li-Chan and Nakai, 1989). SDS-PAGE of egg white protein (EWP) sample (Figure 2, Column 7) showed several bands corresponding to these proteins. The protein corresponding to each band was designated according to the molecular weight and the identifying results from Mass Spectroscopy from Mann (2007). The single band for purified ovalbumin (Figure 2, column 8) confirmed the purity of this fraction. The other proteins remained in the ovalbumin depleted fractions (Figure 2, column 9 and 10). Ovalbumin depleted fraction 1 (OVA-depleted 1) still contained some ovalbumin while the percentage was much less than in EWP (Figure 2, column 9). The OVA-depleted 1 was the only fraction containing lysozyme and had a higher percentage of ovotransferrin than EWP (Figure 2, column 7 and 9). Ovalbumin depleted fraction 2 (OVA-depleted 2) contained mainly ovalbumin and proteins of high MW (Figure 2, column 10). The SDS-PAGE of commercial samples of WPI, BLG, ALAC and EWP showed similar

protein compositions before and after dialysis or ultrafiltration (Figure 2, column 13 through 20), suggesting no protein component was removed due to dialysis or ultrafiltration.

Interfacial rheology of individual components in whey protein isolates

Dialysis was a necessary step during protein purification process, in which salt was removed. The commercial samples of whey protein isolate (WPI), α-lactalbumin (ALAC) and β-lactoglobulin (commercial BLG) were dialyzed and compared with the purified β-lactoglobulin (purified BLG) and β-lactoglobulin depleted fraction (BLG-depleted). The interfacial rheology properties of these samples were determined (Figure 3). In addition, sucrose effect on the interfacial rheology was investigated using 44.3% (w/v) sucrose. This concentration is half of the sucrose concentration found in a normal angel food cake and can be completely dissolved in protein solutions.

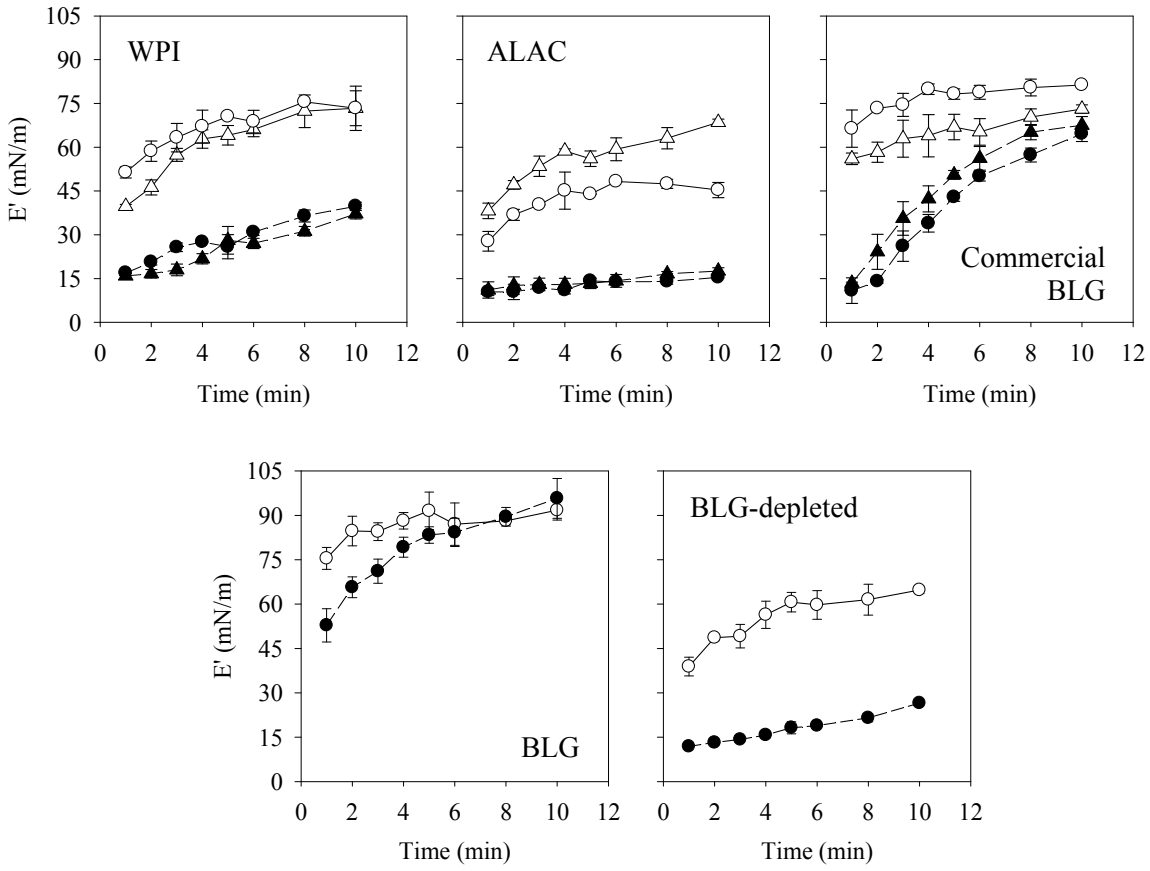

Figure 3. Changes of interfacial dilational elasticity (*E'*) over time for commercial samples of whey protein isolate (WPI), α-lactalbumin (ALAC), β-lactoglobulin (commercial BLG), purified β-lactoglobulin (BLG) and β-lactoglobulin depleted fraction (BLG-depleted) in the absence and presence of 44.3% (w/v) sucrose. Protein concentration is 10% (w/v) in solutions. Before dialysis: △ no sucrose ▲ 44.3% (w/v) sucrose. After dialysis: ○ no sucrose ● 44.3% (w/v) sucrose.

No major difference was observed on the interfacial rheology of the commercial samples of WPI, ALAC and commercial BLG before and after dialysis. The pattern of WPI is similar to that of ALAC, showing decreased interfacial dilational elasticity (*E'*) in the presence of sucrose. The *E'* of BLG (commercial BLG or purified BLG) dropped at the initial stage after sucrose addition; however, it slowly increased over time and reached at almost the same level (for the commercial BLG) as or a slightly lower level (for the dialyzed

commercial BLG) than the pure protein at 10 min. The increasing development of E' suggested a slow build-up process of interfacial elastic film. Davis and Foegeding (2007) observed that 25% (w/w) sucrose increased the interfacial elasticity of β-lactoglobulin, in which E' were compared at a single time point (5 min). E' of commercial BLG increased slightly after dialysis, suggesting decreasing effect of small molecules on the interfacial elasticity. The lower E' of dialyzed commercial BLG than purified BLG is possibly due to the dilution from other proteins. The decreasing effect of sucrose on E' of dialyzed commercial BLG is more obvious than on E' of purified BLG. It's hypothesized that the sucrose decreasing effect on E' of commercial BLG is partially attributing to the small amount of α-lactalbumin contained in the sample. The BLG-depleted fraction exhibited the same patterns as that of ALAC and WPI. Note that the E' of BLG-depleted and WPI were between E' of purified BLG and ALAC in the absence of sucrose, suggesting additive effects. Addition of sucrose caused a great E' decrease of ALAC, BLG-depleted and WPI, suggesting that α-lactalbumin as the only common component in the three fractions determined the interfacial rheology of the mixtures in the presence of sucrose.

E' of BLG-depleted/purified BLG mixtures and ALAC/purified BLG were determined at 5 min after droplet formation (Figure 4).

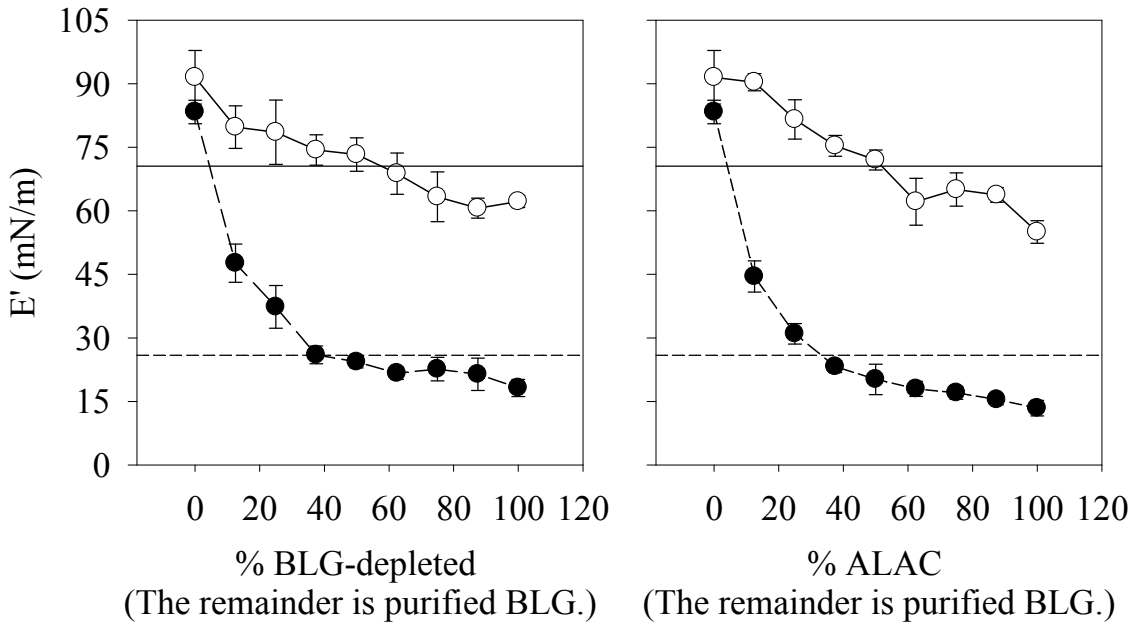

Figure 4. Interfacial dilational elasticity (*E′*) of mixtures of β-lactoglobulin depleted fraction (BLG-depleted) or commercial α-lactalbumin (ALAC) and purified β-lactoglobulin (purified BLG) in the absence and presence of 44.3 % (w/v) sucrose. Protein concentration is 10% (w/v) in solutions. *E′* was measured at 5 min after droplet formation. The solid and dash lines indicate *E′* of dialyzed whey protein isolate in the absence and presence of 44.3% (w/v) sucrose. ○ no sucrose ● 44.3% (w/v) sucrose.

The *E′* of the two mixtures showed similar patterns. The purified BLG had the highest *E′*, which gradually decreased with increasing BLG-depleted or ALAC percentage. Luck et al. (2001) varied the ratio of β-lactoglobulin/α-lactalbumin in protein foams and found that foam yield stress gradually increased with the percentage of β-lactoglobulin. The interfacial rheology data suggested that the gradually increased yield stress of mixture foams was attributing to slowly enhanced *E′* with increasing β-lactoglobulin percentage, as seen in Figure 4. Addition of sucrose dramatically decreased *E′* of BLG-depleted or ALAC but caused insignificant decrease of *E′* of purified BLG (Figure 3). *E′* of mixtures greatly decreased after adding sucrose, representing the characteristics of BLG-depleted or ALAC.

E′ of dialyzed WPI was at a position of approximately 50% BLG-depleted/50% purified BLG. These results again suggested the additive effects of α-lactalbumin and β-lactoglobulin on *E′* in the absence of sucrose and the dominating effect α-lactalbumin on *E′* in the presence of sucrose.

The dynamic change of interfacial tension (γ) of WPI, ALAC, commercial BLG, purified BLG, BLG-depleted fraction and their mixtures were measured from freshly generated pendent droplets (Figure 5 and 6).

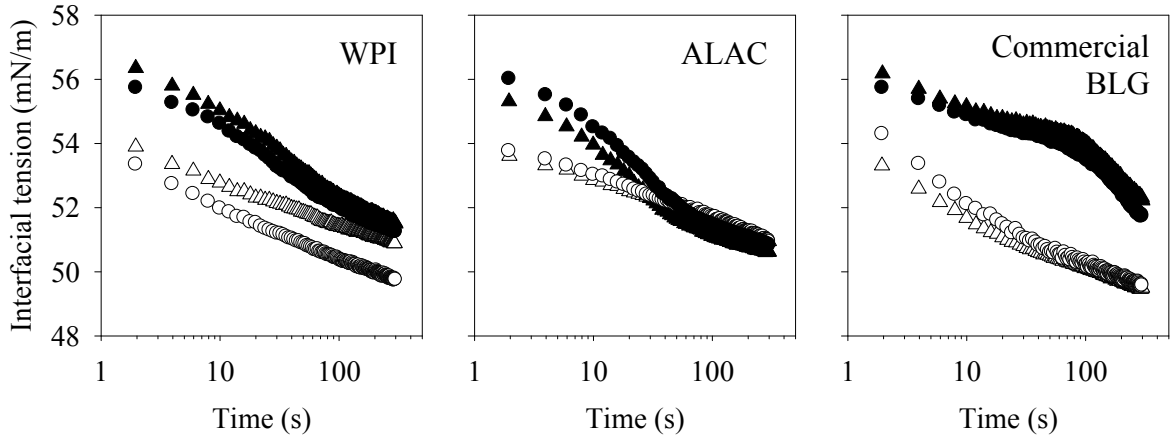

Figure 5. Typical dynamic changes of interfacial tension (γ) over time for commercial samples of whey protein isolate (WPI), α-lactalbumin (ALAC), and β-lactoglobulin (BLG) in the absence and presence of 44.3% (w/v) sucrose. Protein concentration is 10% (w/v) in solutions. Before dialysis: ○ no sucrose ● 44.3% (w/v) sucrose. After dialysis: △ no sucrose ▲ 44.3% (w/v) sucrose.

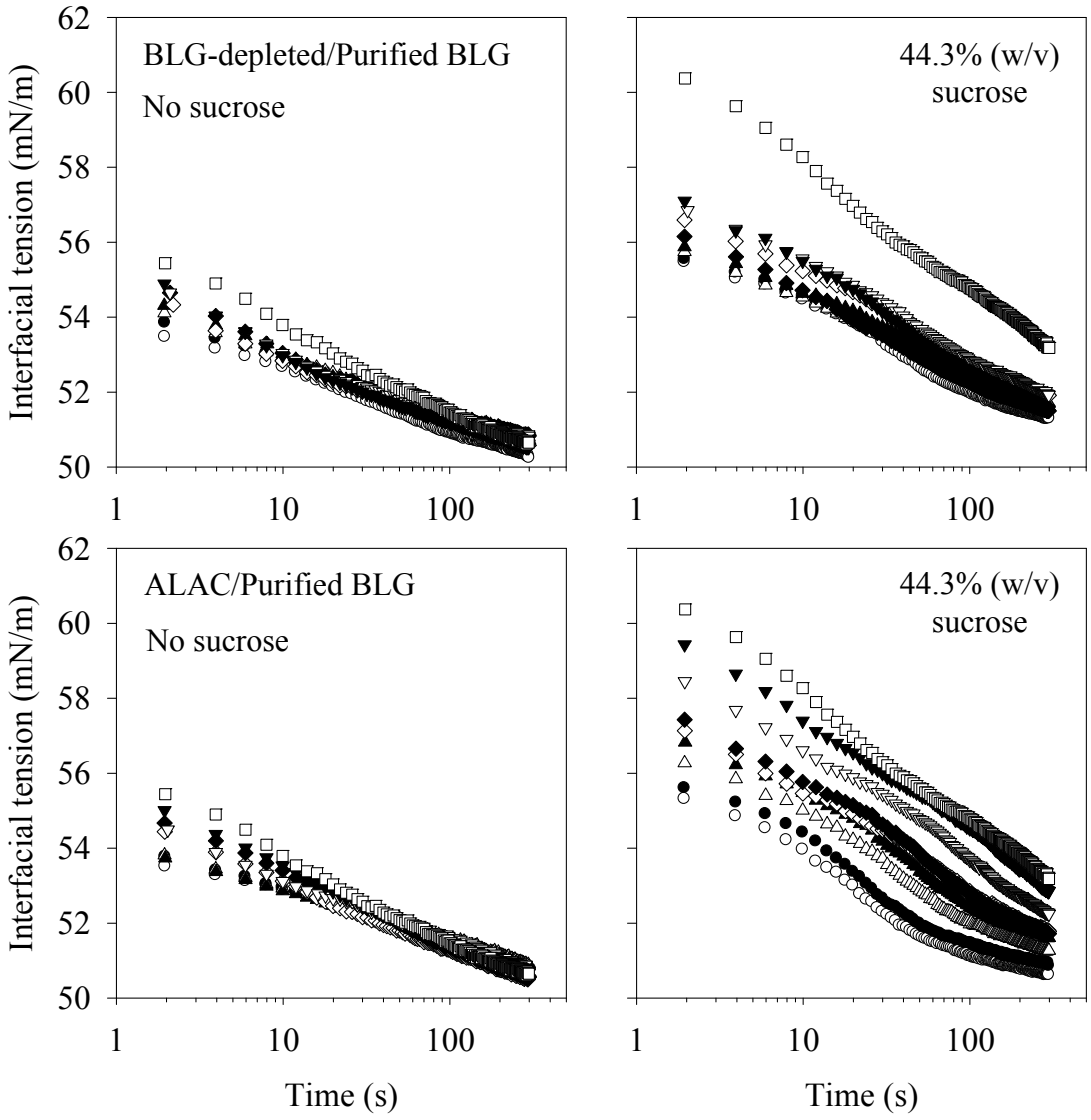

Figure 6. Typical dynamic changes of interfacial tension (γ) of β-lactoglobulin depleted fraction and purified β-lactoglobulin mixtures (BLG-depleted/purified BLG) and commercial α-lactoalbumin and purified β-lactoglobulin mixtures (ALAC/purified BLG) in the absence and presence of 44.3% (w/v) sucrose. Protein concentration is 10% (w/v) in solutions. ○ 100/0 ● 87.5/12.5 △ 75/25 ▲ 62.5/37.5 ◇ 50/50 ◆ 37.5/62.5 ▽ 25/75 ▼ 12.5/87.5 □ 0/100. Ratios are for BLG-depleted/purified BLG or ALAC/purified BLG.

No major difference was observed on the γ decline patterns of commercial protein samples before and after dialysis (Figure 5). The γ decline curves of WPI and ALAC are

similar to each other both in the absence and presence of sucrose. Addition of sucrose increased initial γ but didn't alter γ at 5 min for the two proteins. The γ decline curve of commercial BLG was not much different from those of WPI and ALAC except for a slightly higher initial value. Addition of sucrose increased γ and slowed γ decline rate for commercial BLG. Cornec et al. (1999) investigated the adsorption behaviors of α-lactalbumin and β-lactoglobulin, and suggested that α-lactalbumin unfolded more rapidly than β-lactoglobulin but to a lesser extent at the air/water interface. The difference between α-lactalbumin and β-lactoglobulin became more obvious after adding sucrose, possibly due to slower interfacial adsorption rates. The similarities of γ of WPI and ALAC confirmed that the interfacial characteristics of whey protein isolate was determined by α-lactalbumin in the presence of sucrose.

The γ of purified BLG showed a slightly higher initial value than those of the BLG-depleted fraction and ALAC; however, it reduced to the same level (~50.5 mN/m) as the other two at 5 min (Figure 6). The γ values of mixtures were between those of two individual proteins (purified BLG and BLG-depleted or ALAC). The difference of γ among all samples was no more than 2 mN/m. After sucrose addition, γ of purified BLG increased to a level much higher than those of BLG-depleted and ALAC. The γ decline patterns of BLG-depleted/ purified BLG mixtures followed the pattern of BLG-depleted after adding sucrose, suggesting a domination of BLG-depleted proteins at interface. However, the γ decline patterns of ALAC/purified BLG mixtures gradually changed towards the pattern of ALAC with increasing ALAC percentage after adding sucrose, suggesting co-adsorptions of the two

components at interface. Even so, the γ decline curves of ALAC/purified BLG mixtures showed a similar shape as that of ALAC when containing above 25% ALAC. The γ decline pattern of WPI was represented by those of BLG-depleted/purified BLG mixtures and those of ALAC/purified BLG mixtures containing >75% ALAC, following the patterns of BLG-depleted and ALAC. These results again suggested that ALAC dominates at interface and determines the interfacial characteristic of whey protein isolates in the presence of sucrose.

Interfacial rheology of individual components in egg white protein

Ultrafiltration is a necessary step to remove salt during protein purification (Figure 1). The ultrafiltrated commercial egg white protein (ultrafiltrated EWP) was also obtained and evaluated. The interfacial rheology of egg white proteins was determined both in the absence and presence of 44.3% (w/v) sucrose (Figure 7).

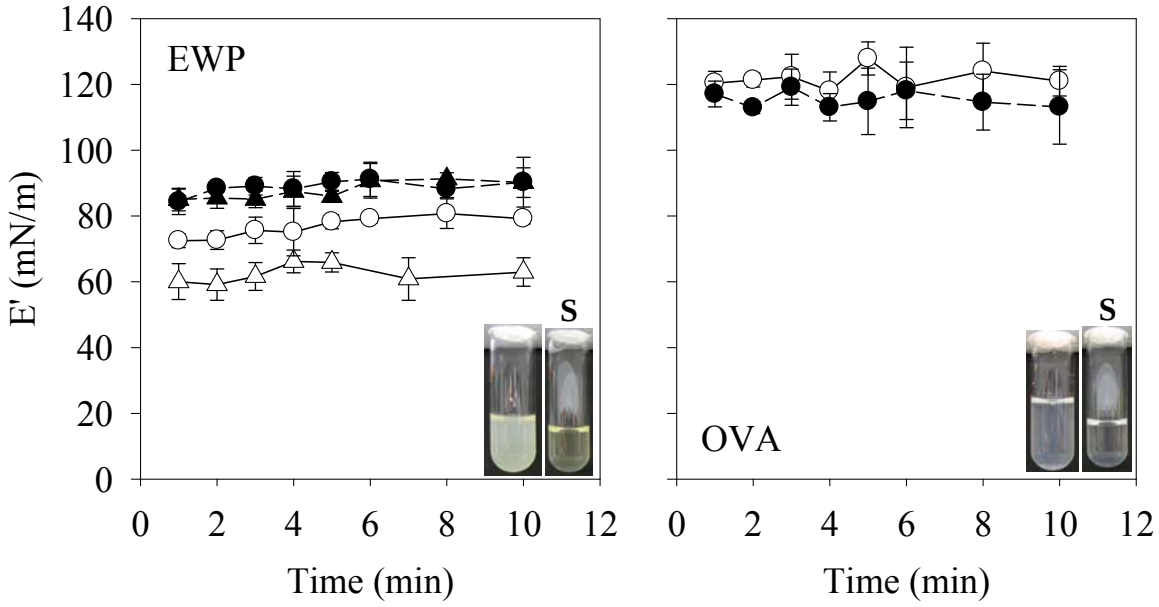

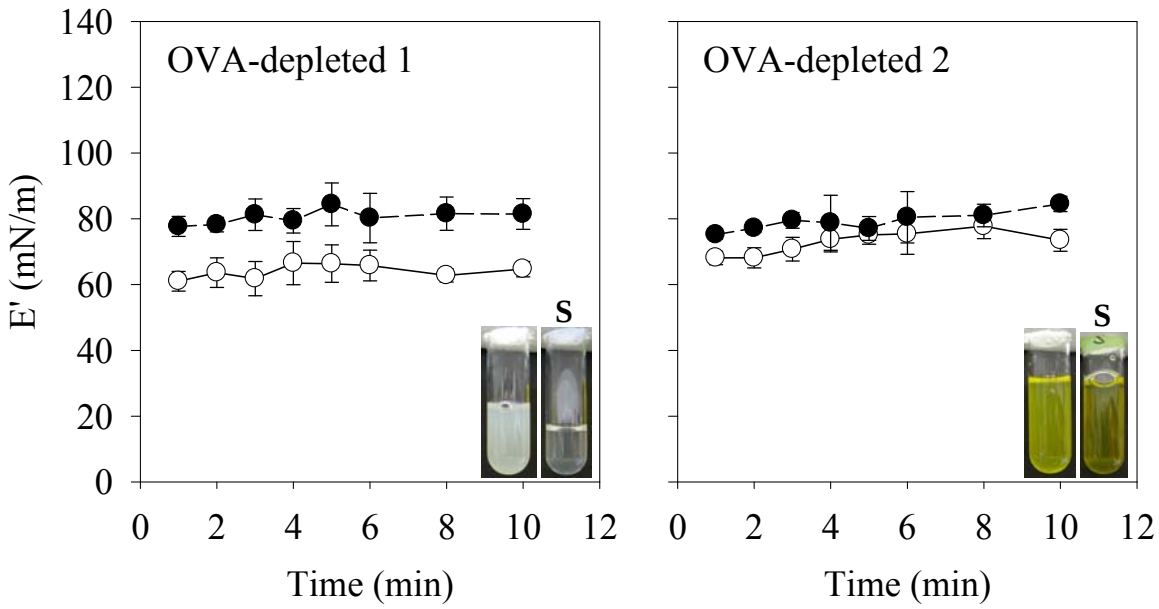

Figure 7. Changes of interfacial elasticity (E') over time for egg white protein (EWP), ovalbumin (OVA), ovalbumin depleted fraction 1 (OVA-depleted 1), ovalbumin depleted fraction 2 (OVA-depleted 2) in the absence and presence of 44.3% (w/v) sucrose. Protein concentration is 10% (w/v) in solutions. Before ultrafiltration: △ no sucrose ▲ 44.3% (w/v) sucrose. After ultrafiltration: ○ no sucrose ● 44.3% (w/v) sucrose. The solution images correspond to ultrafiltrated EWP, OVA, OVA-depleted 1 and OVA-depleted 2 respectively. The "S" above image indicates solutions containing sucrose.

The slight yellow color of EWP was not removed after ultrafiltration and can be attributing to OVA-depleted 2 fraction (Figure 7). This color is possibly from ovoflavoprotein, which tends to bind riboflavin (vitamin B_2) (Li-Chan and Nakai, 1989). E' of all egg white protein samples reached a high value at the first min and did not change over time (Figure 7). The E' of EWP increased about 10 mN/m after ultrafiltration. OVA-depleted 1 and OVA-depleted 2 had approximately the same E' as that of EWP while the E' of ovalbumin (OVA) was much higher than others. Sucrose increased E' of EWP, ultrafiltrated EWP, and OVA-depleted 1 but showed no effect on E' of OVA and OVA-depleted 2. Note that E' of OVA, OVA-depleted 1 and OVA-depleted 2 reached almost the same level after

adding 44.3% (w/v) sucrose. Davis and Foegeding (2007) also observed that sucrose caused no change on the interfacial elasticity of ovalbumin. OVA-depleted 1 had a similar composition as EWP except for less concentration of ovalbumin (Figure 2). The interfacial rheological property of OVA-depleted 1 was also similar to that of ultrafiltrated EWP except for systematically lower values of E'. OVA-depleted 1 contained more globulins (G2 and G3 ovoglobulins and lysozyme) than EWP (Figure 1). The contribution of globulins to the good foaming capacity of egg white was found in several investigations (Johnson and Zabik 1981a, 1981b; MacDonnell et al., 1954). Ovalbumin can produce similar foam overrun as egg white protein but required longer whipping time (Johnson and Zabik 1981a, 1981b; MacDonnell et al., 1954). Our results indicated that removal of ovalbumin only slightly decreased E' of egg white protein, suggesting that other proteins, especially globulins, dominated the interfacial elasticity.

The protein ratio of OVA:OVA-depleted 1:OVA-depleted 2 from each batch was 47:42:11 according to the protein content of the three fractions. The three fractions were mixed to a re-mixed EWP solution based on this ratio. The E' of this mixture was determined at 5 min after droplet formation and compared with that of the original EWP and ultrafiltrated EWP (Figure 8).

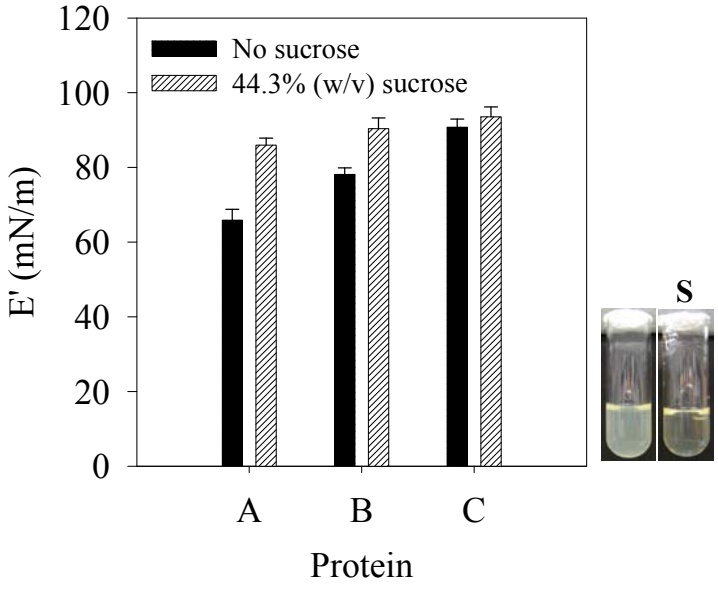

Figure 8. Interfacial dilational elasticity (*E′*) of 10% (w/v) protein solutions in the absence and presence of 44.3% (w/v) sucrose. A: egg white protein (EWP); B: ultrafiltrated egg white protein (Ultrafiltrated EWP); C: re-mixed solution of egg white protein (re-mixed EWP) based on a ratio of 47:42:11 for OVA : OVA-depleted 1 : OVA-depleted 2. *E′* was measured at 5 min after droplet formation. The solution images correspond to re-mixed EWP. The "S" above image indicates solutions containing sucrose.

The *E′* of re-mixed EWP was higher than that of EWP and ultrafiltrated EWP, being minimally affected by sucrose (Figure 8). During the purification process, the 10L of water elution was discarded, causing lower relative content of ovotransferrin in re-mixed EWP (Figure 2). In addition, other proteins, such as ovomucin, may also be removed with the discarded precipitates during purification process (Figure 1). Although the appearances of re-mixed EWP and ultrafiltrated EWP are very close (Figure 7 and 8), their compositions are not identical, resulting in dissimilar interfacial rheological characteristics.

The interfacial rheology of OVA-depleted 1 is similar to EWP, differing from that of OVA. The OVA and OVA-depleted 1 or EWP were mixed and *E′* of the mixtures were measured at 5 min after droplet formation (Figure 9).

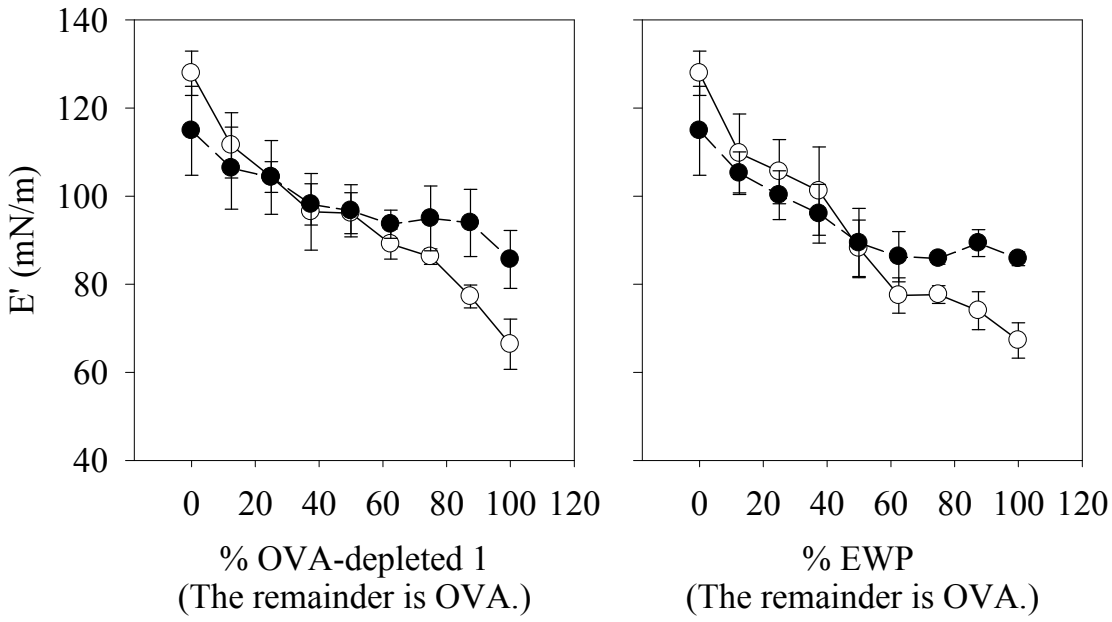

Figure 9. Interfacial dilational elasticity (E') of mixtures of ovalbumin depleted 1 (OVA-depleted 1) or egg white protein (EWP) and ovalbumin (OVA) in the absence and presence of 44.3% (w/v) sucrose. Protein concentration is 10% (w/v) in solutions. E' was measured at 5 min after droplet formation. ○ no sucrose ● 44.3% (w/v) sucrose.

The EWP/OVA mixture and OVA-depleted 1/OVA mixture showed similar interfacial rheological characteristics (Figure 9). E' of the mixtures gradually increased with increasing OVA percentage. The increased E' caused by sucrose was not observed on mixtures containing above 50% OVA. Although OVA had dissimilar E' to those of EWP and OVA-depleted 1, the E' of these mixtures indicated that increasing OVA percentage in egg white protein can cause gradually change of interfacial elasticity, suggesting that the interfacial rheology of egg white proteins is not simply determined by a single component but relies on compositions of several proteins. It should be noted that EWP and OVA-depleted 1 contained high percentage of OVA (Figure 2).

Typical dynamic changes of γ were compared for egg white proteins (Figure 10).

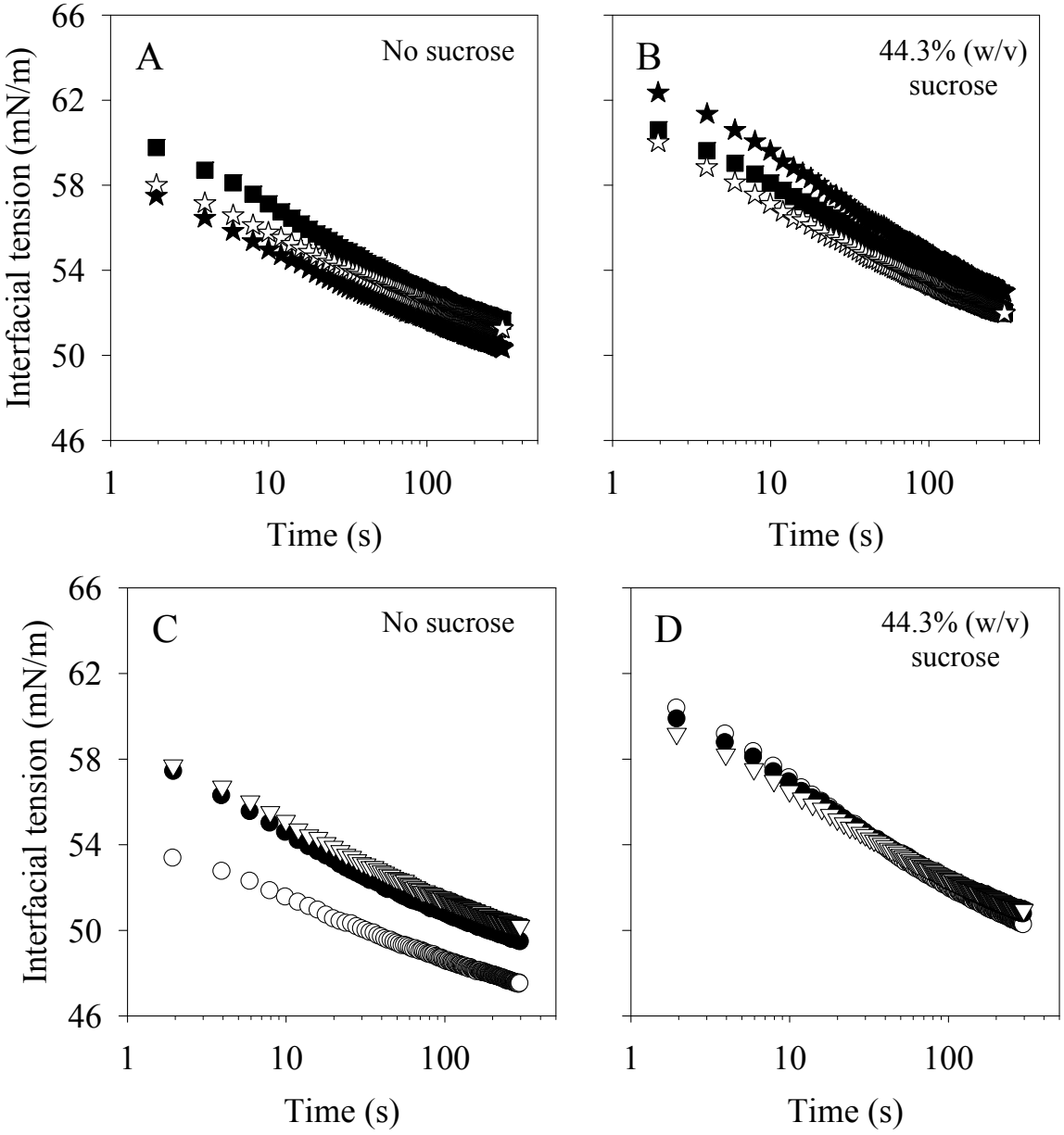

Figure 10. Typical dynamic changes of interfacial tension (γ) over time for 10% (w/v) protein solutions in the absence and presence of 44.3% (w/v) sucrose. ■ ovalbumin (OVA) ★ ovalbumin depleted 1 (OVA-depleted 1) ☆ ovalbumin depleted 2 (OVA-depleted 2) ○ egg white protein (EWP) ● ultrafiltrated egg white protein (ultrafiltrated EWP) ▽ re-mixed solution of egg white protein (re-mixed EWP) based on a ratio of 47:42:11 for OVA : OVA-depleted 1 : OVA-depleted 2.

OVA, OVA-depleted 1 and OVA-depleted 2 showed similar γ decline patterns (Figure 10A). The difference of γ among the three samples is less than the experiment error (1 mN/m). The γ values of separated fractions (OVA, OVA-depleted 1 and OVA-depleted 2) (Figure 10A) are higher than that of EWP (Figure 10C). However, the γ of EWP increased after ultrafilatration and reached the same level as the γ of separated fractions (Figure 10C). The γ decline curve of re-mixed EWP overlapped with that of ultrafiltrated EWP. The γ reached a higher initial value after adding sucrose but reduced to almost the same level as samples containing no sucrose (Figure 10B and 10D). The difference of γ among all samples in the presence of sucrose is no more than the experiment error (1 mN/m). Not much difference can be seen among the γ decline patterns of all samples either in the absence or presence of sucrose.

Typical dynamic changes of γ were determined for the OVA-depleted 1 and OVA mixture (OVA-depleted 1/OVA) and the EWP and OVA mixture (EWP/OVA) (Figure 11).

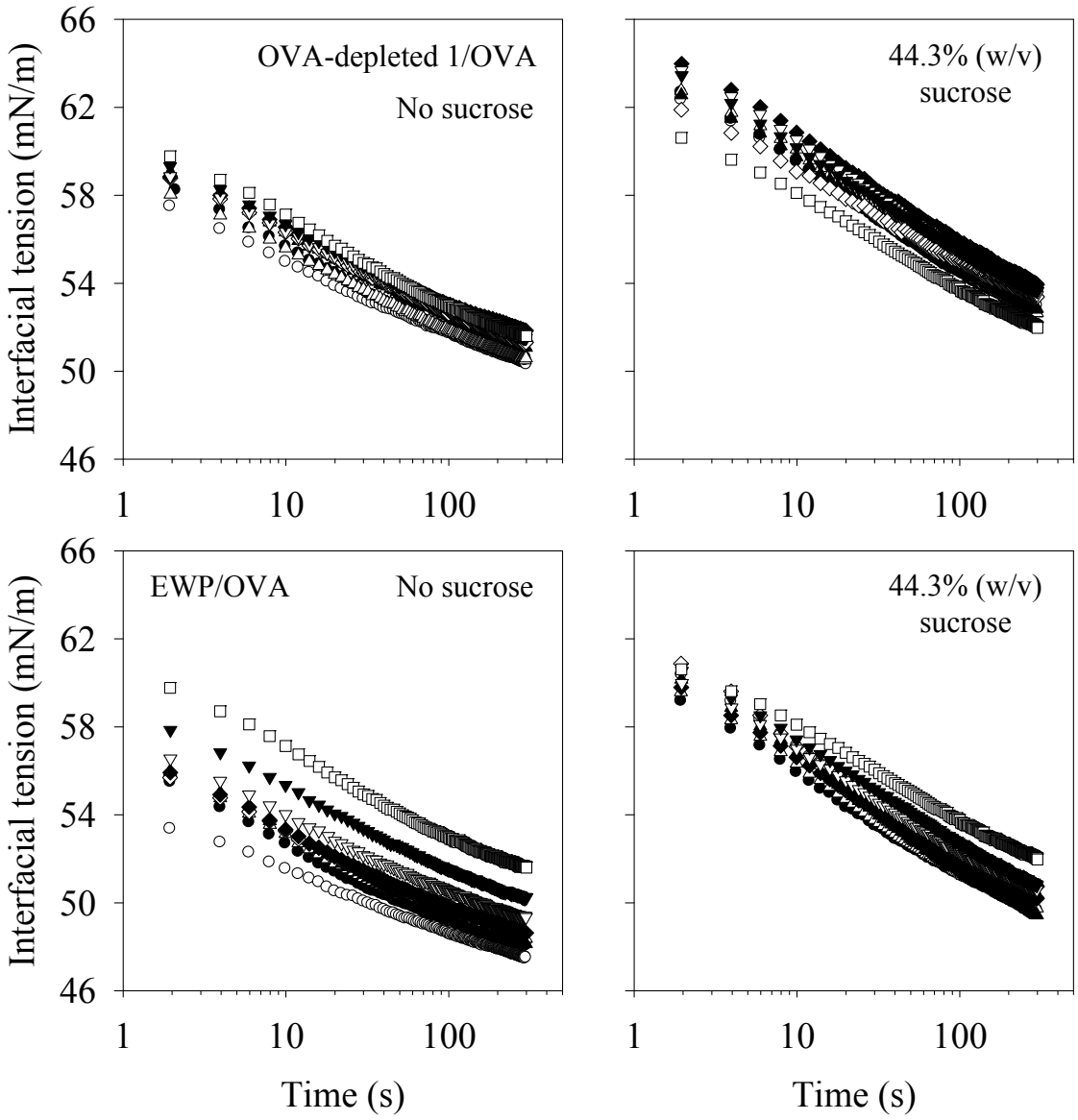

Figure 11. Changes of interfacial tension (γ) over time for egg white protein and ovalbumin mixtures (EWP/OVA) and ovalbumin depleted 1 and ovalbumin mixtures (OVA-depleted 1/OVA) in the absence and presence of 44.3% (w/v) sucrose. Protein concentration is 10% (w/v) in solutions. ○ 100/0 ● 87.5/12.5 △ 75/25 ▲ 62.5/37.5 ◇ 50/50 ◆ 37.5/62.5 ▽ 25/75 ▼ 12.5/87.5 □ 0/100. Ratios are for EWP/OVA or non-OVA1/OVA.

The γ decline curves of OVA-depleted 1, OVA and their mixtures showed no significant difference from each other (Figure 11). The γ decline curve of the EWP/OVA

mixtures gradually shifted from the curve of OVA down to that of EWP with increasing EWP percentage (Figure 11), possibly due to increasing amounts of small molecules with addition of EWP. It is not possible to determine the major occupying molecules at the interface from γ decline curves since the protein components in egg white showed similar γ decline patterns (Figure 10 and 11). Damodaran et al. (1998) found co-adsorption behaviors of various egg white proteins at interface at low ionic strength and low protein concentration. The interfacial rheological characteristics of protein mixtures (Figure 9) suggested a complex co-adsorption of egg white proteins at interface.

Interfacial rheology of protein mixtures

In Chapter 1, we found that the interfacial tension (γ) and foaming properties (yield stress and stability) of the mixtures of whey protein isolate and egg white protein followed the characteristics of whey protein isolate. To clarify the mechanisms of whey protein isolate dominating at interface, we combined whey proteins (WPI, BLG and ALAC) with egg white proteins (EWP and OVA) and determined the interfacial properties (Figure 12).

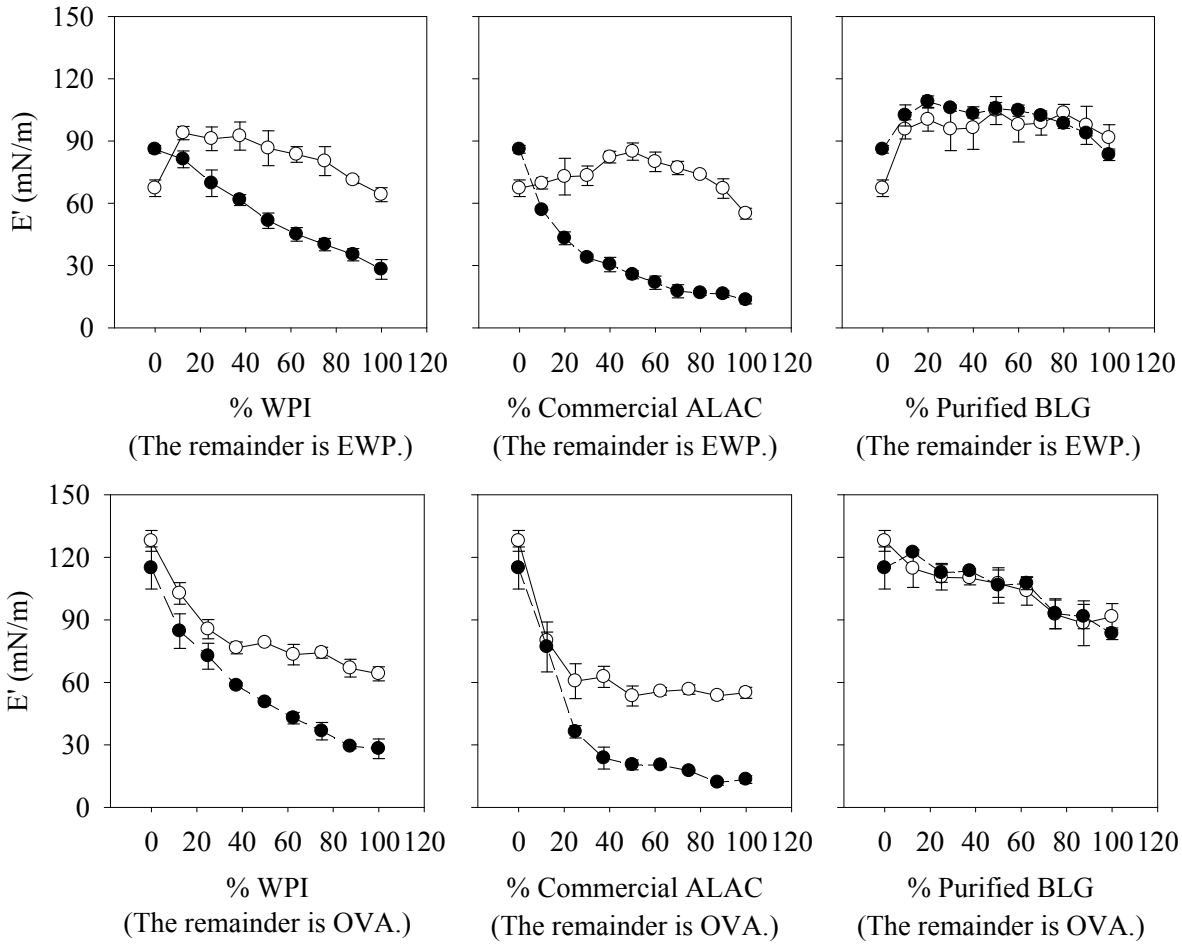

Figure 12. Interfacial dilational elasticity (E') of whey protein isolate and egg white protein mixtures (WPI/EWP), commercial α-lactalbumin and egg white protein mixtures (ALAC/EWP), purified β-lactoglobulin and egg white protein mixtures (purified BLG/EWP), whey protein isolate and ovalbumin mixtures (WPI/OVA), commercial α-lactalbumin and ovalbumin mixtures (ALAC/OVA), purified β-lactoglobulin and ovalbumin mixtures (purified BLG/OVA) in the absence and presence of 44.3% (w/v) sucrose. Protein concentration is 10% (w/v) in solutions. E' was measured at 5 min after droplet formation. ○ no sucrose ● 44.3% (w/v) sucrose.

Although E' of OVA is very different from that of EWP, the E' of the mixtures of the two proteins with whey proteins (WPI, ALAC and BLG) showed some common characteristics (Figure 12). Sucrose increased the E' of EWP and showed no significant effect on the E' of OVA. However, once the two proteins were mixed with WPI or ALAC, the E' of

the mixtures followed the interfacial properties of WPI or ALAC and decreased with sucrose addition. The domination of WPI or ALAC at interface occurred even at a very low percentage of either protein (<20%). Sucrose showed no effect on E' of BLG/EWP mixtures, resembling BLG characteristic. Even with 12.5% substitution of EWP with BLG, the E' of the mixtures jumped to the same level as that of BLG. These results suggested that BLG determined the interfacial elasticity of BLG/EWP mixtures. Increasing BLG percentage in BLG/OVA mixtures gradually decreased E', suggesting additive effects. Sucrose showed no effect on E' of BLG/OVA mixtures as well as two individual proteins.

Typical dynamic change of γ were measured for mixtures of whey and egg white proteins (Figure 13, 14 and 15).

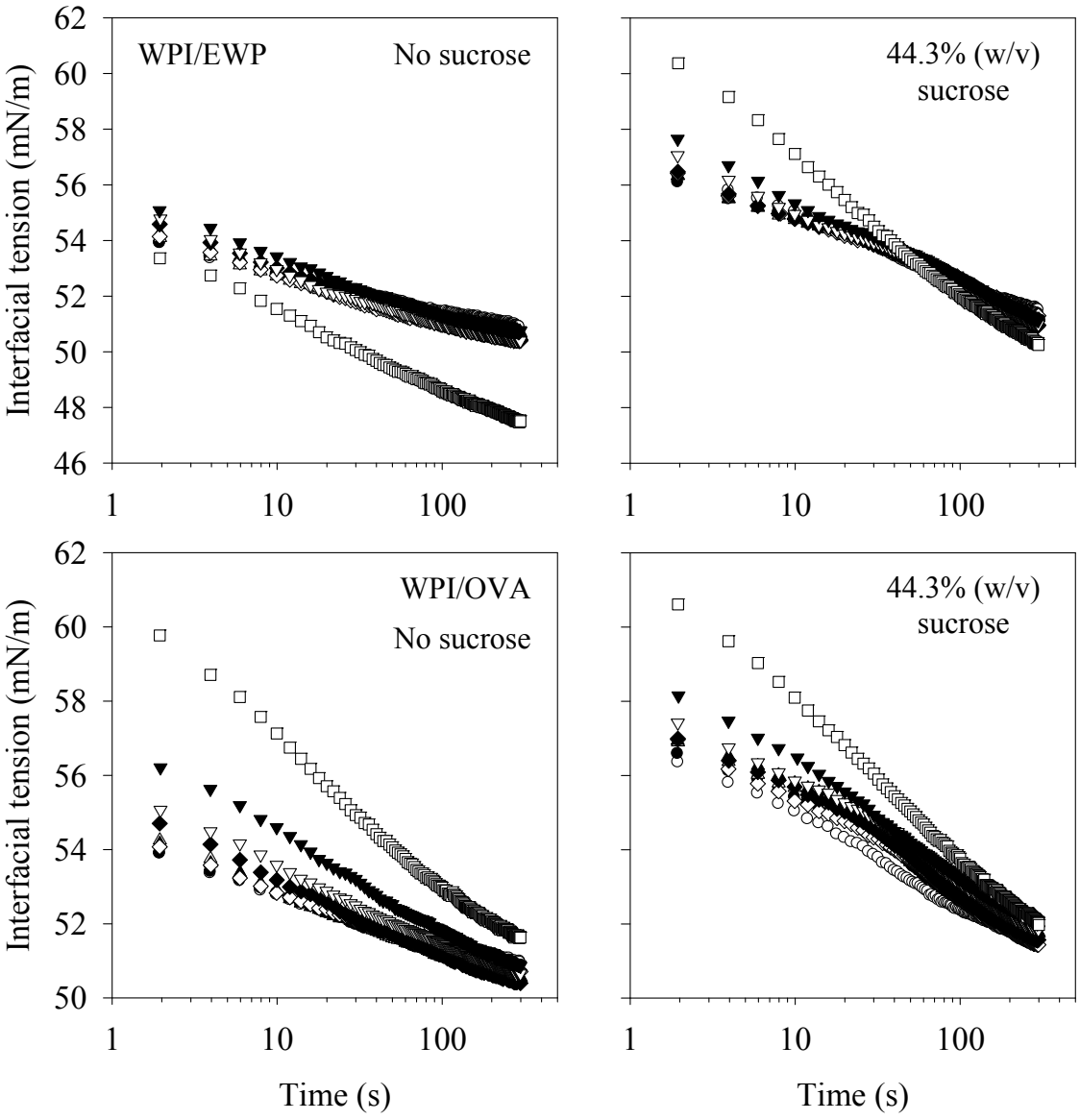

Figure 13. Typical dynamic changes of interfacial tension (γ) over time of whey protein isolate and egg white protein mixtures (WPI/EWP) and whey protein isolate and ovalbumin mixtures (WPI/OVA) in the absence and presence of 44.3% (w/v) sucrose. Protein concentration is 10% (w/v) in solutions. ○ 100/0 ● 87.5/12.5 △ 75/25 ▲ 62.5/37.5 ◇ 50/50 ◆ 37.5/62.5 ▽ 25/75 ▼ 12.5/87.5 □ 0/100. Ratios are for WPI/EWP or WPI/OVA.

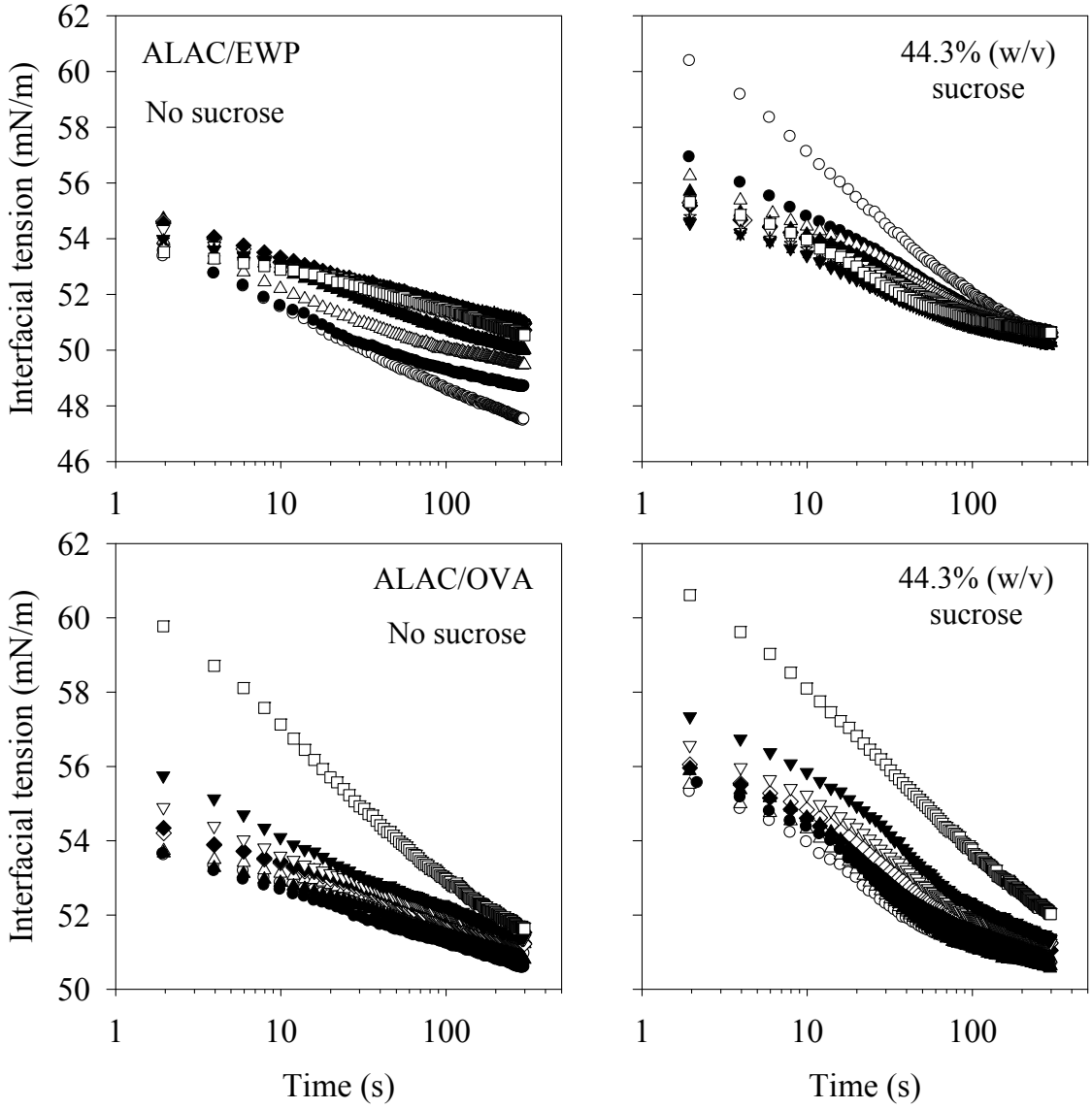

Figure 14. Typical changes of interfacial tension (γ) over time for commercial α-lactalbumin and egg white protein mixtures (ALAC/EWP) and commercial α-lactalbumin and ovalbumin mixtures (ALAC/OVA) in the absence and presence of 44.3% (w/v) sucrose. Protein concentration is 10% (w/v) in solutions. Ratio of ALAC/EWP: ○ 100/0 ● 90/10 △ 80/20 ▲ 70/30 ◇ 60/40 ◆ 50/50 ▽ 40/60 ▼ 30/70 ☆ 20/80 ★ 10/90 □ 0/100. Ratio of ALAC/OVA: ○ 100/0 ● 87.5/12.5 △ 75/25 ▲ 62.5/37.5 ◇ 50/50 ◆ 37.5/62.5 ▽ 25/75 ▼ 12.5/87.5 □ 0/100.

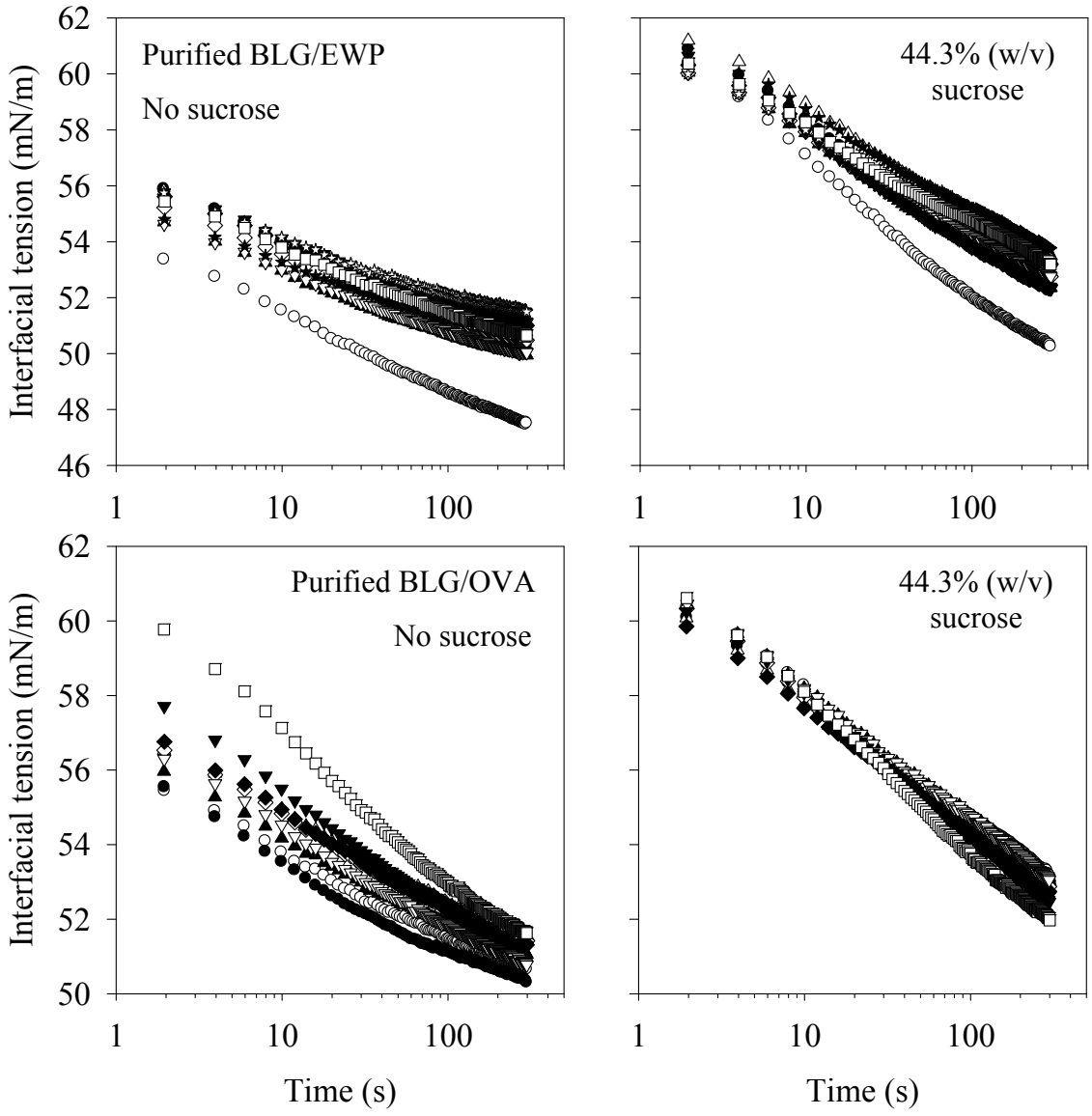

Figure 15. Typical dynamic changes of interfacial tension (γ) over time for purified β-lactoglobulin and egg white protein mixtures (purified BLG/EWP) and purified β-lactoglobulin and ovalbumin mixtures (purified BLG/OVA) in the absence and presence of 44.3% (w/v) sucrose. Protein concentration is 10% (w/v) in solutions. Ratio of purified BLG/EWP: ○ 100/0 ● 90/10 △ 80/20 ▲ 70/30 ◇ 60/40 ◆ 50/50 ▽ 40/60 ▼ 30/70 ☆ 20/80 ★ 10/90 □ 0/100. Ratio of purified BLG/OVA: ○ 100/0 ● 87.5/12.5 △ 75/25 ▲ 62.5/37.5 ◇ 50/50 ◆ 37.5/62.5 ▽ 25/75 ▼ 12.5/87.5 □ 0/100.

The γ of WPI, ALAC and BLG are between the highest γ of OVA and the lowest γ of EWP (Figure 13, 14 and 15). Sucrose increased initial γ of all protein solutions. The γ decline curves of WPI/EWP mixtures and WPI/OVA mixtures followed the pattern of WPI both in the absence and presence of sucrose, confirming the dominance of WPI at interface. The same results were observed in ALAC/EWP mixtures and ALAC/OVA mixtures, in which the ALAC determined γ of mixtures. Again the γ decline trends of mixtures resembled that of purified BLG in the cases of purified BLG/EWP mixtures. Purified BLG and OVA showed similar γ decline patterns and the γ decline curves of purified BLG/OVA mixtures were in between two proteins, suggesting additive effects. These results showed the dominance of WPI, ALAC or BLG at interface when combining any of them with EWP or OVA except for purified BLG/OVA mixture, in accordance with the observations on E'. The individual component in whey protein isolate (ALAC or BLG) always takes over the interface and determines the interfacial properties when mixed with egg white proteins. It appears that α-lactalbumin is the key protein in whey protein isolate to establishing the interface; it can out compete all the other proteins (including β-lactoglobulin) in the mixtures of whey and egg white proteins.

Interfacial and foaming properties of commercial β-lactoglobulin

The decreased E' of whey protein isolate after adding sucrose has been correlated with low foam stability and poor angel food cake quality in Chapter 3. The E' of β-lactoglobulin was not significantly altered with sucrose addition (Figure 3), differing from that of whey protein isolate and α-lactalbumin. Consequently, the interfacial and foaming properties of commercial BLG was evaluated in the presence of different amounts of sucrose

and compared with those of WPI and EWP. Interfacial elasticity and interfacial pressure ($\pi=\gamma_0-\gamma$ where γ_0 is 72.3 mN/m at 25 °C) of commercial BLG, WPI and EWP are shown in Figure 16.

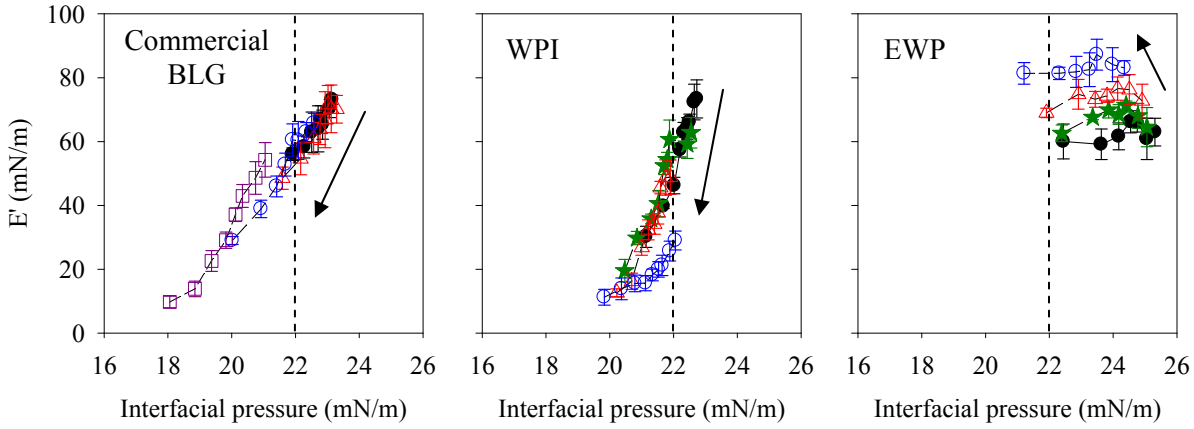

Figure 16. Interfacial dialtional elastic moduli (E') verses interfacial pressure ($\pi=\gamma_0-\gamma$ where γ_0 is 72.3 mN/m at 25 °C) for commercial β-lactoglobulin (commercial BLG), whey protein isolate (WPI) and egg white protein (EWP) in the presence of different sucrose concentrations. Protein concentration is 10% (w/v) in solutions. E' and π were measured at 1 to 10 min after droplet formation. ● no sucrose ★ 12.8 g/100 mL sucrose △ 25.0 g/100 mL sucrose ○ 44.3 g/100 mL sucrose □ 63.6 g/100 mL sucrose. Dash lines correspond to interfacial pressure of 22 mN/m. Arrows are drawn to indicate the change trend of E' with increasing sucrose concentration.

In Chapter 3, we hypothesized that the lower E' of WPI than EWP was attributing to a lower interfacial pressure. The interfacial pressure of WPI decreased below a breaking point of 22 mN/m after adding sucrose, leading to reduced E'. This phenomenon was also observed on commercial BLG (Figure 16). The E' of WPI decreased faster than that of commercial BLG with decreasing interfacial pressure, possibly due to the contribution of α-lactalbumin. Interfacial elasticity and interfacial pressure ($\pi=\gamma_0-\gamma$ where γ_0 is 72.3 mN/m at 25 °C) of ALAC were measured in the presence of different sucrose concentrations (Figure 17).

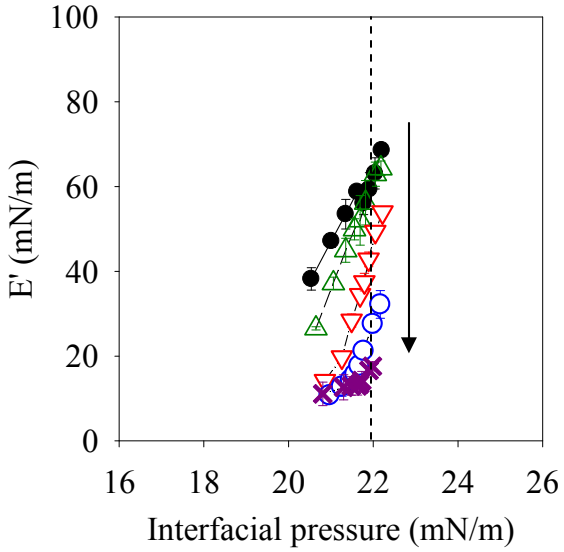

Figure 17. Interfacial dialtional elastic moduli (E') verses interfacial pressure ($\pi=\gamma_0-\gamma$ where γ_0 is 72.3 mN/m at 25 °C) for commercial α-lactalbumin (ALAC) in the presence of different sucrose concentrations. Protein concentration is 10% (w/v) in solutions. E' and π were measured at 1 to 10 min after droplet formation. ● no sucrose △ 11.0% (w/v) sucrose ▽ 22.0% (w/v) sucrose ○ 33.0% (w/v) sucrose ✕ 44.3% (w/v) sucrose. Dash line corresponds to interfacial pressure of 22 mN/m. Arrows are drawn to indicate the change trend of E' with increasing sucrose concentration.

The surface pressure of ALAC was lower than the critical value of 22 mN/m and showed no major shift after adding sucrose. However, E' gradually decreased with increasing sucrose concentration. This result suggests that the sucrose decreasing effect on the interfacial elasticity of ALAC is not due to changes of interfacial pressure. The E' decrease of WPI was mainly attributing to ALAC, resulting in a faster decreasing rate than commercial BLG with increasing sucrose concentration. Note the presence of a small amount of ALAC in commercial BLG (Figure 1), which may contribute to the E' decrease of commercial BLG after adding sucrose. The higher E' of commercial BLG suggested a better foam stability than that of WPI in the presence of sucrose. Foam overrun of the commercial samples of BLG, WPI and EWP were compared in Figure 18.

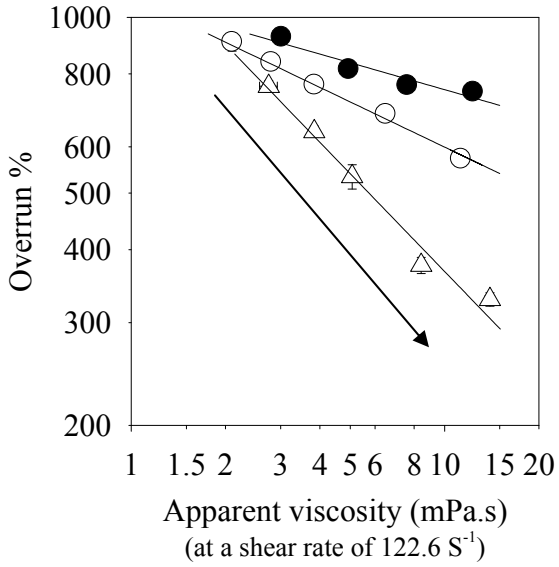

Figure 18. Changes in overrun with the solution apparent viscosity at a shear rate of 122.6 1/s for 10% (w/v) protein solutions in the presence of different sucrose concentrations. ● commercial β-lactoglobulin (commercial BLG) ○ whey protein isolate (WPI) △ egg white protein (EWP). Sucrose concentrations (0.00, 12.8 (only WPI and EWP), 25.0, 44.3, 63.6 g/ 100 mL) increased along with arrow direction. Date of whey protein isolate and egg white protein are from Chapter 3. Equations were showed in Table 1.

Table 1. Relationships among various parameters

y	*x*	*Protein*	*Equations*	R^2
Overrun (%)	Apparent viscosity (mPa.s) (at 122.6 S^{-1})	BLG*	$\ln y = 6.97 - 0.153 \ln x$	0.911
		WPI	$\ln y = 6.99 - 0.257 \ln x$	0.990
		EWP	$\ln y = 7.18 - 0.556 \ln x$	0.973
Drainage ½ life (min)	Apparent viscosity (mPa.s) (at 8.5 S^{-1})	BLG*	$y = 8.52x + 3.14$	0.994
		WPI	$y = 4.66x + 21.2$	0.988
		EWP	$\ln y = 3.89 + 0.128x$	0.983
Drainage ½ life (min)	$\mu\left(E'/\gamma\right)$	All	$y = 11.0x + 4.29$	0.927
Mean bubble area (10^3 μm^2)	Apparent viscosity (mPa.s) (at 122.6 S^{-1})	All	$\ln y = 3.47 - 1.32 \ln x$	0.927
Median bubble area (10^3 μm^2)	Apparent viscosity (mPa.s) (at 122.6 S^{-1})	All	$\ln y = 3.01 - 1.45 \ln x$	0.878
Changes of mean bubble area over 20 min (10^3 μm^2)	Drainage ½ life (min)	All	$\ln y = 11.1 - 2.40 \ln x$	0.923

* BLG is for commercial β-lactoglobulin.

The solution apparent viscosity is calculated at 122.6 1/s, which was estimated using a simplified model for whipping process (Appendix I in Chapter 3). This shear rate is in the shear rate range for mixing process in food industry (Steffe, 1996). Foam overrun decreased with increasing solution viscosity, with linear relationships established between foam overrun and solution viscosity on a ln-ln scale (Table 1). The decreasing rates of foam overrun with increasing solution viscosity followed the order of EWP (slope of -0.556) > WPI (slope of -0.257) > commercial BLG (slope of -0.153). If given a very low solution viscosity ($\mu \rightarrow 1$ mPa.s), EWP, WPI and commercial BLG should have very similar overrun (the intercepts are 7.18, 6.99 and 6.97 for EWP, WPI and commercial BLG respectively). These results suggested an order for foaming capacity of commercial BLG > WPI > EWP at

high solution viscosities (altered by sucrose). The higher the solution viscosity, the greater the difference among the three proteins for foamability. A higher foam overrun of β-lactoglobulin than α-lactalbumin and their mixtures has been observed by Luck et al. (2001).

Drainage ½ life of foams was correlated with solution viscosity (μ) and interfacial elasticity (E') in Chapter 3. In this study, the properties of BLG were fitted into the same models (Figure 19 and Table 1).

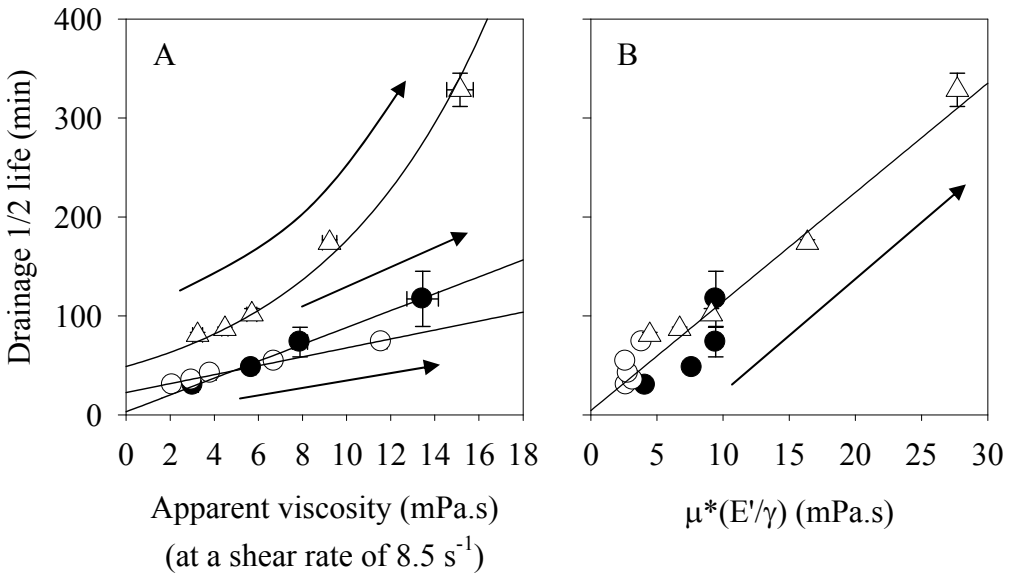

Figure 19. Relationships between foam stability and solution apparent viscosity (μ) at a shear rate of 8.5 1/s, air phase fraction (ϕ) and interfacial elasticity (E'/γ) for 10% (w/v) protein solutions in the presence of different sucrose concentrations. ● commercial β-lactoglobulin (commercial BLG) ○ whey protein isolate (WPI) △ egg white protein (EWP). Sucrose concentrations (0.00, 12.8 (only WPI and EWP), 25.0, 44.3, 63.6 g/100 mL) increased along with arrow direction. Date of whey protein isolate and egg white protein are from Chapter 3. Equations were showed in Table 1.

The solution viscosity was calculated at 8.5 1/s, which is in a range of shear rates experienced by materials under gravity induced drainage (Barnes et al., 1989). A linear relationship (R^2=0.994) was established between foam drainage ½ life and μ for commercial

BLG, with a higher slope than that of the linear relationship for WPI (Figure 19A and Table 1). Note only 4 points were measured and used to fit the linear relationship for commercial BLG. The relationship between drainage ½ life and μ for EWP was described using an exponential equation. The increasing rate of drainage ½ life with increasing solution viscosity followed the order of EWP > BLG > WPI. The differences between EWP and WPI foams were attributing to the dissimilarities in interfacial elasticity (E'/γ), with a common linear relationship being established between foam drainage ½ life and $\mu^*(E'/\gamma)$ for both proteins (Figure 10 in Chapter 3). Involvement of BLG did not affect the validity of the linear relationship (R^2=0.927) between foam drainage ½ life and $\mu^*(E'/\gamma)$, demonstrating the contributions of solution viscosity and interfacial elasticity to the foam stability (Figure 19B and Table 1). Although the drainage ½ life of BLG is higher than that of WPI in the presence of sucrose, it is still much lower than that of EWP. In addition to the sucrose effect, the protein specificity of the interfacial elasticity is a key reason for the superior foam stability of egg white than that of whey protein.

Microstructures of BLG foams were observed using confocal laser microscopic technique (Figure 20).

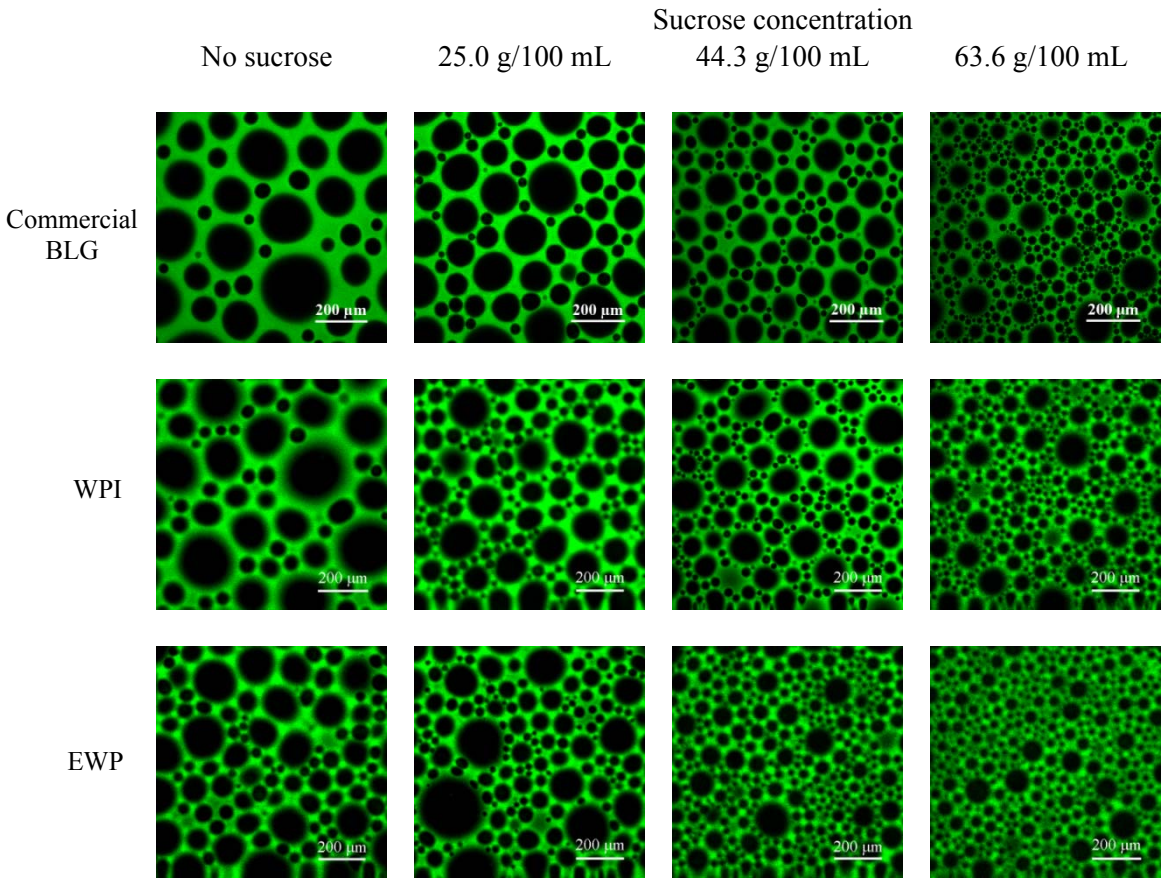

Figure 20. Confocal laser microscopic images of commercial β-lactoglobulin (commercial BLG), whey protein isolate (WPI) and egg white protein (EWP) foams at 0 min. Protein concentration is 10% (w/v) in solutions.

The foam structures changed from dispersions of a low density of large bubbles to dispersions of high density of small bubbles with increasing sucrose concentration. The images of BLG foams showed more similarities to WPI foams than to EWP foams. The size of bubbles in BLG and WPI foams were close and both were larger than EWP foam bubbles when compared at the same sucrose concentration. The area of each bubble in the 2D images was measured using MetaMorph Imaging System software. The mean or median bubble area was determined for each image and averaged from three replication images for each foam (Figure 21).

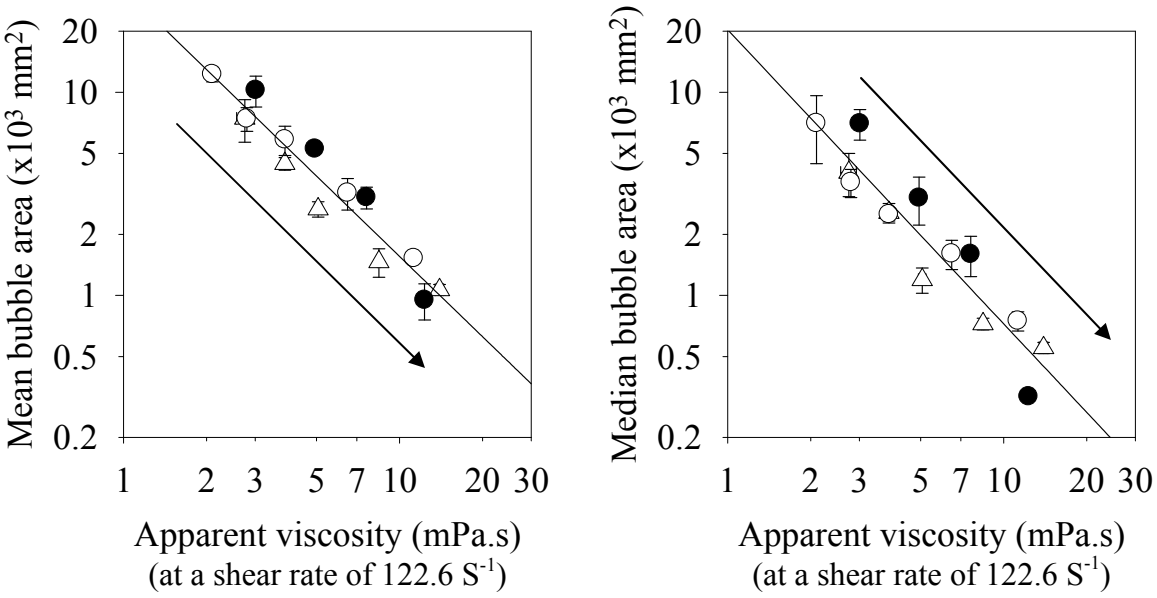

Figure 21. Relationship between mean or median bubble area and solution viscosity for protein solutions in the presence of different sucrose concentrations. Sucrose concentrations (0.00, 12.8 (only WPI and EWP), 25.0, 44.3, 63.6 g/100 mL) increased along with arrow direction. Protein concentration is 10% (w/v) in solutions. ● commercial β-lactoglobulin (commercial BLG) ○ whey protein isolate (WPI) △ egg white protein (EWP). Equations were showed in Table 1.

A common linear relationships were established between mean or median bubble area and solution apparent viscosity (at a shear rate of 122.6 1/s) for WPI and EWP foams on a ln-ln scale (Figure 6 in Chapter 3). The common scaling relationship held for BLG foams (Mean: R^2=0.927; Median: R^2=0.878) (Figure 21 and Table 1). This result indicated that the effect of sucrose decreasing the bubble size is due to increased solution viscosity.

Bubble size can affect the physical properties of foams. Foam yield stress has been correlated to interfacial tension (γ), bubble surface-volume mean radius (R_{32}), air phase fraction (ϕ) and an experimentally derived fitted parameter $Y(\phi)$ according to the model of Princen and Kiss (1989).

$$\tau_0 = \frac{\gamma}{R_{32}} \phi^{1/3} Y(\phi) \qquad \text{Equation 1}$$

The interfacial tension (γ) in this general model can be replaced by interfacial elasticity (E') for protein foams according to our previous results (Foegeding et al., 2006).

$$\tau_0 = \frac{E'}{R_{32}} \phi^{1/3} Y(\phi) \qquad \text{Equation 2}$$

The interfacial properties (γ and E'), foam yield stress (τ_0) and air phase fraction (ϕ) can be directly obtained from measurements. It's impossible to calculate R_{32} without unfolding size distribution of bubbles since the three dimensional (3D) bubble size was unknown. In Chapter 3, we found that the calculation of unfolding bubble size distribution won't affect the validity of Princen and Kiss (1989) model on protein foams. For simple calculations, R_{32} was approximated as $R_{32} \approx R_{20}$ = (mean bubble area / π)$^{1/2}$ or $R_{32} \approx R_{median}$ = (median bubble area / π)$^{1/2}$. The only unknown parameter is the experimentally derived fitted parameter $Y(\phi)$, which has been correlated to ϕ for emulsions and foams in a relationship of (Princen and Kiss, 1989; Figure 13 in Chapter 3):

$$Y(\phi) = -a - b\ln(\phi) \qquad \text{Equation 3}$$

where a and b are constants. The $Y(\phi)$ of BLG foams were calculated from Equation 1 or Equation 2 and fitted to Equation 3 (Figure 22).

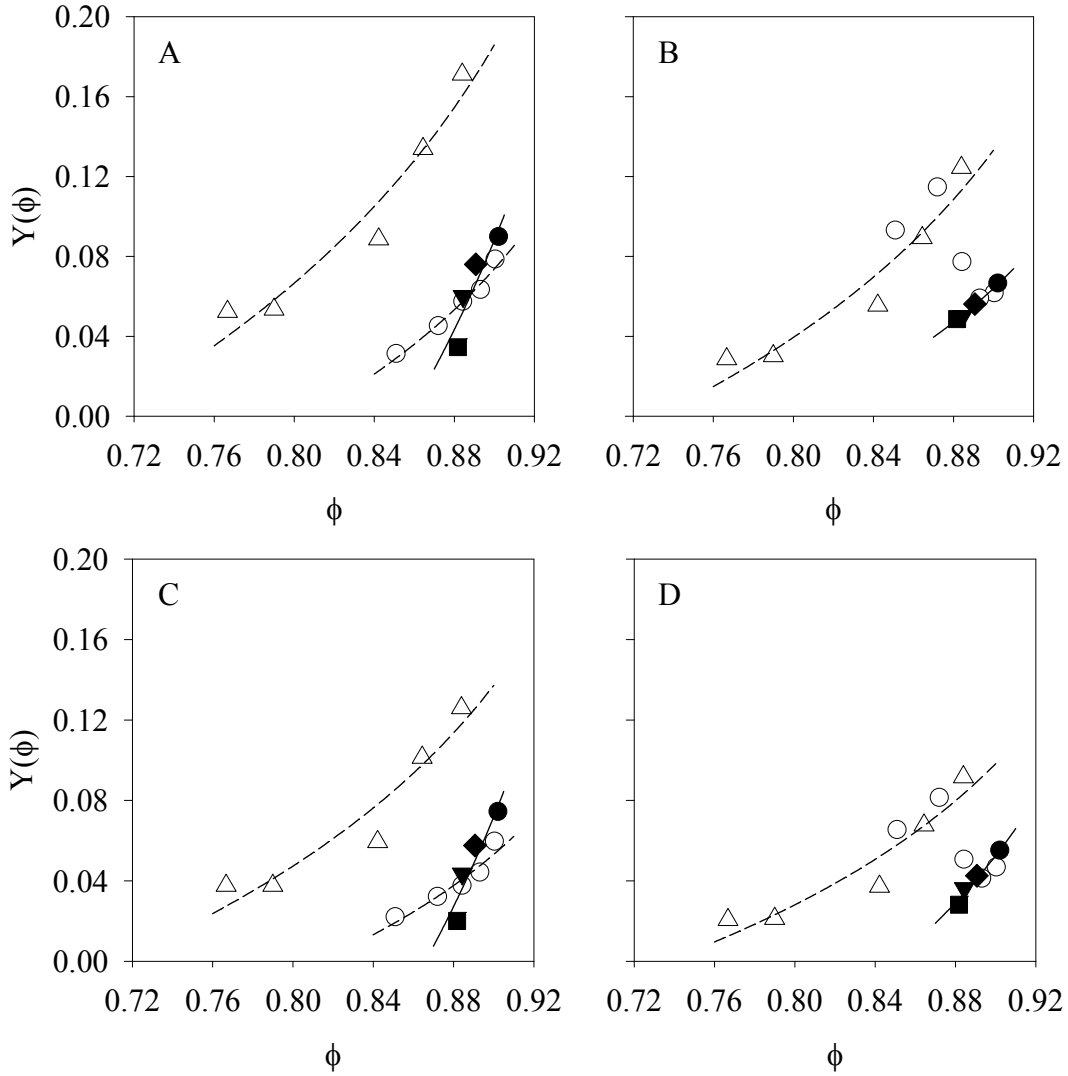

Figure 22. *Y(ϕ)* vs. ϕ calculated from area mean radius (R_{20}) or median radius (R_{median}) for commercial β-lactoglobulin (commercial BLG) foams in the presence of different sucrose concentrations. Protein concentration is 10% (w/v) in solutions. ● no sucrose ▲ 12.8 g/100 mL sucrose ◆ 25.0 g/100 mL sucrose ▼ 44.3 g/100 mL sucrose ■ 63.6 g/100 mL sucrose. Date of whey protein isolate (○) and egg white protein (△) were obtained from Chapter 3. A: *Y(ϕ)* of protein foams was calculated based on R_{20} and γ at 5 min (Equation 1). EWP: $Y(\phi)$=-0.174ln(1-ϕ)-0.213 (R^2=0.940) WPI: $Y(\phi)$=-0.110ln(1-ϕ)-0.180 (R^2=0.979) BLG: $Y(\phi)$=-0.246ln(1-ϕ)-0.478 (R^2=0.803). B: *Y(ϕ)* of protein foams was calculated based on R_{20} and E' at 5 min (Equation 2). EWP: $Y(\phi)$=-0.135ln(1-ϕ)-0.178 (R^2=0.926) BLG: $Y(\phi)$=-0.0931ln(1-ϕ)-0.150 (R^2=0.998). C: *Y(ϕ)* of protein foams was calculated based on R_{median} and γ at 5 min (Equation 1). EWP: $Y(\phi)$=-0.131ln(1-ϕ)-0.164 (R^2=0.914) WPI: $Y(\phi)$=-0.0833ln(1-ϕ)-0.139 (R^2=0.925) BLG: $Y(\phi)$=-0.245ln(1-ϕ)-0.493 (R^2=0.847). D: *Y(ϕ)* of protein foams was calculated based on R_{median} and E' at 5 min (Equation 2). EWP: $Y(\phi)$=-0.101ln(1-ϕ)-0.135 (R^2=0.907) BLG: $Y(\phi)$=-0.128ln(1-ϕ)-0.242 (R^2=0.956).

Three individual relationships can be established between $Y(\phi)$ and ϕ for BLG, WPI and EWP protein foams when $Y(\phi)$ was calculated from γ (Equation 1). This $Y(\phi)$ of BLG and WPI are close to each other while both of them are lower than that of EWP when compared at the same ϕ range (Figure 22A and C). This can be attributing to the higher E' of EWP than that of BLG and WPI whereas the E' is not considered in Equation 1. A higher interfacial elasticity was correlated to the higher foam yield stress for protein foams (Foegeding et al., 2006). After substituted γ with E' (Equation 2), the relationships of Equation 3 still worked for EWP and BLG foams but failed for WPI foams (Figure 22B and D). Two points of WPI (44.3 and 63.6 g/100 mL sucrose concentrations) were close to the curve of EWP while the other two points of WPI (0.00 and 12.8 g/100 mL sucrose concentrations) were close to the curve of BLG. The $Y(\phi)$ of WPI foams with 25 g/100 mL sucrose is in between the two curves. Substituting γ with E' in Princen and Kiss (1989) model leads $Y(\phi)$ and ϕ of the three protein foams closer to a master curve; however, the $Y(\phi)$ are still scattering at high ϕ range. This result confirmed the contribution of interfacial elasticity to foam yield stress and suggested some protein-specific factors were not considered in the theoretical models.

The bubble area change and bubble count number per slide (mm^2 area) were calculated from images taken from 0 to 20 min immediately after foam generation at an interval of 5 min (Figure 23).

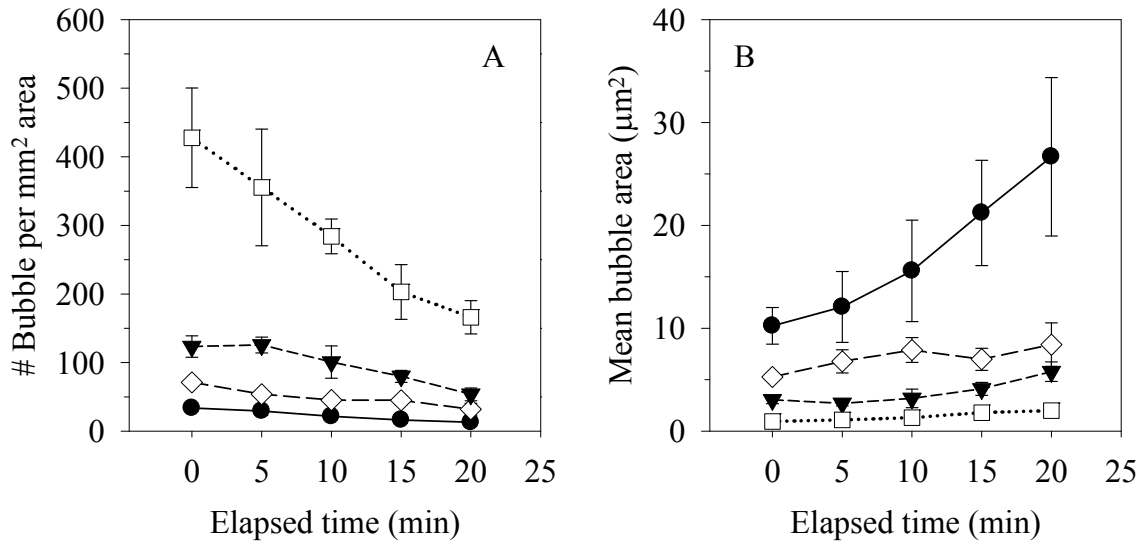

Figure 23. Changes of bubble count per mm^2 area (A) and mean bubble area (B) from 0 to 20 min for commercial β-lactoglobulin (commercial BLG) foams in the presence of different sucrose concentrations. Protein concentration is 10% (w/v) in solutions. ● no sucrose ◇ 25.0 g/100 mL sucrose ▼ 44.3 g/100 mL sucrose □ 63.6 g/100 mL sucrose.

The bubble number per slide (mm^2 area) decreased and the mean bubble area increased over time (Figure 23A). Addition of sucrose increased the bubble number but did not slow down bubble number decreasing rate over time, following the characteristics of WPI foams (Figure 7B in Chapter 3). The bubble number decreasing rate at a high sucrose concentration (63.6 g/100 mL) was faster than others (Figure 23A). The mean bubbles area became smaller and increased slower with increasing sucrose concentration (Figure 23B). The change of mean bubble area over 20 min to some extent indicated the bubble destabilization changes, such as disproportionation and coalescence in the foams. Changes in bubble area has been linearly correlated with the foam drainage ½ life on a ln-ln scale (Figure 8 in Chapter 3). The data from BLG foams was fit to this linear relationship

(R^2=0.923) along with EWP and WPI foams (Figure 24 and Table 1), suggesting that the change of mean bubble area over 20 min can be used as an index to evaluate foam stability.

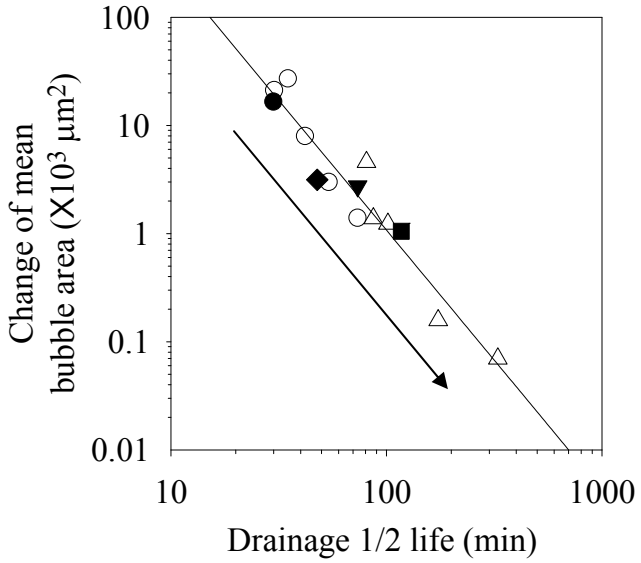

Figure 24. Relationship between the change of mean bubble area and foam drainage ½ life for commercial β-lactoglobulin (commercial BLG) foams in the presence of different sucrose concentrations. Protein concentration is 10% (w/v) in solutions. ● no sucrose ▲ 12.8 g/100 mL sucrose ◆ 25.0 g/100 mL sucrose ▼ 44.3 g/100 mL sucrose ■ 63.6 g/100 mL sucrose. Date of whey protein isolate (○) and egg white protein (△) were obtained from Chapter 3. Sucrose concentration (12.8, 25.0, 44.3, 63.6 g/100 mL) increased along with the arrow indication. Equations were showed in Table 1.

Interfacial elasticity is proposed to increase bubble stability, with a cessation of disproportionation predicted at E'/γ>1/2 (Dickinson, 1992). A condition of E'/γ>2 is more realistic in practice (Walstra, 2003). A negative linear relationship between the change of mean bubble area and E'/γ for EWP foams suggested that E'/γ>2 can effectively retard bubble size growth over time; however, the data for WPI foams were fitted to a positive linear relationship (Figure 9 in Chapter 3). The data from BLG foams were compared with EWP and WPI (Figure 25).

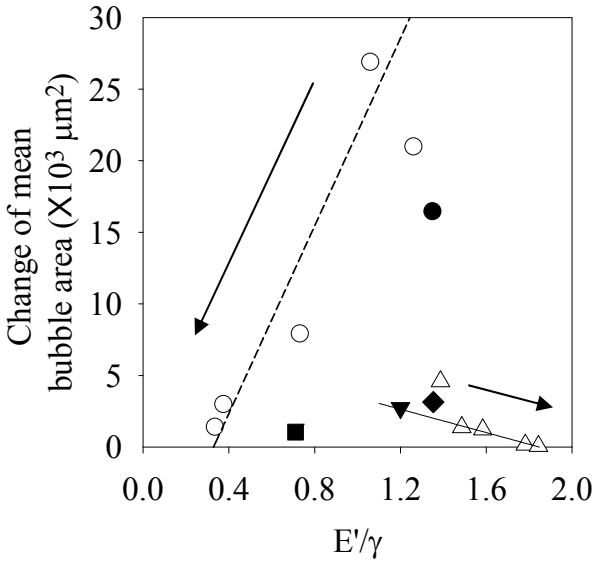

Figure 25. Relationship between the change of mean bubble area and interfacial elasticity (E'/γ) for commercial β-lactoglobulin (commercial BLG) foams in the presence of different sucrose concentrations. Protein concentration is 10% (w/v) in solutions. ● no sucrose ◆ 25.0 g/100 mL sucrose ▼ 44.3 g/100 mL sucrose ■ 63.6 g/100 mL sucrose. Date of whey protein isolate (○) and egg white protein (△) were obtained from Chapter 3. Sucrose concentration (12.8, 25.0, 44.3, 63.6 g/100 mL) increased along with the arrow indication.

Addition of sucrose decreased the change of bubble area. The BLG solutions containing 25.0 and 44.3 g/100 mL sucrose showed properties similar to EWP. However, the other two data points for BLG are very scattered. These results suggested that effect of sucrose on the bubble size growth rate is not solely dependent on the interfacial elasticity. Other properties, such as viscosity, and possible some protein-specific factors also contributed to bubble stability.

Angel food cakes prepared from commercial β-lactoglobulin

The performance of commercial BLG foams in angel food cakes were evaluated and compared with WPI and EWP foams (Figure 26).

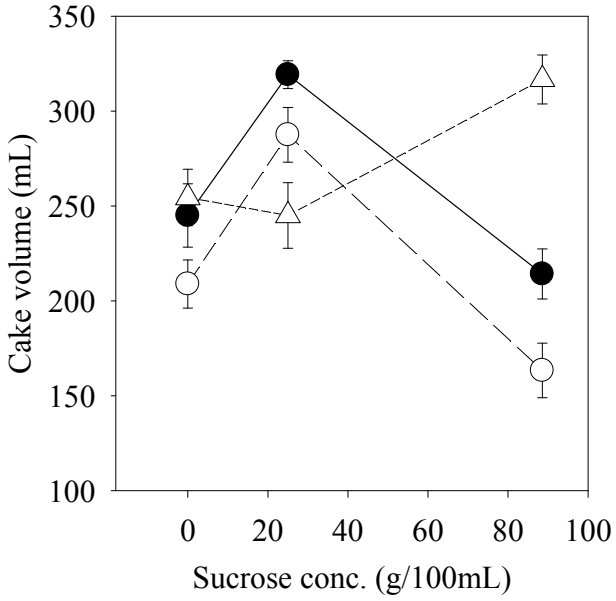

Figure 26. Volume of angel food cakes prepared from 10% (w/v) protein foams with addition of different amount of sucrose. ● commercial β-lactoglobulin (commercial BLG) ○ whey protein isolate (WPI) △ egg white protein (EWP). Date of whey protein isolate (○) and egg white protein (△) were obtained from Chapter 3.

The volume of BLG cakes changed in the same way as that of WPI cakes with varying sugar amounts, with a peak volume at 25.0 g/100 mL sugar concentration (Figure 26). This volume was even higher than the volume of EWP cake at the same sugar concentration. However, the cake volume of BLG and WPI dropped greatly with further increasing sucrose concentration, being much less than that of EWP cakes at a sugar concentration of 88.6 g/100 mL (the standard sugar concentration in an angel food cake). Photos of cross section of angel food cakes showed more similarities between BLG and WPI (Figure 27).

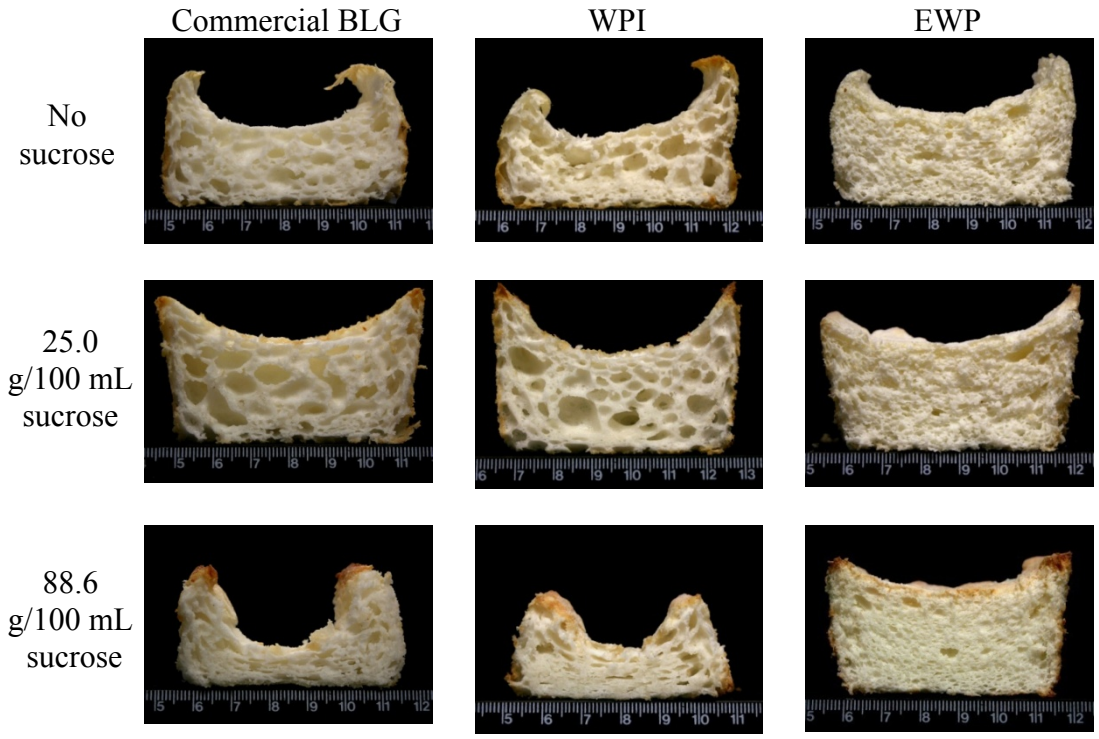

Figure 27. Photos of cross sections of angel food cakes prepared from 10% (w/v) protein solutions at pH 7.0 in the presence of different amounts of sucrose. (Images show scale in cm.) Date of whey protein isolate and egg white protein were obtained from Chapter 3.

The concave shape is observed in angel food cakes containing no sucrose prepared from three proteins. The concave shape of EWP cake decreased continuously while those of commercial BLG and WPI cakes increased. In addition to the cake shape, the cake structure of BLG and WPI showed a domination of large bubbles while that of EWP displayed a majority of small bubbles, regardless of sugar content. Addition of sugar increased the solid content in angel food cake batters and therefore increased cake volume of commercial BLG and WPI at 25 g/100 mL sugar concentration due to bulking effect. However, addition of sugar dilutes the concentration of starch and increases the temperature of starch gelatinization and protein denaturation, delaying cake matrix formation during baking. Due to poor

stability, the bubbles in commercial BLG and WPI became extremely large before the cake matrix formed, resulting in a collapsing of the cake structure at 88.6 g/100 mL sugar concentration. EWP angel food cakes displayed a fine structure with no collapsing, suggesting excellent bubble stability. The commercial BLG produced a coarse structure in angel food cake, similar to that of WPI. However, the interfacial elasticity of β-lactoglobulin is higher than that of whey protein isolate, contributing to increase foam stability and higher cake volume.

Conclusions

The results of this study indicated that the interfacial rheology of whey protein isolate was associated with α-lactalbumin, while that of egg white protein resembled a mixture of proteins. The interfacial properties of mixtures of egg white protein fractions were altered with the protein composition, suggesting a combining interfacial behavior of different fractions. The interfacial domination priority of protein components followed the order of α-lactalbumin > β-lactoglobulin > protein components in egg white, explaining the domination of whey protein isolate at the interface when mixed with egg white protein. Sucrose did not alter the interefacial elasticity (E') of β-lactoglobulin, different from its effect on E' of whey protein isolate. The greater E' of β-lactoglobulin than that of whey protein isolate in the presence of sucrose contributed to a greater stability of the wet foam and increased angel food cake volume. However, the coarse cake structure, indicative of whey protein foams, remained.

REFERENCES

Antipova AS, Semenova MG, Belyakova LE. 1999. Effect of sucrose on the thermodynamic properties of ovalbumin and sodium caseinate in bulk solution and at air water interface. Colloids Surf B: Biointerfaces 12: 261-270.

Baeza R, Carrera Sanchez C, Pilosof AMR, Rodríguez Patino JM. 2004. Interactions of polysaccharides with β-lactoglobulin spread monolayers at the air–water interface. Food hydrocolloids 18: 959-966.

Barnes HA, Hutton JF, Walters K. 1989. An introduction to rheology. Amsterdam: Elsevier. p199.

Berry TK. 2008. Foaming Properties, Interfacial Properties, and Foam Microstructure of Egg White Protein and Whey Protein Isolate, Alone and in Combination. Thesis and dissertation. North Carolina State University.

Bos MA, van Vliet T. 2001. Interfacial rheological properties of adsorbed protein layers and surfactants: A review. Adv Colloid Interface Sci 91: 437-471.

Campbell GM, Mougeot E. 1999. Creation and characterization of aerated food products. Trends Food Sci Tech 10: 283-296.

Cornec M, Cho D, Narsimhan G. 1999. Adsorption dynamics of α-lactalbumin and β-lactoglobulin at air–water interfaces. J Colloid Interface Sci. 214: 129-142.

Damodaran S, Anand K, Razumovsky L. 1998. Competitive Adsorption of Egg White Proteins at the Air-Water Interface: Direct Evidence for Electrostatic Complex Formation between Lysozyme and Other Egg Proteins at the Interface. J Agric Food Chem 46: 872-876.

Davis JP, Foegeding EA. 2004. Foaming and interfacial properties of polymerized whey protein isolate. J Food Sci 69: C404-C410.

Davis JP, Foegeding EA. 2007. Comparisons of the foaming and interfacial properties of whey protein isolate and egg white proteins. Colloids Surf B: Biointerfaces 54: 200-210.

Dickinson E, Murry BS, Stainsby G. 1988. Protein adsorption at air-water and oil-water interfaces. In Advances in food emulsions and foams. Edited by Dickinson E and Stainsby G. Elsevier Applied Science Publishers Ltd. p123.

Dickinson E, Rolfe SE, Dalgleish DG. 1990. Surface shear viscometry as a probe of protein-protein interactions in mixed milk protein films adsorbed at the oil water interface. Int J Biol Macromol 12: 189-194.

Dickinson E. 1992. An Introduction to Food Colloids. Oxford: Oxford University Press.

Dickinson E. 2001. Milk protein interfacial layers and the relationship to emulsion stability and rheology. Colloids Surf B: Biointerfaces. 20(3): 197-210.

Dickinson E, Ettelaie R, Murry BS, Du Z. 2002. Kinetics of disproportionation of air bubble beneath a planar air-water interface stabilized by food proteins. J Colloid Interface Sci 252: 202-213.

Foegeding EA, Luck PJ, Davis JP. 2006. Factors determining the physical properties of protein foams. Food Hydrocolloids 20: 284-292.

Fox PF. 2003. Milk proteins: General and historical aspects. In "Advanced Dairy Chemistry – 1 Proteins" Edited by Fox PF and McSweeney PLH. p1.

Johnson TM, Zabik ME. 1981a. Response surface methodology for analysis of protein interactions in angel food cakes. J Food Sci 46: 1226-1230.

Johnson TM, Zabik ME. 1981b. Egg albumen proteins interactions in an angel food cake system. J Food Sci 46: 1231-1236.

Kloek W, van Vliet T, Meinders M. 2001. Effect of bulk and interfacial rheological properties on bubble dissolution. J colloid interface sci 237: 158-166.

Kosters HA, Broersen K, de Groot J, Simons JWFA, Wierenga P, de Jongh HHJ. 2003. Chemical processing as a tool to generate ovalbumin variants with changed stability. Biotechnol Bioeng 84: 61-70.

Lau CK, Dickinson E. 2005. Instability and structural change in an aerated system containing egg albumen and invert sugar. Food Hydrocolloids 19: 111-121.

Li-Chan E, Nakai S. 1989. Biochemical Basis for the Properties of Egg White. CRC Crit Rev Poultry Biology 2: 21-58.

Luck PJ, Bray N, Foegeding EA. 2001. Factors Determining Yield Stress and Overrun of Whey Protein Foams. J Food Sci 65: 1677-1681.

MacDonnell LR, Feeney RE, Hanson HL, Campbell A, Sugihara TF. 1954. The functional properties of the egg white proteins. Food Technol 8: 49-53.

Magdassi S, Kamyshny A. 1996. Surface activity and functional properties of proteins. In Surface activity of proteins. Edited by Magdassi S. Marcel Dekker, Inc. p3.

Mailliart P, Ribadeau-dumas B. 1988. Preparation of β-lactoglobulin and β-lactoglobulin-free proteins from whey retentate by NaCl salting out at low pH. J Food Sci. 53(3): 743.

Mann K. 2007. The chicken egg white proteome. Proteomics J 7: 3558-3568.

Martin AH, Grolle K, Bos MA, Cohen Stuart MA, van Vliet T. 2002. Network forming properties of various proteins adsorbed at the air/water interface in relation to foam stability. J Colloid Interface Sci 254: 175–183.

McClements DJ. 2002. Modulation of globular protein functionality by weakly interacting cosolvents. Crit Rev Food Sci Nutr 42: 417-471.

Myrvold R, Hansen FK. 1998. Surface elasticity and viscosity from oscillating bubbles measured by automatic axisymmetric drop shape analysis. J Colloid Interface Sci 207: 97-105.

Niño MRR, Wilde PJ, Clark DC, Husband FA, Rodríguez Patino JM. 1997. Rheokinetic analysis of protein films at the air-aqueous subphase interface. 2. Bovine serum albumin adsorption from sucrose aqueous solutions. J Agric Food Chem 45: 3016-3021.

Pernell CW, Foegeding EA, Daubert CR. 2000. Measurement of the yield stress of protein foams by vane rheometry. J Food Sci 65: 110-114.

Pernell CW, Luck PJ, Foegeding EA, Daubert CR. 2002. Heat-induced changes in angel food cakes containing egg-white protein or whey protein isolate. J Food Sci 67: 2945-2951.

Phillips LG, Haque Z, Kinsella JE. 1987. A method for the measurement of foam formation and stability. J Food Sci 52: 1074-1077.

Phillips LG, Yang ST, Schulman W, Kinsella JE. 1989. Effect of lysozyme, clupeine, and sucrose on the foaming properties of whey protein isolate and β-lactoglobulin. J Food Sci 54: 743-747.

Princen HM, Kiss AD. 1989. Rheology of foams and highly concentrated emulsions IV: An experimental study of the shear viscosity and yield stress of concentrated emulsions. J Colloid Interface Sci 128(1): 176-187.

Prins A, Bos M, Boerboom FJG, van Kalsbeek HKAI. 1998. Relation between surface rheology and foaming behaviour of aqueous protein solutions. Proteins at liquid interfaces. Amsterdam: Elsevier Sciences p221–266.

Ridout MJ, Mackie AR, Wilde PJ. 2004. Rheology of mixed β-casein/β-lactoglobulin films at the air-water interface. J Agric Food Chem 52: 3930-3937.

Steffe JF. 1996. Rheological Methods in Food Process Engineering. 2nd ed. East Lansing, MI: Freeman Press. p15, 418.

Swaisgood HE. 1982. Chemistry of Milk Protein. Developments in Dairy Chemistry – 1. Edited by Fox PF. Applied Science Publishers LTD. p1-59.

Walstra P. 2003. Physical Chemistry of Foods. New York: Marcel Dekker.

APPENDIX I

A Simplified Model for Estimating Shear Rate during Whipping

APPENDIX I

The shear rate for whipping was estimated using a simplified model for the Kitchen Aid Ultra Power Mixer (Kitchen Aid, St. Joseph's, MI) with a 4.3 L stationary bowl and rotating beaters (Figure I.1).

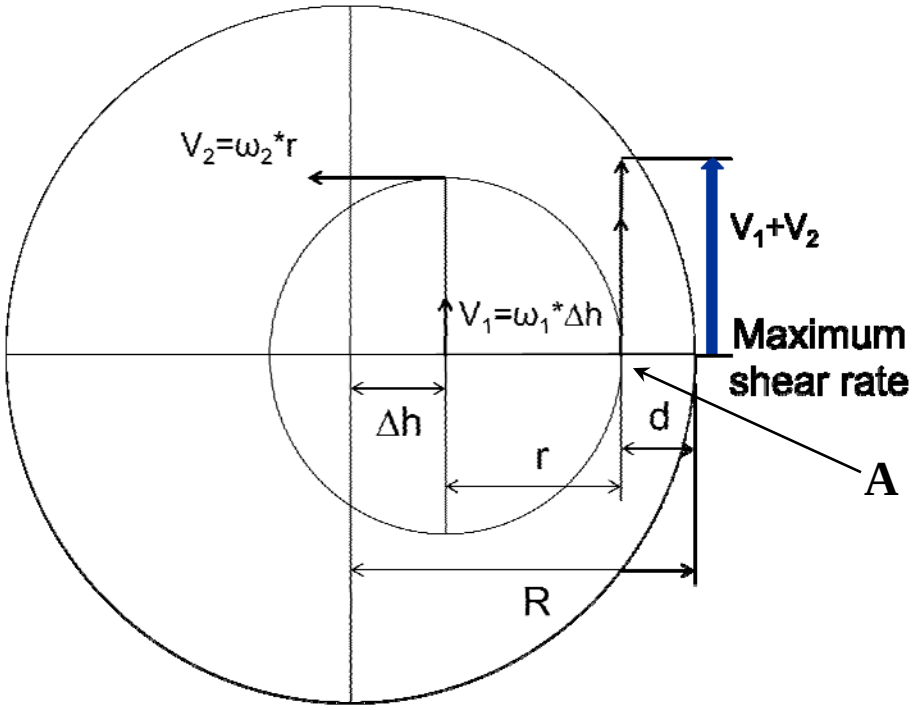

Figure 1. A simplified model for whipping process. *R* is the radius of the big circle (whipping bowl); *r* is the radius of the small circle (beater); *Δh* is the distance between the centers of the two circles; *d* is the shortest distance from the circumference of the small circle to the circumference of the big circle at this position; ω_1 and ω_2 are respectively the planetary and beater rotating rates; V_1 and V_2 are corresponding moving rates and equal to (ω_1*r) and ($\omega_2*\Delta h$) respectively; solid black arrows indicated the magnitude and direction of *V*; the solid blue arrow indicates the magnitude and direction of maximum *V*.

Figure I.1 is a schematic representation for whipping process, in which the beater is rotating as well as doing planetary rotation around the center of the whipping bowl. If we assume no-slip of the flow on the inside wall of the whipping bowl, point A should have the maximum shear rate because it has the shortest distance ($R-(r+\Delta h)$) from the beater (the small circle) to

the inside wall of the whipping bowl (the big circle) and maximum moving rate (V_1+V_2) perpendicular to this distance. Additionally, the movement of fluid was assumed as a simple shear flow for easy calculations. The maximum shear rate can be calculated as $\frac{V1+V2}{R-(r+\Delta h)}$.

The geometry parameters of whipping bowl and beat were measured using a rule. The planetary rpm (ω_1) and beater rpm (ω_2) were given by the manufacture of this mixer.

Known parameters:

R=21.5 cm; r=11cm; Δh=3 cm.

ω_1=225 rpm=225 * 2π/60 s^{-1}= 23.6 s^{-1}; ω_2=737 rpm=737 * 2π/60 s^{-1}= 77.2 s^{-1}.

Calculations:

$V_1= \omega_1 * \Delta h$=23.6 s^{-1} * 3 cm=70.7 cm/s; $V_2= \omega_2 * r$=77.2 s^{-1} * 11 cm=849 cm/s.

$$\text{Maximum shear rate} = \frac{V_1 + V_2}{R - (r + \Delta h)} = \frac{70.7 + 849}{21.5 - (11 + 3)} s^{-1} = 122.6\, s^{-1}$$

According to this model, the shear rate in this whipping bowl is in a range from 0 s^{-1} (near the bowl wall) to 122.6 s^{-1} (the point A) during the whipping process. This is in a shear rate range for normal mixing in food process (10 to 10^3 1/s) (Steffe, 1996). The maximum shear rate of **122.6 s^{-1}** was used to calculate the apparent viscosity of fluids during whipping.

Note that the real situation is far more complex than this model. The movement of fluid in the whipping bowl can be a turbulent flow rather than a simple shear flow. The geometry of the real device is also more complicated than in the model. This simplified model is only used to estimate a reasonable shear rate for the calculation of the apparent viscosity of the fluid during whipping.